

AD-A106 052

ITT AVIONICS DIV NUTLEY N J

F/G 17/2.1

MODULAR MULTI-FUNCTION MULTI-BAND AIRBORNE RADIO SYSTEM (MFBARS--ETC(U)

JUN 81 R A REILLY, C W WARD, A LEE

F33615-78-C-1518

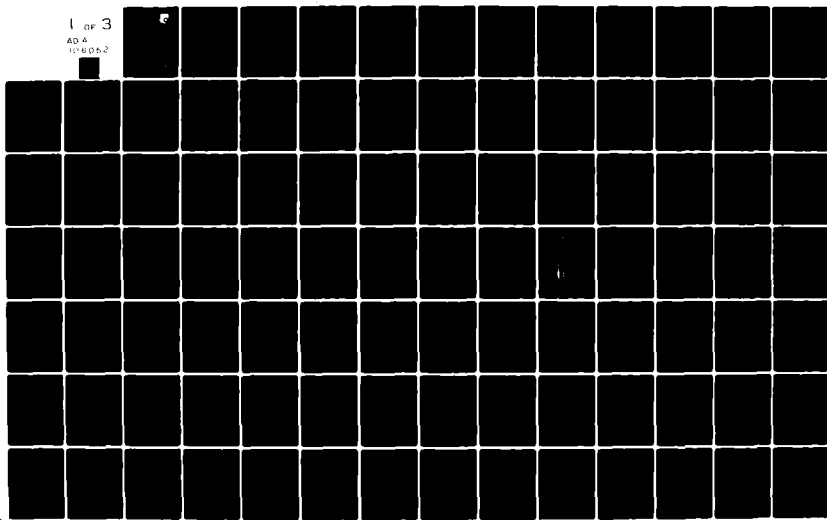
UNCLASSIFIED

AFWAL-TR-81-1077-VOL-2

NL

1 of 3

AD-A  
106052



AD A106052

LEVEL

2

AFWAL-TR-81-1077, Vol. II



## MODULAR MULTI-FUNCTION MULTI-BAND AIRBORNE RADIO SYSTEM (MFBARS)

Volume II - Detailed Report

ITT Avionics Division  
390 Washington Avenue  
Nutley, New Jersey 07110

June 1981

Final Technical Report for Period March 1978 - June 1980

Approved for Public Release; Distribution Unlimited

Avionics Laboratory  
Air Force Wright Aeronautical Laboratories  
Air Force Systems Command  
Wright-Patterson AFB, Ohio 45433

DTIC  
ELECTE  
OCT 23 1981  
S A D

81 10 23

DTIC FILE COPY

NOTICE

When Government drawings, specifications, or other data are used for any purpose other than in connection with a definitely related Government procurement operation, the United States Government thereby incurs no responsibility nor any obligation whatsoever; and the fact that the government may have formulated, furnished, or in any way supplied the said drawings, specifications, or other data, is not to be regarded by implication or otherwise as in any manner licensing the holder or any other person or corporation, or conveying any rights or permission to manufacture use, or sell any patented invention that may in any way be related thereto.

This report has been reviewed by the Office of Public Affairs (ASD/PA) and is releasable to the National Technical Information Service (NTIS). At NTIS, it will be available to the general public, including foreign nations.

This technical report has been reviewed and is approved for publication.

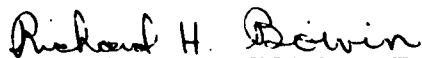


DARLOW G. BOTHA  
PROJECT ENGINEER  
AFWAL/AAAD



CHARLES R. REGISTER, Major, USAF  
Acting Chief, Info Transmission Br  
Avionics Laboratory

FOR THE COMMANDER



RICHARD H. BOIVIN, Colonel, USAF  
Chief, System Avionics Division  
Avionics Laboratory

"If your address has changed, if you wish to be removed from our mailing list, or if the addressee is no longer employed by your organization please notify AFWAL/AAAD-3 W-PAFB, OH 45433 to help us maintain a current mailing list".

Copies of this report should not be returned unless return is required by security considerations, contractual obligations, or notice on a specific document.

17 REPORT DOCUMENTATION PAGE		READ INSTRUCTIONS BEFORE COMPLETING FORM
1. REPORT NUMBER AFWAL TR-81-1077, Vol 2 AD-A106052	2. GOVT ACCESSION NO.	3. RECIPIENT'S CATALOG NUMBER
4. TITLE (and Subtitle) Modular Multi-Function Multi-band Airborne Radio System Volume II, Detailed Report.	5. TYPE OF REPORT & PERIOD COVERED Final Technical Report Mar 1978 - Jun 1980	6. PERFORMING ORG. REPORT NUMBER
7. AUTHOR(s) R. A. Reilly C. W. Ward A. Lee R. Schineller ITT Avionics; A. Clemens, W. Robertson, ITT/AOD Dr. J. Rome, Univ. of Lowell Mass.	8. CONTRACT OR GRANT NUMBER(s) Contract No. F33615-78-C-1518	
9. PERFORMING ORGANIZATION NAME AND ADDRESS ITT Avionics Division 390 Washington Ave. Nutley, N.J. 07110	10. PROGRAM ELEMENT PROJECT, TASK AREA & WORK UNIT NUMBERS 62204F 2003, 02A7	
11. CONTROLLING OFFICE NAME AND ADDRESS Avionics Laboratory (AFWAL/AAAD) Air Force Wright Aeronautical Laboratories Wright-Patterson AFB, Ohio 45433	12. REPORT DATE Jun 1981	
14. MONITORING AGENCY NAME & ADDRESS (if different from Controlling Office)	13. NUMBER OF PAGES 230	
	15. SECURITY CLASS (of this report) Unclassified	
16. DISTRIBUTION STATEMENT (of this Report) Approved for public release, distribution unlimited.		
17. DISTRIBUTION STATEMENT (of the abstract entered in Block 20, if different from Report)		
18. SUPPLEMENTARY NOTES This report consists of two volumes.  Volume 1 contains the executive summary.		
19. KEY WORDS (Continue on reverse side if necessary and identify by block num. or) Integrated Communication Navigation    Integrated Radio System Avionics Identification Avionics    Avionics Integrated CNI Avionics    Agile Transversal Filter ICNIA    ATF CNI    Wideband Agile Transversal Filter (cont)		
20. ABSTRACT (Continue on reverse side if necessary, and identify by block number) This report describes the results of the first two phases of the MFBARS radio architecture study. This study was aimed at establishing a cost effective and volume-conserving method of integrating tactical CNI avionics equipments. The goal was innovative integration of these systems, by a method which would allow the incorporation of new capabilities and which would take advantage of technological advances, both in-hand and projected within the near-term future (1985). Such integration is needed to reduce spiraling		



20. ABSTRACT (cont.)

life cycle costs and to alleviate severe hardware space limitation problems in tactical aircraft.

During Phase I, a set of viable MFBARS candidate architectures was developed, together with a cost evaluation of these with respect to a government-provided baseline of existing equipment, to allow meaningful comparisons.

The three MFBARS architectures proposed during Phase I were keyed to a reasonable expectation of techniques and devices projected to be available when MFBARS advanced development would be initiated in the mid '80's. The three architectures provided a graduated increase in payoff potential with associated increases in technical risk.

The Government then selected the most advanced of the three Phase I candidate system architectures for more detailed study.

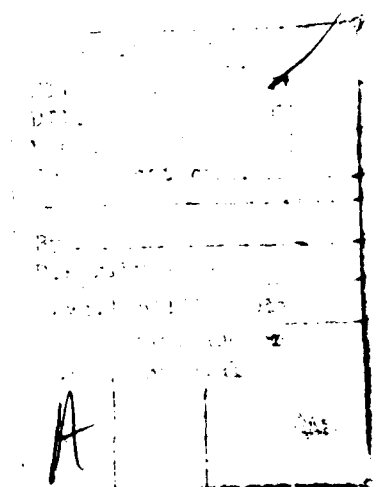
During Phase II, ITT conducted a top-down, system-oriented study of the selected system approach. System configuration details and performance parameters were refined. In addition, to minimize system development risk and to provide guidance on the best direction along which MFBARS should proceed, recommended plans were defined for development of the system and supporting technology.

The main emphasis of this report is on the final recommended system configuration and associated performance parameters and recommended development plans.

19. KEY WORDS (con't.)

WBATF  
Narrowband Agile Transversal Filter  
NBATF  
JTIDS  
GPS  
GPS/JTIDS

Integrated GPS/JTIDS  
Integrated GPS/JTIDS/INS  
SEEK TALK  
AFSATCOM



## C O N T E N T S

	<u>Page No.</u>
1. INTRODUCTION.....	11
1.1 STUDY OBJECTIVES.....	11
1.2 STUDY APPROACH.....	13
1.3 BASELINE DEFINITION.....	16
2. DESCRIPTION OF MFBARS CANDIDATE SYSTEM ARCHITECTURES.....	21
2.1 GENERAL PERFORMANCE REQUIREMENTS.....	21
2.2 THE THREE (PHASE I) CANDIDATE SYSTEM ARCHITECTURES.....	24
2.2.1 Architecture No. 1.....	28
2.2.2 Architecture No. 2.....	32
2.2.3 Architecture No. 3.....	36
2.3 COMPARISON OF (PHASE I) CANDIDATE SYSTEM ARCHITECTURES.....	40
3. DETAILED DESCRIPTION OF THE DESIGN OF THE SELECTED MFBARS ARCHITECTURE.....	43
3.1 AIRCRAFT INTERFACES.....	43
3.2 OVERALL SYSTEM BLOCK DIAGRAM.....	43
3.3 ANTENNA SUBSYSTEM.....	45
3.3.1 Conventional Antenna Elements and Antenna Coupling Network.....	45
3.3.1.1 GPS.....	49
3.3.1.2 JTIDS/TACAN.....	50
3.3.1.3 IFF Transponder and Interrogator.....	50
3.3.1.4 VHF/UHF Communications....	50
3.3.1.5 AFSATCOM.....	51
3.3.1.6 VOR/Localizer/Glideslope/ Marker Beacon.....	51

VOLUME II  
CONTENTS

	<u>Page No.</u>
3.3.1.7 Antenna Coupling Network..	51
3.3.2 Adaptive Antenna Arrays.....	53
3.3.2.1 Separate Arrays for each spread spectrum signal....	53
3.3.2.2 Partial Array Integration.	53
3.3.2.3 Full Array Integration....	60
3.3.2.4 Adaptive Algorithms and Antenna Weighting Circuits.....	68
3.4 RF SUBSYSTEM.....	69
3.4.1 Wideband Agile Transversal Filters (WBATF's).....	71
3.4.1.1 Introductory Description of WBATF.....	71
3.4.1.2 WBATF Application to MFBARS.....	72
3.4.2 VHF/UHF Preselection Filters.....	72
3.4.3 Log-Video Amplifiers.....	79
3.4.4 AGC Amplifier.....	84
3.4.5 VHF/UHF Transmitters.....	84
3.4.5.1 Transmitter Architecture..	85
3.4.6 L-Band Transmitter.....	89
3.4.6.1 Oscillator.....	89
3.4.6.2 Modulator.....	89
3.4.6.3 Upconverter.....	91
3.4.6.4 RF Driver/Exciter.....	91
3.4.6.5 Power Amplifier.....	94
3.5 SIGNAL PROCESSOR SUBSYSTEM.....	96
3.5.1 Baseband Converters.....	96
3.5.2 Signal Switching Network.....	96
3.5.3 Narrowband Agile Transversal Filter (NBATF) Assembly.....	100
3.5.3.1 JTIDS NBATF's.....	106
3.5.3.2 GPS NBATF's.....	109
3.5.3.3 TACAN NBATF's.....	109
3.5.3.4 IFF NBATF's.....	109

VOLUME II  
CONTENTS

	<u>Page No.</u>
3.5.3.5 SEEK TALK NBATF's.....	113
3.5.3.6 NBATF Requirements for Narrowband MFBARS Signals.	114
3.5.4 Code Generators.....	114
3.5.5 Special Purpose Dedicated Signal Processors.....	115
3.5.5.1 GPS Processor.....	117
3.5.5.2 JTIDS Processor.....	121
3.5.5.3 JTIDS Wedge Delay Line....	123
3.5.5.4 TACAN Processor.....	127
3.5.5.5 IFF Processor.....	129
3.5.5.6 SEEK TALK Processor.....	133
3.5.5.7 AFSATCOM Processor.....	133
3.5.5.8 SINCGARS Processor.....	133
3.5.5.9 Analog Voice Processor....	133
3.6 DATA AND CONTROL PROCESSOR SUBSYSTEM.....	135
3.6.1 Architecture.....	137
3.6.2 Microprocessors.....	137
3.6.3 Main Memory.....	138
3.6.4 I/O's (Input/Output Devices).....	138
3.6.5 Interconnection Structure.....	138
3.6.6 Software.....	139
3.7 BITE SUBSYSTEM.....	141
3.8 PHYSICAL DESCRIPTION.....	146
4. TECHNOLOGY PROJECTIONS.....	151
4.1 WBATF TECHNOLOGY.....	152
4.2 DIGITAL CIRCUITS.....	155
4.3 SAW PRESELECTION FILTERS.....	156
5. COST ANALYSES.....	157
5.1 BASELINE DATA AND ESTIMATING GROUND RULES...	157
5.2 RESULTS.....	161
6. INTEGRATED NAVIGATION CONCEPTS.....	163
6.1 SUMMARY OF RESULTS OF INTEGRATED NAVIGATION FUNCTION STUDY TASK.....	163

VOLUME II  
CONTENTS

	<u>Page No.</u>
6.1.1 Opportunities for Hardware Integration.....	163
6.1.2 Operational Benefits to JTIDS Users.	163
6.1.3 Operational Benefits to GPS Users...	164
6.2 DETAILS OF INTEGRATED GPS/JTIDS/INS NAVIGATION FUNCTION.....	165
6.2.1 GPS Tracking Loops.....	169
6.2.2 Kalman Filter.....	174
6.2.2.1 Filter State Structure....	174
6.2.2.2 Filter Timing.....	178
6.2.2.3 Filter Operation.....	179
6.2.3 Navigation Data Set Source Selection.....	181
6.2.3.1 Dynamic Behavior of Navigation Data Set Source Selection.....	184
6.2.4 Acquisition and Maintenance of Time-base.....	185
6.2.5 Geodetic Navigation with Less Than Four GPS Satellites in View.....	186
7. CONCLUSIONS AND RECOMMENDATIONS.....	189
7.1 REVIEW OF THE STUDY FINDINGS.....	189
7.2 RECOMMENDATIONS FOR FUTUE DEVELOPMENT.....	191
7.3 SUGGESTED PROGRAM PLAN.....	191
APPENDIX A. DETAILED DESCRIPTION OF WIDEBAND AGILE TRANSVERSAL FILTER (WBATF) DESIGN.....	197

## I L L U S T R A T I O N S

<u>Figure No.</u>	<u>Title</u>	<u>Page No.</u>
1	MFBARS CNI Signals (HF not shown).....	12
2	Approach to Phase I.....	14
3	Approach to Phase II.....	15
4	MFBARS Architecture No. 1 Physical Description.....	25
5	MFBARS Architecture No. 2 Physical Description.....	26
6	MFBARS Architecture No. 3 Physical Description.....	27
7	MFBARS Architecture No. 1, HF and VHF/UHF Receivers.....	29
8	30-400 MHz Receiver.....	30
9	MFBARS Architecture No. 1, L-Band Receiver and Processing Subsystems.....	31
10	MFBARS Architecture No. 2, VHF/UHF Receiver.....	33
11	MFBARS Architecture No. 2, L-Band Receiver and Processing Subsystems.....	35
12	MFBARS Architecture No. 3.....	38
13	Projected MFBARS Benefits for Each Candidate System Architecture, as Compared to Baseline.....	41
14	Interface of MFBARS with Other Aircraft Systems.....	44
15	MFBARS Top Level Block Diagram.....	44
16	Antenna Subsystem.....	46
17	Block Diagram of Conventional Antenna Elements and Antenna Coupling System.....	47
18	Nominal Antenna Locations, Conventional Antennas.....	48

VOLUME II  
ILLUSTRATIONS

<u>Figure No.</u>	<u>Title</u>	<u>Page No.</u>
19	MFBARS Antenna Coupling Network.....	52
20	A Non-integrated Approach to Adaptive Arrays.....	55
21	Partially Integrated Adaptive Antenna Array.....	56
22	Eleven Element Array Concepts.....	58
23	Integrated Adaptive Antenna Array Processor/Spread Spectrum RF Processor....	62
24	Time-sharing and Up/Down Conversion for Integrated Processing.....	63
25	Integrated Adaptive Array Processor/ Wideband RF Processor.....	65
26	RF Subsystem.....	70
27	WBATF Block Diagram.....	73
28	VHF/UHF Preselection Filters.....	75
29	30-88 MHz Filter Bank.....	76
30	108-174 MHz Filter Bank.....	77
31	225-400 MHz Filter Bank.....	78
32	Gain, Noise Figure, and Intermodulation Budgets.....	80
33	Log Video RF Amplifier.....	81
34	Log Video RF Amplifier for TACAN Signal Processing.....	82
35	MFBARS Synthesized Block Diagram.....	86
36	L-Band Transmitter Block Diagram.....	90
37	CPSM Code Modulator.....	90
38	Fast Hopping Indirect Frequency Synthesizer.....	92
39	RF Driver/Exciter.....	93

VOLUME II  
ILLUSTRATIONS

<u>Figure No.</u>	<u>Title</u>	<u>Page No.</u>
40	Dual Power Amplifier.....	95
41	Signal Processor Subsystem.....	97
42	Baseband Converter.....	98
43	Signal Switching Network.....	99
44	NBATF Block Diagram.....	101
45	Standard NBATF Building Block.....	102
46	NBATF Assembly.....	104
47	NBATF Configuration, ATDMA/TDMA JTIDS Sync.....	107
48	NBATF Configuration, ATDMA/TDMA Data Mode.....	108
49	NBATF Configuration for JTIDS DTDMA, Both Sync and Data Modes.....	110
50	NBATF Configuration, GPS.....	111
51	NBATF Configuration, TACAN.....	111
52	NBATF Configuration, IFF.....	112
53	NBATF Configuration, Narrowband Signals...	112
54	PN Code Generator Designs.....	116
55	GPS Receiver Processor Block Diagram.....	118
56	GPS Signal Processor Block Diagram.....	120
57	JTIDS Processor Block Diagram.....	122
58	The JTIDS Synchronization Problem.....	125
59	The Wedge Delay Line Block Diagram.....	126
60	TACAN Processor Block Diagram.....	128
61	IFF Interrogation Block Diagram.....	130
62	IFF Transponder Block Diagram.....	132



VOLUME II  
ILLUSTRATIONS

<u>Figure No.</u>	<u>Title</u>	<u>Page No.</u>
63	Analog Voice Processor Block Diagram.....	134
64	Data and Control Processor Subsystem.....	136
65	Block Diagram of Monitor Circuit for Typical Antenna Channel.....	144
66	MFBARS Phase II, LRU No. 1.....	147
67	MFBARS Phase II, LRU No. 2.....	148
68	MFBARS Phase II, LRU No. 3.....	149
69	Domain of Operation for Various Trans- versal Filter Technologies.....	154
70	Fully Integrated System Structure GPS/ JTIDS/INS.....	166
71	Time-Locked Loop, Normal Operation.....	170
72	Combined Conventional Tracking and Loop Slewing.....	172
73	Kalman Filter Operation.....	180
74	Source Selection Algorithm Functional Flow Chart.....	183
75	Geometry of Three Platforms in a Field of Hyperbolic LOP's.....	187
76	Comparison, MFBARS Versus Baseline.....	190
77	Program Flow Chart.....	192
78	Detailed Program Flow Chart.....	193

## T A B L E S

<u>Table No.</u>	<u>Title</u>	<u>Page No.</u>
1	Baseline CNI Radio Functions.....	17
2	Potential Growth Functions for Integrated CNI Avionics (ICNIA) Architecture.....	20
3	MFBARS Radio Spectral Requirements.....	22
4	Functional Requirements.....	23
5	MFBARS Phase I Candidate Architectures Compared to Phase I Baseline.....	41
6	Adaptive Array Requirements.....	54
7	NBATF Building Block Requirements.....	105
8	Software Requirements (Preliminary Estimate).....	140
9	RF Subsystem Bite Functions.....	142
10	Summary of Physical Characteristics.....	146
11	CCD WBATF Performance Projections.....	153
12	SAW Filter Performance Comparison.....	156
13	CNI Baseline.....	158
14	Software Requirements (Preliminary Estimate).....	160
15	Cost Comparisons (1978 \$).....	162
16	Outputs of Navigation Equations.....	175
17	Error States Used in the Kalman Filter....	176

## 1. INTRODUCTION

This report describes the results of the first two phases of the Modular Multi-function Multi-band Airborne Radio System (MFBARS) radio architecture study. This study identifies cost effective and volume-conserving methods of integrating tactical Communication, Navigation and Identification (CNI) avionics equipments for the signals shown in Figure 1.

The study goal was to develop concepts for innovative integration of these equipments by methods which would allow the incorporation of new capabilities, and which would take advantage of technological advances, both in-hand and projected to be available within the near-term future (1985). Such integration is needed to reduce spiraling life cycle costs and to alleviate a severe space problem in tactical aircraft.

### 1.1 STUDY OBJECTIVES

The primary objectives of the MFBARS study were to define smaller and more cost effective CNI avionics through an architecture characterized by standardization of common functional modules and interfaces designed to provide:

- reduced proliferation of unique modules
- the ability to configure, from a set of common modules, a given total CNI capability on specific platforms for a given mission
- the ability to take advantage of technological advances to improve specific common modules with a minimum of retrofit/transition cost
- the ability to incorporate new capabilities
- improved reliability with graceful degradation
- redundancy of critical functions

In meeting these objectives, it was necessary to comply with two overriding Government-imposed guidelines:

- performance standards (of each individual radio function) must be maintained or could be improved, but could not be degraded.
- signal-in-space waveforms (of each individual radio function) could not be modified.

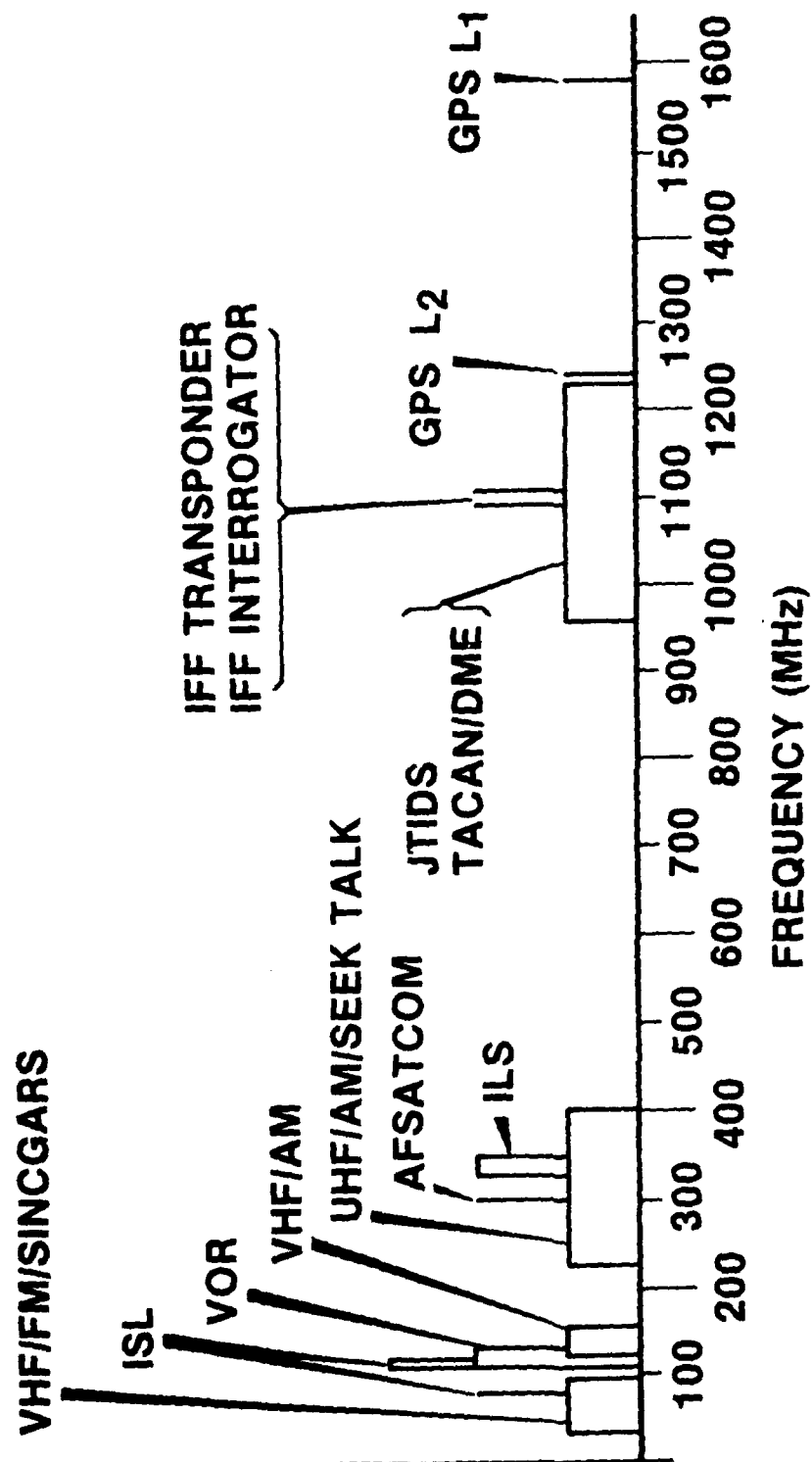


Figure 1. MFBARS CNI signals (HF not shown)

In addition, the Government directed that MFBARS designs should incorporate technology as projected to be available in 1985, the planned start of hardware development. This was done to avoid constraining MFBARS designs by technology which would be seven years old by the time hardware development started.

Finally, MFBARS interfaces with other aircraft systems were to maximize use of other standard avionics equipment, both in-being and under development as standard avionics modules. For example, all MFBARS digital interface with cockpit controls and displays would utilize DAIS. The controls and displays themselves would be standard DAIS-compatible controls and displays, not special items developed as part of the MFBARS design effort.

## 1.2 STUDY APPROACH

Phase I of the MFBARS study addressed broad conceptual issues of MFBARS design. Three specific candidate system architectures were defined, each with a different degree of technical risk and associated projected payoff in terms of reduced size and cost and improved operational flexibility. At the end of Phase I, the Government directed ITT to proceed with the highest risk/highest payoff candidate system design. During Phase II, more detailed levels of this design were developed, as were recommended associated technology development plans. Figures 2 and 3 show the approaches taken during Phases I and II.

It was clear at the onset that the MFBARS approach confronts multiple complex issues, and that it would dilute the current effort to attempt to address all of the issues, assuming that all could be identified. The study concentrated, therefore, on the areas that promised the highest payoffs. In doing this, a system-oriented top-down study approach was utilized.

The study started with an analysis of operational and mission requirements. This analysis showed that no more than 4-6 VHF/UHF radio functions were ever used simultaneously (of up to 14 VHF/UHF radios carried). This meant that considerable systems savings could be achieved by integrating VHF/UHF RF front end modules, and by adding software-controlled flexible switching and signal processing capabilities.

Similar analysis of the L-band radio functions led to the conclusion that software-controlled high speed time sharing would provide the best approach to meeting MFBARS objectives for L-band signals.

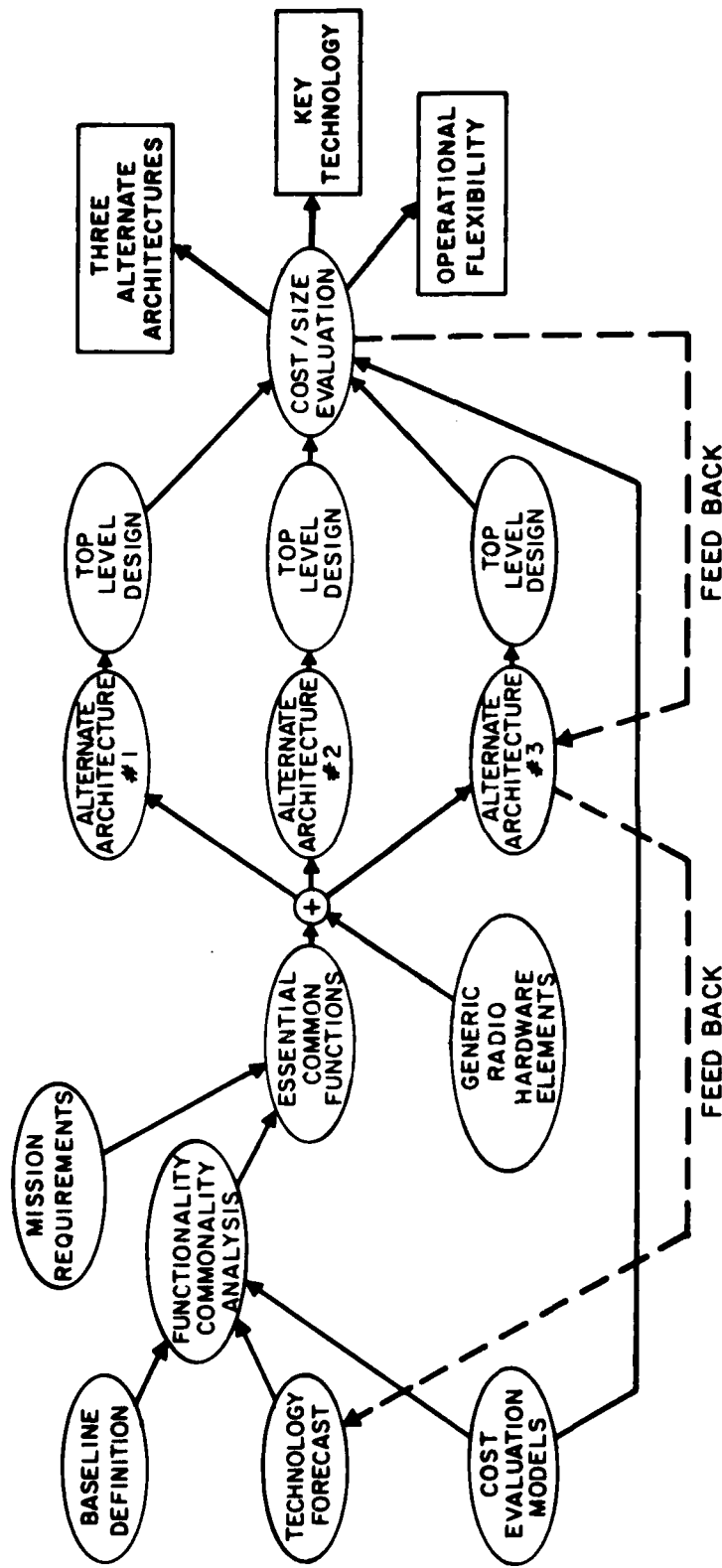


Figure 2. Approach to Phase I

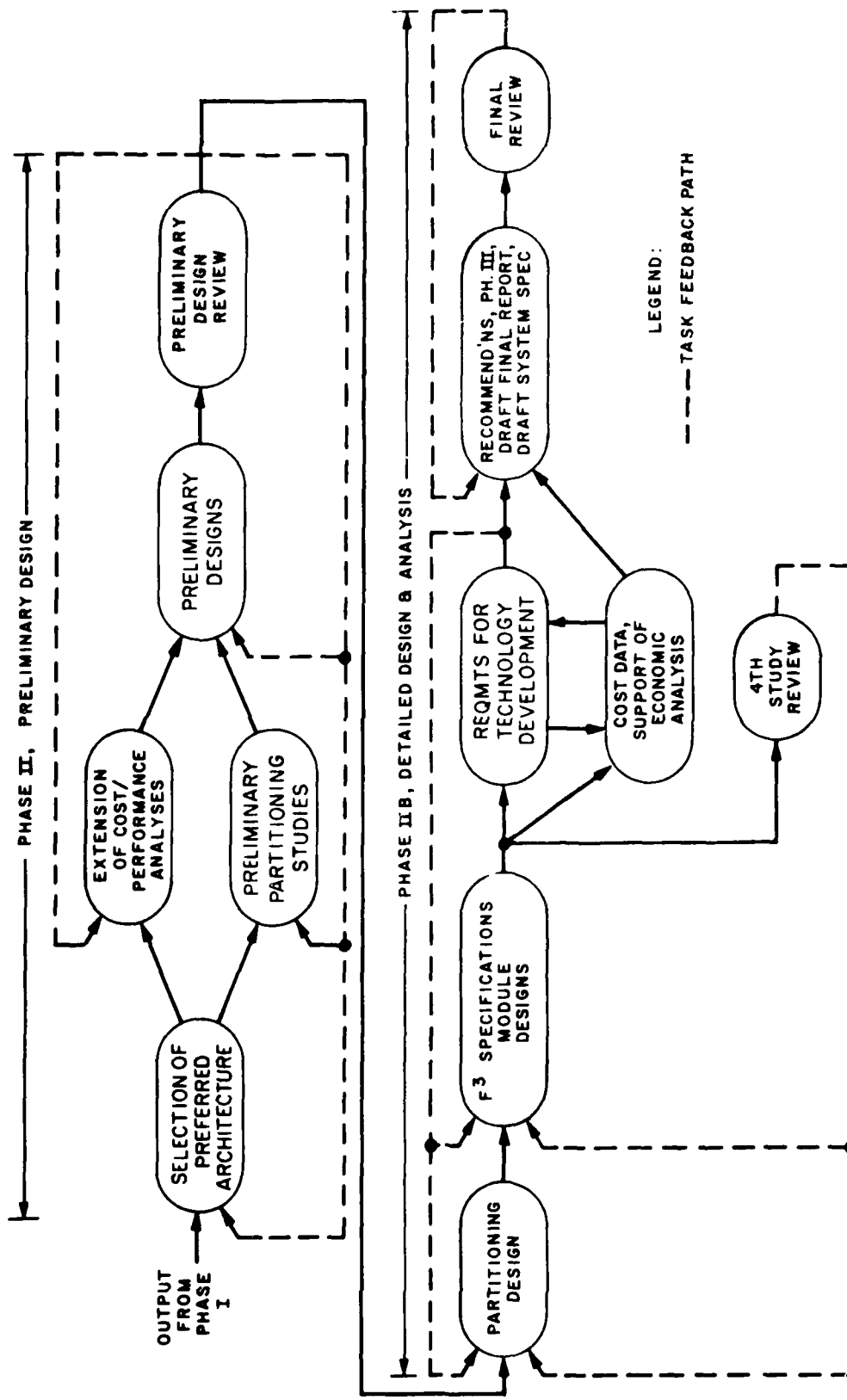


Figure 3. Approach to Phase 11

Analysis of HF radio functions led to the conclusion that only marginal (approximately 5 percent) savings would be realized by integration of HF radio functions. Furthermore, tactical mission use of HF is very limited. Therefore, unless new factors (such as widespread introduction of new adaptive HF techniques) were considered, it would not be cost effective to integrate HF with the other radio functions. The resultant design approaches, therefore, consider HF as an optional future add-on only, not as a mainline system capability.

In addition to identification of flexible switching (for VHF/UHF bands) and high speed time sharing (for L-band) as candidate techniques for CNI radio integration, cost analyses were performed for generic radio sets. It was revealed that more than 50 percent of their cost is commonly contained in the RF circuitry. One focus of the study was therefore concentrated in the reduction of or simplification of the many RF components and related RF signal processing circuits. Common RF modules and other potential RF cost saving approaches were identified and evaluated. Promising cost effective design approaches were incorporated in candidate designs.

Three candidate system architectures emerged from these top-level analyses of the most promising areas for size and cost reduction. These three architectures are described in Section 2 of this report. Section 3 of the report then provides expanded details on the architecture selected by the Government as most appropriate in terms of meeting MFBARS objectives.

### 1.3 BASELINE DEFINITION

In order to evaluate each candidate MFBARS system design concept, a reference point had to be established. To this end the Government provided a baseline list of (non-integrated) CNI radio equipment which provided all of the functional capabilities required of MFBARS. This baseline list changed somewhat during the course of the study, as explained in the following paragraphs. The baselines are summarized in Table 1.



TABLE 1. BASELINE CNI RADIO FUNCTIONS

<u>Radio</u>	<u>Band; Type</u>	<u>Phase I</u>	<u>Phase II</u>
ARC 112	HF; Comm	X	
ARC 131	Low VHF, FM; Comm (30-88 MHz)	X	X
ARC 115	High VHF, AM/FM; Comm (108-156 MHz)	X	X
ARC 164	UHF, AM; Comm	X	X
ARN 118	L-Band; TACAN	X	X
APX 76	L-Band; IFF Interrogator	X	X
APX 101	L-Band; IFF Transponder	X	X
JTIDS	L-Band; Spread Spectrum Comm/Nav	X	X
GPS	L-Band; Spread Spectrum Nav	X	X
SEEK TALK	UHF Spread; Spectrum Comm	X	X
SINCGARS	VHF; Freq. Hop Comm		(some platforms)
AFSATCOM	UHF; Satellite Comm		(some platforms)

The baseline list of equipment was subjected to a PRICE cost analysis (RCA's Programmed Review of Information and Costing Evaluation) to determine projected costs, as well as improved size and weight for the total baseline list if individual baseline equipment items were to be updated to take advantage of available technology, but without integration. This provided a more realistic comparative reference point than a simple summation of baseline equipment size, weight and cost without allowing any update of older equipments on the baseline list.

All MFBARS candidate system architectures were then also analyzed by PRICE. However, the MFBARS candidate system architectures had the opportunity to take advantage of benefits of integration. In addition, two of the candidate system architectures were based on technology improvements above and beyond what would otherwise be available in the normal course of technology growth. These two architectures entailed higher risk, which had to be assessed against the projected added benefits. Comparative results are discussed in Section 3.

The original baseline contained an HF radio function. As the MFBARS program progressed, it was decided to make HF an optional add-on only. This was done because it was found that the benefits of system integration could not efficiently be extended to HF. The primary reasons for this were:

1. Very high power (400 watt) CW HF transmitters would be required, which would constrain potential reduction in system size reduction, because of fundamental transmitter efficiency limits and thermal dissipation requirements. (Such transmitters were not required for any other MFBARS radio functions.)
2. The many octaves of operating frequency in the HF band require complicated and bulky dedicated antenna matching circuitry, not required for any other MFBARS radio functions.
3. Relatively few tactical aircraft are presently (or expected to be) equipped with HF radios.

The above conclusions are based on consideration of conventional HF systems only. If an adaptive HF system using new spread spectrum concepts were to be implemented, then integration of HF into MFBARS would require reconsideration. The system is designed in such a way that HF could be added as an optional add-on.

The original baseline GPS radio set was considered to be the production version of the Magnavox X-set (simultaneous 4-channel receiver capability for high accuracy computations for high dynamics maneuvering platforms). It was recognized, however, that MFBARS should incorporate the results of parallel on-going GPS improvement programs which would increase GPS jam resistance and add other system performance improvements. Therefore, the baseline GPS performance was changed to an "improved X-set" capability. With the exception of an adaptive antenna array for improved GPS anti-jam performance (which is addressed as a separate item), these GPS improvements

would all be incorporated in software or with very minor hardware changes. Therefore, the physical elements of the Magnavox X-set were retained for baseline purposes (except for the addition of an adaptive antenna array), with the improved baseline capabilities reflected in the software area.

The JTIDS baseline capability was defined to be the "worst case" of three different versions of JTIDS under consideration by the Government: TDMA (Time Division Multiple Access), ATDMA (Advanced TDMA), and DTDMA (Distributed TDMA). TDMA has been tentatively selected by the Government as the interim version of JTIDS, scheduled for limited deployment on AWACS and F-15's. Either DTDMA or ATDMA, but not both, will be selected later as the advanced follow-on JTIDS for deployment on all other platforms. The advanced JTIDS system selected must be "downward compatible" with interim JTIDS (TDMA) for interoperability between AWACS, F-15's and other platforms. Thus, MFBARS had to have a capability for either ATDMA/TDMA or DTDMA/TDMA. Since ATDMA/TDMA imposes the "worst case" conditions for hardware and software design purposes, ATDMA/TDMA was used as the baseline and for projection of worst case MFBARS requirements. If the Government should select DTDMA/TDMA instead, the impact on MFBARS would be to reduce MFBARS hardware and software requirements.

Finally, the baseline was modified to reflect packaging improvements projected possible if GPS and JTIDS were integrated rather than considered each as separate sets. This combined GPS/JTIDS packaging, based on a Draper Labs study, would not change functional performance of either radio set, but would provide a more realistic advanced technology baseline against which to compare projected MFBARS architectures.

The only other significant modifications to the original baseline were the addition of two new capabilities. The first was SINCGARS, a VHF secure voice communication system, and the second was AFSATCOM, a UHF, low data rate digital data satellite communication system. These are not required for all platforms and are therefore considered optional modules of MFBARS.

A summary of some of the more important specifications of the baseline equipments appears in Section 2.1 of this report.

It is recognized that as the MFBARS development progresses, further changes or additions to the baseline may occur. Several radio functions which are candidates, but as yet not incorporated in the baseline, are listed in Table 2.

TABLE 2. POTENTIAL GROWTH FUNCTIONS FOR INTEGRATED  
CNI AVIONICS (ICNIA) ARCHITECTURE

Adaptive HF

MLS (Microwave Landing System)

CAS (Collision Avoidance System)

DABS (Discrete Address Beacon System)

NIS (NATO IFF System)

## 2. DESCRIPTION OF MFBARS CANDIDATE SYSTEM ARCHITECTURES

### 2.1 GENERAL PERFORMANCE REQUIREMENTS

The functions and modes of operation required to fulfill the requirements for communication, navigation and identification for MFBARS are shown in Tables 3 and 4.

Four simultaneous VHF/UHF communications and navigation receive channels are required to provide three simultaneous voice channels (including one guard channel) and one time-shared channel containing four navigation signals. Transmission is required on one VHF/UHF channel, but not simultaneously with VHF/UHF receive. These channels cover the bands of 30-88 MHz, 108-156 MHz, and 225-440 MHz. Two VHF/UHF receivers are required for redundancy, but only one is used at a time. VHF/UHF receive channels cover the bands of 30-88 MHz, 108-156 MHz, and 225-440 MHz. Transmit channels are the same except for 118-156 MHz instead of 108-156 MHz (VOR and ILS signals do not require airborne transmission).

In addition to conventional voice communication modes, the UHF band capability must also provide SEEK TALK, AFSATCOM, and secure voice modes.

VHF FM low-band operation requires secure voice and frequency hopping modes of operation, in addition to conventional voice communication modes.

For L-band, the system must provide 10 channels of simultaneous receive capability for: four GPS signals (two time-shared frequencies), one IFF frequency (at a time), and up to eight simultaneous JTIDS frequencies (required for "worst case" ATDMA/TDMA acquisition and sync, although four channels would be adequate for DTDMA JTIDS). TACAN, when utilized, would be received on a single TACAN frequency at a time.

L-band transmissions will be from a single L-band transmitter, shared between JTIDS, TACAN (when utilized) and IFF. IFF transmissions would interrupt receipt or transmission of other L-band signals, as at present in conventional suites of CNI avionics.

Within both the VHF/UHF bands and L-band, the system will be in either a transmit or receive mode; there is no requirement for simultaneous receive and transmit within either band. However, the two bands may operate

TABLE 3. MFBARS RADIO SPECTRAL REQUIREMENTS

RECEIVE:				
VHF/UHF:				
		Freq. MHz	Modulation	Baseline Equivalent
1. VHF LO-Band Comm/Homing	Tunable/Freq. Hopped	30-88	PM	ARC-131
2. VHF LO-Band Guard	Fixed	40.5	PM	
3. VHF LO-Band Marker Beacon	Fixed	75.0	AM	ARC-108
4. VHF HI-Band Localizer	Tunable	108-117	AM	
5. VHF HI-Band VOR	Tunable	112-118	AM	
6. UHF Glide Slope	Tunable	329-335	AM	
7. VHF HI-Band Comm/ADF	Tunable	108-156	AM	ARC-115
8. VHF HI-Band Guard	Fixed	121.5	AM	
9. UHF Comm/ADF	Tunable	225-400	AM	ARC-164
10. UHF Guard	Fixed	243	AM	
11. UHF SEEK TALK	Direct Seq. PN	225-400	PN	SEEK TALK
12. UHF AFSATCOM (a)	Hopped	225-400	FSK	AFSATCOM
L-Band:				
13. JTIDS Comm/Nav	Freq. & Time Hopped & Dir. Seq. PN	960-1215	PN, PULSE	(b)
14. IFF	Fixed	1030/1090	PPM	APX-76/APX-101
15. Tacan	Tunable	960-1215	PULSE	APN 118
16. GPS	Fixed	1227/1575	PN	(c)
17. SINGCARS (a)	Freq. Hopped	30-88		SINGCARS-V
TRANSMIT:				
VHF/UHF:				
		Freq. MHz	Modulation	Baseline Equivalent
1. VHF LO-Band Comm	Tunable/Freq. Hopped	30-88	PM	ARC-131
2. VHF HI-Band Comm	Tunable	118-156	AM	ARC-115
3. UHF Comm	Tunable	225-400	AM	ARC-164
4. UHF SEEK TALK	Direct Seq. PN	225-400	PN	SEEK TALK
5. AFSATCOM (a)	Freq. Hopped	225-400	FSK	AFSATCOM
L-Band:				
6. JTIDS Comm/Nav	Freq. & Time Hopped & Dir. Seq.	960-1215	PN, Pulse	(b)
7. Tacan	Tunable	960-1215	Pulse	APN-118
8. IFF	Fixed	1030/1090	PPM	APX-76/APX-101
9. SINGCARS (a)	Freq. Hopped	30-88		SINGCAR V
(a) Some platforms only				
(b) JTIDS ATDMA/TOMA or RTDMA/TDMA, to be determined by Government				
(c) Improved X-set				
		Power (Watts)		
		10/1		
		10		
		10		
		10		
		40		
		200/1000		
		1000		
		500		

TABLE 4. FUNCTIONAL REQUIREMENTS

VHF/UHF Communications

- Up to three simultaneous receive voice channels, including one guard channel.
- Transmission on one channel at a time (dual VHF/UHF transmitters provide redundancy, but only one transmits at a time).
- Transmit and receive capability in each of the bands: 30-88 MHz, 108-156 MHz, and 225-400 MHz.
- 25 kHz channel separation.
- Ability to pre-program channels and processors.
- Ability to pre-program information transfer functions.
- SEEK TALK spread spectrum voice capability.
- AFSATCOM low data rate capability.
- SINCGARS-V frequency hopping voice capability.

L-Band Communications

- JTIDS ATDMA/TDMA or DTDMA/TDMA (8 simultaneous channels for worst case ATDMA/TDMA acquisition and sync; 4 channels adequate for DTDMA/TDMA).

Navigation and IFF (VHF/UHF and L-band)

- ILS/VOR: Marker beacon, localizer, glide slope, VOR
- GPS: Precision navigation.
- TACAN: Air-to-ground and air-to-air; receive and transmit.
- JTIDS: Relative navigation; receive and transmit.
- IFF: Transponder and interrogator; all modes including Mark XII; receive and transmit.
- VHF FM: Homing (back-up nav).
- VHF AM: ADF (back-up nav).

independently of each other. That is, both could be receiving simultaneously or both transmitting or either could be receiving while the other is transmitting.

## 2.2 THE THREE (PHASE I) CANDIDATE SYSTEM ARCHITECTURES

Although many potential MFBARS architectures could be considered, three generic designs were selected as representative of the variations that could be expected as a function of selected tradeoff parameters. The three selected architectures are categorized in terms of risk. The first design represents a minimum, or low risk approach using technology currently in hand or in advanced development. The second design represents a medium risk approach using slightly more sophisticated technology as well as novel approaches to signal processing which require more extensive development effort. While this architecture represents a higher risk than the first architecture, it also offers further improvements in size, weight and cost as well as enhanced performance characteristics. Finally, the third design is a higher risk approach utilizing some technology which requires considerable development effort. As might be expected, the payoff for this investment is the greatest improvement in size, weight, cost and performance.

Each of the three architectures is described fully in the forthcoming sections. For the purpose of comparing size and weight between the baseline and each candidate MFBARS architecture, a consistent packaging method was used. Component packaging into standard size cards or modules was based on the Hughes Aircraft Company advanced JTIDS packaging technique as described in the GPS/JTIDS/INS Integration Study Final Report, prepared by the Charles Stark Draper Laboratory, Incorporated, April 1978. In packaging modules into LRU's, a standard LRU size of 3/4 ATR (long) was used. In all architectures a normal growth of general purpose component technology (with respect to such things as digital gate densities or active devices per chip, power dissipation, operating frequency range, etc.) was assumed.

Figures 4, 5, and 6 show the three different Phase I physical packages resulting from the three different architectural approaches. There was a direct correlation between size and weight reduction and degree of sophistication of technology utilized.



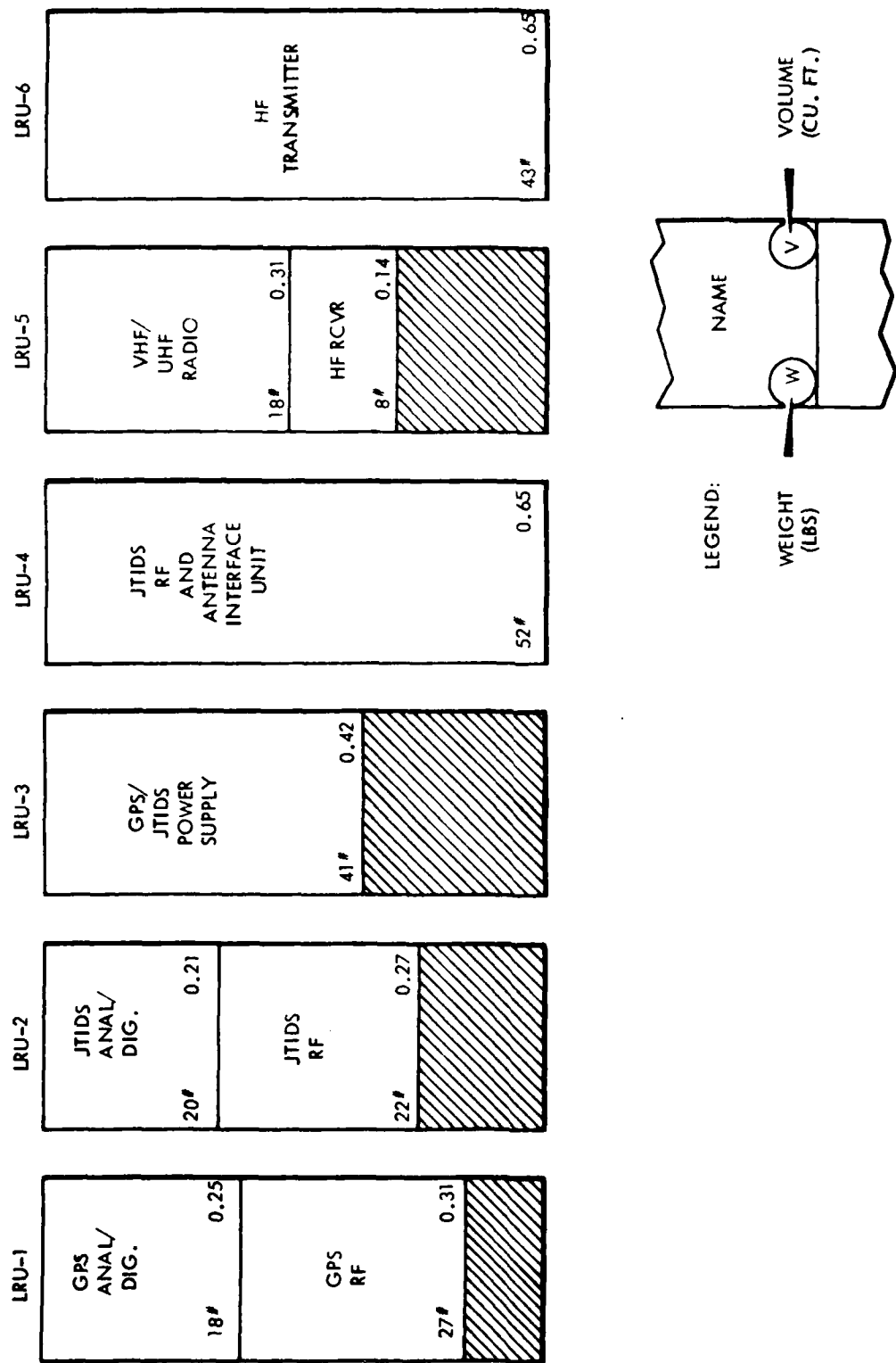
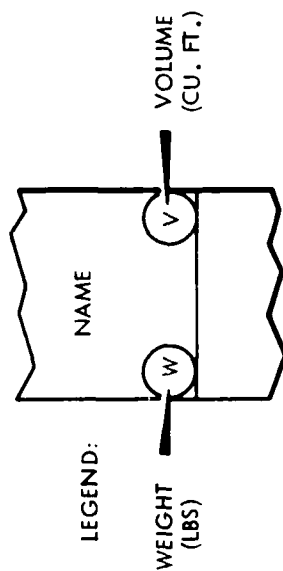
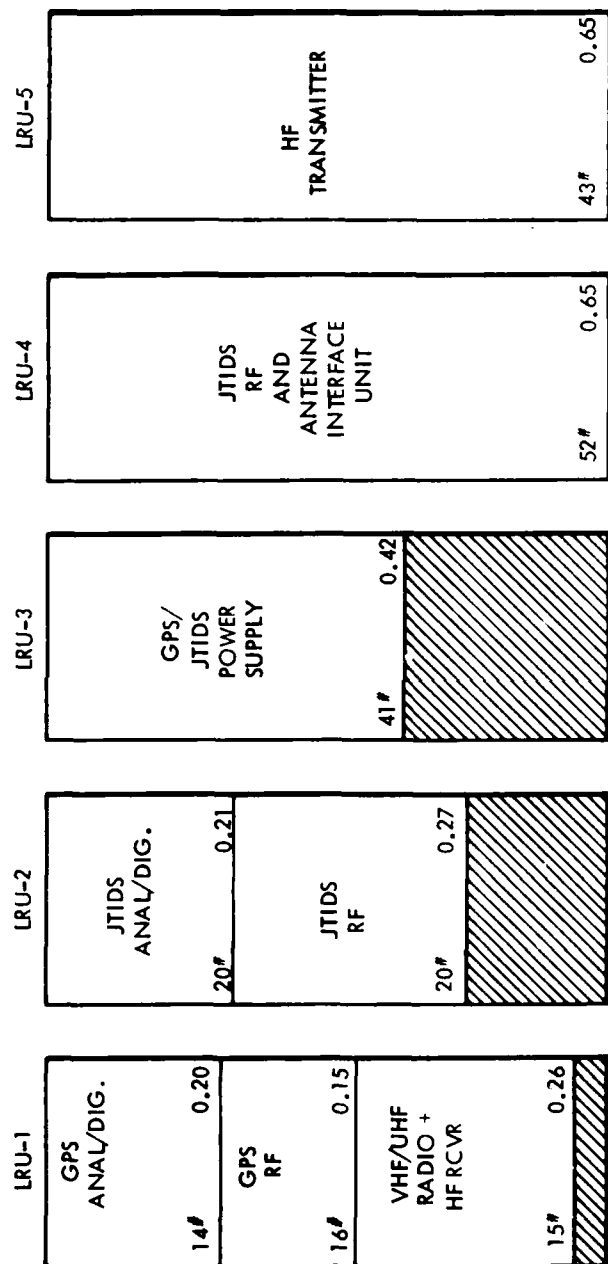


Figure 4. MFBARS architecture no. 1 physical description



- 1) ALL LRU'S ARE 3/4 ATR - LONG
- 2) SHADED AREAS ARE UNUSED VOLUMES

Figure 5. MFBARS architecture no. 2 physical description

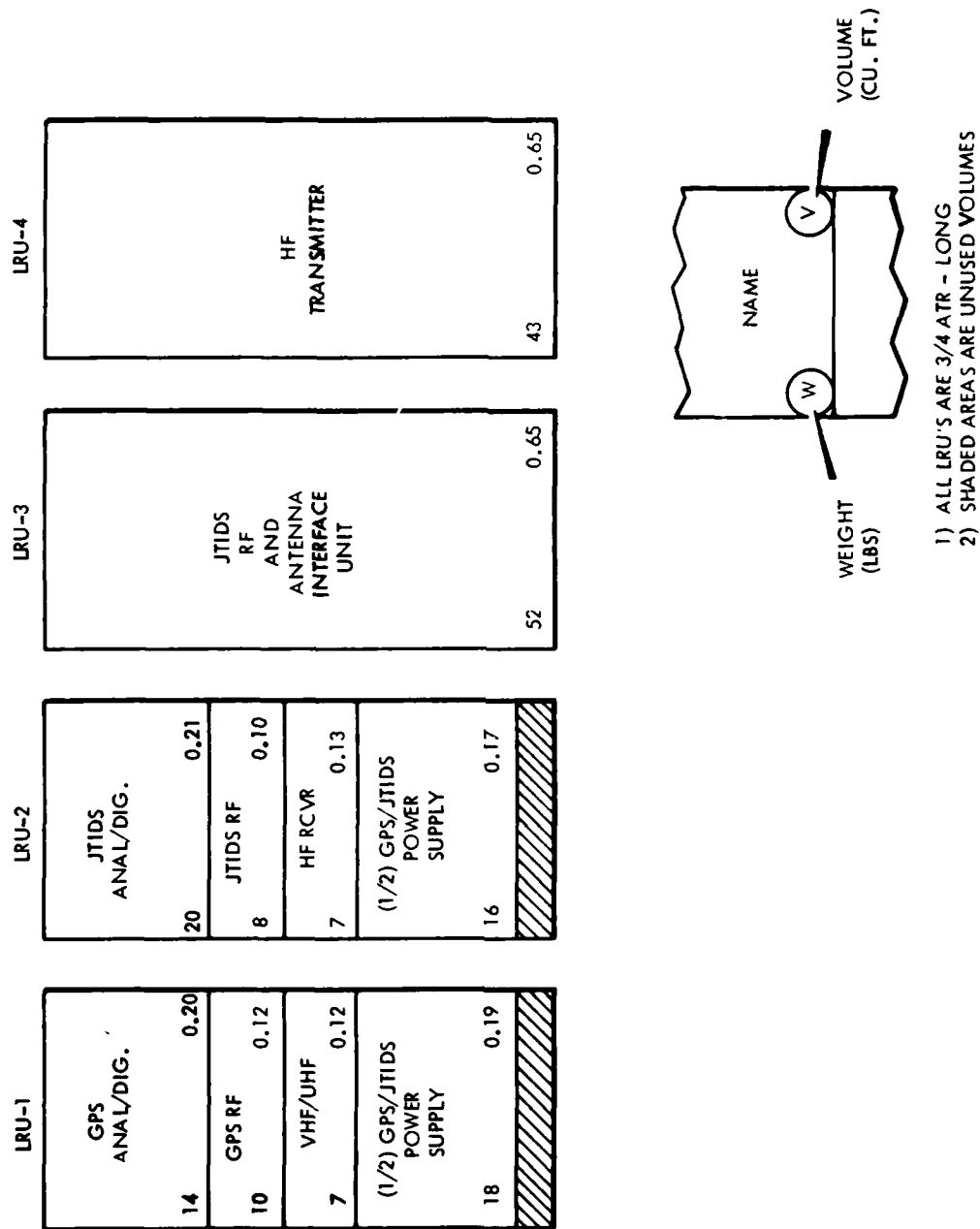


Figure 6. MFBARS architecture no. 3  
physical description

### 2.2.1 Architecture No. 1

MFBARS architecture No. 1 was designed to provide a low risk approach to system integration which was not critically dependent upon new or unique technology. Particular use was made of evolving integrated monolithic RF circuitry such as integrated IF amplifiers and "receiver-on-a-chip" phase locked demodulation devices where applicable. Time-sharing was incorporated to the maximum extent possible consistent with the constraint that performance was not to be degraded. The issue of commonality was exploited in this architecture to the maximum extent possible within the bounds of other assumptions or constraints.

The issue of timesharing is a very fundamental consideration for integrated systems. By its very nature it maximizes the utilization efficiency of existing hardware. Analysis of operational requirements in conjunction with adaptive timesharing concepts showed that a set of four identical, frequency agile receivers would satisfy all operational requirements in the 30-400 MHz VHF/UHF band. It was also shown that the HF requirement in the 2-30 MHz band would best be satisfied by a dedicated (non-integrated) receiver. The HF requirements associated with bandwidth, tuning and antenna matching were sufficiently unique that it was not reasonable to integrate HF with VHF/UHF. At most, only about a 5 percent savings would result, not enough to justify HF redesign and development as part of an integrated configuration.

Figure 7 is a block diagram of MFBARS architecture No. 1 for the HF and VHF/UHF receivers. The HF receiver is a conventional HF design. The VHF/UHF receiver would up-convert to 1300 MHz and then down-convert to 110 MHz (see Figure 8). At this point the IF frequencies would be the same and common circuitry could be used for further signal processing. This common circuitry would consist of phase-locked demodulators similar to the "receiver-on-a-chip" type devices presently under development. The outputs of the receivers would be provided to an array of communication and navigation signal processors through the data/control distribution subsystem. A real time control processor would control the time-shared operation of the receivers in such a way as to be responsive to mission requirements, operational priorities, and the nature of the jamming environment.

(Not shown in Figure 7 are two multiband VHF/UHF transmitters and a single HF transmitter of relatively conventional design.)

Figure 9 is a block diagram of the L-band receiver portion of MFBARS architecture No. 1. All receivers are down-conversion superheterodyne designs. For commonality, a

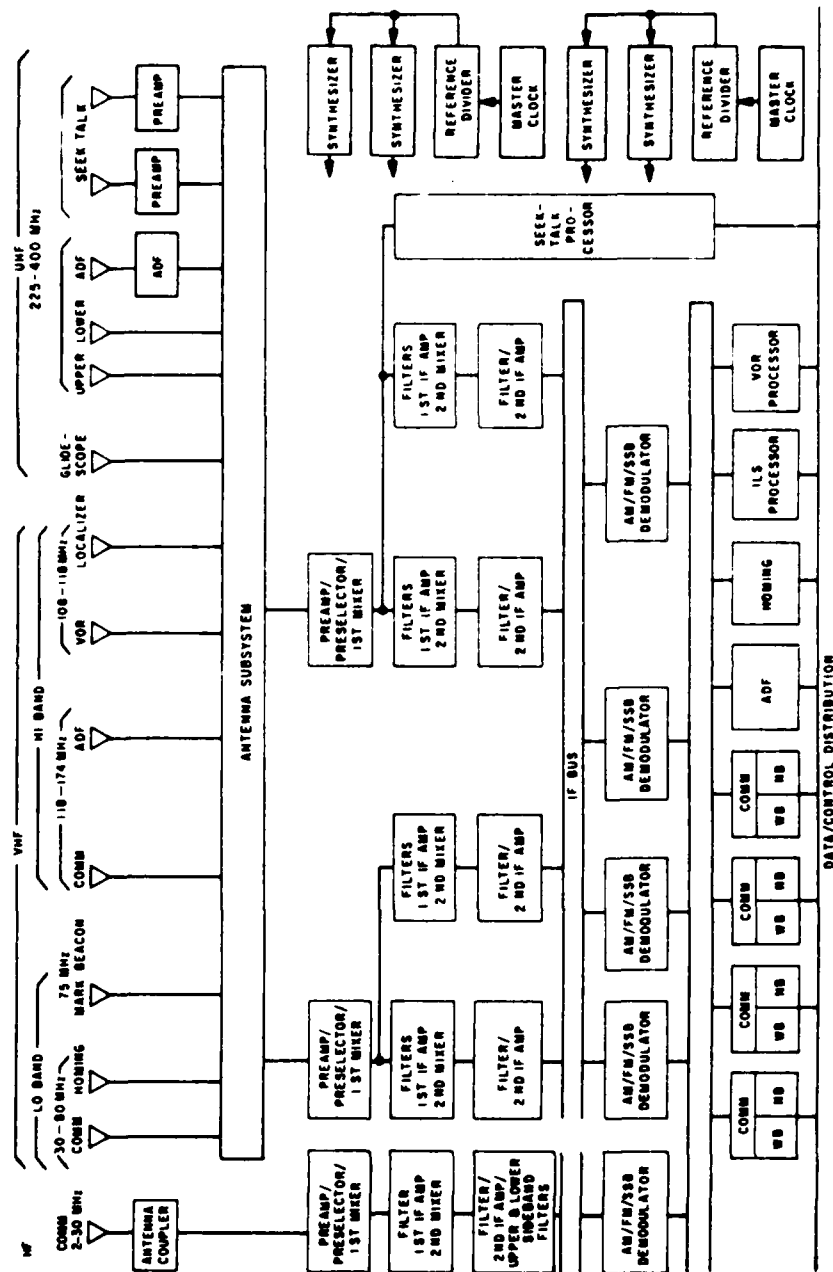


Figure 7. MFBARS architecture no. 1,  
HF and VHF/UHF receivers

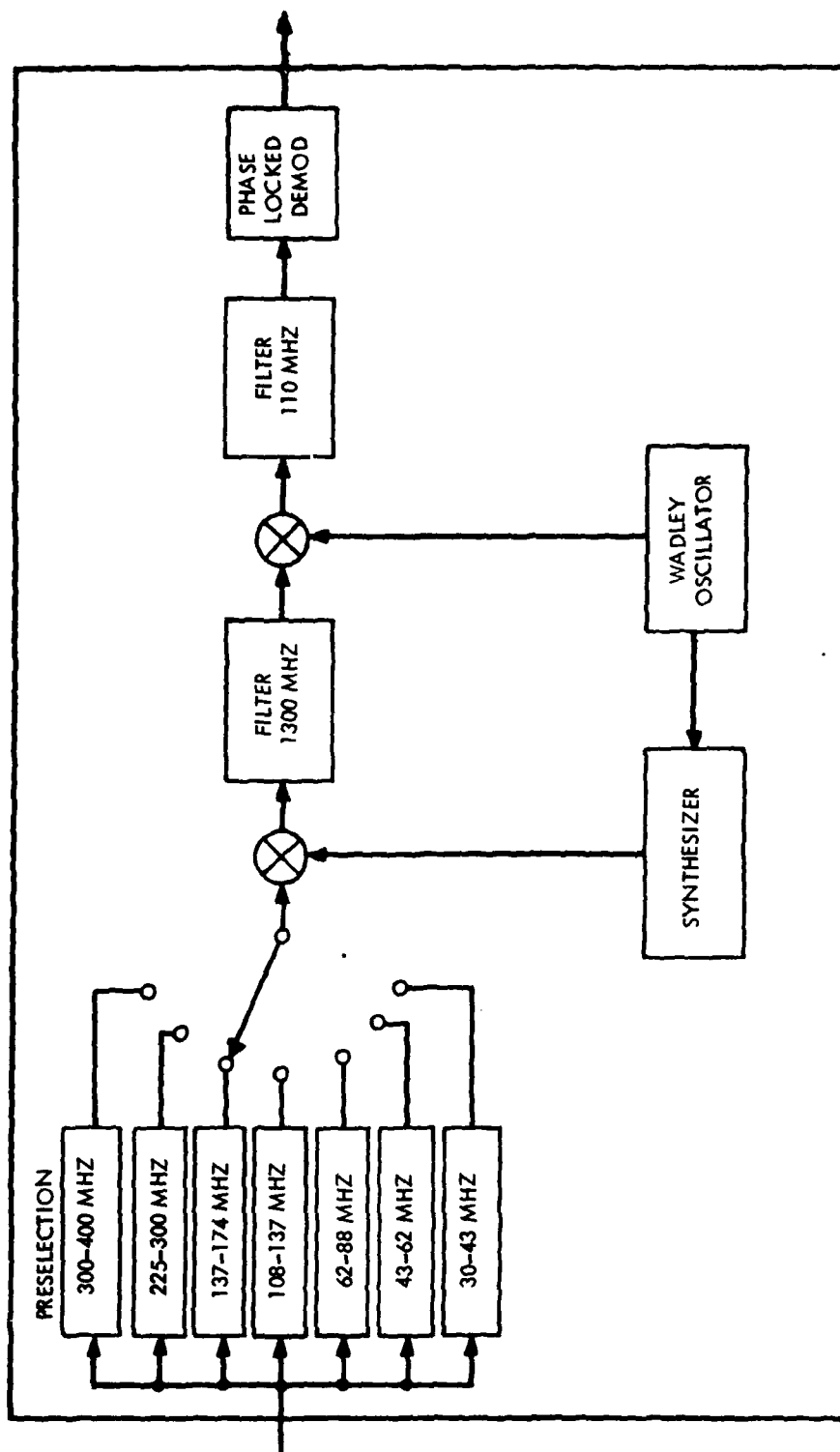


Figure 8. 30-400 MHz receiver

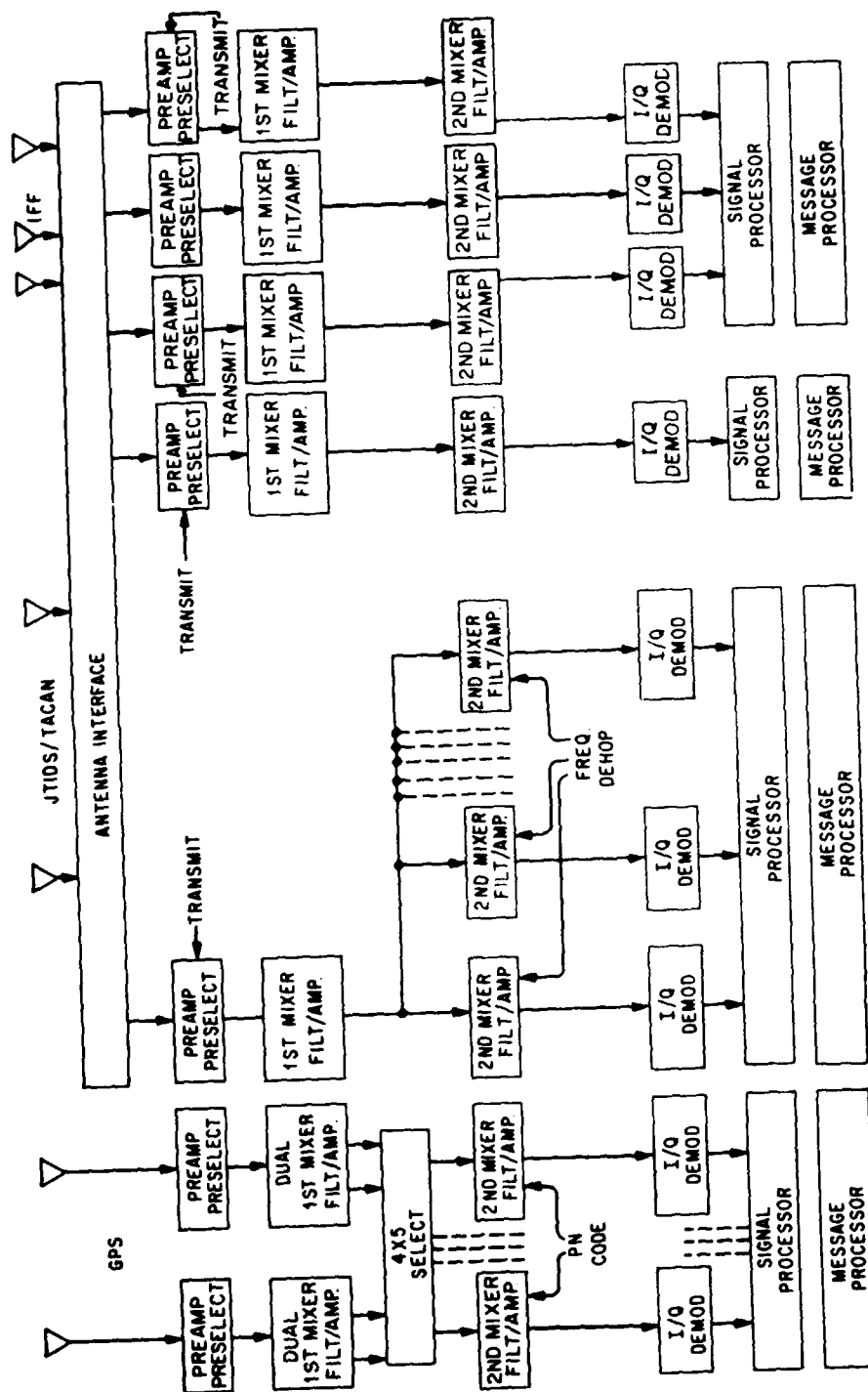


Figure 9. MFBARS architecture no. 1, L-band receiver and processing subsystems

common IF frequency of approximately 110 MHz is derived at the output of the second mixer.

Common integrated devices are employed for demodulation as they were for the 2-400 MHz band. Aside from this commonality, there is very little difference from this architecture and the baseline. There are several reasons for this situation which are described in the following paragraph.

The L-band systems which contribute the most to the overall complexity of the system (GPS and JTIDS) are still under development and incorporate the latest system and component technology. Using conventional system approaches to redesign these systems results in very little improvement. Conventional time-sharing as an approach to integration is not productive because it results in some performance degradation. Performance degradations are unavoidable for conventional time-sharing designs because 1) GPS employs a continuous (CW) signal structure and any interruption represents signal power loss, and 2) JTIDS (ATDMA/TDMA) requires eight receivers to be dedicated full time over the range uncertainty time of approximately 2 msec for processing the sync preamble to a message.

Also included but not shown in Figure 9 is a single L-band transmitter. All the L-band systems requiring a transmit capability are pulsed and can be combined in a single L-band time-shared transmitter.

#### 2.2.2 Architecture No. 2

MFBARS architecture No. 2 represents a medium risk system approach. Some moderate device technology development and advanced signal processing techniques development would be required, particularly within the L-band portion of the system. MFBARS architecture No. 2 would utilize sophisticated Surface Acoustic Wave (SAW) technology for filters, oscillators and correlators. Some applications of the SAW devices would represent new and powerful signal processing techniques which would permit (non-conventional) time-sharing of system hardware resources, without performance degradation.

There was no change in the HF receiver, HF transmitter or VHF/UHF transmitters in architecture No. 2.

The block diagram of the VHF/UHF receiver subsystem is shown in Figure 10. This subsystem consists of four receiver channels grouped into two dual receivers. Each dual receiver shares the majority of synthesizer and preselection hardware. The synthesizer is a tree structured SAW



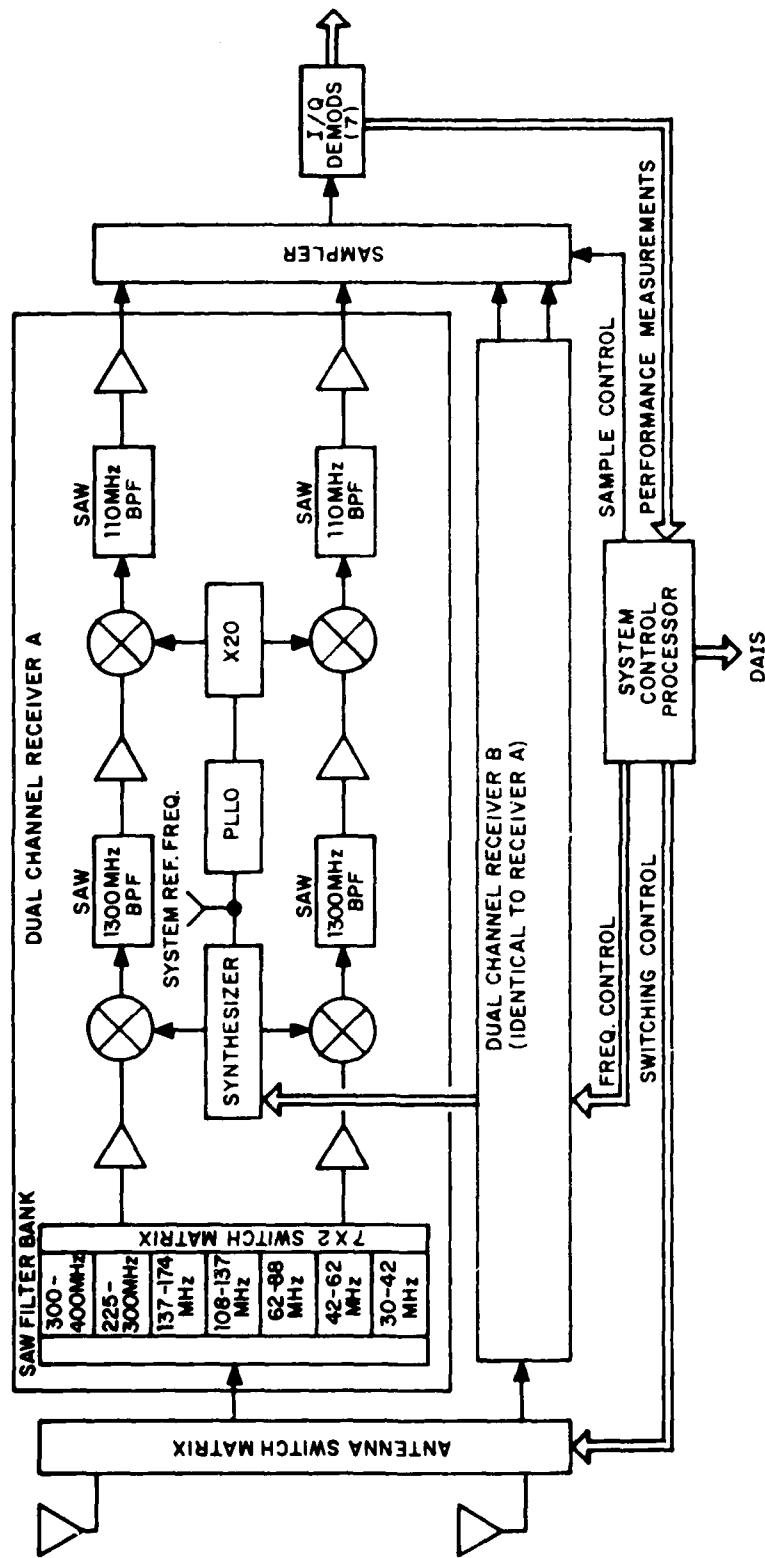


Figure 10. MFBARS architecture no. 2, VHF/UHF receiver

synthesizer using SAW comb filters and switched filter banks to select a desired local oscillator frequency. The synthesizer uses a single acoustic substrate with independent frequency selection switches for each of the dual output lines. The preselectors use the same principle, that is, a single substrate and dual switches for the outputs. A common SAW substrate theoretically could have been used for all four receiver channels; however, this would have been undesirable from a reliability standpoint.

The preselector filters are fabricated using SAW technology and are semi-octave in bandwidth. The design is an up-converter with a first IF frequency of 1300 MHz. A SAW device is again selected (due to its very small size) as a filter providing approximately a 3 MHz IF bandwidth. After a second stage of frequency conversion to 110 MHz, the system is essentially the same as MFBARS architecture No. 1. The outputs of the four receiver channels are provided to demodulators in a time-shared sampled sequence under the direction of the system control processor. A real time adaptive time-sharing algorithm, as in MFBARS architecture No. 1, is utilized for control.

The L-band portion of MFBARS architecture No. 2, shown in Figure 11, makes use of new device and system technologies. The major innovation is a device called a "universal correlator" which is capable of processing any one at a time of several different types of spread spectrum signals. The spread spectrum signals may have various modulation formats such as BPSK (for GPS) or CPSM (for JTIDS). Furthermore, even though SEEK TALK is a UHF-band spread spectrum signal, by up-converting to L-band, it could be processed by the same "universal correlator".

Nine L-band channels would be required for MFBARS architecture No. 2, eight for worst case JTIDS requirements (ATDMA/TDMA signal acquisition and sync), and one channel to be shared with other spread spectrum signals on a time-shared basis. Normally, ATDMA/TDMA JTIDS would not require all eight allocated worst case channels and other spread spectrum signals could use some of the allocated JTIDS channels; also, DTDMA/TDMA JTIDS, if selected by the Government as the final JTIDS configuration, would require only four channels maximum for signal acquisition and sync, which would either free some of the allocated channels for other spread spectrum signals or would permit a reduction in the number of channels required for the system.

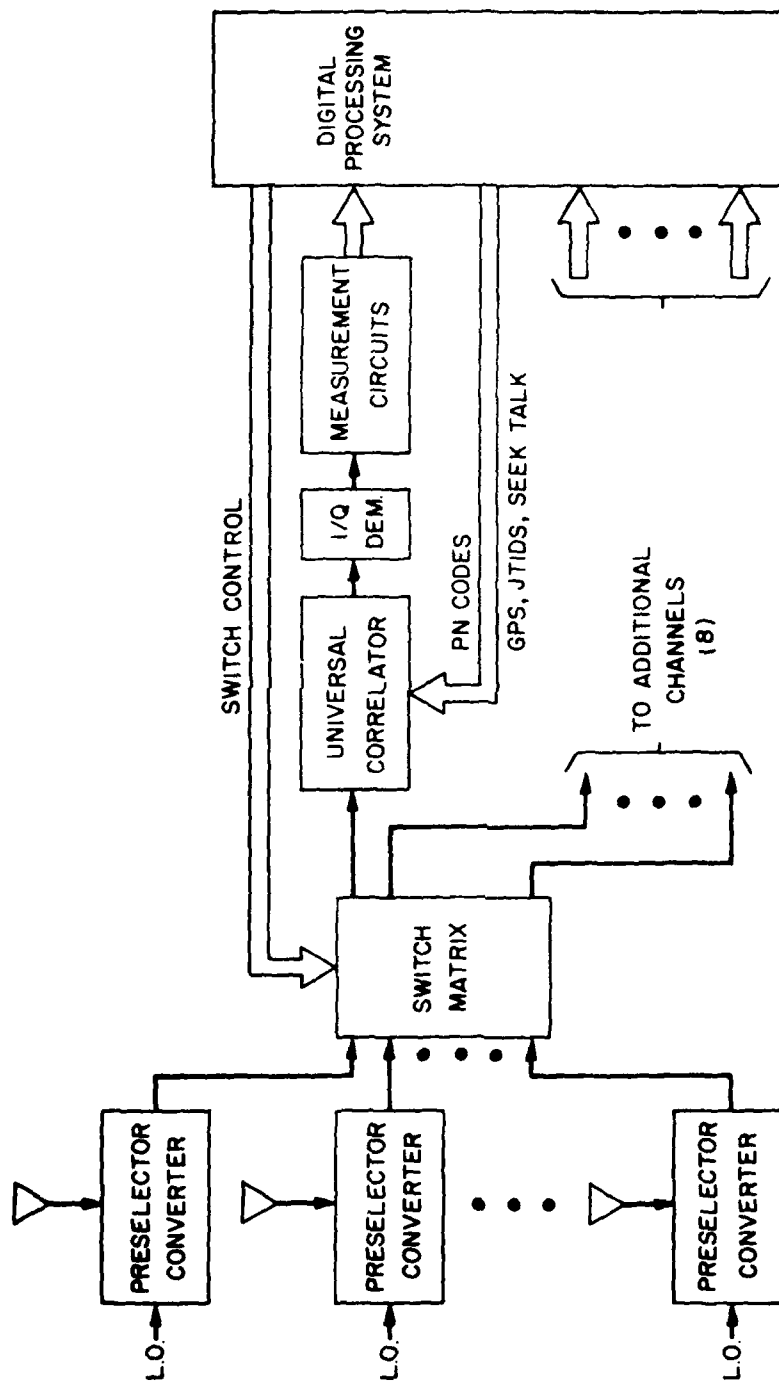


Figure 11. MFBARS architecture no. 2, L-band receiver and processing subsystems

Each channel would have its own "universal correlator". The universal correlator would be an advanced technology tapped delay line device, utilizing either SAW correlator or CCD correlator techniques, with processor-controlled switching of correlator reference signals, as required for each specific signal of interest.

All nine channels would be identical and would be under the control of an adaptive time-sharing algorithm. By comparison to L-band MFBARS architecture No. 1, the total number of receiving channels could be reduced from 17 to 9, with no loss in performance. Furthermore, since all channels would be identical and under software assignment control, processor-controlled resource reassignment would enable "fail soft" system degradation in the event of failure.

### 2.2.3 Architecture No. 3

MFBARS architecture No. 3 is intended to be the most powerful design in terms of performance and ultimate cost and size reduction. As such, it also represents the design with the highest degree of risk.

In analyzing the cost distribution of modern electronic systems such as JTIDS and GPS it can be determined that the majority of system costs reside in the RF area. RF assemblies cost from two to three times as much as analog or digital assemblies of approximately the same size. From this we may conclude that if a potential new design is to be cost effective it must exploit new concepts in RF signal processing.

A particular complication in JTIDS is the fast frequency hopped signal structure used to achieve improved A/J performance. This feature requires the use of a fast frequency hopping synthesizer for which considerable research and development effort has been expended in recent years. Before the input signal is dehopped, the bandwidth is large and particular care must be exercised in the design with regard to dynamic range and spurious responses.

MFBARS architecture No. 3 was an attempt to overcome some of the aforementioned problems in a cost-effective manner.

Many classical problems of radio design could be greatly simplified if very narrow-band (preferably information bandwidth) filters could be realized at RF frequencies. By placing such a filter in the signal path as close to the

antenna as possible, adjacent channel interference rejection and cross modulation distortion could be improved, and the design of the remaining radio system required to process the signals could be greatly simplified.

MFBARS architecture No. 3 uses new devices called "agile transversal filters" (ATF's). There are two forms of these devices used in the system, a wideband agile transversal filter (WBATF) and a narrowband agile transversal filter (NBATF). The WBATF filter forms a highly agile preselection filter which directly reduces an RF input bandwidth from approximately 400 MHz to as narrow as 5 MHz (which is the spectrum bandwidth of a JTIDS pulse). The filter is capable of switching tuning frequencies in the order of 6 nsec. This rapid tuning feature allows a single WBATF to scan a selected set of frequencies (for example eight ATDMA/TDMA JTIDS sync burst frequencies) all within the total delay time of the tapped delay line of the WBATF. Since the WBATF performs parallel integration of the signal over the total filter delay time, all time segments of all selected frequencies are processed with no degradation in signal to noise ratio (as long as the cycle time through the frequencies is less than the total delay time of the filter). The WBATF is described in detail in section 3.4.1 and in Appendix A.

The NBATF is essentially the same as the "universal correlator" described previously as part of architecture No. 2. It is described in detail in Section 3.5.3.

Figure 12 is a simplified block diagram of MFBARS architecture No. 3. The design is conceptual in nature and many alternative variations centering around the WBATF's are possible. HF is not integrated because, as has been mentioned previously, integration of HF with the other bands is not cost effective. There are two WBATF's in architecture No. 3, one for L-band signals and one for VHF/UHF. Each of these bands is approximately 400 MHz in total RF input bandwidth. Switching allows either band to be processed by either WBATF. This provides redundancy for "fail soft" system performance in the event one WBATF should fail.

It should be noted that, since the WBATF's are just entering development and since their ultimate performance characteristics and cost performance variables are not known, several optional system implementations of the WBATF are under consideration. At one extreme, the WBATF would be used for selection of all signals in a band (JTIDS, TACAN, GPS, IFF for L-band; SEEK TALK, and conventional narrowband comm and nav channels



in the VHF/UHF band). The other extreme would use the WBATF for only some of the MFBARS signals (basically non-fixed frequency signals, such as JTIDS and TACAN in the L-band); other signals (basically fixed frequency signals such as GPS and IFF) would be selected by fixed frequency bandpass filters rather than the WBATF's. There are technical merits to both extremes and also for some intermediate points. The best implementation approach cannot be determined until WBATF development work, starting in late 1980, proceeds far enough to provide WBATF performance characteristics and cost data required for system level tradeoff decisions. Therefore, the current MFBARS system design concepts include a range of WBATF implementation alternatives as feasible system design options. A final system level decision will be made after device performance characteristics and limitations are better known and final tradeoffs can be made between optional WBATF designs and other optional elements of the overall system design.

As shown in Figure 12, the outputs from the WBATF's (and/or from fixed frequency bandpass filters for any fixed frequency signals which may not be processed by the WBATF), are frequency-translated by a baseband converter to a "zero-IF" baseband frequency prior to further signal processing by narrowband ATF's (NBATF's). In the case of spread spectrum signal samples (GPS, JTIDS, SEEK TALK), the NBATF's then provides correlation (also referred to as PN code stripping) so that baseband information can be recovered. Following recovery of baseband information, each selected signal is then processed as appropriate in digital and/or analog processors.

In addition to achieving a significant reduction in RF hardware, architecture No. 3 meets another objective, the elimination of the need for an expensive agile frequency synthesizer to de-hop the JTIDS signal. The JTIDS signals are transmitted on pseudo-randomly selected frequencies spaced 3 MHz apart, and each frequency is a harmonic of 3 MHz. Since the signal has been passed through a narrow-band filter, the noise is well correlated within time intervals corresponding to a 3 MHz rate.

Therefore the signal can be sampled at that rate without significant S/N degradation. And since the signal frequency is some harmonic of 3 MHz, successive samples maintain a consistent phase relationship regardless of the frequency. An example will help illustrate this point. If a JTIDS frequency of 999 MHz is selected, there are exactly (except for Doppler offsets which are small) 333 cycles of this frequency in one cycle of three MHz. If the next lower JTIDS frequency of 996 MHz were selected, then there would

be exactly 332 cycles in one cycle of 3 MHz. In other words there is always an integral number of cycles of a JTIDS frequency in a 3 MHz period, and therefore, successive samples at a 3 MHz rate have a constant phase relationship. Actually, there are other aspects of this problem which may require higher sampling rates than 3 MHz. But in this case, sampling at integer multiples of 3 MHz can be used at the price of some increased complication with respect to the phase relationship between successive samples.

## 2.3 COMPARISON OF (PHASE I) CANDIDATE SYSTEM ARCHITECTURES

There were several criteria for comparing each candidate MFBARS architecture with the baseline. These included:

- development cost
- unit cost of production
- LCC savings
- volume savings
- weight savings
- operational flexibility
- growth capability
- technical risk

Figure 13 provides a graphical presentation of the benefits projected for each MFBARS architecture, compared to the baseline.

The figures from which the bar charts were constructed are tabulated in Table 5.

The increased savings with successive architectures is related to technology. Each successively higher performance architecture requires acceptance of successively greater technology risks in order to obtain the projected increase in system benefits. Later sections of this report describe details of the technology and technology development plans required for architecture No. 3, the architecture selected by the Government for detailed study.



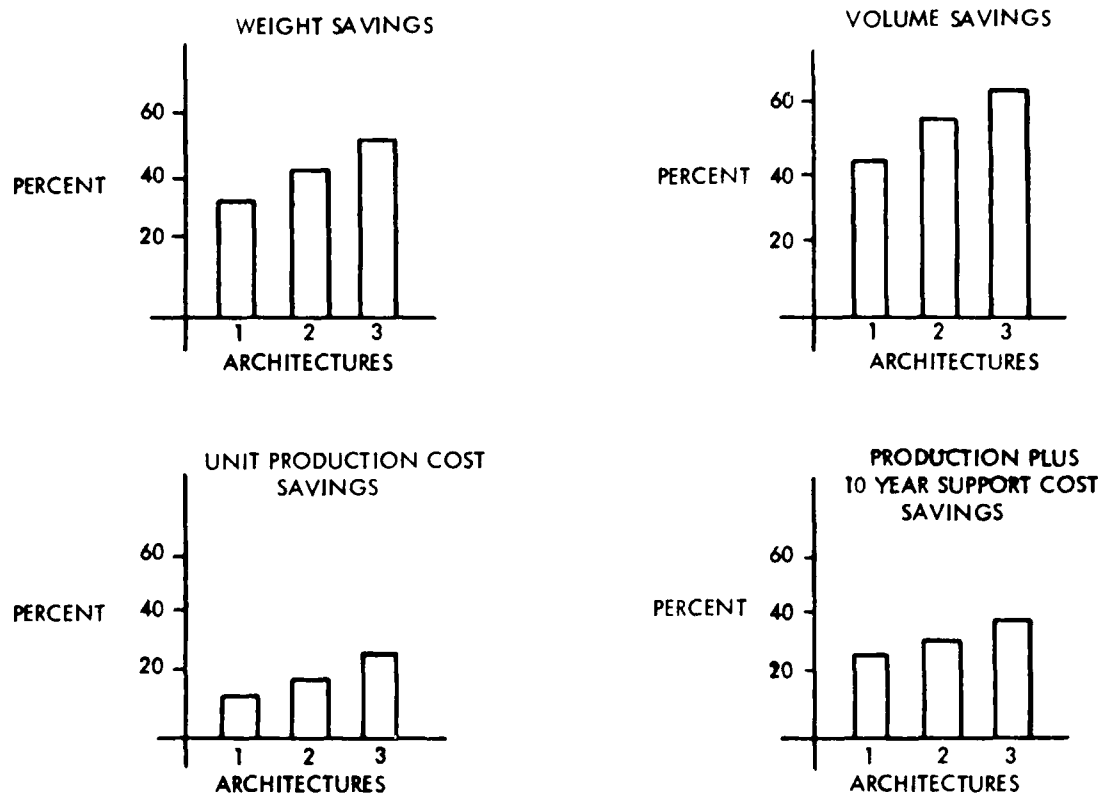


Figure 13. Projected MFBARS benefits for each candidate system architecture, as compared to baseline

TABLE 5. MFBARS PHASE I CANDIDATE ARCHITECTURES COMPARED TO PHASE I BASELINE

	Phase I Baseline	MFBARS No. 1	MFBARS No. 2	MFBARS No. 3
Weight	420#	290#	253#	215#
MFBARS Savings	-	31%	40%	49%
Volume	7.0 cu.ft.	3.9 cu.ft.	3.3 cu.ft.	2.6 cu.ft.
MFBARS Savings	-	44%	53%	63%
Unit Prod Cost (1050 units)	\$200K	\$176K	\$168K	\$152K
MFBARS Savings	-	12%	16%	24%
Prod Cost (1050 units) Plus Support Costs (10 years)	\$302M	\$231M	\$221M	\$203M
MFBARS Savings	-	24%	27%	33%

### 3. DETAILED DESCRIPTION OF THE DESIGN OF THE SELECTED MFBARS ARCHITECTURE

Of the three candidate architectural approaches to MFBARS, the third, which was the most sophisticated approach, was chosen for further study during Phase II. This architecture offered the greatest potential cost and size savings for an integrated system. Further design refinements during Phase II substantiated the previously projected savings in volume, weight and cost. In addition, further relative savings were realized by the net effect of eliminating the HF function from the baseline and adding AFSATCOM and SINGARS. Details are provided in Sections 3.8 (physical description) and 5.0 (cost analyses).

A detailed description of the theory of operation, design tradeoffs, and recommended implementation for the selected architecture is presented in the remainder of this section.

#### 3.1 AIRCRAFT INTERFACES

A top level block diagram of the electrical interfaces between MFBARS and other aircraft systems is shown in Figure 14. MFBARS performs all the required radio functions on the aircraft. Non-digital (e.g., audio) information interfaces with the aircraft intercom system. Digital data interfaces with the Digital Avionics Information System (DAIS) which in turn interfaces with the cockpit controls and displays and with other aircraft systems (INS, weapon system and fire control computers, etc.) There is also a direct interface between the Inertial Navigation System (INS) and MFBARS for some signals (e.g., high speed tracking loops).

#### 3.2 OVERALL SYSTEM BLOCK DIAGRAM

Figure 15 shows the MFBARS top level block diagram.

The Antenna Subsystem consists of antenna elements, antenna selection switches and antenna coupling circuitry. The antenna elements may be either conventional antenna elements or adaptive antenna arrays, depending on the specific type of aircraft. Adaptive antenna array concepts are still under evaluation. One is a conventional multi-band self-contained adaptive array, with minimum control signal and RF interfaces with the rest of MFBARS. The other is a more highly integrated design concept in which portions of the RF subsystem hardware would be shared with the antenna array processor to achieve a higher degree of total system integration. These concepts are explored in more depth in Section 3.3.

The RF Subsystem consists of receiver RF front ends, including the Wide Band Agile Transversal Filters (WBATF's),

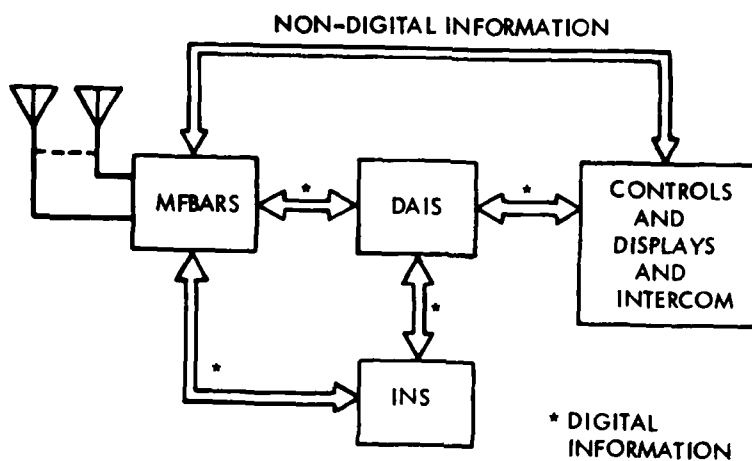


Figure 14. Interface of MFBARS with other aircraft systems

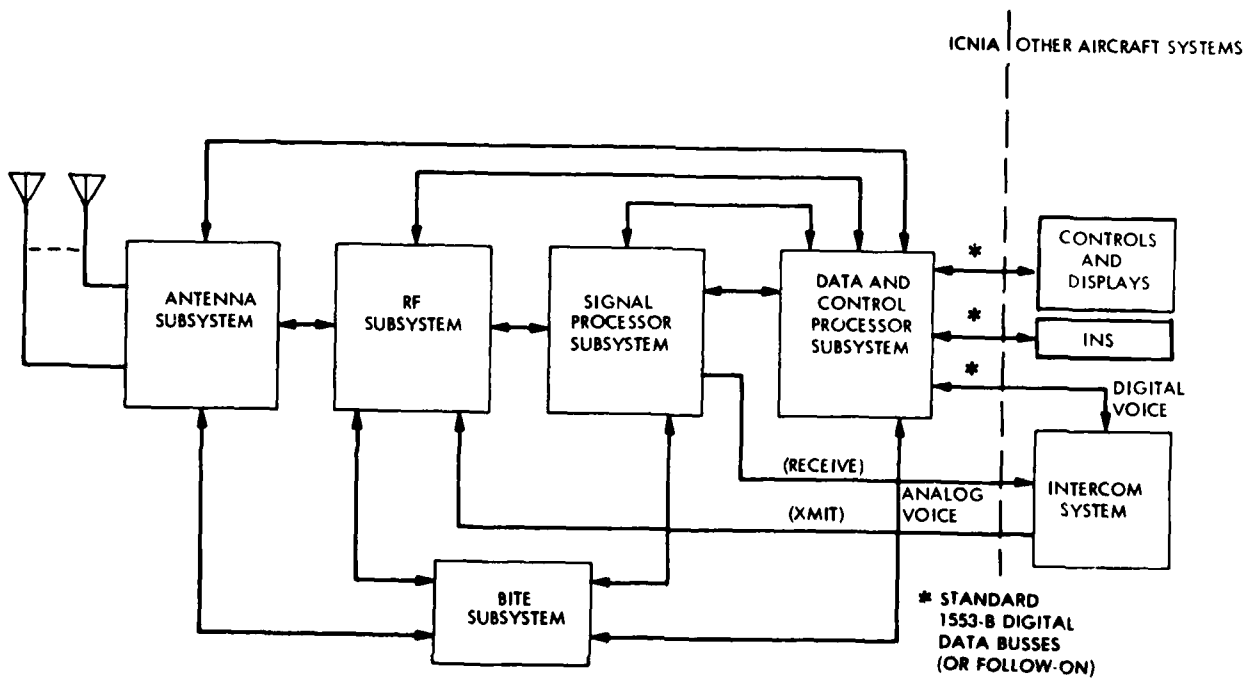


Figure 15. MFBARS top level block diagram

plus three transmitters. Details are discussed in Section 3.4.

The Signal Processor Subsystem contains baseband converters, a Narrow Band Agile Transversal Filter (NBATF) Assembly, a signal switching network, code generators, and special purpose dedicated signal processors. Details are discussed in Section 3.5.

The Data and Control Processor Subsystem consists of a dynamically reconfigurable multiprocessor array, modularized main memory (in which is stored all system operating programs and the system data base), internal and external input/output devices (I/O's), and an interconnection structure. Details are discussed in Section 3.6.

The BITE Subsystem is a processor-controlled built-in test subsystem for testing, monitoring and evaluating system health. It contains analog and digital test signal generators and analog sensors and digital logic for determining whether the system is operating within performance limits, and for fault-isolation in the case of detection of out-of-limit performance. The BITE Subsystem can provide inputs to the Data and Control Subsystem for in-flight system reconfiguration in the event of detected failures. Details are discussed in Section 3.7.

### 3.3 ANTENNA SUBSYSTEM

Figure 16 is a simplified block diagram of the Antenna Subsystem. Each of the blocks in this figure is discussed in greater detail in the subparagraphs of this section.

Since MFBARS must operate with both conventional antennas and with adaptive antenna arrays, both options are discussed. Section 3.3.1 addresses conventional antennas and antenna couplers for MFBARS. Section 3.3.2 then addresses adaptive arrays for MFBARS.

#### 3.3.1 Conventional Antenna Elements and Antenna Coupling Network

Figure 17 shows a block diagram of the Antenna Subsystem with conventional antennas and antenna coupling elements. (Note that this block diagram shows separate GPS and IFF signals. This is for the system design option in which GPS and IFF interrogator signals are not processed by the WBATF's, as discussed in section 2.2.3. For the alternate system option, GPS and IFF signals would be part of the channel A and/or B outputs.)

Figure 18 shows nominal antenna element locations on a typical tactical aircraft for conventional antennas. It

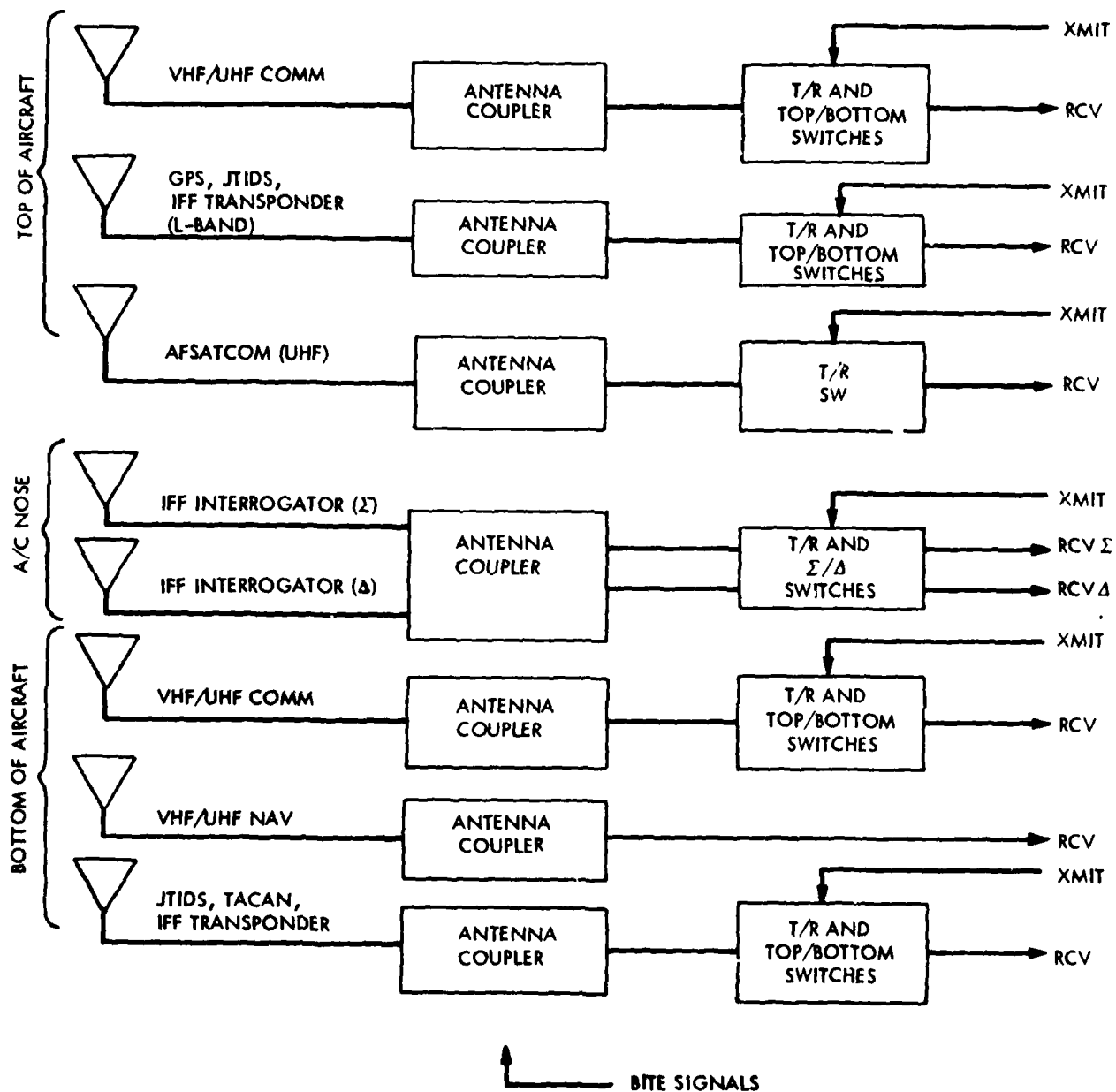


Figure 16. Antenna Subsystem

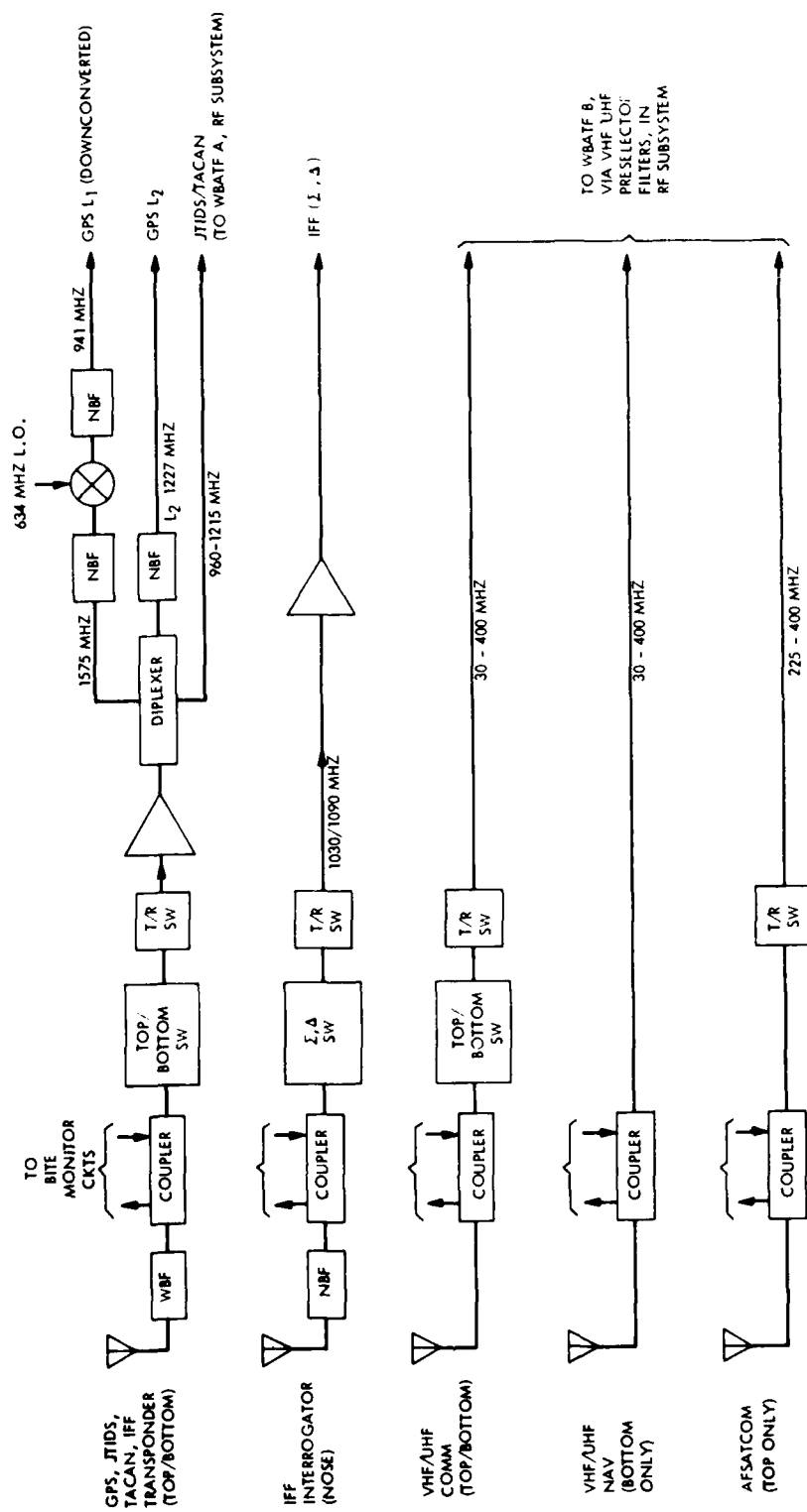


Figure 17. Block diagram of conventional antenna elements and antenna coupling system

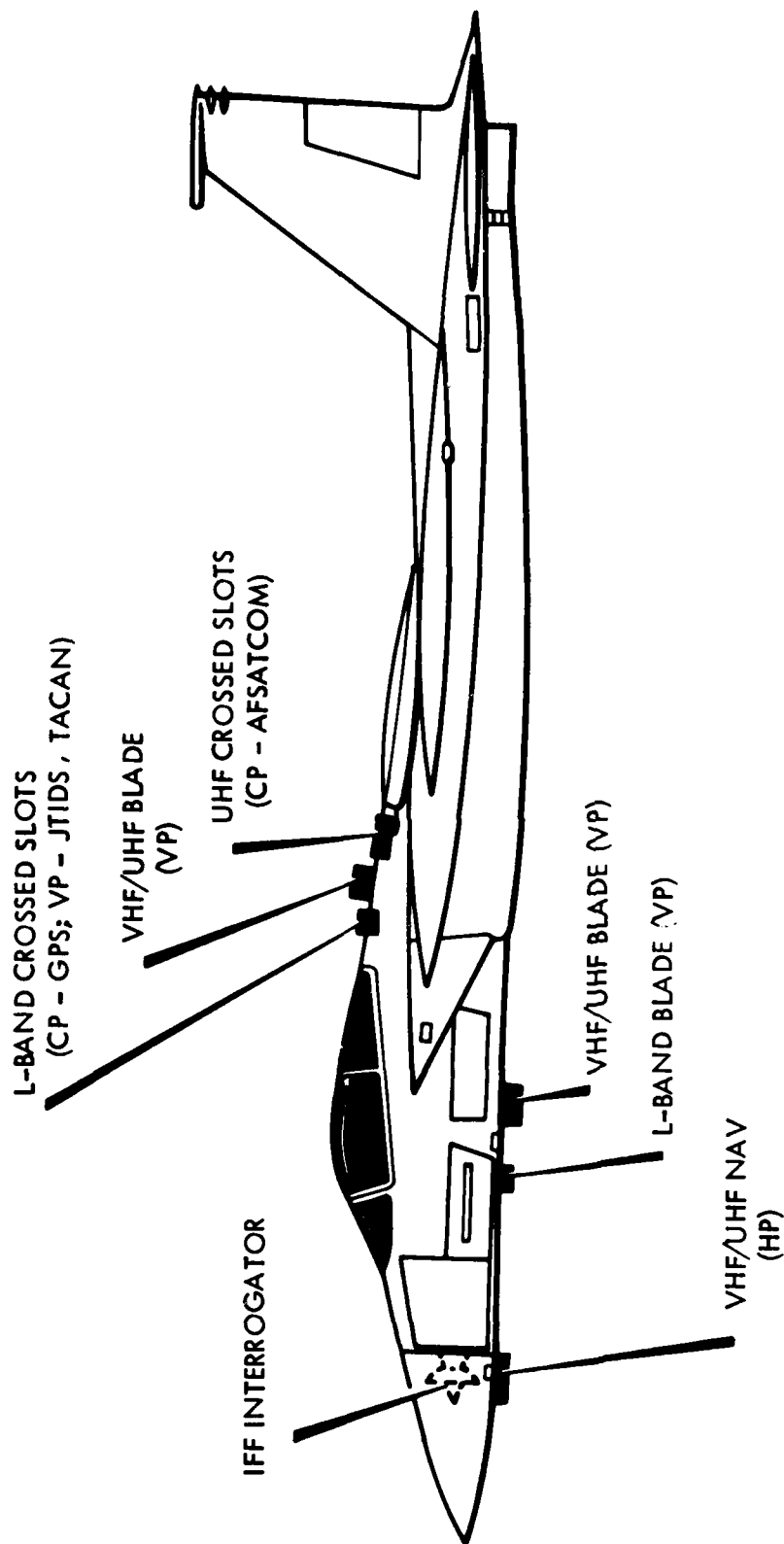


Figure 18. Nominal antenna locations,  
conventional antennas

should be emphasized that these are nominal locations only, for discussion purposes; final selection of antenna locations for a specific aircraft must take into account specific electrical, mechanical, aerodynamic, and logistics requirements.

Three antennas are located on top of the aircraft: (1) an L-band antenna for GPS, JTIDS, TACAN and the IFF transponder; (2) a VHF/UHF antenna for VHF/UHF communications, and (3) a UHF AFSATCOM antenna. The IFF interrogator antenna is co-located with the radar in the nose of the aircraft. Three more antennas are located on the bottom of the aircraft, one each for L-band and for VHF/UHF communications as on top, and another (horizontally polarized) VHF/UHF antenna for navigation functions, including VOR, localizer, glideslope and marker beacon.

A description of each of the antennas and the signal flow through the coupling network is presented for each of the radio functions served.

#### 3.3.1.1 GPS

The GPS antenna, located on top of the aircraft, consists of a pair of crossed slots designed to receive circular polarization over as much of the upper hemisphere as possible. The polarization is circular near the zenith direction, for GPS signals operating in the L1 (1575 MHz) and L2 (1227 MHz) bands, and deteriorates to vertical polarization near the horizon for both GPS and JTIDS signals in the 960 to 1215 MHz band. For a flush mounted, or low profile antenna, the presence of the aircraft skin prevents achieving good circular polarization from any antenna element at low elevation angles, i.e., near the horizon. If greater antenna gain were required at low angles for either GPS or JTIDS, an additional linearly-polarized, monopole-type antenna could be added.

The received signal from this antenna is coupled to a bandpass filter covering the 960 to 1585 MHz band. Directional couplers sample the forward and reflected waves for BITE test and monitoring purposes. The signal is then coupled through a circulator and T/R switch and on to a diplexer. The diplexer splits the GPS L<sub>1</sub>, GPS L<sub>2</sub> and JTIDS signals into three separate channels as shown. (Unless the alternate system option is selected, in which the WBATF processes GPS signals, as well as JTIDS.) The L<sub>1</sub> signal is then narrowband filtered, amplified and mixed down to 941 MHz. The L<sub>2</sub> signal is narrowband filtered, amplified and connected directly to a switching matrix.



### 3.3.1.2 JTIDS/TACAN

The JTIDS and TACAN functions, are served by the L-band antenna on top of the aircraft (described above) and by a separate L-band antenna on the bottom. The bottom L-band antenna is a vertically polarized monopole type with omnidirectional coverage in azimuth. The signal from each antenna is filtered, sampled and preamplified in a similar manner to the GPS L<sub>1</sub> signal. The preamplifier has a noise figure of 3 dB, and 20 dB gain for a range of input signal levels from -95 to 0 dBm. The signals from the top and bottom antenna are combined in a linear combiner, as shown, to form a single output (channel A). The linear combiner is a switch which selects either the top or the bottom antenna, whichever has the stronger signal. If a feedback signal is generated, the signals can be adaptively weighted and combined in such a way as to maximize the total signal.

The same radiating elements are used for JTIDS transmissions. The signal from the transmitter is switched to either the top or bottom antenna, depending on which received the stronger input signal. The T/R switch and circulator provide the necessary isolation between the transmitter and receiver.

### 3.3.1.3 IFF Transponder and Interrogator

IFF transponder signals are received and transmitted through the same antennas and circuitry as for the JTIDS signals described above.

IFF interrogator signals (if part of the aircraft mission functions) are transmitted and received through separate antennas as shown in Figure 17. These antennas are co-located with a radar in the front of the aircraft.

### 3.3.1.4 VHF/UHF Communications

All of the VHF/UHF communication signals are vertically polarized and are received on the top and/or bottom wideband antennas. These are identical monopole-type antennas designed to radiate an omni pattern over the frequency band from 30 to 400 MHz. The signals are coupled directly to the VHF/UHF preselector where they are switched through a filtering matrix and preamplified. A detailed description of the VHF/UHF preselector is given in Section 3.4.2.

#### 3.3.1.5 AFSATCOM

The UHF AFSATCOM system is served by a crossed slot antenna located on top of the aircraft. The antenna is essentially a scaled version of the GPS antenna, designed to radiate circular polarization over most of the upper hemisphere. The received AFSATCOM signal is coupled to the VHF/UHF preselector.

#### 3.3.1.6 VOR/Localizer/Glideslope/Marker Beacon

Since the VOR/Localizer Glideslope and Marker Beacon functions all utilize horizontal polarization with coverage in the lower hemisphere, all will be served by a common antenna. The antenna output is switched to the appropriate filter bank in the preselector and amplified and filtered in the same manner as the VHF Comm signals.

#### 3.3.1.7 Antenna Coupling Network

The Antenna Coupling Network will be fabricated with a combination of technologies including microwave integrated circuits (MIC), thick film hybrids (TFH) and discrete components. A diagram illustrating a proposed breakdown of the various components by the circuit technology used to fabricate them is given in Figure 19. The symbols identify the type of construction and the numbers within the symbols are keyed to the listing of the component functions. The numbers in parenthesis give an estimate of the circuit area for each component. The total board area for the circuits shown is 10 inches by 12 inches. This assumes the MIC circuits are fabricated from a high dielectric constant material such as Epsilon 10 or Duroid 6010.

The coupling network will probably be divided into several separate modules, but the final breakdown will depend on the particular installation. For good electrical performance, it is desirable to locate all components through the first amplifier stage as near as possible to the antenna, to minimize cable losses and RF pickup. However, from a packaging standpoint, it is desirable to locate all of the circuits together in one module. Consequently, compromises will be required, based on each specific installation requirement.

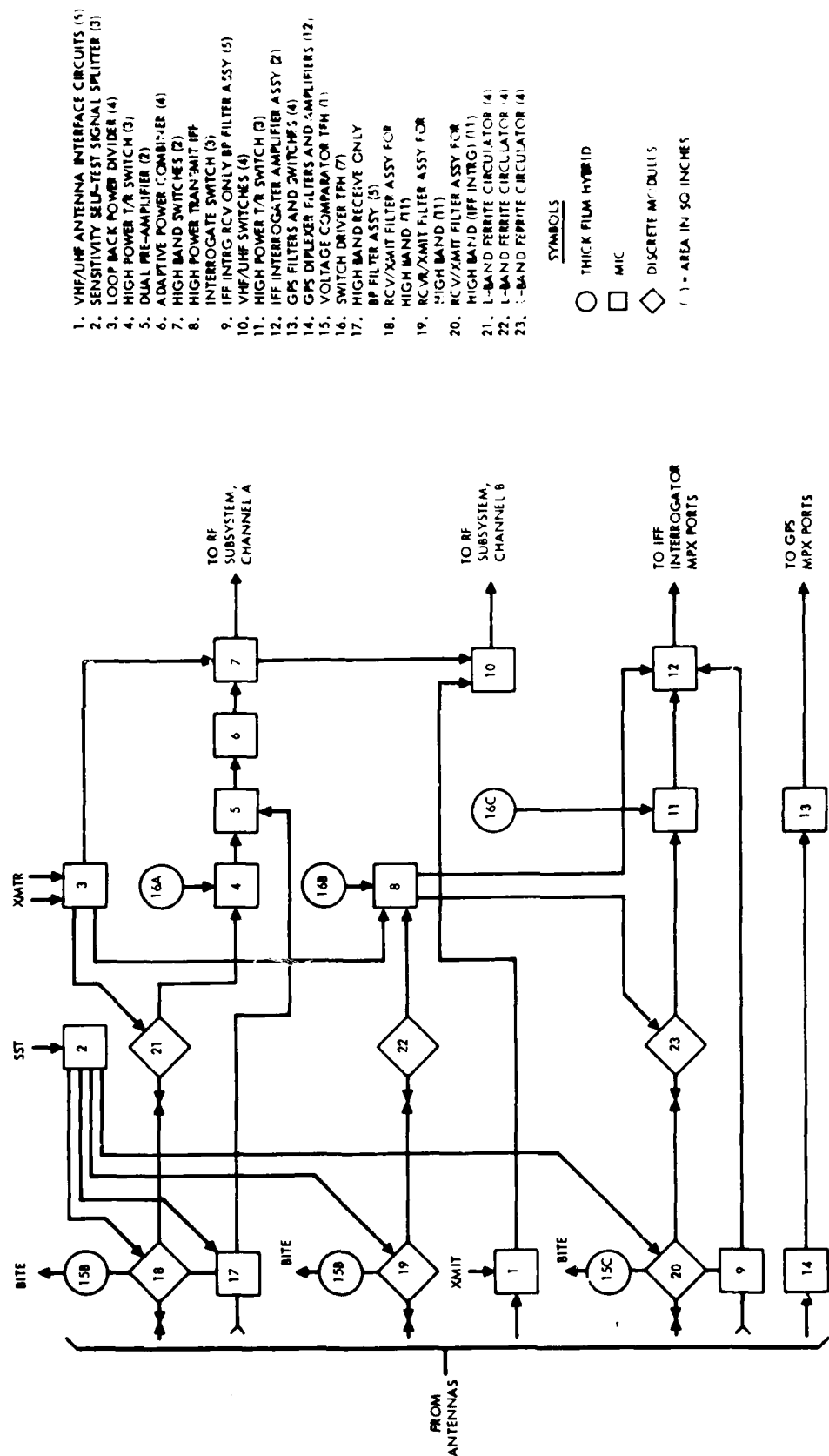


Figure 19. MFBARS antenna coupling network

### 3.3.2 Adaptive Antenna Arrays

Some MFBARS-equipped aircraft will have adaptive antenna arrays for additional anti-jam (AJ) protection of spread spectrum signals. (GPS, JTIDS, SEEK TALK). The antenna array design effort has not been completed; at present, there are three basic approaches under consideration:

- separate stand-alone arrays for each spread spectrum signal
- integration of arrays with each other, but no integration between array hardware elements and other MFBARS hardware elements
- integration of the arrays with each other, plus integration of some array processor elements with other MFBARS processor hardware elements

The first two approaches are the subject of other Air Force contracts, both in-being and planned. (In-being for the RADC-sponsored SEEK TALK program, and planned for the AFWAL-sponsored Adaptive Multi-Function Antenna (AMA) program, which will address integration of GPS and JTIDS in the initial phase and of all CNI functions in a later phase.) The third approach has been addressed to date only in context of this MFBARS study. At this point in time, no final conclusions have been reached on the best of the three approaches for MFBARS. This will have to be resolved in a future phase of the MFBARS program. The following paragraphs describe current status for each of the three basic approaches under consideration.

#### 3.3.2.1 Separate Arrays for Each Spread Spectrum Signal

Table 6 summarizes basic adaptive antenna array requirements for each of the three spread spectrum signals. Figure 20 shows a top level block diagram of interfaces with other elements of MFBARS.

The separate array approach would be the most demanding, in terms of aircraft integration, and would not provide any opportunity for cost savings through integration of antenna or antenna processor hardware elements. However, it would represent the lowest technical risk.

#### 3.3.2.2 Partial Array Integration

Figure 21 illustrates a concept for partial array integration, through sharing of common antenna elements and use of time-sharing techniques in a common weight control and timing system.

TABLE 6. ADAPTIVE ARRAY REQUIREMENTS

<u>Operational capabilities</u>	<u>Null Bandwidth</u>	<u>Potential Discriminants</u>
GPS	● 20 MHz at both Frequencies Simultaneously	● Power Inversion
- 1227.6, 1575.42 MHz		● LMS with Spread Spectrum Reference
- Upper Hemisphere		● Known Direction of Arrival
- Circular Polarization		● Sidelobe Canceller
JTIDS	● 3 MHz Frequency Hopper	● Look Ahead to Next Channel
- 960 - 1215 MHz	● Alternative is Entire Band	● Weight Storage
- Omnidirectional	● Avoid Tacan/DME Nulls	● Known Direction of Arrival
- Linear Polarization		
SEEK TALK	● 10 MHz Channels	● Power Inversion for Acquisition
- 225 - 400 MHz		● LMS with Summed Reference
- Omnidirectional		
- Linear/Polarization		

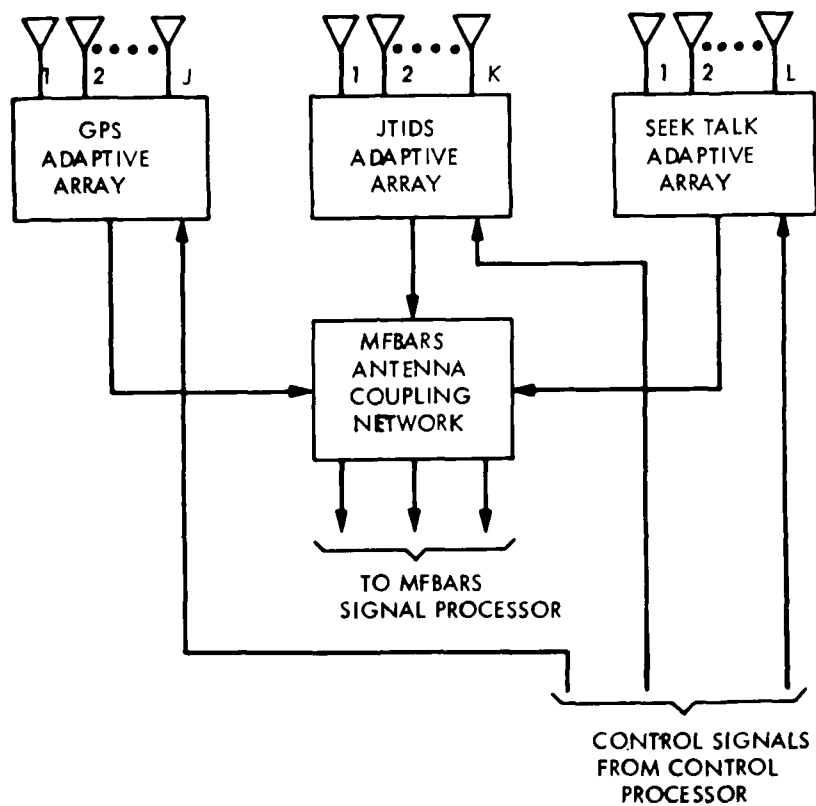


Figure 20. A non-integrated approach to adaptive arrays

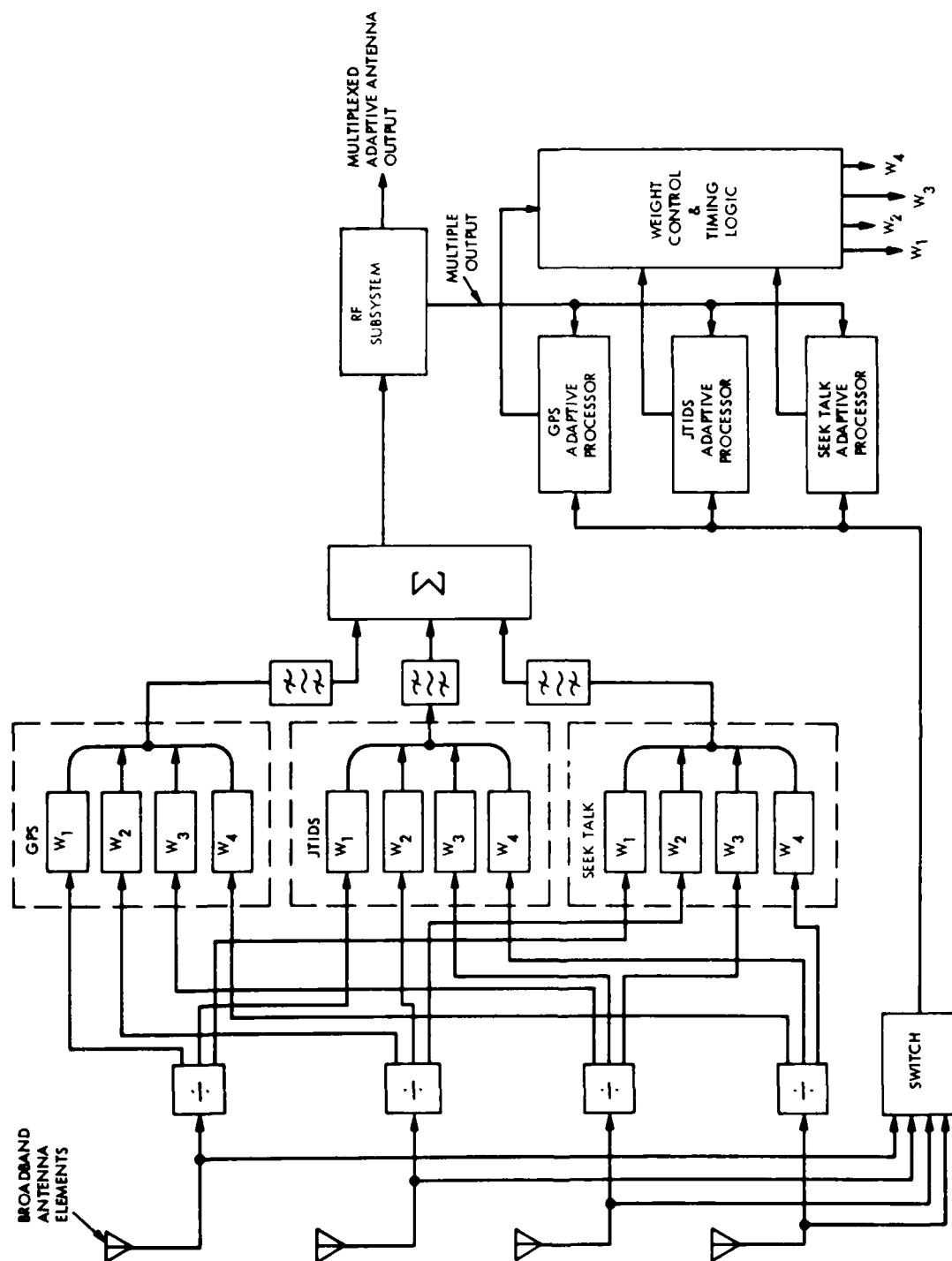


Figure 21. Partially integrated adaptive antenna array

Figure 22 illustrates a concept for integration of the antenna elements. There would be two such arrays on the aircraft, one on the top and one on the bottom.

In order to provide improved anti-jam performance, each array must be capable of spatial filtering of one or more undesired signals in each band of interest. This requires each part of each array to function as an adaptive null steering array. The number of undesired signals which can be steered into a null is one less than the number of independently controlled elements in a given array. For purposes of this concept, the number of elements per array has been selected as 5, so that up to 4 interference signals from different directions can be rejected.

The next element of this partial integration concept is the amount of commonality of antenna elements which can be used for the three different spread spectrum signals (SEEK TALK, GPS, JTIDS). Optimum design of an adaptive array utilizes element spacing of approximately one half a wavelength, in order to avoid a multiplicity of grating nulls. The range of wavelengths for the signals of interest is from 19 to 133 cm. Some compromises are therefore required.

The two extremes of commonality are:

- (a) Use 5 antenna elements common to all three functions.
- (b) Use a separate group of 5 antenna elements for each of the 3 functions, resulting in 15 antenna elements for each array.

Extreme (a) is undesirable because the array cannot even approach the optimum element spacing for all three functions simultaneously.

Extreme (b) is undesirable because of complexity and cost.

For the proposed concept, an array configuration of 11 elements was selected. As shown in Figure 22, optimum spacing is closely approached for the GPS and JTIDS functions, and for the high frequency end of the SEEK TALK function. In this configuration, four of the elements (2, 3, 5 and 7) are common to two functions. The aircraft surface area required for this configuration is essentially the same as would be required for the SEEK TALK array alone.



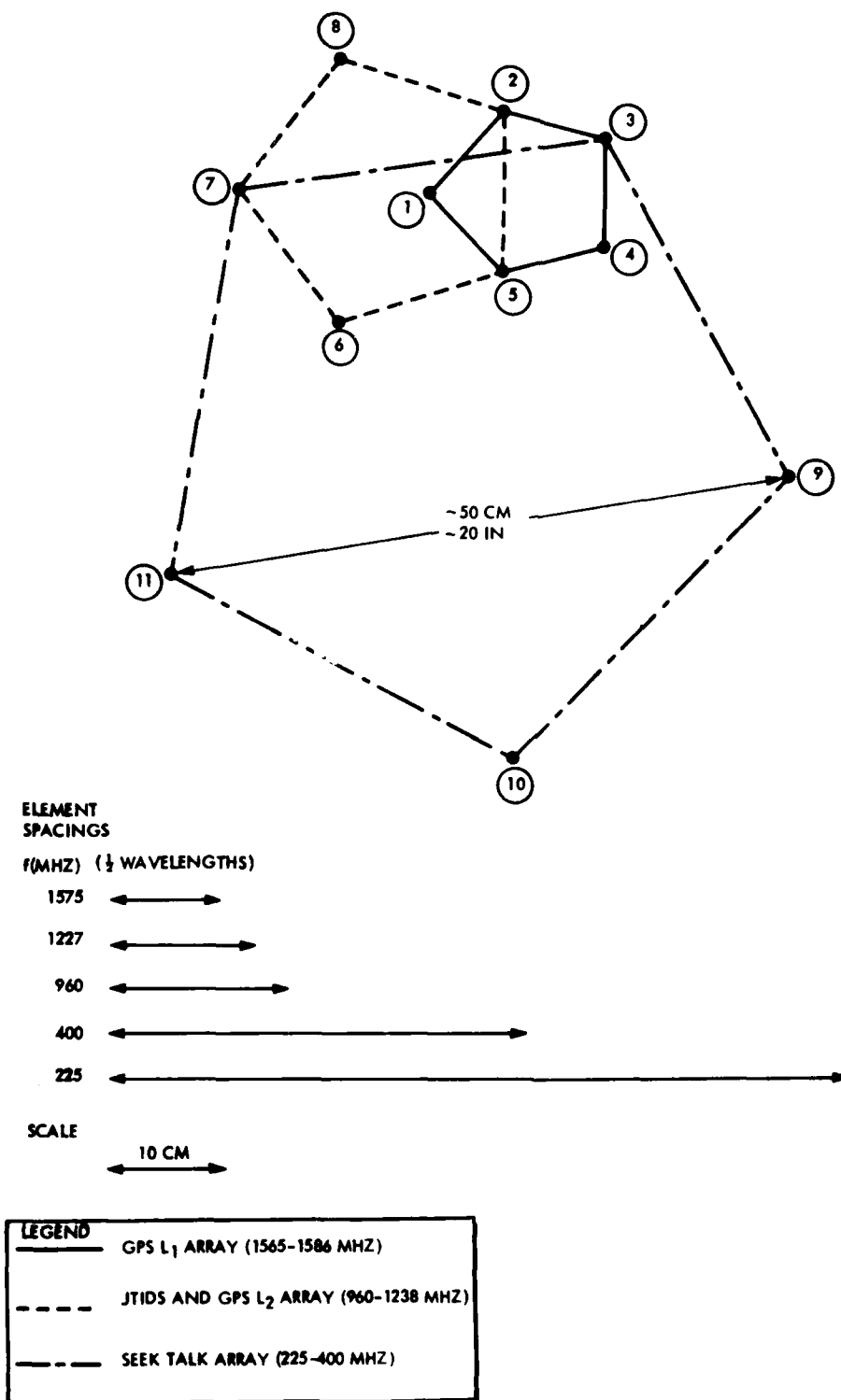


Figure 22. Eleven element array concepts

The jamming scenario requirements may be such that different numbers of jammers would exist in each of the three bands of interest. In that case, the configuration of Figure 21 could be modified accordingly. For example, if the SEEK TALK array were required to reject only two jammers instead of four, elements 9, 10 and 11 could be replaced by a single element, thereby materially reducing the surface area required for the array.

Polarization and element type of each element are matched to the signals. Crossed slots provide circular polarization toward the zenith for GPS and vertical polarization toward the horizon for GPS and JTIDS. Dual band blades provide coverage toward the horizon for vertically polarized SEEK TALK signals and GPS and JTIDS. Since GPS L<sub>2</sub> (1225 MHz) is directly adjacent to the JTIDS band (960 - 1215 MHz), we have chosen, for the proposed concept, to utilize the JTIDS array to receive the GPS L<sub>2</sub> signal.

Although the signals transmitted from the GPS satellites are all circularly polarized, the combination of CP and LP antennas is believed to provide the best overall coverage. For a flush mounted, or low profile antenna, the presence of the aircraft skin prevents achieving good circular polarization from any antenna at low elevation angles, i.e., near the horizon. Since an optimum satellite geometry for GPS navigation is to use one satellite at the zenith and the remaining three satellites at low angles, the combination of a CP antenna with good coverage up to zenith, and LP antennas with maximum gain near the horizon was selected.

For coverage in the downward direction, the elements of the array will be mounted on the bottom of the fuselage to provide coverage for vertically polarized signals coming from sources beneath the aircraft. The antennas will be dual band blades identical to the top mounted blades.

Narrowband UHF and L-band signals would use one or more elements of the UHF and L-band arrays, depending on the most effective interface. Narrowband VHF signals would require the same separate VHF antenna elements as described previously, as there is no VHF array.

The adaptive processors would employ individually tailored adaptive weight control algorithms. In the partially integrated implementation, dedicated weighting circuits would be required for continuous operation on all radio functions simultaneously. (See Section 3.3.2.4 for more detailed discussion.)

Time-shared adaptive weighting is not a trivial design problem. For example, if one considers JTIDS, one notes that the input signals to the weighting elements are wideband. While it is true that in the JTIDS data mode only one signal frequency at a time is received, in the ATDMA/TDMA JTIDS synchronization mode, eight frequencies must be received simultaneously. A single set of complex weights cannot produce nulls at all eight frequencies simultaneously. There are several solutions to this problem. One solution would be to replace the single complex weight by a tapped delay line and complex weight vector. Each element of the vector would then operate on an output tap of the delay line. In addition to the obvious increase in hardware complexity, the computation requirements would then become much more complex. Another approach would be to frequency dehop and narrowband the signals prior to weighting. However, in the ATDMA/TDMA JTIDS sync mode, thirty-two independent receivers (8 frequencies x 4 antennas) would be required, with complex weights at the output of each receiver. This approach would require much more hardware than the first approach. An advantage of this 32 receiver approach, however, is that by performing frequency selective filtering before weighting, the probability of an out-of-band jammer saturating the weighting elements would be reduced.

Further work is required before costs, risks, and benefits of the partial integration approach can be assessed and tradeoff design decisions made.

### 3.3.2.3 Full Array Integration

A third approach to adaptive arrays for MFBARS is still in the definition and evaluation stage. This approach would attempt to achieve the greatest possible overall system efficiencies by sharing of adaptive array and RF processing functions.

The antenna elements would be the same as described for the partially integrated concept; the differences would be in RF processor hardware and software, and in hardware and software interfaces with other elements of MFBARS. At this level of integration, conventional interfaces between antenna subsystem and RF subsystem would disappear and a new level of system integration would emerge. The major impact would be replacement of large portions of separate, conventional RF and adaptive array processor hardware with a unique integrated configuration.

This highly integrated concept is based on the use of a wideband agile transversal filter (WBATF) and agile tapped delay line weights (similar to WBATF's) for each antenna element, to allow simultaneous adaptive antenna array

processing and first stage spread spectrum RF processing, utilizing one common set of processor hardware elements.

Figure 23 illustrates the basic concept for this fully integrated approach. First, frequency filtering is provided by WBATF's. Then, spatial filtering is provided by null formation through adaptive weighting of the signals from each antenna element. Figure 23 shows the signals from each antenna element transmitted through a separate WBATF and weighting circuit and then combined in a common summing network. In principle, a single summing network is sufficient; however, in order to provide some redundancy for increased reliability, two separate combining networks would be used, as described later. The time multiplexed signal at the output of the summing network is divided into three separate channels in a demultiplexing circuit as shown. This permits independent processing of the JTIDS, GPS and SEEK TALK signals with algorithms optimized for the individual characteristics of each.

The unweighted signals ( $X_i$ 's) from each antenna element are picked off from the WBATF's, as shown, and then switched and demultiplexed for correlation with the weighted signal ( $Y$ ) from the summing network. The weight commands are derived in the array processor and then multiplexed prior to transmission to the weighting circuits. It should be noted that the basic MFBARS signal processing design requires high speed signal sampling. This must be taken into consideration in the design of an integrated RF processor/adaptive array processor.

Time multiplexing for the WBATF's and their associated complex weight circuits must be such that all input signals are sampled at a rate sufficient to retain all the data inherent in the received signals. Each sampling interval ( $T_s$ ), must be divided by a minimum factor of 12, in order to provide time-shared outputs for each of up to eight JTIDS channels for ATDMA/TDMA sync burst) along with two samples each for GPS and for SEEK TALK. The result is a switching rate interval of  $T_s/12$  of approximately 6 nsec. The time-sharing sequence is illustrated in Figure 24. Note, however, that even though the adaptive weights must be cycled (reprogrammed) at a high data rate (consistent with the sampling frequency), the adaptive processing circuitry can operate much more slowly, at a rate dictated by the relative motion between jammer and platform. This permits filtering and integration of the adaptive signals in the usual way.

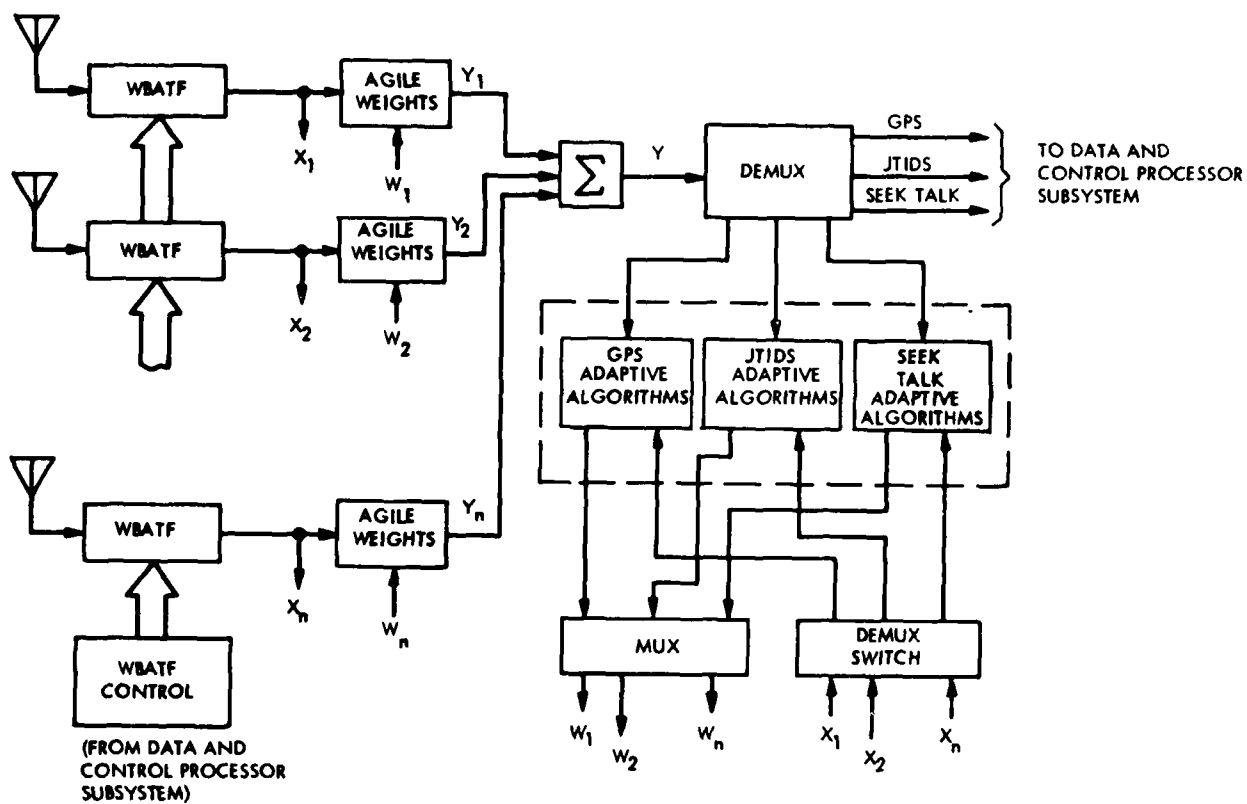


Figure 23. Integrated adaptive antenna array processor/  
spread spectrum RF processor

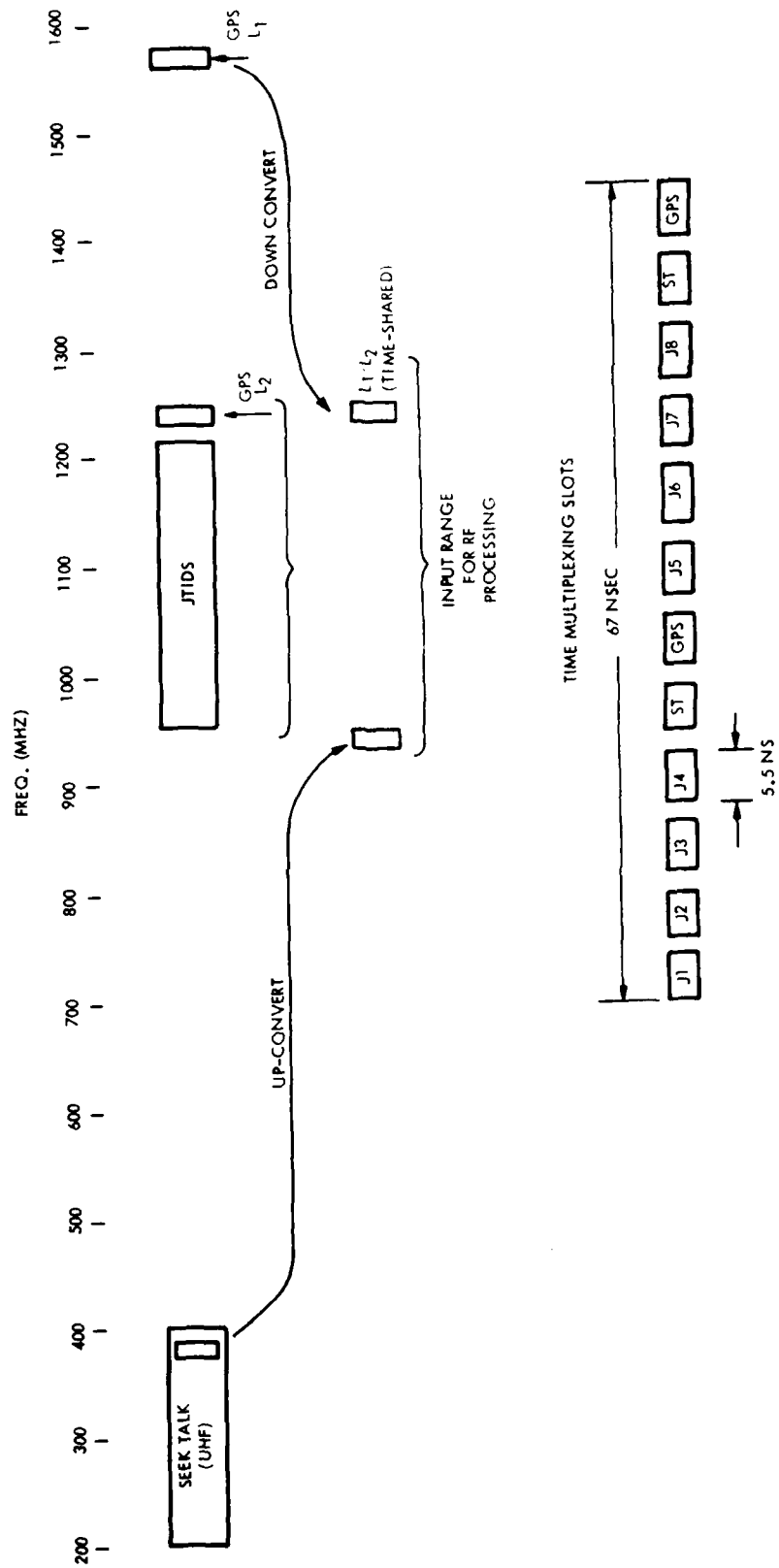


Figure 24. Time-sharing and up/down conversion for integrated processing

Also shown in Figure 24 is spectral up- and down-conversion of SEEK TALK and GPS L<sub>1</sub> signals. This is required for reasons of RF processor functional requirements rather than array processor functional requirements. (These RF functional processing requirements are described in this section, rather than in Section 3 which describes the basic RF processing approach, to aid in understanding the fully integrated concept).

In order to limit the bandwidth of the WBATF input signals to a reasonable number, some restructuring of the RF signal processing must occur. All wideband spread spectrum signals (GPS, JTIDS, SEEK TALK) must be combined to allow common processing by one set of WBATF's (with one WBATF per antenna element for any one selected array, at any point in time).

This requires up-converting the UHF SEEK TALK signal from UHF to 950 MHz, right below the lower end of the JTIDS band (960-1215 MHz) and down-converting the GPS L<sub>1</sub> signal from 1575 MHz to 1225 MHz, right above the upper end of the JTIDS band. Since the WBATF's have an input RF frequency bandwidth of 400 MHz, this bandwidth compression then allows processing of all three signals by only one WBATF per element per selected array.

Figure 25 (sheet 1 and sheet 2) shows a more detailed block diagram of this fully integrated concept, including the up and down conversions just described. Each antenna element of each array has an associated preamplifier, for establishing the system noise figure. For the case where an antenna element is part of more than one sub-array, a band separator (inverse of a diplexer) separates the various bands into multiple lines. Signals outside of the bands of interest are filtered out to prevent circuit saturation by out-of-band signals. For single band antenna elements, only a harmonic (semi-octave bandwidth) filter is required. For the L-band elements, the JTIDS and the GPS L<sub>2</sub> signals will be similarly separated, so that the L<sub>2</sub> signals can be processed separately.

Next, SEEK TALK (UHF-band) and GPS L<sub>1</sub> (1575 MHz) signals are up and down-converted respectively. The L<sub>1</sub> signals are down-converted from 1575 MHz to 1225 MHz using a fixed L.O. The SEEK TALK signals are up-converted by a controllable L.O. such that the resultant translated center frequency is at 950 MHz.

The control processor will select one at a time of either L<sub>1</sub> or L<sub>2</sub> signals for GPS processing. Note that the GPS signals, along with the JTIDS and the SEEK TALK signals, are all carried through in parallel for the upper and lower antenna arrays. This makes it possible for the control

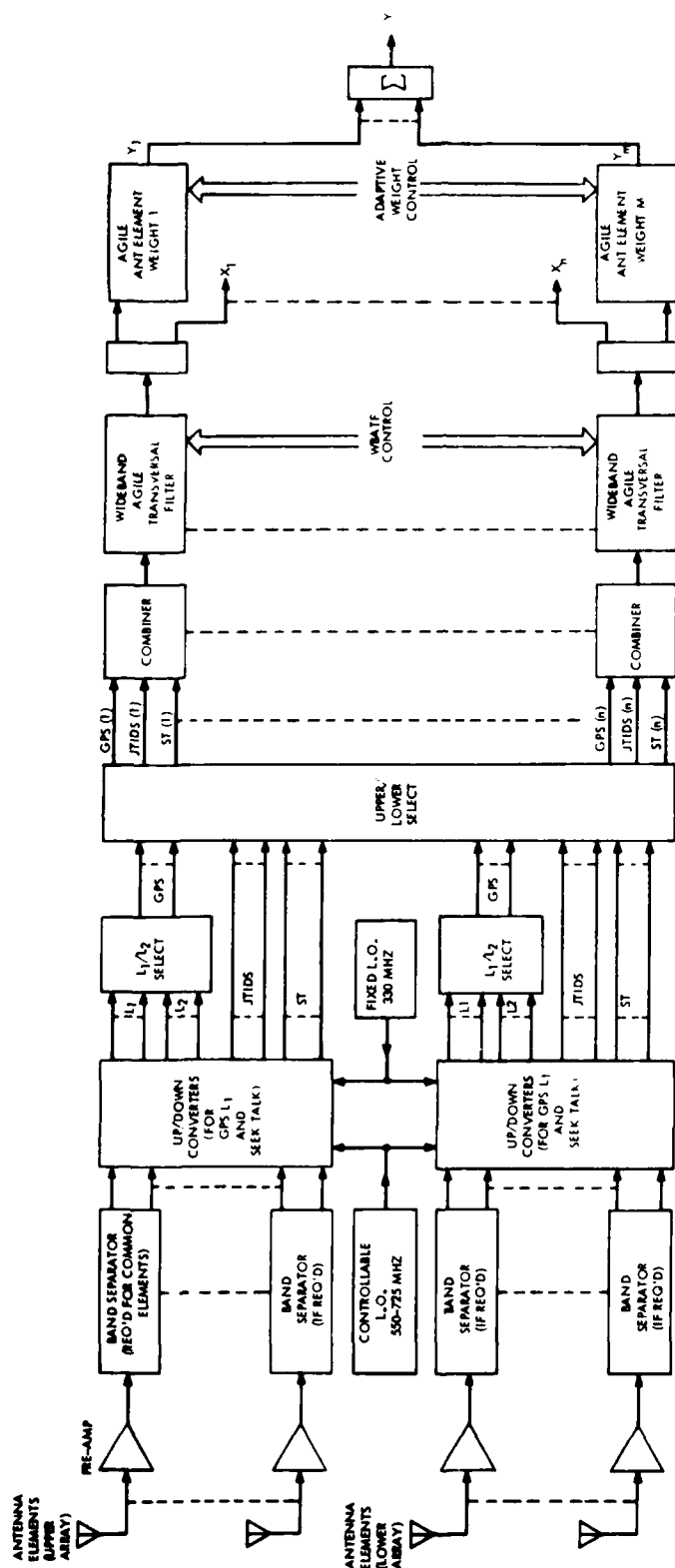


Figure 25. (Sheet 1 of 2) Integrated adaptive array processor/wideband RF processor



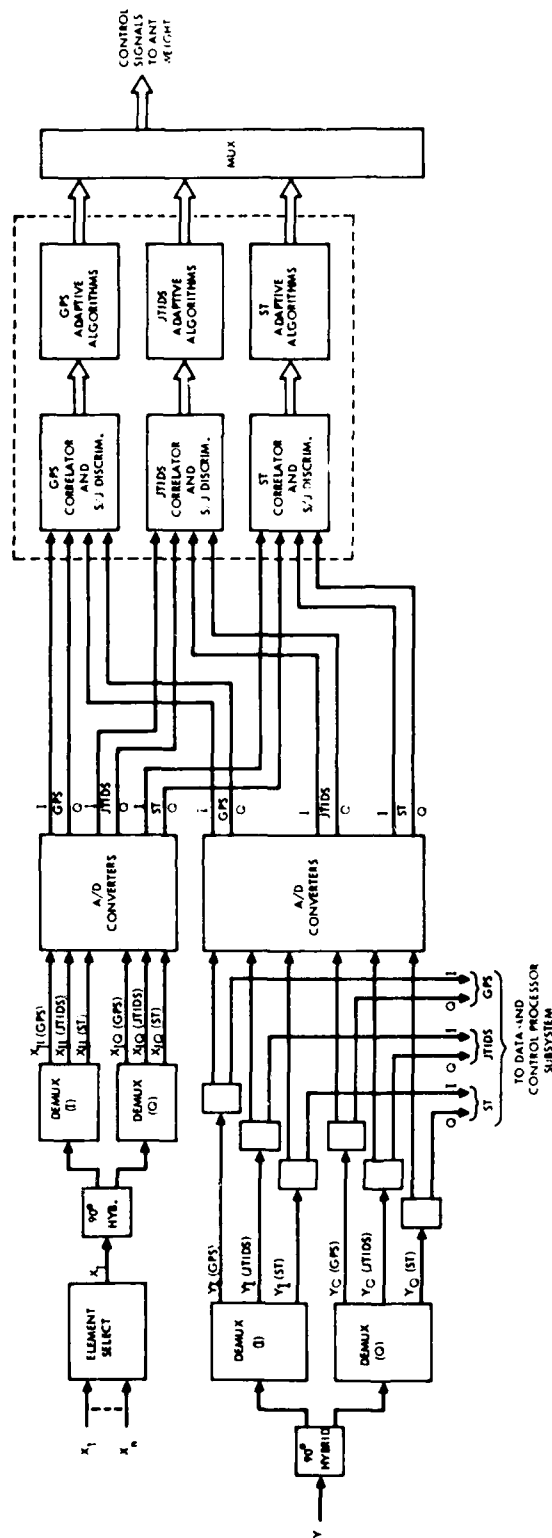


Figure 25. (Sheet 2 of 2) Integrated adaptive array processor/wideband RF processor

processor to independently select the upper or lower sub-array for each of the functions (GPS, JTIDS or SEEK TALK) as indicated in the box labeled "Upper/Lower Select".

The lines emerging from this box then represent the selected signals for each function for each active element in the associated sub-array. The signals from each active element may then be combined to form inputs to their associated WBATF's.

Each WBATF output signal then contains the time-multiplexed series of signals illustrated at the bottom of Figure 24 for RF and adaptive null control processing. The X components are then split (see right side of Figure 25, sheet 1) to provide signals to the antenna weighting elements. These signals are sent to the antenna element weights (see Figure 25, sheet 1) in synchronism with WBATF tap weight reference control signals, so that the desired spatial nulls are formed for each signal of interest as each is being sampled by the WBATF's. The outputs from the agile antenna element weight circuits are also summed into a composite Y signal, which is then demuxed into separate signals of interest which are then sent to the Data and Control Processor Subsystem for baseband information processing (see bottom part of Figure 25, sheet 2). Also, the composite Y signal, after demuxing, is A/D converted for use in the adaptive weight controlling correlator circuits. The functions of correlation, S/J discrimination, and processing of the adaptive algorithms are all handled digitally, as illustrated in the top part of Figure 25, sheet 2, resulting in a desired complex weight for each active element in each active sub-array, on an iterative basis.

Viability of this fully integrated concept depends upon ultimate device-to-device uniformity characteristics of the WBATF's (which are still in an early stage of development) and also on ultimate WBATF production quantity unit costs. Device-to-device uniformity (across wide frequency bands) is very critical to successful adaptive nulling of an antenna array. Low unit cost is critical to this full integration concept because one WBATF would be required for each antenna element in any selected array (5 at a time in this concept), rather than only two (one for VHF/UHF, one for L-Band, within the RF subsystem), in the basic MFBARS designs. It is expected that the added cost of the larger quantity of WBATF's would be more than offset by elimination of other, more costly, hardware elements in both the array processor and in the RF subsystem. Since the WBATF devices are projected to be achievable as standardized monolithic devices, it is projected that sufficiently uniform device-to-device characteristics and low device unit cost can be achieved. But this requires verification from the results of the WBATF development program.

It is also possible that unit costs could turn out to be low enough that one WBATF per antenna element (22, including both top and bottom arrays) could be affordable. This could enable elimination of other hardware elements, such as the up and down converters and selection switches. Also, control could be simplified. This option will be explored if and when forthcoming projected WBATF unit costs make this option economically attractive.

#### 3.3.2.4 Adaptive Algorithms and Antenna Weighting Circuits

For any of the adaptive antenna array concepts, each spread spectrum signal would have its own algorithm, optimized to each specific spread spectrum signal. Each algorithm would generate a complex (phase and amplitude) control signal for complex weighting of each antenna element. Control signals would be fed to the weighting circuits in a time-multiplexed manner, in synchronism with the tap weight control signals fed to the WBATF's for frequency tuning and filtering. Discrimination of desired from undesired signals will be different for each signal, as described below.

JTIDS will utilize knowledge of expected frequency hopping patterns and signal times of arrival after each frequency hop as discriminants. The JTIDS algorithm will utilize a narrow band, asynchronously hopped, closed loop scheme with storage for 51 sets of weights (corresponding to the 51 available center frequencies for JTIDS transmission).

GPS will utilize the known signal level of the received satellite signals and their spread-spectrum PSK codes for identification. The baseline adaptive algorithm for GPS ( $L_1$  and  $L_2$ ) will be the pattern search method with variable step size, as recommended in the Harris report (AFAL Contract F 33615-77C-1274) in Section 4.2. However, because of the advantage of combining the  $L_2$  array with that used for the JTIDS signals in the MFBARS, no attempt will be made to combine the  $L_1$  and  $L_2$  adaptive algorithms, as was done in the Harris study. In MFBARS, the  $L_1$  array and the  $L_2$  array will be adapted independently. In this manner, no compromises need be made to compromise between the two bands, which are widely separated in frequency.

There also will be a specific algorithm for SEEK TALK. However, since the Government has not yet released design information on the two competitive waveforms being considered for SEEK TALK, or on the proposed stand-alone SEEK TALK adaptive antenna array subsystem design, it is impossible to comment at this time on details of SEEK TALK algorithms or other aspects of the SEEK TALK adaptive antenna array design.

### 3.4 RF SUBSYSTEM

The RF Subsystem consists of RF receiver front-end hardware and three transmitters. Figure 26 shows a top level block diagram of the RF Subsystem.\*

The RF Subsystem contains the most innovative device technology utilized by MFBARS, a pair of wideband agile transversal filters (WBATF's). The WBATF's, described in detail in Section 3.4.1 and in Appendix A, allow the system to use direct frequency tuning for variable tuned signals, rather than superheterodyne techniques. This is one of the major contributions to MFBARS hardware simplification, which in turn provides significant MFBARS system size and cost savings.

Note from Figure 26 that the GPS L<sub>1</sub> and L<sub>2</sub> signals and IFF signals are shown as bypassing the WBATF's. This is because they are fixed frequency signals, for which conventional fixed frequency bandpass filters are adequate for signal selection. (The WBATF provides greatest efficiencies for variable tuned signals, rather than fixed tuned signals.) However, as discussed earlier in this report (Section 2.2.3), alternate configurations are still under consideration. It may turn out better for overall tradeoff reasons to also have the WBATF's select the GPS and IFF fixed frequency signals, as well as the variable-tuned signals. Tradeoffs in subsequent phases of the program will determine the best final configuration. The balance of this section presents the RF subsystem description for the case where the IFF and GPS signals are not selected by the WBATF. This is a "worst case" situation in terms of hardware component count. If the design ultimately incorporates processing of these signals in the WBATF, then overall system size will be smaller.

Other elements of the RF Subsystem described in this section include a bank of pre-selector filters for the VHF/UHF band signals, a signal switching network, and log video and AGC amplifiers.

\*Note from the previous section that one of the adaptive antenna array concepts being considered would change the conventional boundary lines between the Antenna Subsystem and the RF Subsystem. If this approach were to be implemented, there would be two different RF Subsystem configurations for MFBARS: (1) a highly integrated configuration for those aircraft having adaptive antenna arrays; and (2) a conventional configuration for those aircraft not having adaptive antenna arrays. This section of the report describes only the latter configuration. Refer to Section 3.3.2.3 for a description of the integrated array processor/RF processor configuration.

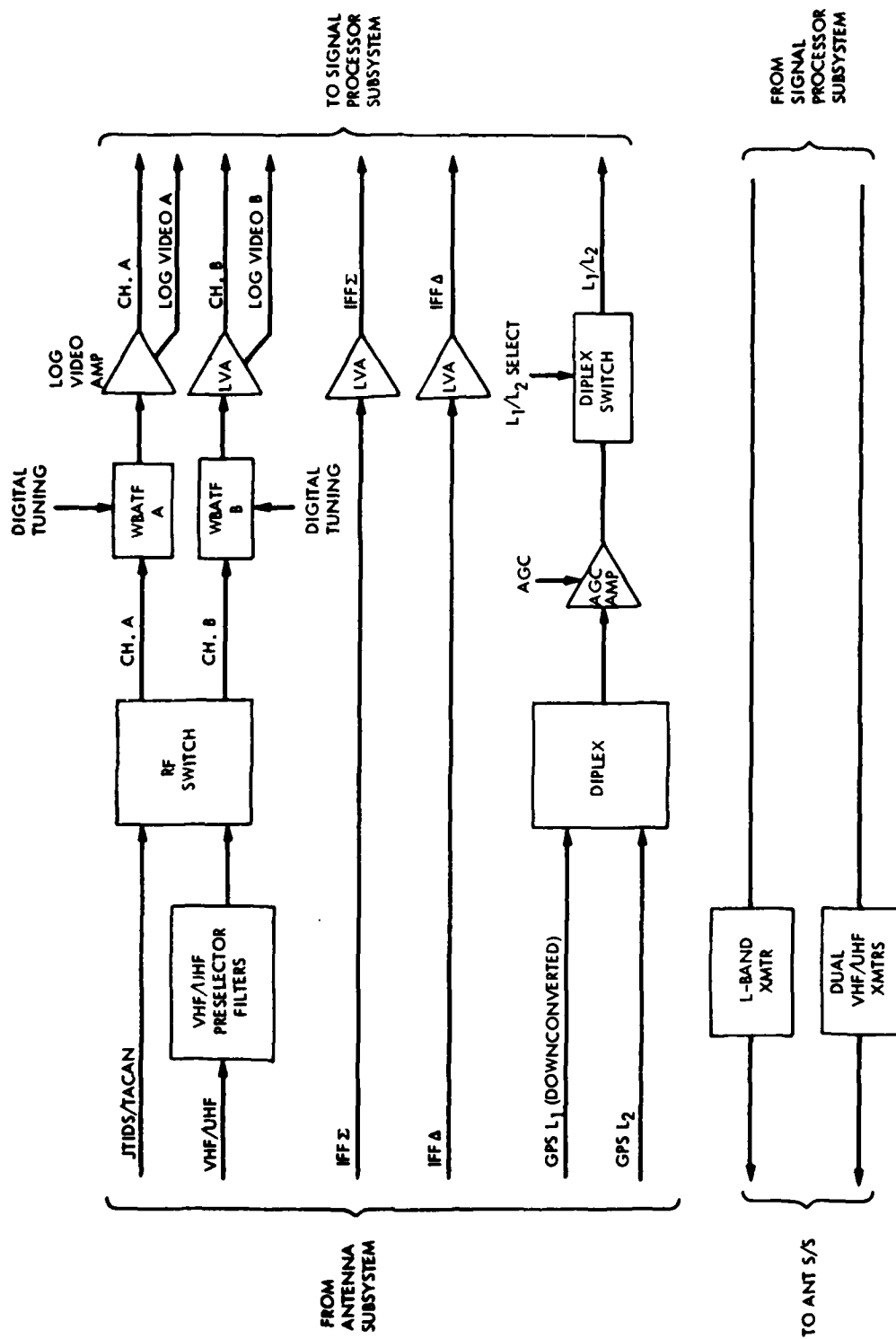


Figure 26. RF Subsystem

### 3.4.1 Wideband Agile Transversal Filters (WBATF's)

The heart of the selected MFBARS architecture is an advanced technology device called a wideband agile transversal filter (WBATF). The following paragraphs provide a brief introductory description of the WBATF, prior to describing its utilization in the RF Subsystem. Refer to Appendix A for a more detailed description of the WBATF device.

#### 3.4.1.1 Introductory Description of WBATF

A WBATF is a special form of a generic device called a transversal filter, which is a device containing:

- a lossless delay line through which an input signal propagates
- a large number of equally spaced lossless taps which sense signal energy as the input signal traverses the taps
- tap weights, one for each tap
- a summing bus output, which sums the weighted energy detected by the taps.

If the incoming RF contains a signal whose shape matches the predetermined reference shape stored in one of the tap weight sets, then the summing bus output will peak during the sampling interval. If there is no match, the weighted tap outputs will selectively cancel out and the summing bus will not peak. Amplitude measurement of the summing bus outputs can provide successive samples of detected signals of interest. These successive samples are at rates greater than the Nyquist rate of the signals of interest, so that the outputs will be (multiplexed) samples of the modulated waveforms of the signals of interest. The multiplexed sampled waveforms can then be demultiplexed in subsequent MFBARS circuitry so that each signal of interest can be processed separately.

The major differences between the generic transversal filter and the WBATF are: an extraordinarily wide input bandwidth (400 MHz); high speed sampling of the input signal (870 MHz); a large number of taps (500); and the ability to change the tap weights rapidly (6 ns), under software control, as the sampled signal propagates through the device. The usual transversal filter either has fixed tap weights which cannot be changed at all or tap weights which can be changed only slowly relative to the propagation time of the input signal through the delay line. By contrast,

the WBATF weighting circuits can be changed at a high rate relative to input signal transit time through the delay line. With this capability, the tap weight reference characteristics can be changed at several times the Nyquist sampling rate (for all signals of interest) as they propagate through the delay line. This allows high speed switching between several different tap weight references during signal transit through the delay line. Thus, several different signals of interest can be sampled, on a time multiplexed basis, during propagation through a single WBATF. Most importantly, there is no signal to noise degradation in these multiplexed samples, because of the Nyquist sampling and because the tap process is (theoretically) lossless. These features provide the ability for a WBATF-equipped MFBARS to offer considerable savings in hardware for multiple signal tuning, compared to conventional RF tuning approaches.

Figure 27 shows a general block diagram of the WBATF. As an input signal travels through the delay line, the summing bus output provides successive instantaneous summations of the input signal, as shaped by the tap weights, which are set by the tap weight register. The tap weights can be changed by input control signals to provide different sets of tap weights for several selected signals of interest. As shown in Figure 26, multiple sets of tap weights can be pre-stored in holding registers within the WBATF. These several sets of tap weights are then advanced one set at a time to the tap weight register, where they reset the tap weights for one sampling interval. Then a different set of tap weights is advanced to set the weights for the next sampling interval, recycling indefinitely. Any pre-stored set can be replaced at any time by control inputs, so that any new signal reference can replace any prior signal of interest reference at any time.

#### 3.4.1.2 WBATF Application to MFBARS

The WBATF performs the following functions for the selected MFBARS architecture.

- It provides a capability for high speed (multiplexed) switching (tuning) between several different frequencies of interest.
- It is fully programmable in terms of center frequency and bandshape, making it useful for processing various signal formats in a multi-function environment.

As shown in Figure 26, the selected MFBARS architecture contains two identical WBATF's, one for L-band signals and one for VHF/UHF signals. Each has an RF input bandwidth

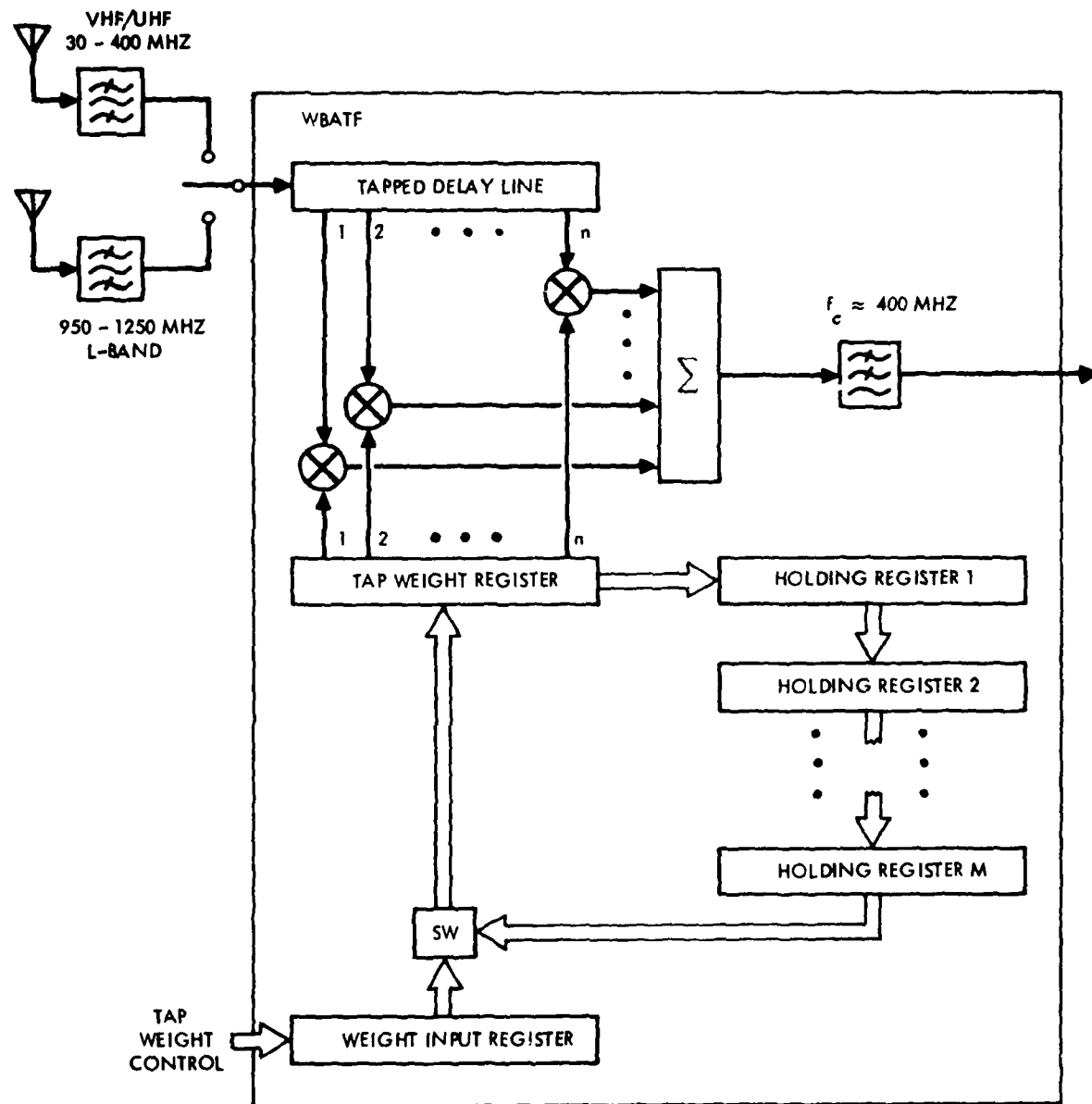


Figure 27. WBATF block diagram



of approximately 400 MHz. Either WBATF can be switched to the other band, or either can handle both bands, on a multiplexed basis. This flexibility provides fail soft system degradation in the event of failure.

#### 3.4.2 VHF/UHF Preselection Filters

As shown in Figure 26, one of the WBATF's is preceded by a bank of SAW VHF/UHF preselection filters. This filter bank is required for improved dynamic range performance of VHF/UHF signal detection. The filter bank and whichever WBATF is assigned to VHF/UHF processing work as complementary successive filters in detecting VHF and UHF signals. Figure 28 shows a block diagram of the preselection filter bank.

The preselection filter bank establishes sensitivity and provides selectivity to prevent desensitization by off-channel signals. No (conventional) explicit down-conversion is required, due to the WBATF frequency conversion which follows.

The preselection filters consist of two filter bank modules; the first covers the 30 to 88 MHz band, the low frequency VHF band, while the second module covers both the 108-174 MHz (high VHF) band and the 225-400 MHz (UHF) band. In addition, the second module contains an antenna switching matrix so that two antennas can be used simultaneously in each band. The selectivity is provided by three SAW filter banks, one for each band. Each filter bank has two RF amplifiers whose inputs may be connected to any selected filter output within the filter bank. The outputs of the RF amplifiers are summed and filtered further by either of the WBATF's.

The SAW filter banks are matched to 50 ohms and have PIN switches at both the input terminal and output terminal of each filter so that input signals are routed to one appropriate filter and amplifier. The center frequency and one dB bandwidth for the 30-88 MHz, 108-174 MHz, and 225-400 MHz filter bands are shown in Figures 29, 30 and 31 respectively.

Power VMOS RF amplifiers were chosen because of their low noise figure (4 dB) and high third order output intercept point (45 dBm).

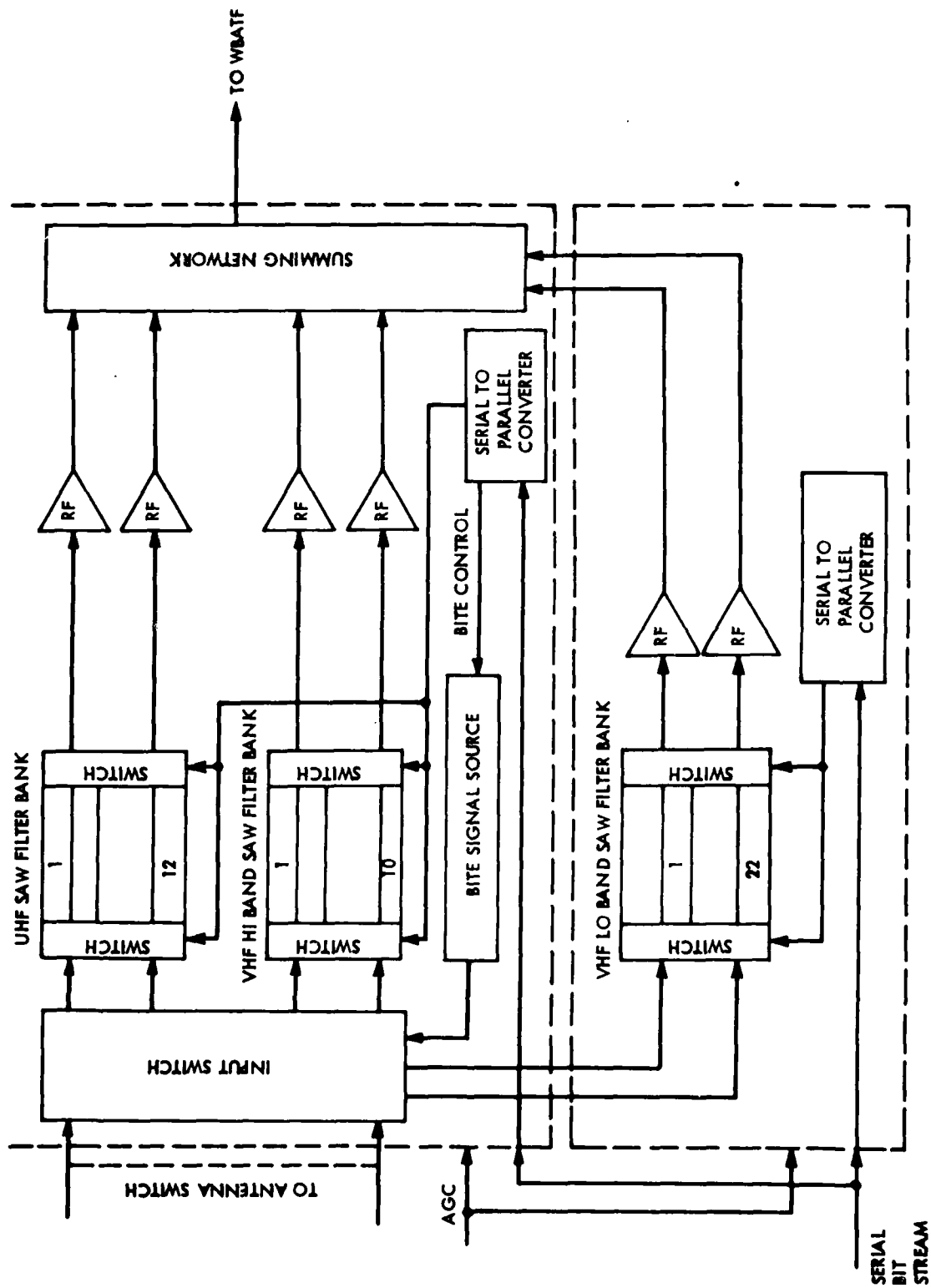
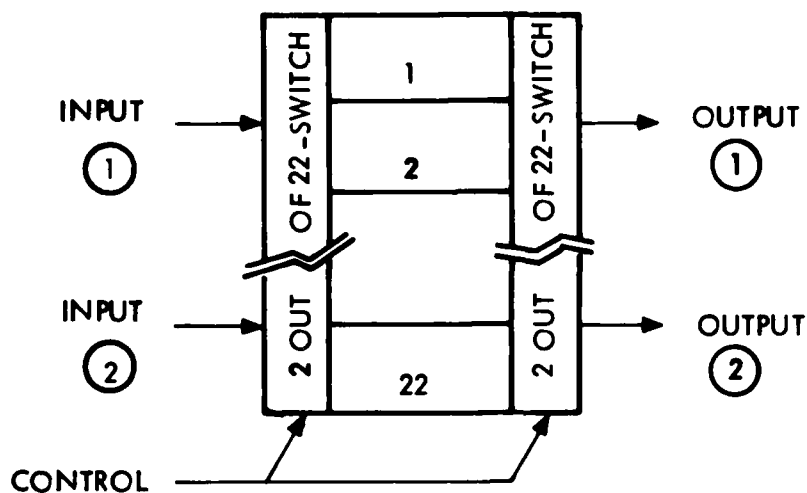
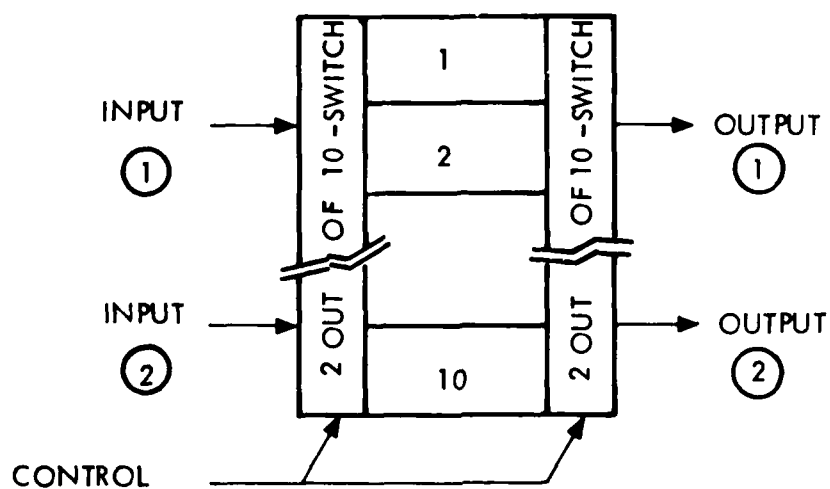


Figure 28. VHF/UHF preselection filters



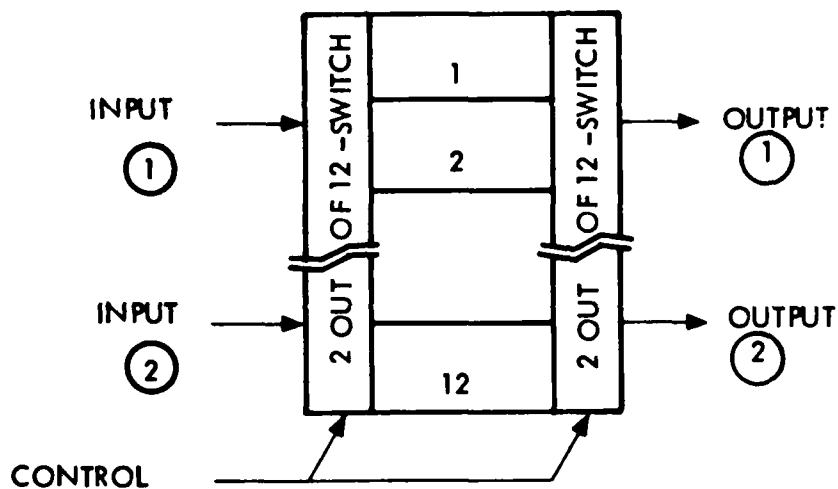
<u>FILTER NUMBER</u>	<u>CENTER FREQUENCY, MHZ</u>	<u>1 dB BANDWIDTH, MHZ</u>
1	30.7519	1.5038
2	32.2933	1.5791
3	33.9121	1.6583
4	35.6119	1.7414
5	37.3970	1.8287
6	39.2715	1.9204
7	41.2400	2.0166
8	43.3072	2.1177
9	45.4780	2.2239
10	47.7576	2.3353
11	50.1515	2.4524
12	52.6654	2.5753
13	55.3053	2.7044
14	58.0775	2.8400
15	60.9887	2.9823
16	64.0458	3.1318
17	67.2561	3.2889
18	70.6273	3.4537
19	74.1675	3.6268
20	77.8852	3.8086
21	81.7893	3.9995
22	85.890	4.2000

Figure 29. 30-88 MHz filter bank



<u>FILTER NUMBER</u>	<u>CENTER FREQUENCY, MHZ</u>	<u>1 dB BANDWIDTH, MHZ</u>
1	110.6378	5.2756
2	116.0422	5.5333
3	121.7106	5.8036
4	127.6560	6.0871
5	133.8917	6.3844
6	140.432	6.6963
7	147.292	7.0234
8	154.487	7.3665
9	162.033	7.7263
10	169.9481	8.1037

Figure 30. 108-174 MHz filter bank



<u>FILTER NUMBER</u>	<u>CENTER FREQUENCY, MHZ</u>	<u>1 dB BANDWIDTH, MHZ</u>
1	230.5254	11.0509
2	241.8477	11.5937
3	253.7261	12.1631
4	266.1879	12.7605
5	279.2617	13.3872
6	292.9776	14.0447
7	307.3673	14.7345
8	322.4636	15.4582
9	338.3014	16.2174
10	354.4171	17.0140
11	372.3489	17.8496
12	390.6369	18.7263

Figure 31. 225-400 MHz filter bank

Gain, noise figure, and intermodulation distortion budgets for the preselection filters are shown in Figure 32. The noise figure of the preselection filters is less than 10 dB while the input third order intercept point is greater than 20 dBm. The input and output impedance of the RF amplifiers is 50 ohms.

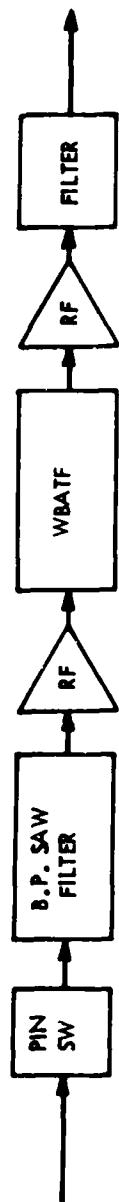
#### 3.4.3. Log-Video Amplifiers

There are two types of log-video amplifiers in the RF Processor Subsystem. The first is used for RF amplification of the IFF signals. The second is used for amplification of the WBATF outputs.

The log video amplifiers used for the IFF functions are conventional units. A simplified block diagram is shown in Figure 33. The RF center frequencies of the signals of interest are either 1030 MHz or 1090 MHz. The RF bandwidth will be approximately 6 MHz and the logarithmic gain compression range will be at least 60 dB. Only the log-video output of the amplifier is required for IFF functions.

The WBATF log video amplifiers are more complex than the IFF log video amplifiers. The output of the WBATF's will be JTIDS, TACAN, and various communication and navigation signals. For TACAN operation, both the log-video and hard-limited outputs of the amplifier are used as shown in Figure 34. For JTIDS, only the hard-limited output is used. The various communication and navigation functions may use either one or both of these outputs. Also, these devices will be required to operate over a broader frequency range, from 30-400 MHz.

The signal time-sharing requirements are also an important design consideration. The output of the WBATF is a time division multiplexed sequence of signals. These signals are passed through a 400 MHz low pass filter. After the instant of transition from one signal to the next, the low pass filter will have a transient response which must decay before a sample can be taken on the output signal. As the time-sharing rate is increased to handle more simultaneous signals the decay interval decreases and some portion of the previous signal begins to contaminate the sample of the present signal. We can estimate the degree of contamination



NF/D8	1	3	4	15	4
GAIN/D8	-1	-3	20	-15	20
ACCUM GAIN/D8	-1	-4	16	1	21
3 I /DBM	50	50	45	50	45
<u>ACCUM</u>					
NF					9.17 DB
3					
I					22.79 DBM

Figure 32. Gain, noise figure, and intermodulation budgets

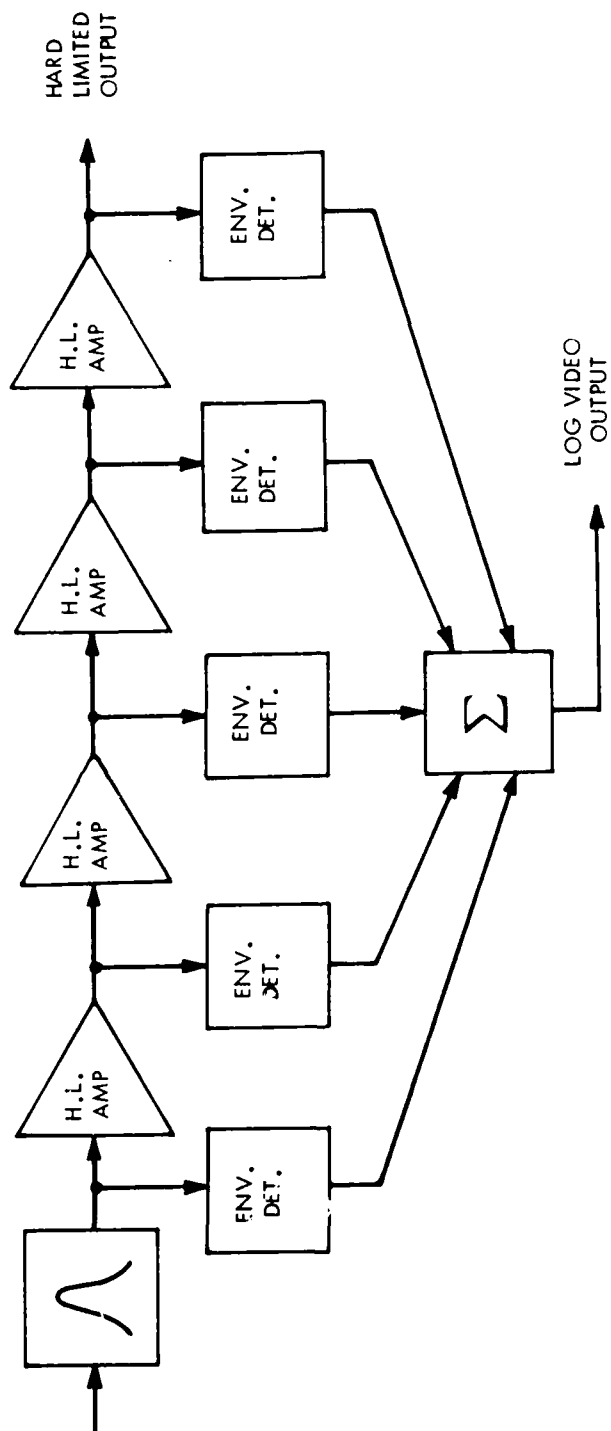


Figure 33. Log video RF amplifier



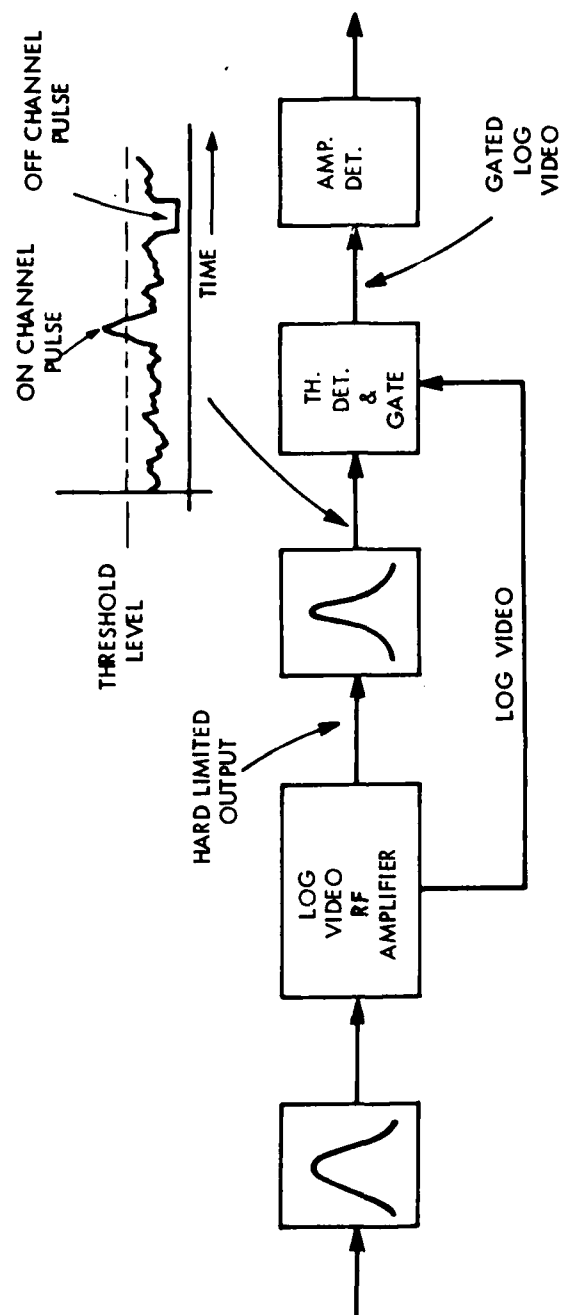


Figure 34. Log video RF amplifier for TACAN signal processing

by assuming that the low pass filter has a single pole and a transfer function:

$$\frac{E_{OUT}}{E_{IN}} = \frac{1}{\sqrt{1 + \omega^2 T^2}}$$

where

$$\omega = 2 \pi f$$

$$T = \text{time constant} \quad (1)$$

Using the low pass filter cutoff frequency (3 dB) of 400 MHz, we can find the time constant T.

$$\frac{E_{OUT}}{E_{IN}} = \frac{1}{\sqrt{2}} = \frac{1}{\sqrt{1 + \omega^2 T^2}}$$

$$T = \frac{1}{2 \pi f_c} = 3.98 \times 10^{-10} \text{ seconds.} \quad (2)$$

The fraction of voltage remaining at the output of the filter after t seconds is the impulse response of the filter.

$$\frac{e_{out}}{e_{in}} = e^{-(t/T)} \quad (3)$$

If we assume that the sampling rate for each signal of interest is 15 MHz and we wish to process between 10 and 14 signals, then the time interval between successive signals at the WBATF is:

$$t_{min} = \frac{1}{(15 \times 10^6)} = 4.76 \times 10^{-9} \text{ Sec} \quad (4)$$

$$t_{\max} = \frac{1}{(15 \times 10^6) (10)} = 6.67 \times 10^{-9} \text{ sec.} \quad (5)$$

Substituting equations (2), (4) and (5) into equation (3) yields:

$$\left( \frac{e_{\text{out}}}{e_{\text{in}}} \right)_{\max} = e^{-\frac{t_{\min}}{T}} = 6.37 \times 10^{-6} = -104 \text{ dB}$$

$$\left( \frac{e_{\text{out}}}{e_{\text{in}}} \right)_{\min} = e^{-\frac{t_{\max}}{T}} = 5.24 \times 10^{-8} = -146 \text{ dB} \quad (6)$$

Based on the above results, timesharing the WBATF among 10 to 14 signals would be satisfactory.

#### 3.4.4 AGC Amplifier

The AGC amplifier for the GPS signals is a conventional AGC amplifier. The diplexed  $L_1/L_2$  signals are amplified by a common RF (AGC) amplifier which provides 120 dB of gain and +20 dB gain control. Since up to 40 dB of signal variation might be encountered between different GPS satellites, and since the AGC amplifier operates on all GPS signals simultaneously, an additional AGC system will be implemented in software to normalize individual signal amplitudes.

#### 3.4.5 VHF/UHF Transmitters

There are two identical (for redundancy) 10 watt transmitters for the following frequency ranges: 30 to 88 MHz, 108 to 174 MHz, and 225 to 400 MHz. They each operate in a single channel mode with 25 KHz channels. In addition, they operate in a wideband spread spectrum mode in the 225-400 MHz range for SEEK TALK. Also, some MFBARS configurations provide a SINCGARS capability which uses slow frequency hopping of 25 kHz channels in the 30-88 MHz band.

The VHF/UHF transmitters consist of a synthesizer, and a 10 Watt power amplifier. A 40 Watt power amplifier module can be added for those MFBARS configurations containing AFSATCOM capability.

For the 30-88 MHz single channel mode, the transmitters provide frequency modulation with a 6.5 kHz peak deviation and binary FM (16 kbs) with a peak deviation of 5.6 KHz. Only binary FM is used for SINCGARS.

For the 108-150 MHz range, amplitude modulation and on-off keying (16 kbs) is provided. For the 150-174 MHz range, frequency modulation and binary FM is provided, with 5 KHz frequency deviation for voice and 5.6 kHz for binary FM.

For the 225-400 MHz range, amplitude modulation and on-off (16 kbs) keying is provided. FSK is also provided for those MFBARS configurations with AFSATCOM capability.

#### 3.4.5.1 Transmitter Architecture

The MFBARS synthesizer uses a three loop architecture to provide FM modulation, frequency hopping and frequency offsets.

Figure 35 shows the block diagram of the synthesizer and associated exciter stages. It consists of three loops: a frequency modulation loop, a main loop and a follower loop. All three loops are phase locked to the 3.2 MHz TCXO which in turn may be locked to a Rubidium standard (if available, external to MFBARS) for even greater accuracy.

The modulation loop uses a VCXO to provide  $\pm 6.5$  kHz peak deviation for analog FM voice and  $\pm 5.6$  kHz deviation for 16 Kbps digital voice and data.

The follower loop VTO generates +22 dBm level in the 30 to 400 MHz range in three bands. The high level VTO is required so that the noise floor at the transmitter output is -190 dBc/Hz. SEEK TALK modulation is accomplished in the high level balanced modulator at the output of the follower loop which phase modulates the carrier with the PN sequence from the SEEK TALK PN Generator.

Amplitude modulation is achieved in the amplitude modulation loop which is capable of 90 percent modulation.

The main loop generates frequency hopping in the 38.8-368.8 MHz range for the follower loop, and has less than 1 millisecond dead-time per hop. The buffered 16 kbps data is sent at 18 kbps for 9 milliseconds thus preventing the loss of any data.

The digital control logic contains the buffers and ROM's needed to coarse tune and control all loops.

**MODULATION LOOP DESIGN** - The modulation loop provides  $\pm 6.5$  kHz and  $\pm 5.6$  kHz peak frequency deviation from 10 Hz to 9 kHz needed for frequency modulation of voice and data respectively.

The modulation loop is locked to the 3.2 MHz TCXO by a phase lock loop having 10 Hz loop bandwidth, thus permitting modulation down to 10 Hz.

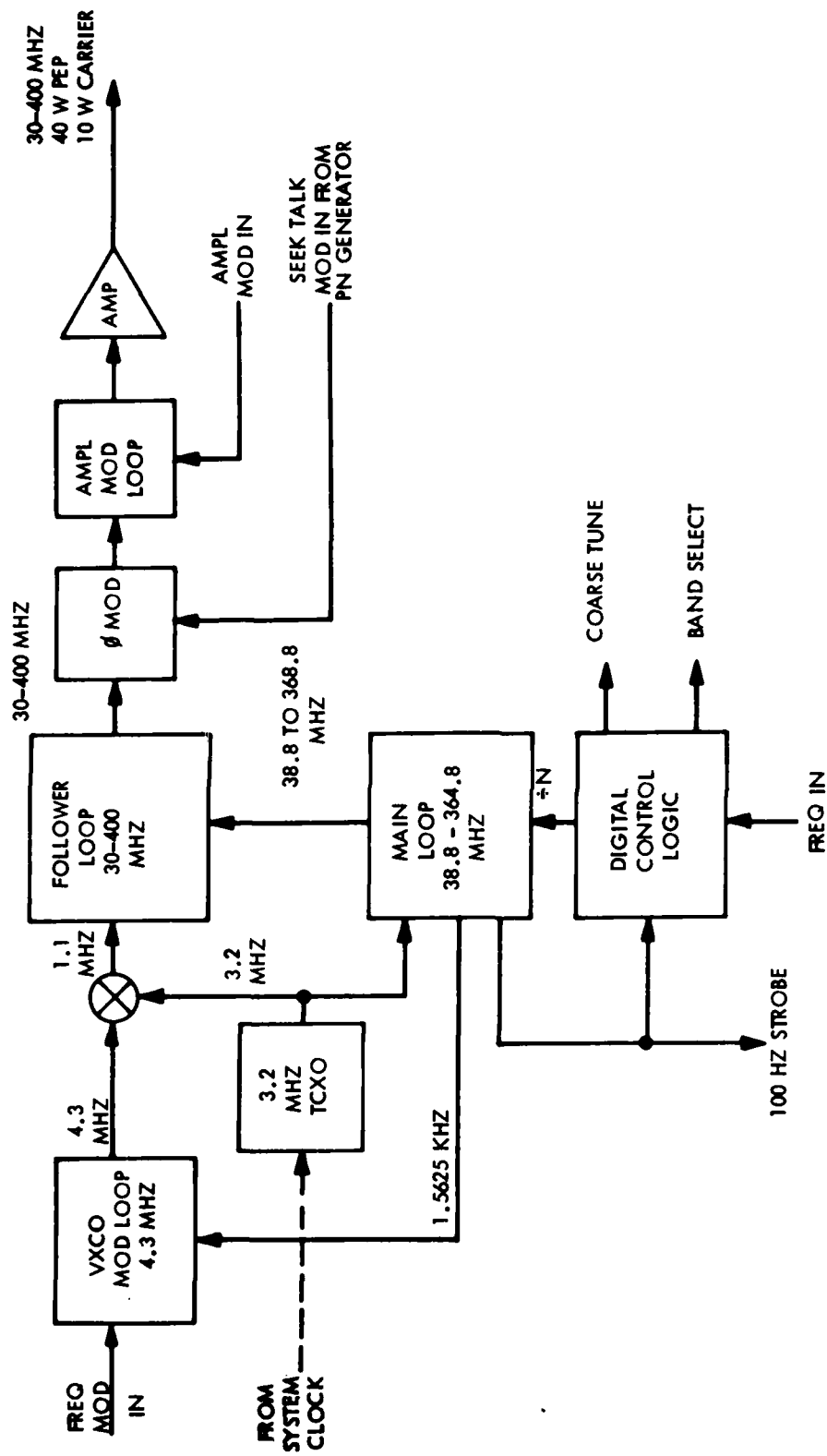


Figure 35. MFBARS synthesized block diagram

Because of the  $\pm 8$  and the  $\pm 32$  in the follower loop, the VXCO must have a peak deviation of  $\pm 700$  kHz for  $\pm 5$ V digital voice in the 30 to 88 MHz band and  $\pm 175$  Hz for  $\pm 5$ V digital voice in the 150-174 MHz band. A  $\pm 5.8$ V analog voice signal will then yield  $\pm 812.5$  Hz deviation at the VXCO in the 30-88 MHz band and  $\pm 203$  Hz deviation in the 150-174 MHz band. An attenuator is used in the 30-88 MHz band to compensate for this difference.

The worst case clock spurs in this loop are -115 dBc. The modulation loop has an 8 Hz loop bandwidth and can, therefore, be modulated down to 10 Hz. The loop has a 67 degree phase margin and is, therefore, very stable. The loop tunes to within 100 Hz in less than one second and therefore, does not require fast acquisition circuitry. The spurs which appear in the 1.1 MHz band-passed output of the modulation loop will not affect the system.

FOLLOWER LOOP DESIGN - The follower loop follows the VCXO and the frequency hopping main loop, generating a frequency modulated carrier from 30 to 400 MHz in three bands.

The follower loop mixes the main loop output with the follower loop output, the difference frequency is then divided by 8 or 32 and phase locked to the 1.1 MHz from the modulation loop.

The coarse tune input shown activates inductors to coarse tune the VTO to the approximate frequency so that it cannot lock on the image frequency. The image frequency is 17.6 MHz above the desired frequency in the 30 to 88 MHz band and is 70.4 MHz above or below the desired frequency in the other two bands. The  $\pm 8$  is used in the 30 to 88 MHz band and the  $\pm 32$  in the other bands.

VMOS transistors are used in the oscillator in order to generate an output of +20 dBm with a noise floor of approximately -194 dBc/Hz at the VTO.

The worst case clock spur (-57 dBc) is reduced to less than -77 dBc by a "bridged-T" notch filter. The loop has a worst case closed loop zeta of .9178, open loop phase margin is  $70^\circ$  and gain margin is 22 dB. The loop has a loop bandwidth of 160 KHz which will allow it to follow the hopping rate and the 10 Hz to 9 KHz modulation. This loop will tune to within 100 Hz in 0.133 milliseconds and will, therefore, not limit the synthesizer's ability to settle within one millisecond.

There are no significant spurs in the #8 loop in the 30 to 88 MHz band or in the #32 loop in the other two bands. The VTO output is 30 to 88 MHz in band 1; 108 to 174 MHz in band 2 and 225 to 400 MHz in band 3. The main loop is 8.8 MHz above the follower loop in band 1, 35.2 MHz above the follower loop in band 2, and in the 225 to 300 MHz portion of band 3 and 35.2 MHz below the follower loop in the 300 to 400 MHz portion of band 3.

MAIN LOOP DESIGN - The main loop generates a frequency hopping frequency from 38.8 to 364.8 MHz and tunes to within 100 Hz in less than .8 millisecond.

This loop uses a phase/frequency detector with switchable gain so that it first converges with high gain for the first .6 milliseconds of a frame and then switches to lower gain for the next 9.4 milliseconds.

The coarse input is controlled by the digital control logic to limit the tuning range of the varactors. In the normal mode, the worst case clock spur is -64.6 dBc. The worst case zeta of this loop is .6156, the phase margin is 48°, the gain margin is 20 dB and it tunes to within 100 Hz in 3 milliseconds. In the fast mode, the worst case zeta is .55, the phase margin is 43° and the gain margin is 13 dB. The main loop tunes to within 100 Hz in less than .8 milliseconds in fast mode enabling it to be settled within 1 millisecond after the start of the data frame assuring that data is not missed in the next 9 milliseconds. The fast/slow technique is used to reduce clock spurs during the 9 milliseconds of data.

OUTPUT STAGES - The output stages provide phase and amplitude modulation with low noise to provide a -190 dBc/Hz noise floor.

In the output stages the mixer is a double balanced active modulator using VMOS transistors for low loss.

The amplitude modulation loop uses a power sensor and PIN attenuator in a feedback loop to provide 300 Hz to 10 KHz modulation with less than 10 percent total harmonic distortion with up to 90 percent modulation. The PIN attenuator has a nominal -6 dB gain in order to provide 90 percent upward modulation. The output is a nominal 10 watts and 40 watts peak.

The two lowpass filters shown are switched by the band selection lines from the control logic in order to provide harmonic rejection in each band.

The output stages have a noise floor of -190 dBc and an output third order intercept point of +55 dBm. This is adequate for a nominal 40 dBm output.

**DIGITAL CONTROL LOGIC** - The digital control logic provides the coarse tuning mode for both VTO's and the band select for the filters,  $\pm 8/\pm 32$  and the FM gain attenuator.

The digital control logic accepts parallel input frequency hop words. It can also be configured to accept serial input data at 640 KHz rate.

The control logic uses ROM's to generate the proper coarse tune word for each of the two VTO's in accordance with the incoming frequency hop word.

This logic also gives the required "fast" signal to the main loop phase comparator for the first .6 millisecond of each frame.

#### 3.4.6 L-Band Transmitter

The L-band transmitter generates all the signals required to be transmitted for the JTIDS, IFF, TACAN and DME functions. An overall block diagram is given in Figure 36. The transmitter consists of a stable oscillator at 450 MHz, a modulator, a frequency upconverter and power amplifiers. All circuitry, including the power amplifiers, is solid state construction.

The transmitter interfaces with the antenna coupling network as shown in Figure 17. In addition to the signals to be radiated, the transmitter provides low level signals for monitoring and self-test of the receiver signal processing circuitry.

##### 3.4.6.1 Oscillator

The oscillator is a 450 MHz stable oscillator, phase locked to a system reference clock. The reference frequency is not critical, but is expected to be around 1 MHz. The oscillator can be a VCO or a SAW oscillator, so long as it is locked to the system reference.

##### 3.4.6.2 Modulator

The modulator provides continuous phase shift modulation (CPSM) as required for the JTIDS function. A block diagram of the circuit is shown in Figure 37. It consists of a preamplifier, a PSK modulator with driver, a second amplifier and a SAW filter. The first amplifier raises the signal level to about 20 dBm. The PSK modulator is a double



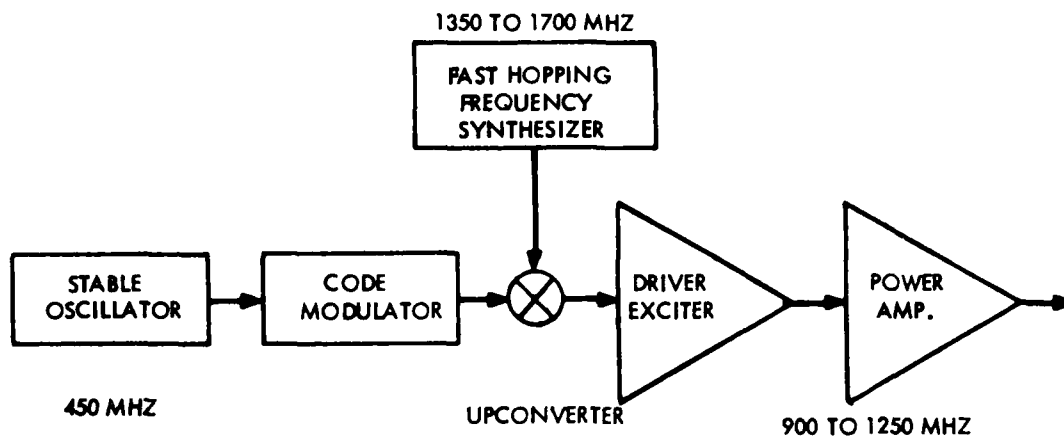


Figure 36. L-band transmitter block diagram

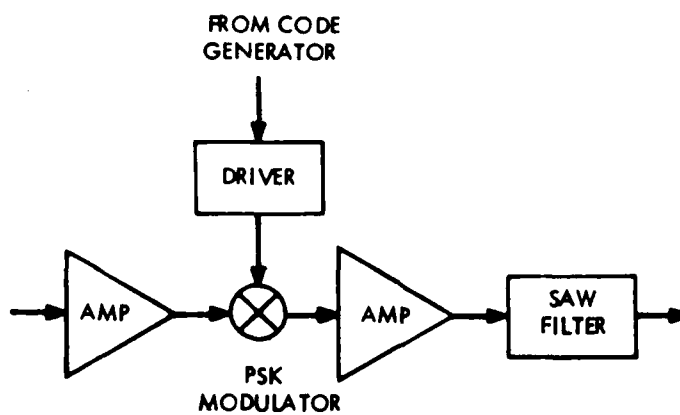


Figure 37. CPSM code modulator

balanced mixer, connected to provide 180° phase reversal of the incident signal on command from an external digital control. Its output is amplified and then coupled to a SAW filter, designed to convert the PSK modulation to CPSM. The center frequency of the SAW filter is 450 MHz; 3 dB bandwidth is 4 MHz and ultimate attenuation is greater than 50 dB. The output of the modulator is a fixed frequency, continuous wave signal with CPSM coding for JTIDS and unmodulated for Tacan, IFF and DME.

#### 3.4.6.3 Upconverter

The function of the upconverter is to convert the fixed frequency signal at 450 MHz to a frequency hopped signal in the 900 to 1250 MHz band. This is accomplished by using a fast hopping Frequency Synthesizer (FS) at the local oscillator of a mixer. A block diagram of the FS is given in Figure 38. This synthesizer uses the indirect synthesis (phase locked loop) approach. The key component in the design is a programmable frequency divider operating in the frequency range of 1350 to 1700 MHz. Such a device is presently under development at several laboratories using Gallium Arsenide FET technology. Required specifications for the fast hopping synthesizer are as follows:

Frequency (MHz)	1350 to 1700
Frequency Increments (MHz)	1
Switching Speed (usec)	6
Power Dissipation (watts)	3
Volume (cu. inches)	3
Weight (oz.)	7

A high pass filter is required at the output of the upconverter to reject the 450 MHz input frequency.

#### 3.4.6.4 RF Driver/Exciter

The RF Driver/Exciter module takes the output of the upconverter, amplifies it and imparts the required amplitude modulation for TACAN, IFF and DME. A block diagram of the driver/exciter is given in Figure 39. The CW input signal is first amplified and pulse modulated by a PIN diode switch as shown. This premodulation limits the duty cycle to about 25 percent. The switch is followed by two stages of amplification which raises the signal level to 50 Watts peak. The second

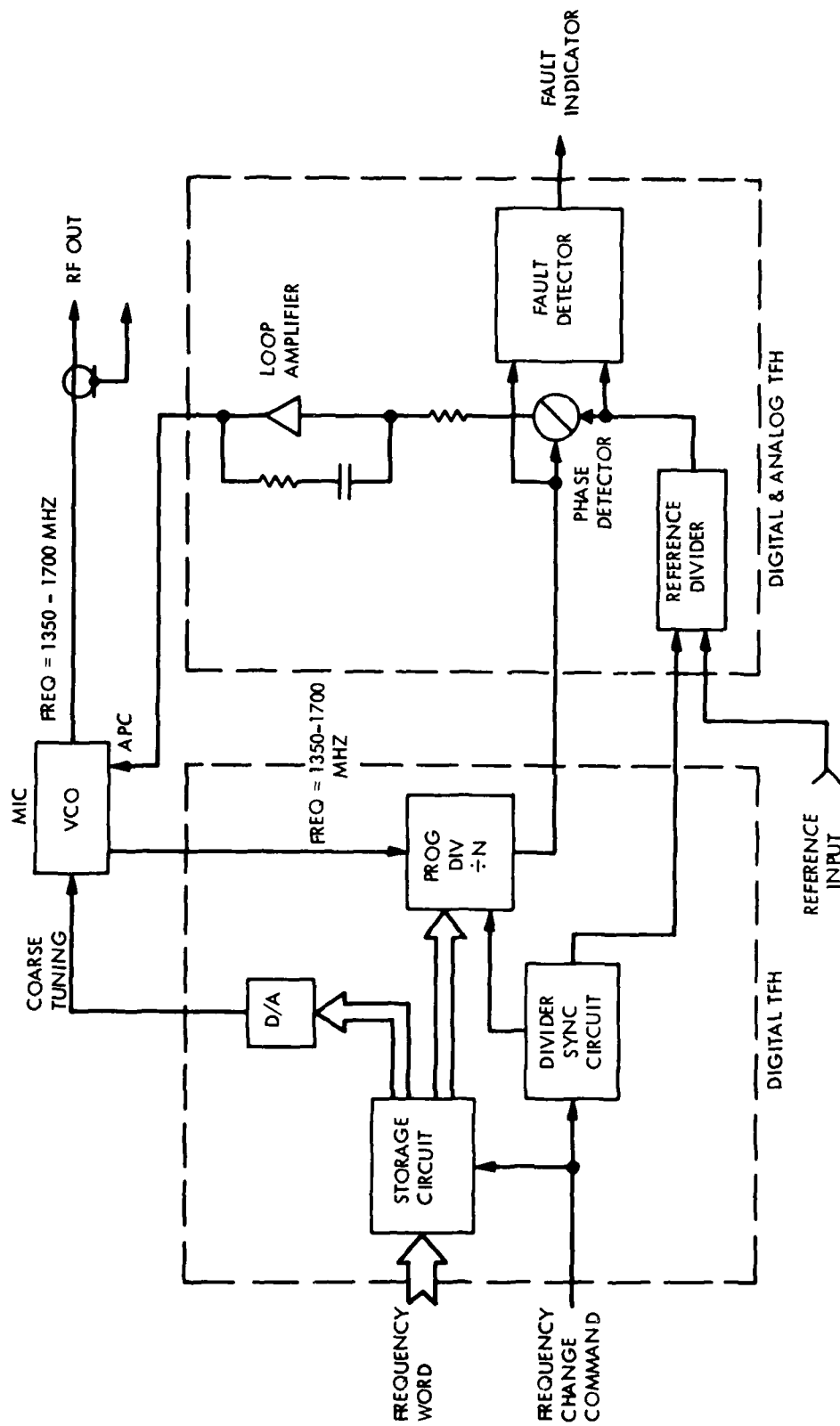


Figure 38. Fast hopping indirect frequency synthesizer

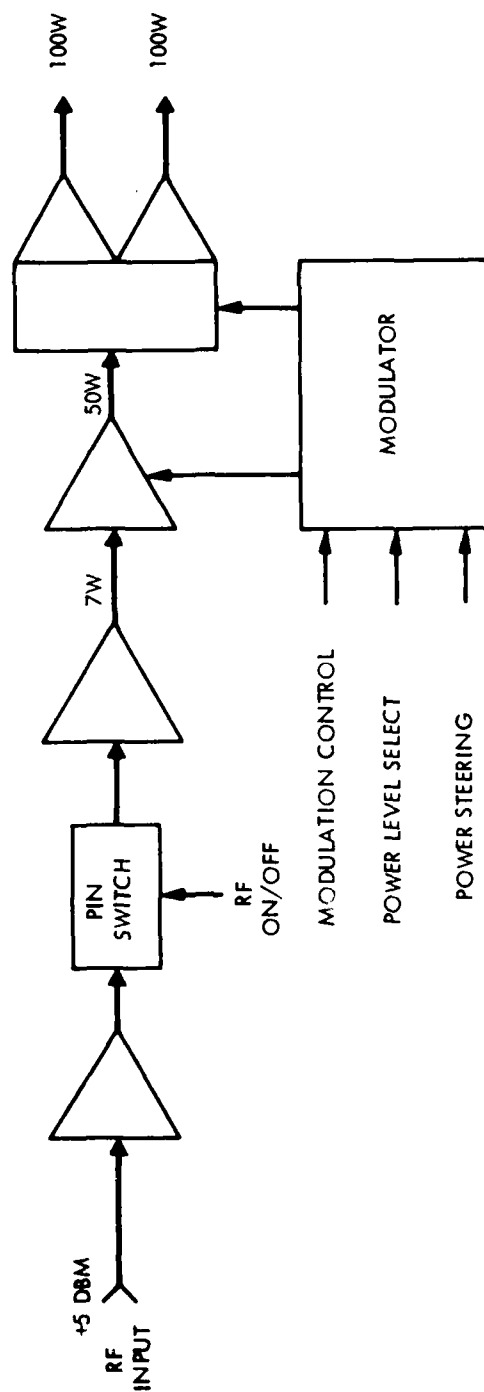


Figure 39. RF driver/exciter

amplifier also imparts the final amplitude modulation, i.e., square pulses for JTIDS and IFF, and Gaussian shaped pulses for Tacan and DME. The signal is then divided into two channels and further amplified to provide two 100 Watt outputs.

A phase modulator is included which can shift the relative phase of the two outputs by +90 degrees. This is used to steer the power to either one or both antennas as described below.

#### 3.4.6.5 Power Amplifier

The outputs of the driver/exciter module drive two parallel power amplifiers which provide outputs of 650 Watts each. A diagram of the power amplifier module is given in Figure 40. The amplifier outputs are connected to circulators, filters and finally to the antennas. The total output power of 1300 Watts can be supplied from either the upper port or the lower port of the hybrid, or divided equally between the two, depending on the relative phase of the inputs as determined by the phase shifter in the exciter. The primary specifications of the transmitter are summarized below:

Frequency Band	960-1215 MHz
Peak Power Output	1000 Watts (single output) 500 Watts (dual outputs)
Gain (overall)	55 dB
Efficiency	40 percent
Duty Cycle	
Short Term (6 msec)	52 percent
Long Term	20 percent
Operating Modes	Tacan, JTIDS, IFF, DME
Input Power Required	900 Watts (max.)
Module Size	
RF Exciter/Driver	40 cu. in.
Dual Power Amp.	100 cu. in.
Power Supply	150 cu. in.

AD-A106 052

ITT AVIONICS DIV NUTLEY N J

F/G 17/2.1

MODULAR MULTI-FUNCTION MULTI-BAND AIRBORNE RADIO SYSTEM (MFBARS--ETC(U)

JUN 81 R A REILLY, C W WARD, A LEE

F33615-78-C-1518

UNCLASSIFIED

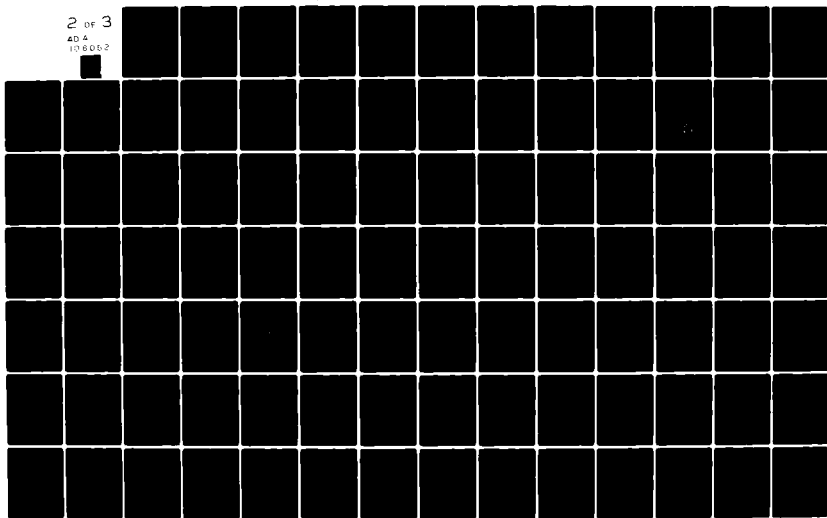
AFWAL-TR-81-1077-VOL-2

NL

2 OF 3

40 4

1980062



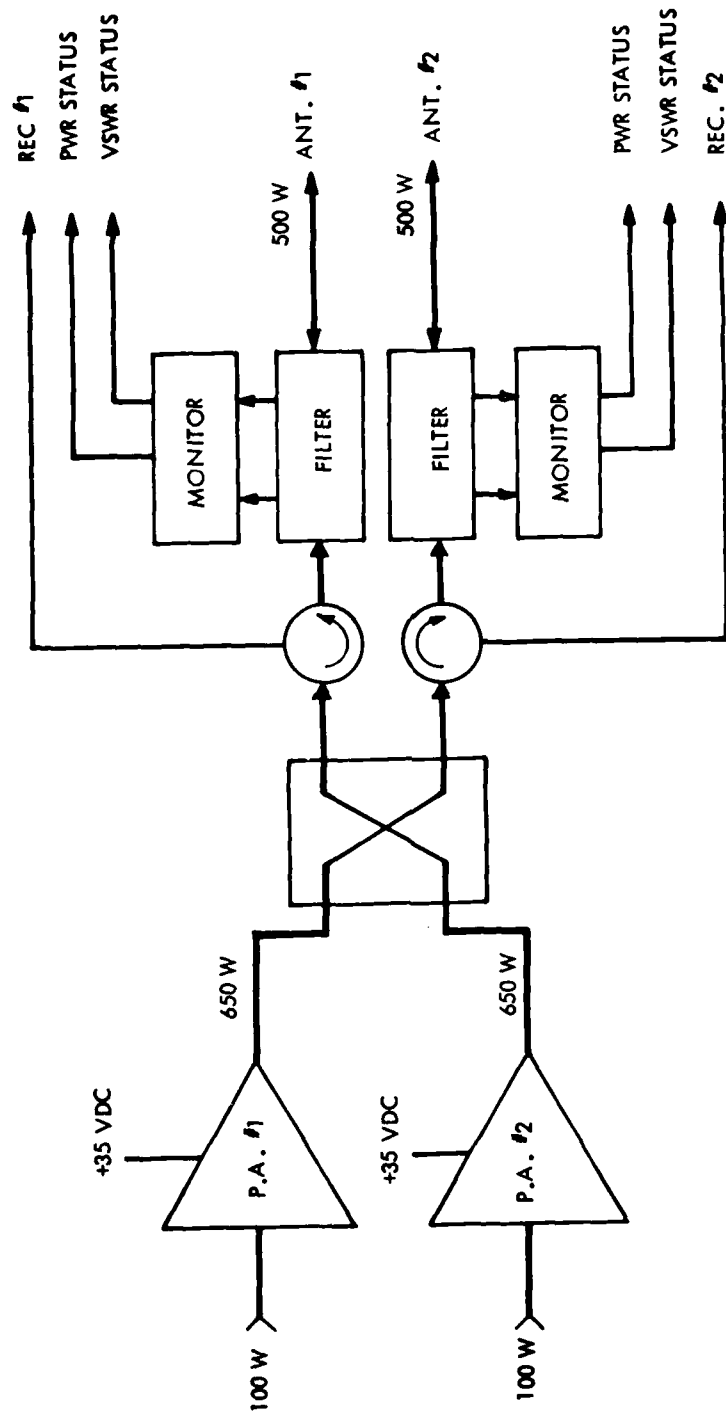


Figure 40. Dual power amplifier

### 3.5 SIGNAL PROCESSOR SUBSYSTEM

The Signal Processor Subsystem consists of two baseband converters, a signal switching network, a narrowband agile transversal filter (NBATF) Assembly, code generators, and special purpose dedicated signal processors. Figure 41 shows a top level block diagram of the Signal Processor Subsystem.

#### 3.5.1 Baseband Converters

The baseband converters are frequency translation devices, similar in function to a down-conversion mixer, which convert signals to "zero-IF" for baseband processing. They provide final frequency translation of signals not converted to zero-IF and/or baseband in the WBATF's. (Only those signals whose carrier frequencies are exact multiples of the WBATF output sampling rate are translated directly to baseband in the WBATF's.) Figure 42 shows a block diagram of the baseband converter. The technology required for this device is similar to that developed for the WBATF, but a new circuit design is required specifically for MFBARS application.

An additional input to the digital sine function generator is the TRANSEC PN codes utilized in JTIDS for spectrum spreading. These codes are superimposed in real time on the SIN and COS outputs of the generator and produce sign (+/-) changes in the polarity of the output resulting in a PN code stripping process in the baseband converter.

#### 3.5.2 Signal Switching Network

The signal switching network is a signal routing device which, in conjunction with other circuitry, provides the high degree of flexibility required in a multi-function radio system. This flexibility is achieved through the ability to dynamically reconfigure the system resources to meet the requirements of a particular mission profile to minimize single point failure modes and to generally improve significantly the probability of mission success.

Figure 43 is a simplified block diagram of the signal switching network. It receives outputs from the baseband converters, each of which may be in either the VHF/UHF band or the L-band. Switches S1 and S2 allow these bands to be interchanged with respect to their normal routing. (The



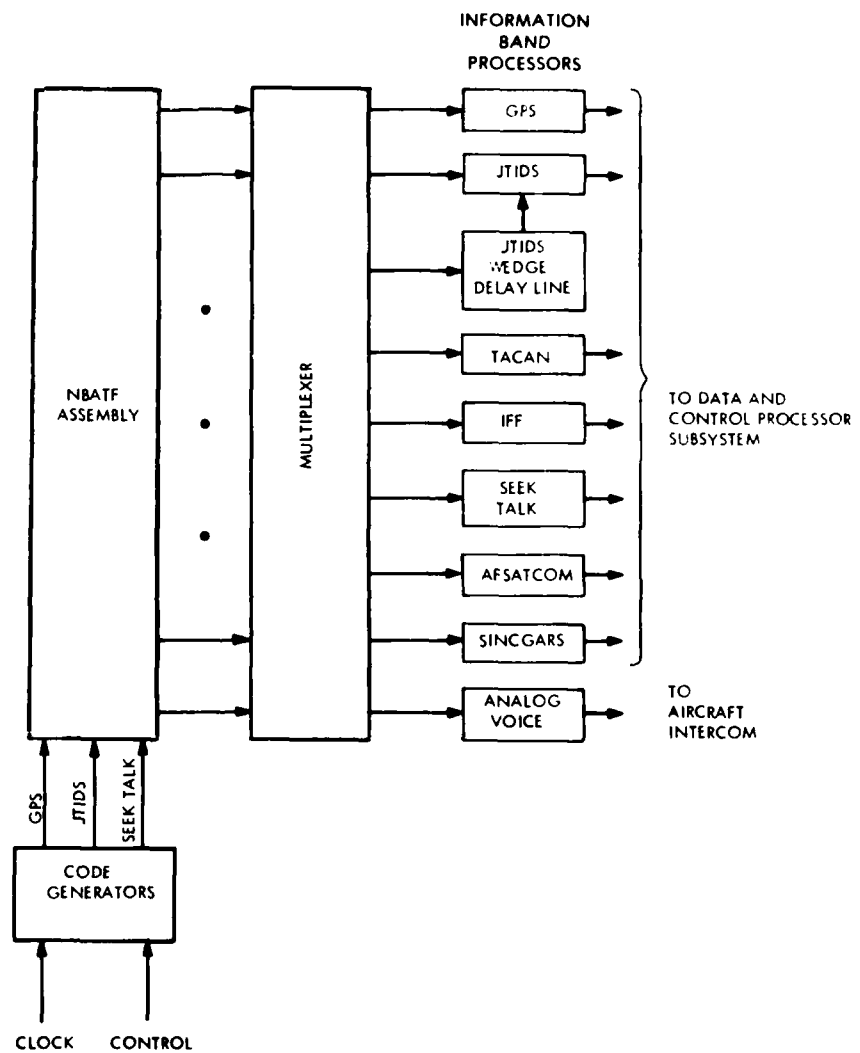


Figure 41. Signal Processor Subsystem

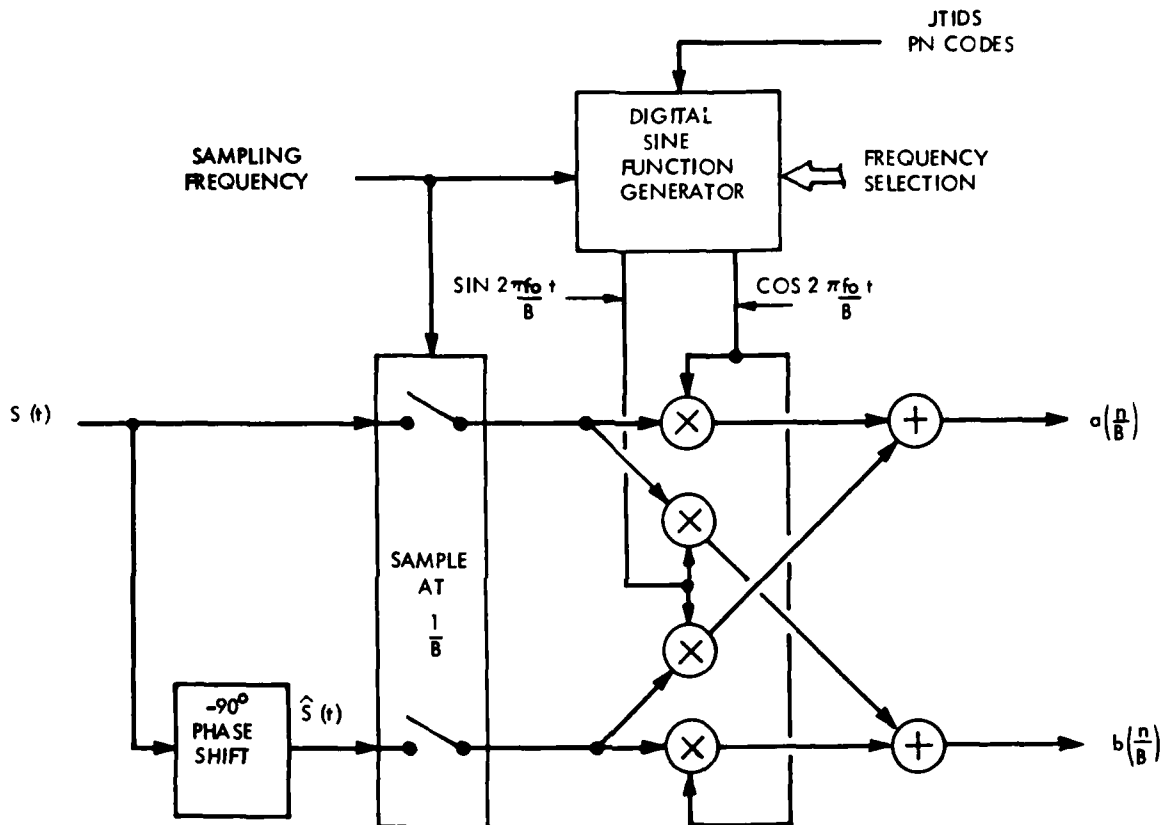


Figure 42. Baseband converter

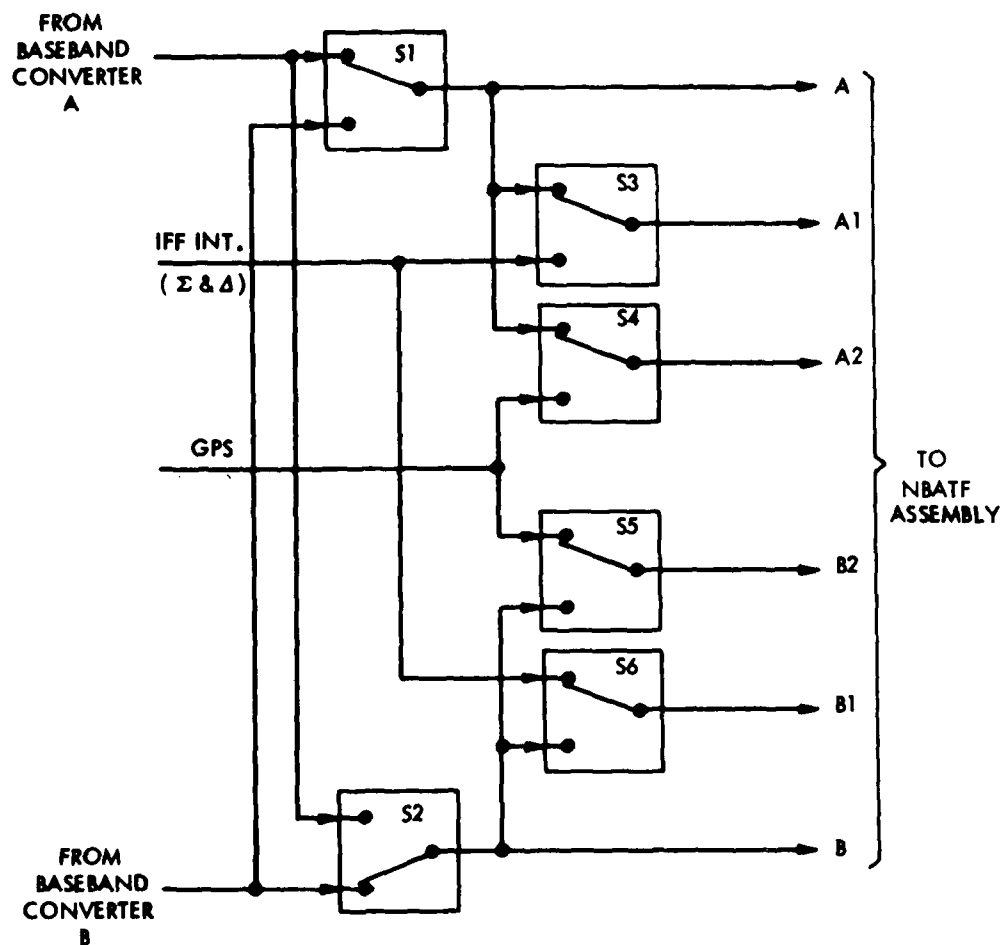


Figure 43. Signal switching network

switch positions of all switches S1-S6 are shown in their normal positions.) Also, either baseband converter can drive both inputs simultaneously, if required.

The IFF and GPS inputs are routed by switches S3-S6 to the auxiliary outputs A1, A2, B1, and B2. The auxiliary outputs provide the capability of reconfiguring some portion of the otherwise identical, duplicate resources driven by the "A" and "B" baseband converter outputs.

The isolation required in the signal switch should be at least 100 dB to eliminate cross-interference between channels. The switches need not be fast. Switching times on the order of a few tenths of a second are adequate.

### 3.5.3 Narrowband Agile Transversal Filter (NBATF) Assembly

Further bandlimiting is required following the baseband converter and the signal switching network. Bandwidths of from 5 to 15 MHz must be reduced to bandwidths of as little as 25 KHz, commensurate with IF bandwidths in conventional radios, prior to baseband processing. In addition, the spread spectrum signals (GPS, JTIDS, SEEK TALK) must be "despread" by correlation with PN spread spectrum references. Both processes (bandlimiting and PN despreading) can be accomplished with a common device, a narrowband agile transversal filter (NBATF). The NBATF is similar to the wideband agile transversal filter (WBATF) described previously, but operates at slower signal clock speeds (approximately 30 MHz maximum versus 870 MHz for the WBATF). The NBATF utilizes variable input clocking rates and flexible input/output interconnections.

Figure 44 shows a block diagram of an NBATF. It is a CCD-type device, with 195 taps and an adjustable input clocking rate. Tap weights can be changed, under processor control, to provide variable bandpass shaping and/or variable PN code references for PN correlation. Each NBATF has a capability for storing up to four sets of tap weights for cyclic utilization. New tap weight inputs are entered under processor control. NBATF's are used in sets, with inputs and outputs of each set interconnected as required for optional cascading, optional parallel in-phase and quadrature-phase processing, and/or optional squaring and summing of outputs, according to specific processing requirements for each different type of MFBARS signal being processed (as explained below). Since a good many of the MFBARS signals require four NBATF's or multiples thereof, it is convenient to configure the NBATF's in standard building block sets of four. Figure 45 shows a standard NBATF

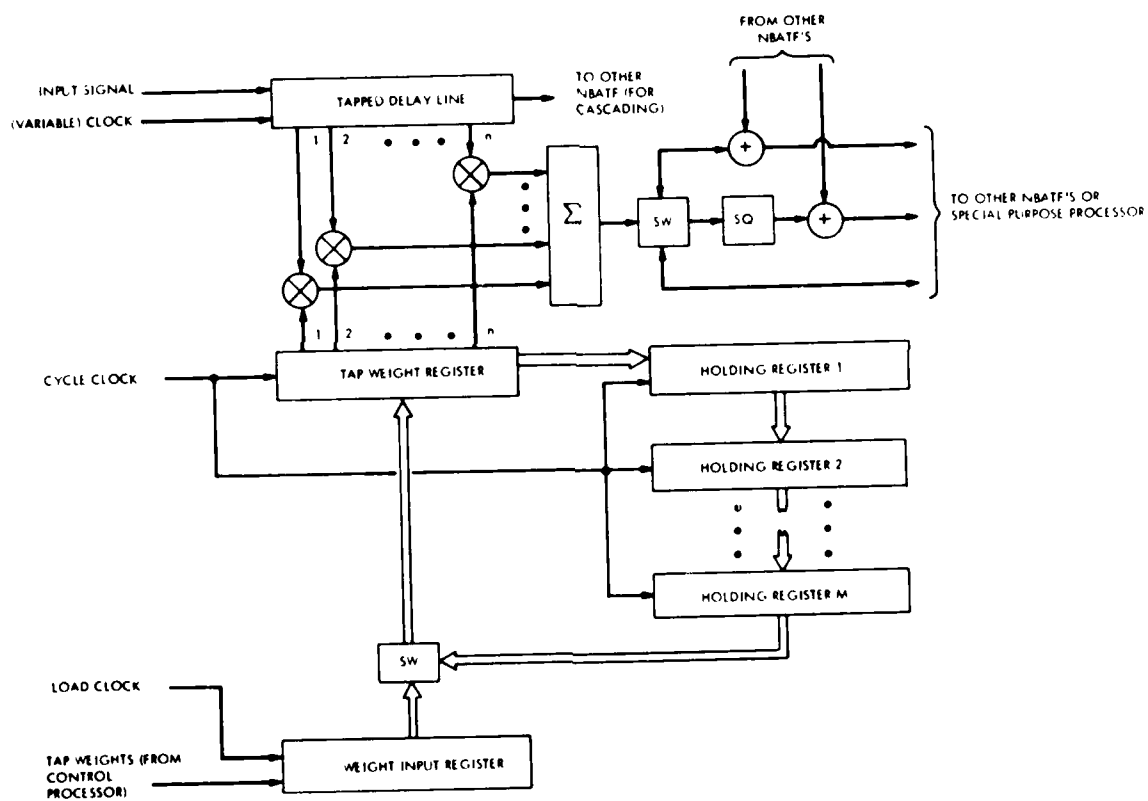


Figure 44. NBATF block diagram

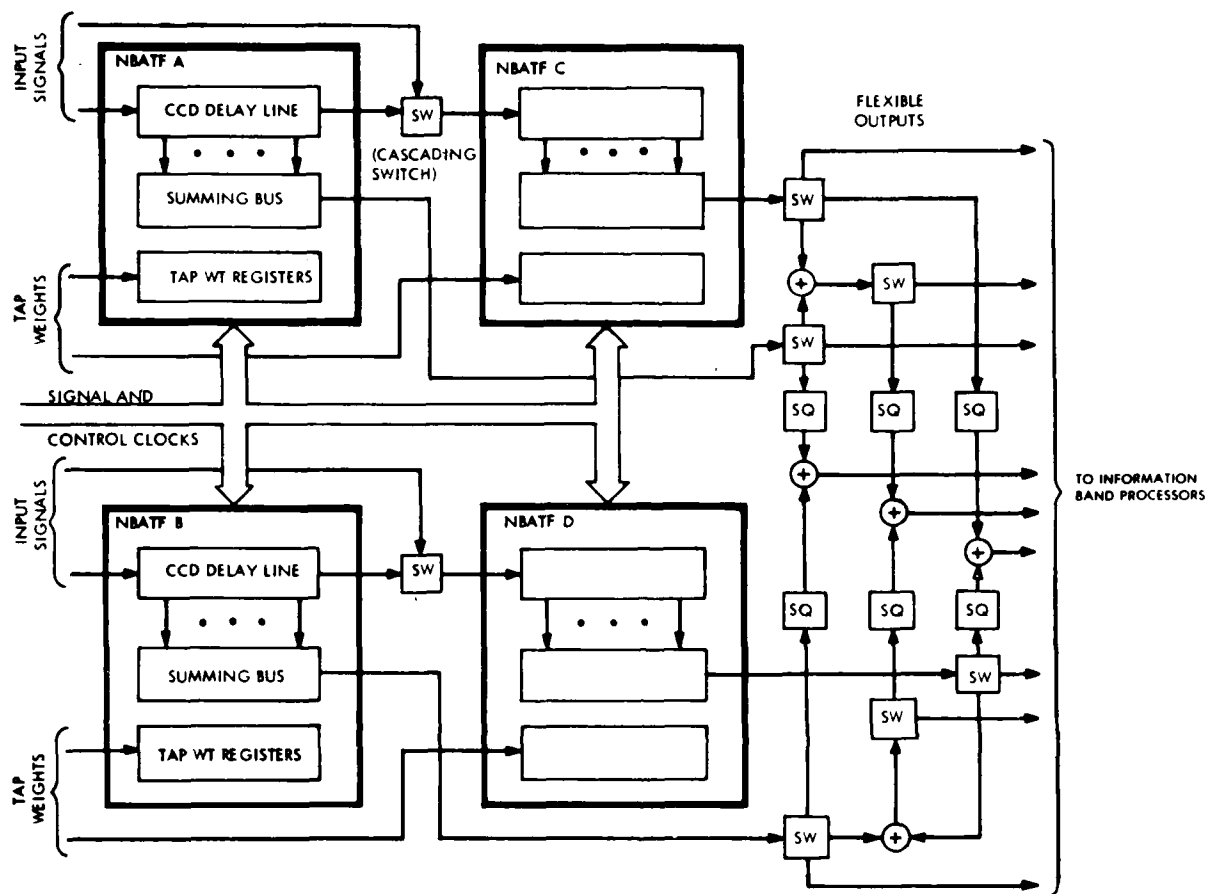


Figure 45. Standard NBATF building block

building block, including the standard flexible interconnections. It is projected that, by the production phase of the program, it may be cost-effective to put each set of four NBATF's and their associated support circuits and flexible interconnections on a single monolithic chip.

All of the NBATF building blocks taken together constitute what is referred to as the NBATF Assembly, shown in Figure 46. Although there is only one NBATF Assembly for MFBARS, each NBATF building block is separately accessible, for system reliability purposes. Since each NBATF building block in the assembly is identical, any signal may be processed by any NBATF building block(s), as assigned under processor control. This provides for fail-soft system operation in the event of failure.

The total number of NBATF building blocks in the NBATF Assembly has not yet been determined, primarily because applicable SEEK TALK design information is not available and because the Government has not yet made a final choice on which form of JTIDS will be utilized, both of which may affect requirements. It is estimated that approximately 20 NBATF building blocks (with four NBATF's per building block) represent a reasonable upper limit. However, since it is possible to time share NBATF's for some signals, the final number is expected to be less than 20. Table 7 summarizes the NBATF requirements for the system.

Sections 3.5.3.1 through 3.5.3.6 following, provide details on specific NBATF configurations required for each specific type of MFBARS signal.

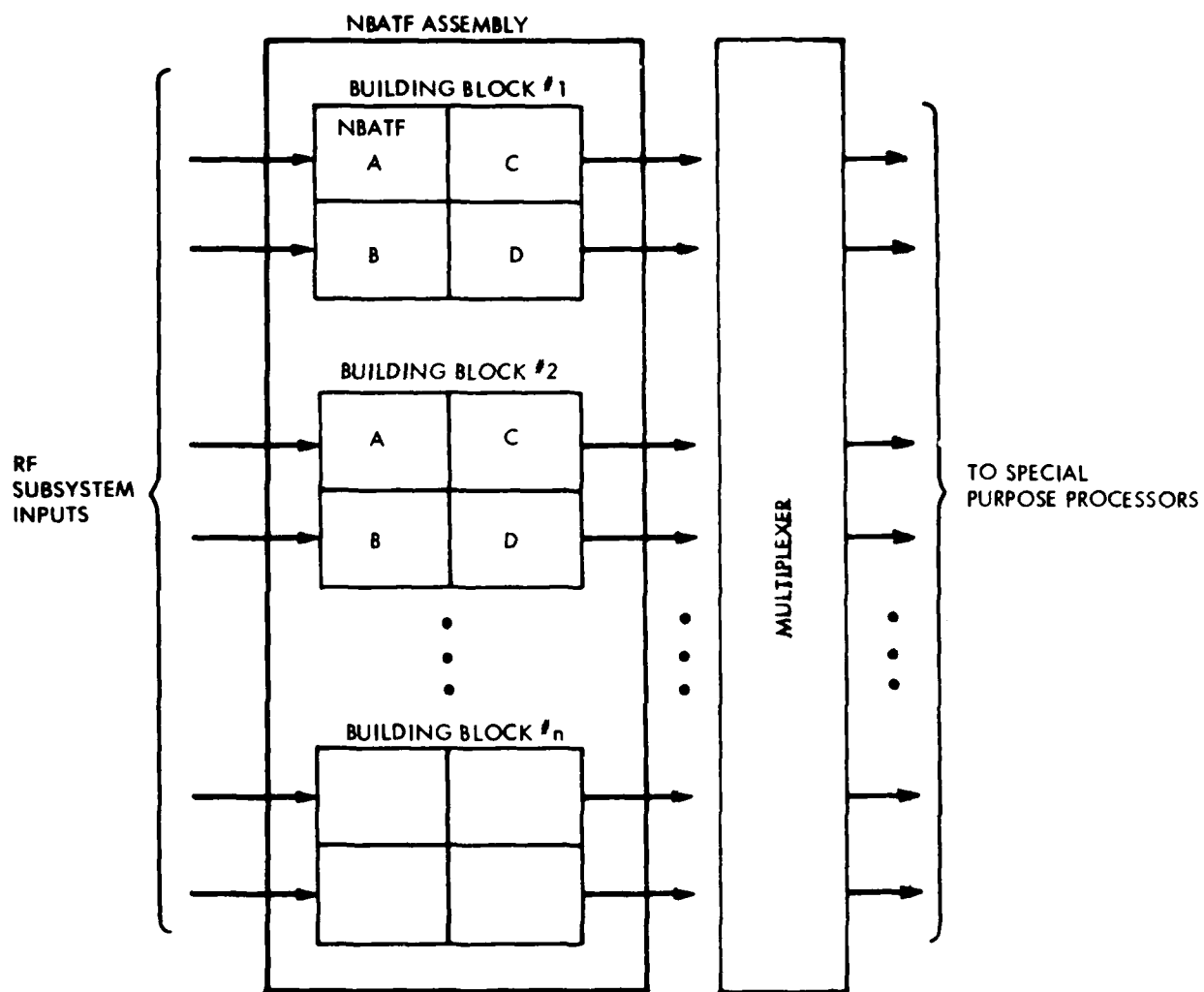


Figure 46. NBATF Assembly



Table 7. NBATF BUILDING BLOCK REQUIREMENTS

	<u>NATF Building Blocks</u>	<u>NBATF's Utilized</u>	<u>Comments</u>
JTIDS, ATDMA/TDMA, Sync	4	16	12 NBATF's available for other signals except during sync.
JTIDS, ATDMA/TDMA, Data	1	4	
JTIDS, DTDMA, Sync and Data	2	8	All 8 required for both data and sync
JTIDS Subtotal	2-4	8-16	
GPS	1	4	
TACAN	1	3	1 NBATF available for other signals
IFF	1	3	1 NBATF available for other signals
SEEK TALK	4	16	(estimated)
VHF/UHF Comm	3	12	
VHF/UHF Nav	1	4	4 time-shared signals
Subtotal	13-15	50-58	
AFSATCOM	1	4	some platforms only
SINCGARS	1	4	some platforms only
	15-17	58-66	
VHF FM homing	(1)	(4)	backup nav
VHF AM ADF	(1)	(4)	backup nav
UHF AM ADF	(1)	(4)	backup nav
	(15-17)	(58-66)	(backup nav not an additive NBATF requirement)

### 3.5.3.1 JTIDS NBATF's

JTIDS will require either 2 or 4 NBATF building blocks (8 or 16 NBATF's) depending on whether the Government selects DTDMA/TDMA or ATDMA/TDMA JTIDS formats as the operational JTIDS systems. Of the three JTIDS formats, ATDMA/TDMA are the more demanding in terms of NBATF's. Sixteen NBATF's are required for ATDMA or TDMA because of the necessity for simultaneous tuning to eight different frequencies during sync, with each frequency requiring two NBATF's for in-phase (I) and quadrature-phase (Q) signal processing. Each JTIDS NBATF has a 15 MHz input clock, which provides a 13 usec delay time through the 195 taps. Figure 47 shows the NBATF configuration for ATDMA/TDMA JTIDS sync.

It should be noted that these 16 NBATF devices replace 64 PN correlators in a conventional ATDMA/TDMA JTIDS system. This is because each of the eight sync frequencies uses 4 different PN codes during sync. With conventional PN correlators, PN reference codes cannot be changed fast enough to permit time-sharing, thus requiring 4 sets of 16 correlators, or 64 total. The NBATF's, however, permit changing of PN reference codes at high rates relative to the sync pulses, which allows rapid reprogramming which enables reduction of device count by a factor of four.

Following sync, only 1 NBATF building block (4 NBATF's) is required to receive ATDMA/TDMA JTIDS data pulses. This is because data is transmitted in pulse pairs but it is only necessary to tune to one frequency at a time for data pulses (versus eight for sync). The first pulse of each pulse pair is I and Q processed (requiring 2 NBATF's), then sent through delay lines (2 more NBATF's), while the first 2 NBATF's are used for I and Q processing of the second pulse. (The delayed first pulse and the subsequent second pulse are then in time-synchronization and are added together prior to further processing.) Thus, 1 NBATF building block is adequate for ATDMA/TDMA data pulses. Figure 48 shows the NBATF configuration for the ATDMA/TDMA data mode. During the data pulse portion of the JTIDS message, the other 3 NBATF building blocks could be used for other signals, if desired.

DTDMA JTIDS requires only 2 NBATF building blocks (8 NBATF's). This is because DTDMA sync pulses are distributed throughout the DTDMA message and are processed as if they were data. Two simultaneous pulse frequencies are required to achieve the same overall system performance as for ATDMA, with eight frequencies. This is because the number of channels in DTDMA is dependent upon data rate, whereas the number of channels in ATDMA/TDMA is dependent upon synchronization performance.

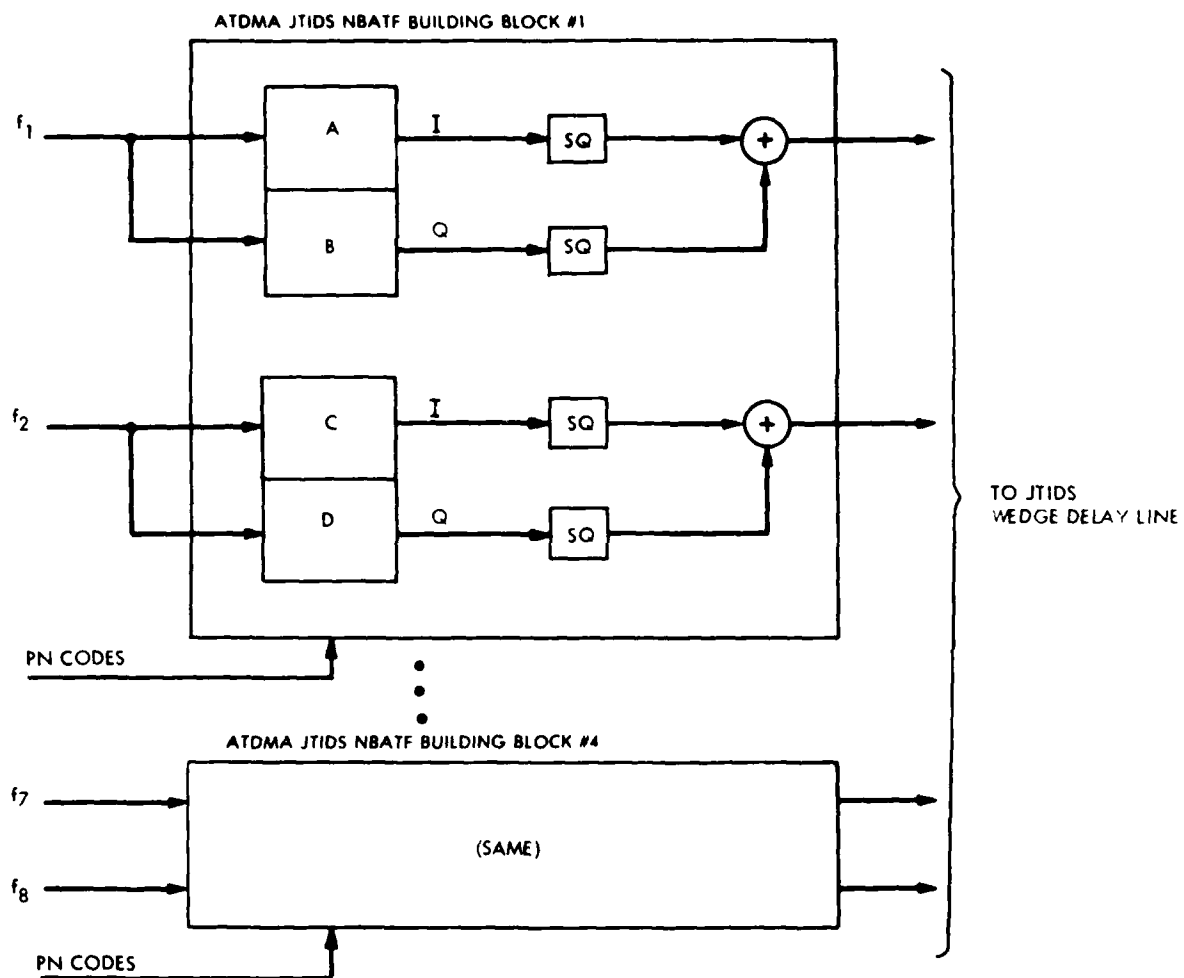


Figure 47. NBATF configuration, ATDMA/TDMA JTIDS sync

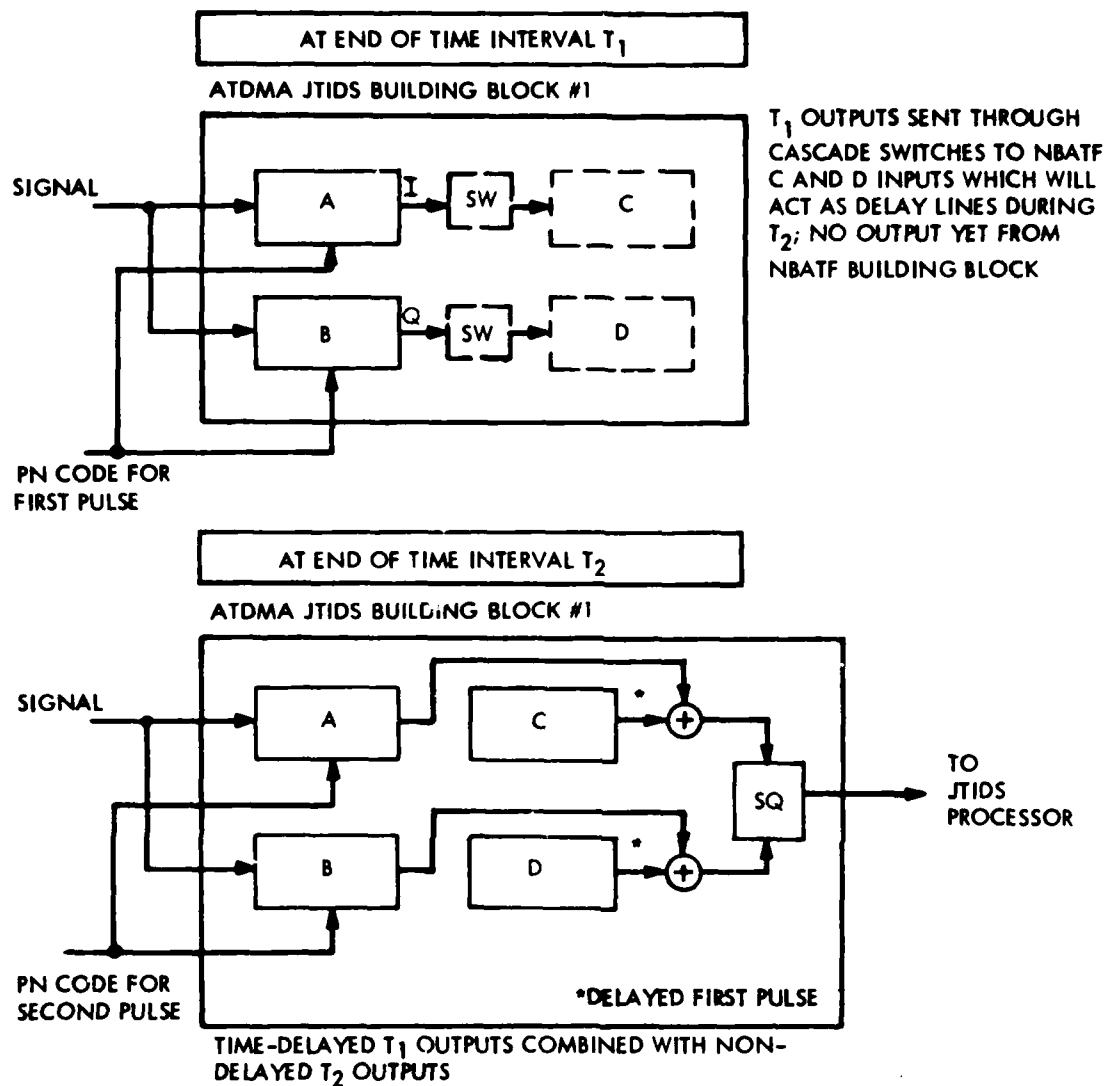


Figure 48. NBATF configuration, ATDMA/TDMA data mode

During DTDMA data pulse detection, there is no reduction in simultaneous channel requirements, as with ATDMA or TDMA, because the distributed nature of the DTDMA message requires the same number of channels for both sync and data detection. Thus, DTDMA JTIDS always requires 2 NBATF building blocks. Figure 49 shows this NBATF configuration.

#### 3.5.3.2 GPS NBATF's

GPS requires 1 NBATF building block (4 NBATF's). This is because: the system must track 4 different satellites simultaneously (same  $L_1$  or  $L_2$  frequency, one at a time, but with different PN codes); and with I and Q processing required for each separate signal. Normally, four individual correlators (equivalent to 4 NBATF building blocks) would be required for this function. With the MFBARS design, however, a single NBATF building block is adequate due to the high speed agile time-sharing capabilities of the NBATF's. One time-shared NBATF building block can produce equivalent performance to four conventional non-time-shared correlators for the four GPS signals of interest.

Note that the GPS signal PN chipping rate is 10.23 MHz, which is not a simple integral relationship to the 5.0 MHz JTIDS PN chipping rate. Thus, a different clock input rate must be used for GPS than for JTIDS. This is one of the advantages of using CCD-type devices for the NBATF's, as they can accept variable input clock rates without processing degradation. Figure 50 shows this NBATF configuration.

#### 3.5.3.3 TACAN NBATF's

TACAN requires 3/4 of one NBATF building block (3 NBATF's). Two NBATF's are used for I and Q processing of the hard limited output of the log video amplifier. One NBATF is required for processing of the log video output of the log video amplifier, as only amplitude information is required, with no phase information required. For either case, the tap weights are shaped to allow the NBATF's to function as matched filters for TACAN pulses. Figure 51 shows this NBATF configuration.

#### 3.5.3.4 IFF NBATF's

IFF requires 3/4 of an NBATF building block (3 NBATF's). One NBATF is required to process incoming IFF messages from an external interrogator platform. Two NBATF's are required for processing incoming IFF replies to own-platform IFF interrogations. Figure 52 shows this NBATF configuration.

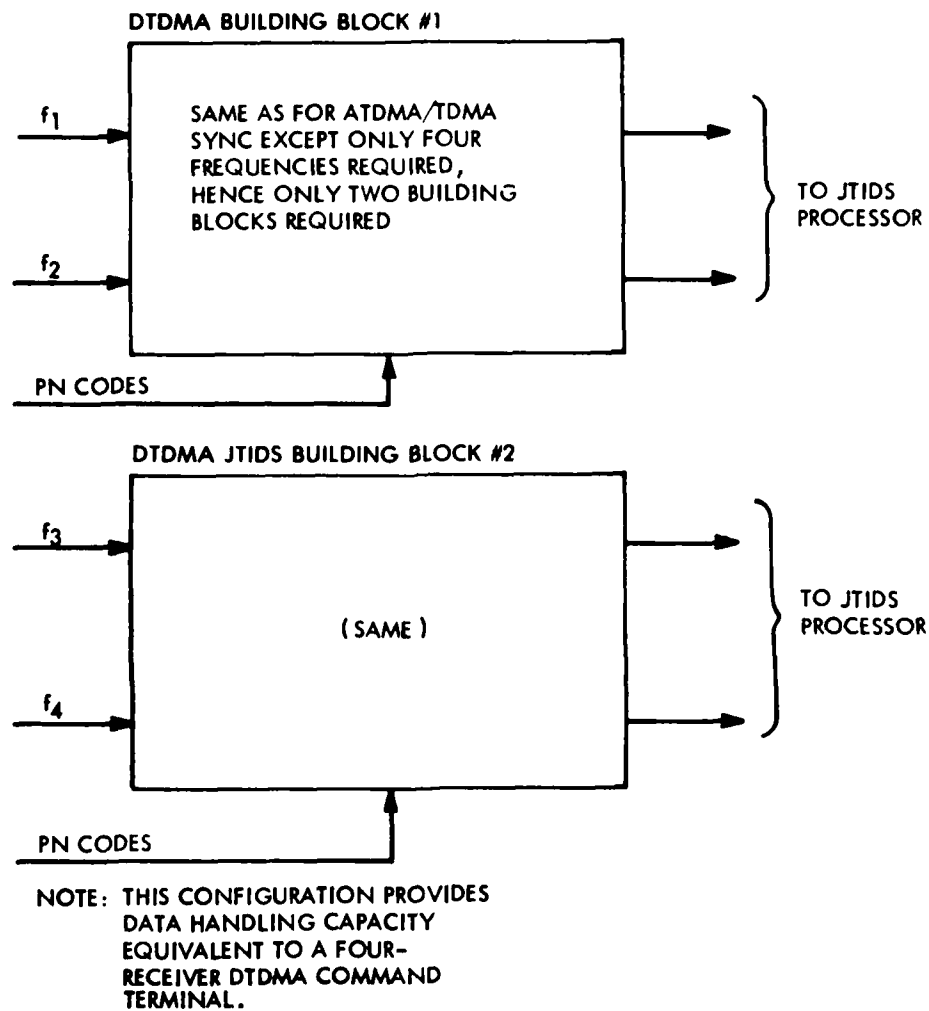
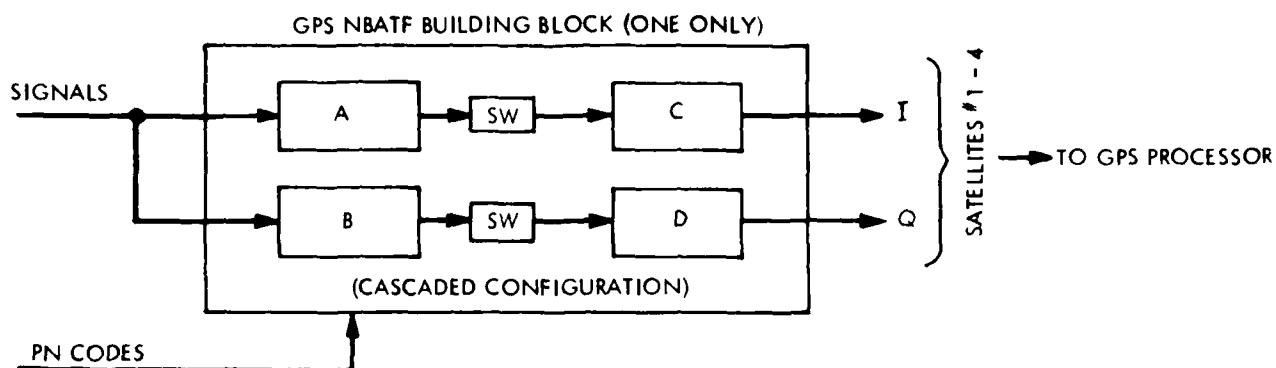


Figure 49. NBATF configuration for JTIDS DTDMA, both sync and data modes



- NOTES: (1)  $CLOCK = 10.23 \times n$  FOR GPS PROCESSING  
 (2) PN REFERENCE CODES WILL BE AGILELY CYCLED TO PROVIDE SIGNAL PROCESSING CAPACITY EQUIVALENT TO FOUR CONVENTIONAL GPS CHANNELS.

Figure 50. NBATF configuration, GPS

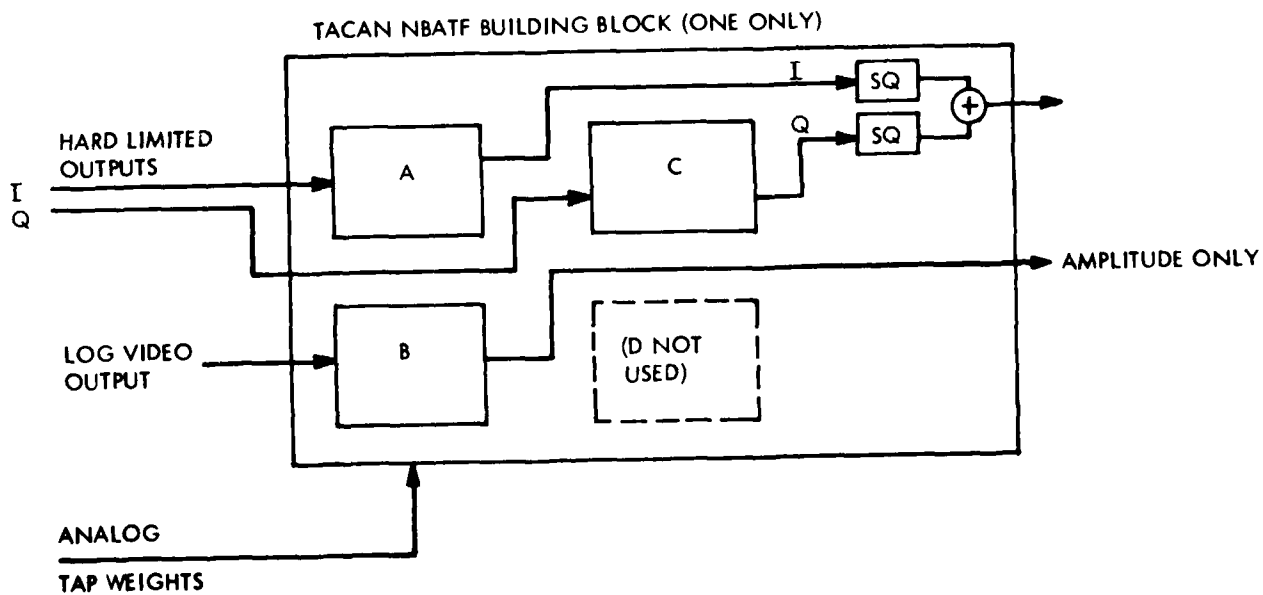


Figure 51. NBATF configuration, TACAN

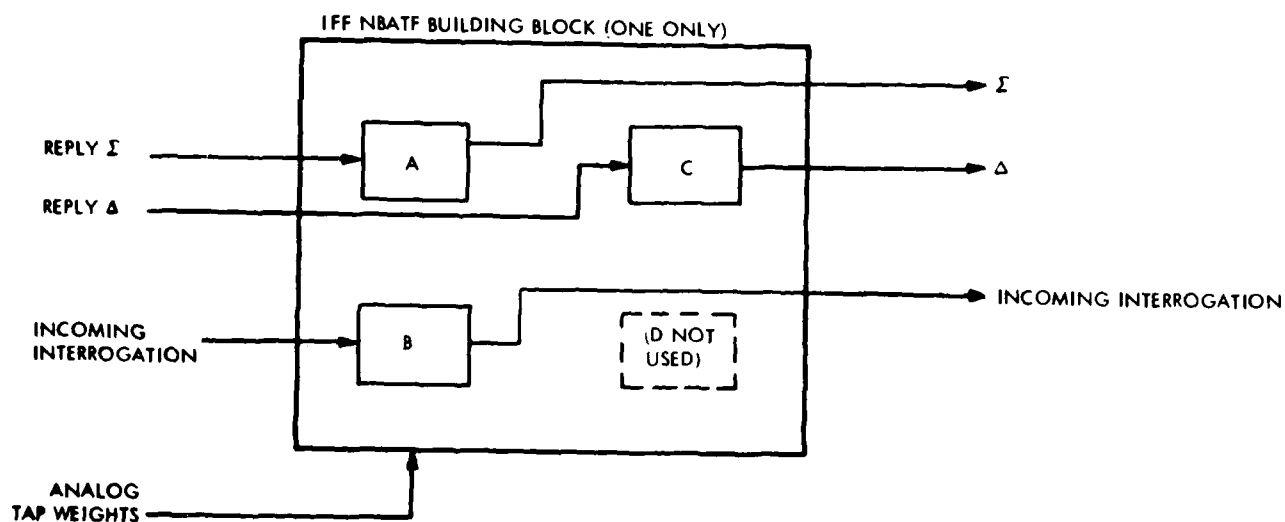
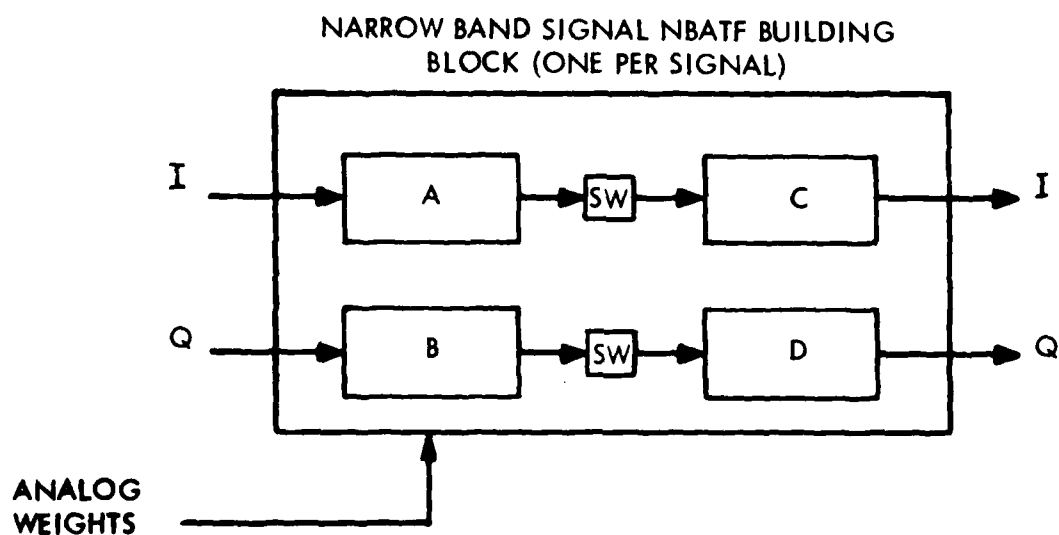


Figure 52. NBATF configuration, IFF



(CASCADED CONFIGURATION, WITH INPUT CLOCK CHANGED TO  $\sim 8$  MHZ TO PROVIDE  $\sim 50 \mu\text{SEC}$  DELAY THROUGH CASCADED DELAY LINES)

Figure 53. NBATF configuration, narrowband signals



When some other platform is acting as an interrogator, the incoming IFF pulsed signals will be received by an omni antenna and will be processed as a single-channel input signal. Therefore, only one NBATF is required for transponder operation. For the situation where the MFBARS' own platform is acting as the interrogator, return responses from a (friendly) external transponder will require parallel two-channel sum ( $\Sigma$ ) and difference ( $\Delta$ ) processing of the signals received by the own platform IFF differential antenna elements. In this case, two NBATF's are required, one for IFF  $\Sigma$  input and one for IFF  $\Delta$ .

For either case, only log video amplitude detection is processed by the NBATF's. The tap weights of the IFF NBATF's are shaped to allow the NBATF's to function as matched filters for IFF pulses. Some care is required in doing this. First, the bandwidth of the IFF pulse spectrum is relatively wide, due to the narrow IFF pulse width. This means that the matched filter impulse pulse width is also small, implying that only a relatively small number of the available taps in the NBATF should be used. This being the case, it is very important that the taps used are the very first taps of the filter, without waiting for full propagation of the input signal through the entire length of the NBATF. This is because there is a critical timing requirement of about 2 microseconds for the start of a reply after an interrogation has been received. Using later taps would not change the filter characteristic but does introduce a proportional group delay factor. This delay, if excessive, could make it impossible to meet the response time requirements.

#### 3.5.3.5 SEEK TALK NBATF's

NBATF requirements for SEEK TALK can only be estimated at this time, as critical SEEK TALK design information has not yet been released by the Government. The factors affecting the number of NBATF's required include final design information on: spreading function, modulation technique, range window, number of parallel audio output channels, command message override technique, and other factors. For purposes of this phase of MFBARS, an upper limit of 4 NBATF building blocks (16 NBATF's) was assumed and was used for preliminary system sizing computations.

### 3.5.3.6 NBATF Requirements for Narrowband MFBARS Signals

All other signals are narrowband signals, requiring one NBATF building block (4 NBATF's) per signal. Each building block is configured as a double-length cascaded set of NBATF's, with parallel I and Q channels for each. Figure 53 shows the NBATF configuration for narrowband signals. They include:

- Three parallel VHF/UHF comm channels
- One VHF/UHF nav channel (four time-shared ILS/VOR navigation signals)
- AFSATCOM (some platforms)
- SINCGARS (some platforms)
- VHF FM homing (backup nav)
- VHP AM ADF (backup nav)
- UHF AM ADF (backup nav)

For the narrowband signals, the input clock is adjusted to approximately 8 MHz to provide about 50 usec of delay time through the cascaded NBATF's ( $2 \times 195 = 390$  taps). This provides the narrowbanding required to go from 5 MHz input bandwidths to 25 KHz output bandwidths. Filter taps are adjusted to provide optimum filter characteristics for the narrowband signals.

### 3.5.4 Code Generators

Several system functions included in MFBARS such as JTIDS, GPS, and SEEK TALK use pseudo-random noise (PN) generators to perform spectrum spreading of transmitted signals to increase A/J performance. An advanced technique of PN generation is under consideration for MFBARS, as described in the following paragraphs. This technique provides an easier means for timesharing through providing code in word groups rather than in bit streams.

PN generators most often use linear feedback shift registers to produce binary PN code sequences. This technique is shown in Figure 54. The modulo-two summer operates on a set of feedback taps selected by closing some prearranged number of tap switches ( $s_1-s_n$ ). The binary result is used to drive the input of the shift register. Unique non-repeating codes of maximum length ( $2^n-1$ ) can be produced in this fashion. One difficulty with this approach is that it is not easily timeshared because to preset the generator to an arbitrary state in the code sequence requires either complex computation, or presetting to an epoch state and sequencing the generator to the desired state. The first approach is undesirable due to the complexity of extra hardware (or software) required to perform the calculation, and the time required to make the calculation. Similarly, the second approach requires considerable time to advance the shift registers to their desired state.

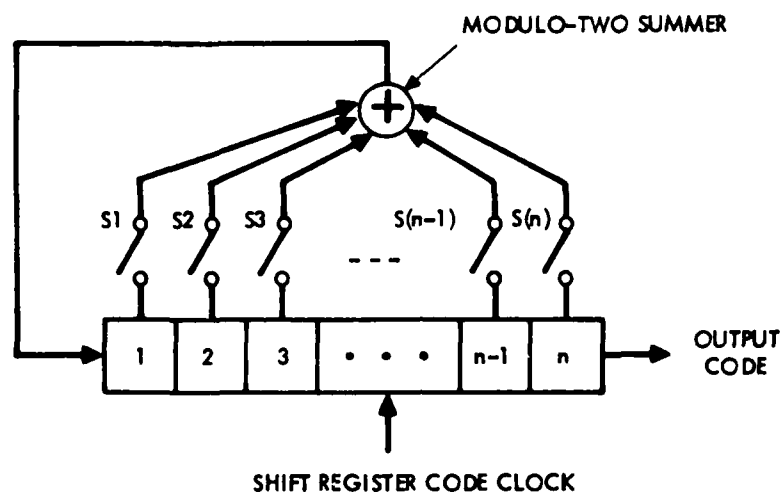
With the advent of inexpensive digital memories, a more direct solution to this problem is to store the entire code sequence ( $2^n-1$  bits) in a digital memory. Then, it is not necessary to generate the code, since it is immediately available by appropriate addressing. Since the code is stored in time sequence, to begin producing code at any particular state requires an address proportional to the code/time state. This situation is depicted in Figure 54.

Another advantage of the digital memory approach is that segments (words) of code may be extracted from the memory during a single read cycle. The size of the word depends on the organizational structure of the memory. But as the word size gets larger the access rate decreases for the same output code rate. Therefore, the digital memory generator can produce more code at a given clock rate than the conventional approach.

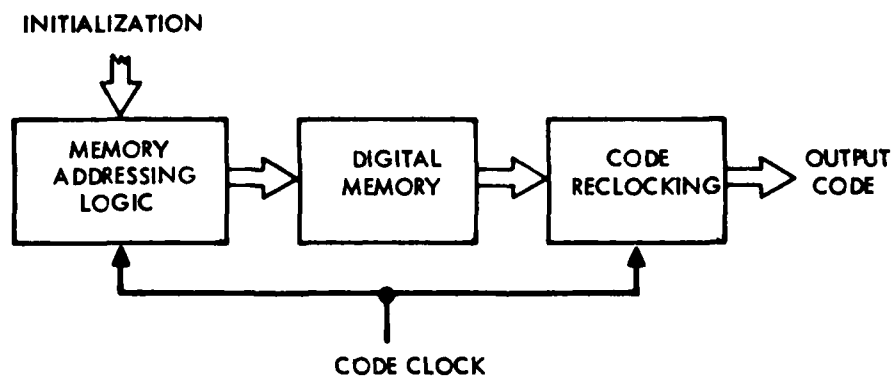
Although the code structures are not completely defined for all spread spectrum systems under consideration for MFBARS, analysis for GPS has indicated that there is a (approximately) 50 percent savings in hardware for a full four channel code generator using the digital memory code generator concept.

### 3.5.5 Special Purpose Dedicated Signal Processors

There are several hardware elements in the Signal Processing Subsystem which are dedicated to processing of one specific type of signal. This is because unique signal characteristics or other factors make time-sharing or use of a general purpose processor non-cost-effective. This section describes the special purpose dedicated signal processors.



A) THE CONVENTIONAL PN CODE GENERATOR



B) THE DIGITAL MEMORY CODE GENERATOR

Figure 54. PN code generator designs

### 3.5.5.1 GPS Processor

The function of the GPS processor is to receive signals from at least four earth satellites, measure the relative propagation time to determine pseudo-range to each of the satellites, and compute a three-dimensional position of the receiver with respect to the earth and derive accurate time. All satellite transmissions are continuous PN BPSK coded signals on the same two center frequencies, termed  $L_1$  and  $L_2$ . Various satellite signals are differentiated from one another by the structure of their PN codes.

Figure 55 is a simplified block diagram of the GPS receiver processor. The  $L_1$  and  $L_2$  signals are provided from the antenna coupling system which performs a chip matched filtering operation and establishes the system noise figure. The  $L_1$  and  $L_2$  signals are diplexed together and amplified in a common RF amplifier. This amplifier provides 120 dB of gain and +20 dB gain control. Analysis of nominal received signal levels for all satellites only produces a gain variation of 2 dB between isotropic antennas; however, at least 40 dB might be encountered under extreme fading conditions. Since the AGC amplifier operates on all signals simultaneously, an additional AGC system will be implemented in software to normalize the individual signal amplitudes.

After amplification, the  $L_1$  and  $L_2$  signals are separated again in a diplexer and one or the other is selected by a PIN diode switch. The normal mode of operation will be to dwell on the  $L_1$  frequency about 90 percent of the time, and regularly switch to the  $L_2$  frequency for ionospheric refraction correction measurements for the remaining 10 percent of the time.

The sum of the in-view satellite signals enter the GPS NBATF's simultaneously, and by rapid rotation of four selected PN codes in a high speed timesharing fashion, process the selected signals without significant signal-to-noise ratio degradation. The output of the GPS NBATF's produces a timed sequence of I&Q baseband correlation functions for the selected signals (only one function is shown in the figure for simplicity). These correlation pulses may be sampled and processed to perform carrier phase/frequency tracking, code timing tracking, data extraction, and AGC processing. Each pulse will be sampled (I&Q) at the expected peak, as well as either (approximately) 50 nanoseconds early or late. Consecutive samples will dither between early and late correlation time, comparing the resultant samples which, if equal, imply perfect straddling of the correct pulse position.

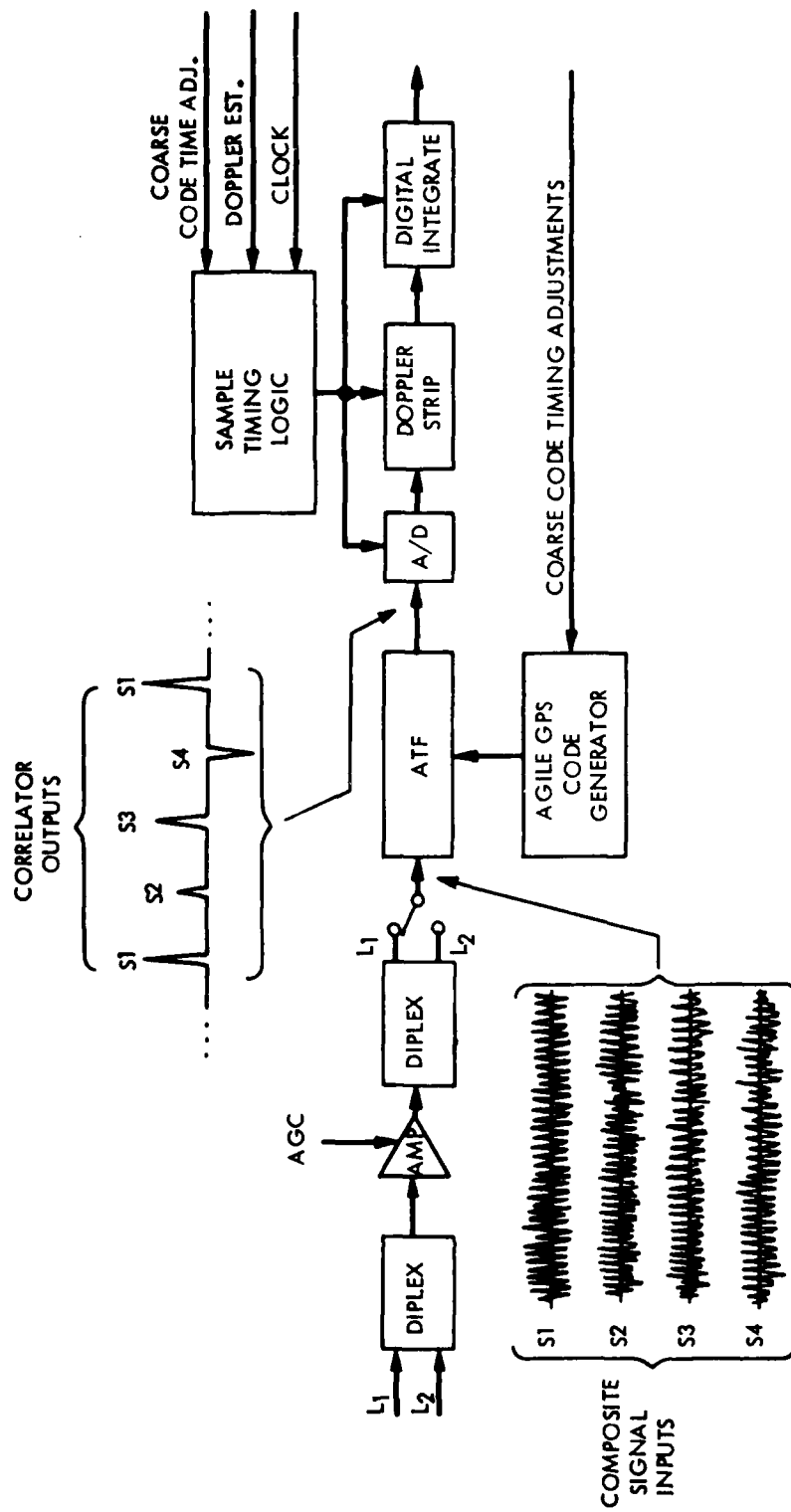


Figure 55. GPS receiver processor block diagram

Imperfect straddling produces an error voltage which is used to drive a code tracking loop, implemented in software.

In general, each of the selected satellite signals will arrive at the receiver with an independent Doppler shift due to the dynamics of the satellites and the platform. This Doppler shift was of no great significance to most of the systems used in MFBARS because their final detection bandwidth was large compared to the Doppler offset. For GPS, however, the carrier tracking loop bandwidth may be a small fraction of 1 Hz while the worst case total Doppler shift could approach 10 KHz. Therefore, the Doppler shift causes the amplitudes of the correlation pulses at the NBATF output to beat at the Doppler frequency. Doppler shift cancellation circuitry, which is similar in function to the baseband converter, is used to correct for this. Figure 56 shows this circuitry.

In addition to Doppler stripping, some intermediate integration of the samples is desirable before sending the samples to a digital processor. This intermediate integration further enhances the signal-to-noise ratio and relieves the input processing burden to the computer interface. As shown in figure 56, the I&Q output of the NBATF's will be discrete time in nature and will be filtered by low pass filters to produce a continuous correlation function. The correlation functions are then provided to a set of four A/D converters. Four converters were chosen because there are exactly four samples required on each correlation pulse. That is, I&Q carrier samples (at the peak), and I&Q code samples (either early or late). Only two A/D converters could have been used, but then they would have to be able to perform a conversion in real time (50 nanoseconds). With the four converter approach, the conversion time is reduced such that a 12-bit converter with a 3 usec conversion time is adequate.

The switches at the input of the multipliers in Figure 56 select alternately the two input terms required (compare with the baseband converter function, as described in section 3.5.1) while the switch from the Doppler frequency generator alternately provides the appropriate sine or cosine term. The accumulators following the multiplier sum the results of the two multipliers.

The digital integrator consists of four sets (for four satellites) of four, sixteen bit word memories (one per satellite) which keep the samples separate, and provide for summation of consecutive samples until they are transferred to the computer for further processing. The digital

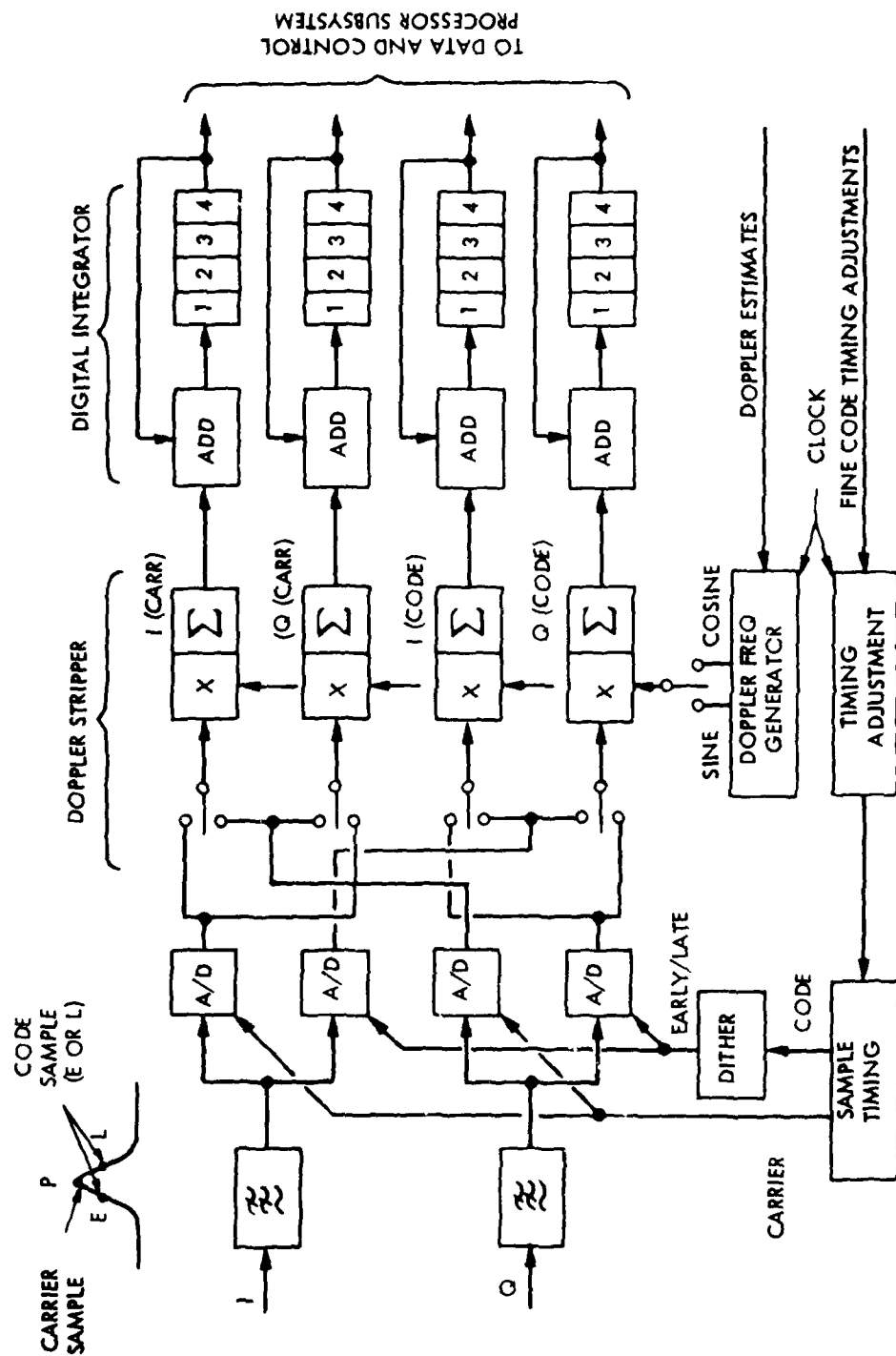


Figure 56. GPS signal processor block diagram



computer interface rate places an upper limit on the bandwidth of the various tracking loops implemented in software. It also puts a limit on the resolution of the BPSK 50 Hz data recovery timing. For these reasons a computer interface rate of 1 KHz per integrator has been chosen.

As the satellites and the platform move about in space, the times of arrival of the correlation pulses move about. The tracking loops in the digital computer strive to keep the carrier samples timed to the peaks of the pulses. Fine adjustments in the times of occurrence of the samples are provided by timing adjustment circuits which shift the phase of the signal triggering the sample timing circuits. In order to meet the accuracy requirements of the GPS specification, the resolution of timing adjustment circuits should be less than 10 nsec, preferably 5 nsec. Coarse adjustments of PN code timing may be obtained by causing the code generator to advance or retard one chip of code. This will keep the time of occurrence of consecutive correlation pulses regularly spaced regardless of how the signal dynamics change.

#### 3.5.5.2 JTIDS Processor

The JTIDS processor contains all the dedicated hardware necessary to perform JTIDS signal transmission and reception. (The details which follow are for ATDMA/TDMA JTIDS, which represents worst case JTIDS processor requirements; DTDMA JTIDS would be less complex.)

Figure 57 is a simplified block diagram of the JTIDS signal processor. The processor requires a time reference from the MFBARS system clock. The system timing drives the slot control function which creates the JTIDS-peculiar timing signal associated with the time division multiplexed structure of ATDMA/TDMA JTIDS.

In the receive mode, time compressed JTIDS pulses from the NBATF Assembly (for data) or from a wedge delay line (for sync, as described in the following section) are provided to a threshold detector and time of arrival (TOA) measurement circuit. During reception of the sync preamble the TOA measurement is used to establish a time reference to strobe the data pulses as they are received. In the data mode the TOA measurement is interpreted as a character detection process. That is, the TOA could fall into any one of 32 (200 nanosecond wide) time slots, each time slot corresponding to one of 32 characters. The receive event controller supervises this process.



The detected character is then sent to receive interleaving storage. This is basically digital memory which stores the characters as they are received in sequential addresses. They are then read out in accordance with a prescribed pattern. Since this pattern was used to scramble (interleave) the characters before they were transmitted, this receive process unscrambles the character string. The deinterleaved characters are then sent to the Reed-Solomon (R-S) decoder. The decoder removes parity characters from the string that were originally inserted by the R-S encoder at the transmitter. These extra characters are used to detect and correct errors. The remaining decoded character data is then routed to the Secure Data Unit (SDU) control, then to the SDU for baseband decryption, and back to the SDU control where it is stored as a block of data. Finally, the data is transferred to the MFBARS computer system through the data processing I/O circuits.

In the transmit mode, the operation is essentially the reverse of the receive process. Data is transferred from the MFBARS computer system through the data processor interface to the SDU control. It then passes through the SDU for baseband encryption, and is sent back in the SDU control. From there it is routed to the R-S encoder and on to the transmit interleaved storage where the characters are scrambled. Next, the five bit characters are sent to the Cyclic-Code-Shift-Keyed (CCSK) encoder which transforms each character into a 32 bit binary code sequence. Then these codes are sent to the SDU control, the SDU, and back to the SDU control. This second pass through the SDU superimposes a 32 bit PN code on the CCSK encoded data for the purpose of TRANSEC (spectrum spreading). At this time, the slot processor is going through a frequency selection algorithm, to choose a set of pseudo-randomly selected frequencies for transmission. The selected frequencies together with the TRANSEC encoded data is provided to the parameter storage function. When the transmit event controller receives a transmit command it extracts the contents in parameter storage and sends the data to the L-Band transmitter.

Built-in-test equipment implemented primarily in software, creates self test events which are processed by the common hardware to check system health.

### 3.5.5.3 JTIDS Wedge Delay Line

A wedge delay line is required for JTIDS (ATDMA/TDMA only; not required for DTDMA). Its function is to integrate 32 pulses of the ATDMA/TDMA JTIDS synchronization preamble which precedes the message in every ATDMA/TDMA JTIDS time

slot. The integrated pulses are used for synchronizing a data strobe to optimally recover the information contained in the data pulses following the sync preamble.

Figure 58 is a simplified block diagram which demonstrates the principle of ATDMA/TDMA JTIDS sync. The 32 sync pulses are evenly spaced in time, and are detected by a matrix of JTIDS code correlators within the NBATF Assembly. The code correlators are connected to the wedge delay line which can be visualized as a shift register with equally spaced taps. The order of interconnection is such that the first pulse detected is fed to the earliest (longest delay) tap of the shift register, the second pulse detected is fed to the next to longest delay tap, and so on until the last pulse is connected to the tap with the shortest delay (or no delay at all). If the time delay between taps is exactly equal to the time delay between the occurrence of successive pulses, then the first pulse previously introduced at tap 1 will add to pulse 2, which is then introduced to the delay line at tap 2. The third pulse then adds to the first and second as they arrive at tap 3, and so on until the output of the delay line (shift register) is the simultaneous sum of all 32 pulses.

There are many different ways to implement the wedge delay line. If a binary shift register is used as the wedge delay line, as shown in Figure 58, it implies that a decision as to whether an individual pulse has been detected or not must be made at the output of each correlator. This decision is equivalent to a hard-limiting function at the correlator outputs. Since non-linear operations tend to degrade noise performance, an improvement of between one and two dB in signal-to-noise ratio can be obtained by providing the correlator output video to a linear delay line and making a threshold detection and time of arrival measurement on the video integration of the 32 pulses. Besides the performance improvement, this technique also eliminates the 32 threshold detectors required in the binary integration case.

Figure 59 is a simplified block diagram of the wedge delay line. A multiplexer in the NBATF interconnects the outputs of the code correlators to the proper delay elements shown on the left of the figure. The multiplexing is performed in such a way as to cause the first 8 of the 32 JTIDS sync pulses to arrive at the first summing point simultaneously. This signal then enters the first 97.5 usec delay line.

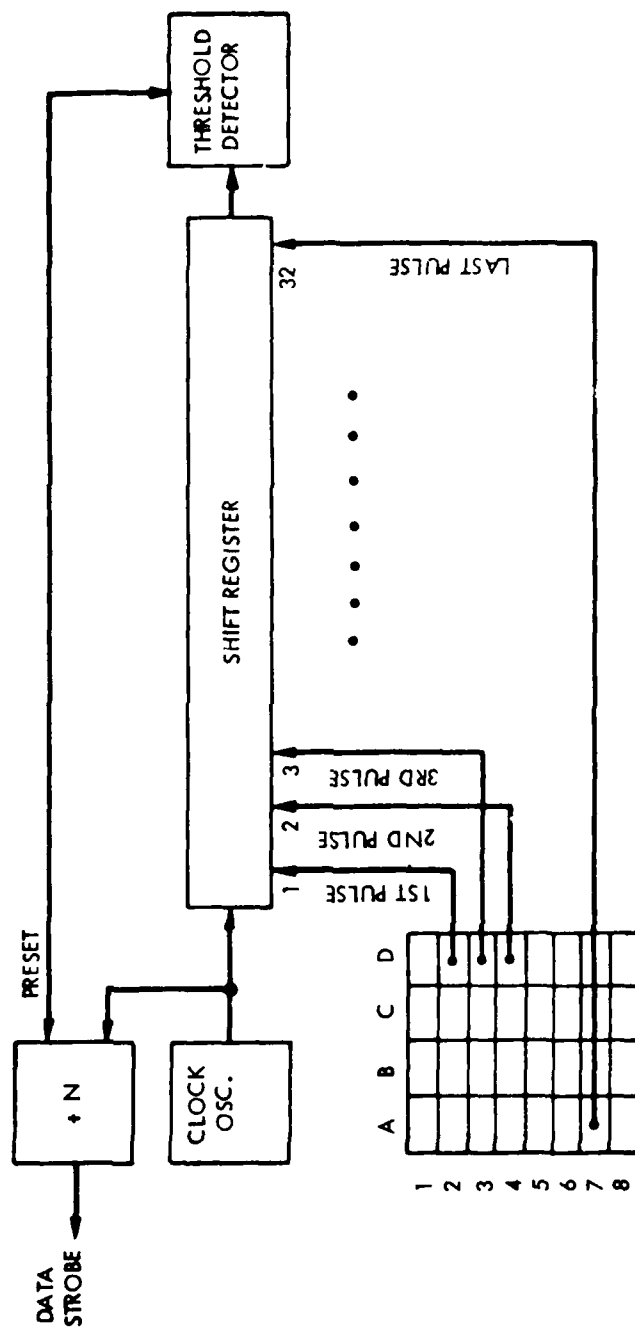


Figure 58. The JTIDS synchronization problem

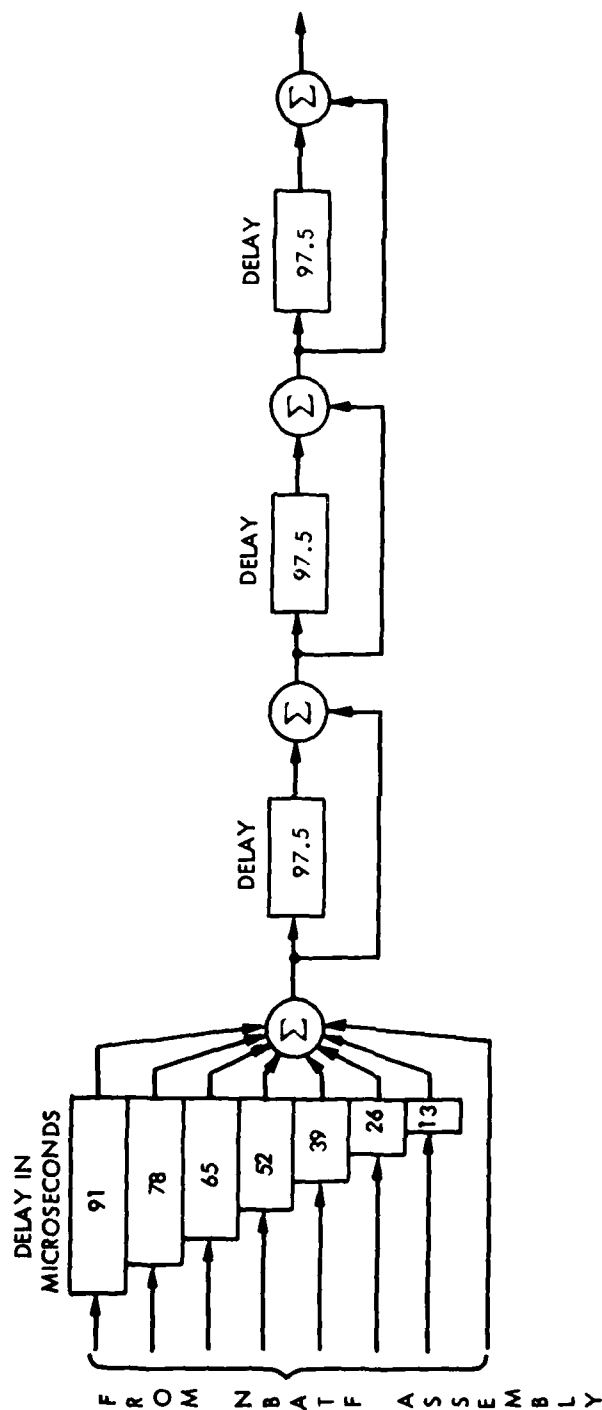


Figure 59. The wedge delay line block diagram

Exactly 97.5  $\mu$ sec later the second group of 8 sync pulses arrive at the first summing point and adds to the first group at the second summing point. The process is continued until all 32 pulses effectively arrive at the last summing point simultaneously.

One method of implementing the various delay elements is by the use of CCD delay lines. These delays are rather long in duration, however, and many stages (cells) will be required. The input clocking rate required would be 60 MHz which is determined by the agile timesharing of the NBATF's. The number of states required for each of the 97.5  $\mu$ sec delay elements is then:

$$(60 \times 10^6 \text{ Hz}) \times (97.5 \times 10^{-6} \text{ sec}) = 5850 \quad (7)$$

There are three of these and what amounts to about four more in the wedge structure on the left, so we can see that we need something on the order of 40,000 stages. Although this type of CCD would not need the complex tap weighting circuitry required for the NBATF's, this may still be a difficult task.

An alternative would be some form of SAW device, the technology employed in current JTIDS wedge delay line design. A final decision has not yet been made for MFBARS.

#### 3.5.5.4 TACAN Processor

The TACAN processor contains all the dedicated circuitry required to perform the TACAN navigation function. Only a high level functional description of the processor will be presented here because the techniques employed are well known and relatively straight-forward from an implementation standpoint.

Figure 60 is a simplified block diagram of the TACAN processor. Both the hard-limited RF and log video signals are provided to the width, time, and amplitude detection circuits. The hard limited signal produces a gating function which gates through the log-video signal when an on-channel pulse is received. This operation desensitizes the processor to off-channel (adjacent frequency bands) pulses. A further selection function is performed by a range window gate which eliminates all pulses arriving at times much different than the expected beacon reply time. In the track mode this eliminates most on-channel beacon replies resulting from other interrogators. In addition, pulse shaping is performed on the selected pulses such that their width is well defined as a digital signal. A pulse width screen passes only pulses which are approximately 3  $\mu$ sec in duration. In this way shorter IFF pulses and longer JTIDS

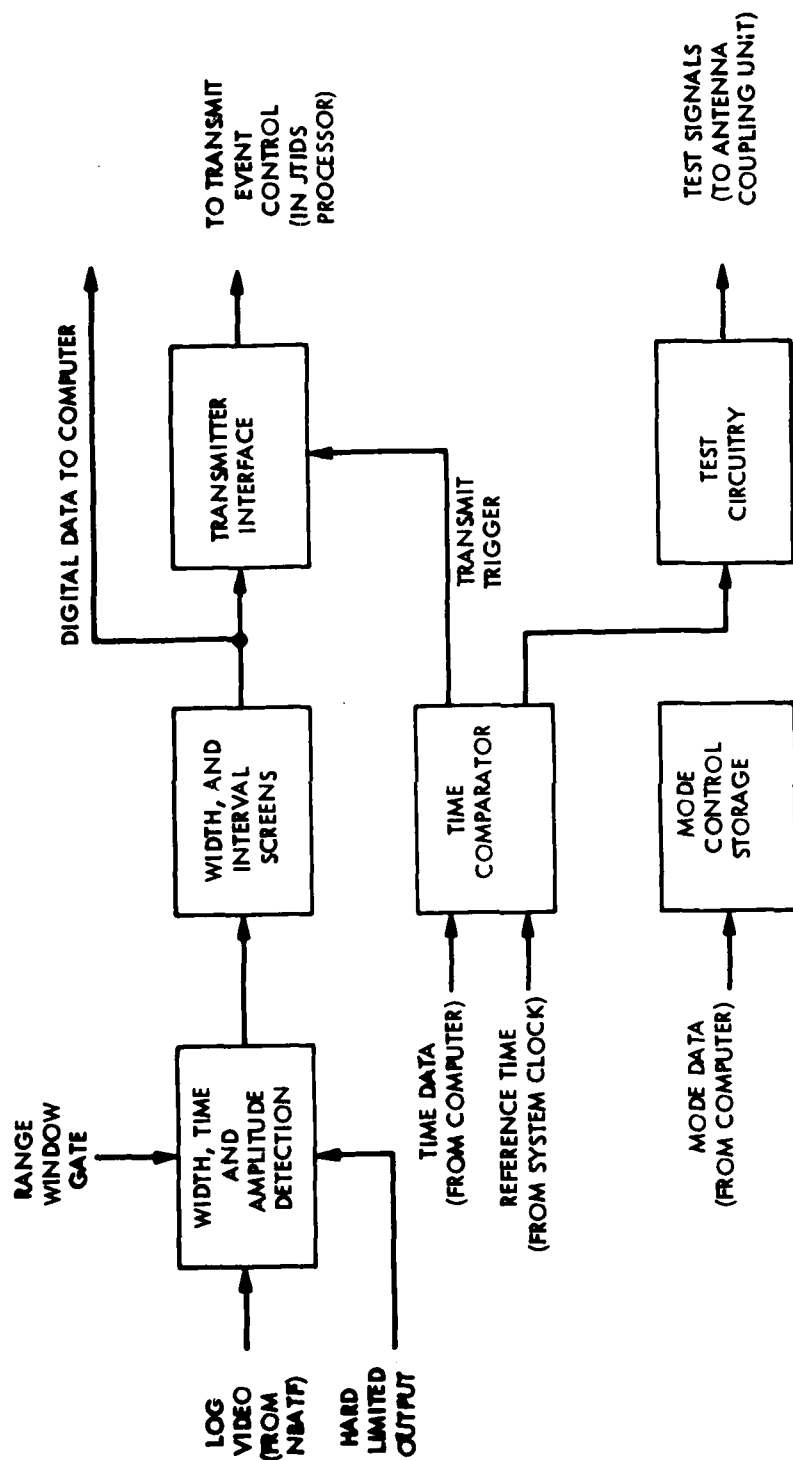


Figure 60. TACAN processor block diagram



pulses are eliminated. Finally, a pulse interval screen eliminates all pulses except those occurring in pairs with the designated spacing.

For each pulse pair that survives the screening process, there are digital words generated which define the Time of Arrival (TOA) and the amplitude. This data is then provided to the computer interface which processes it to calculate range and bearing from the aircraft to the beacon relative to true north. The computer also calculates the times of occurrence of interrogation pulses which nominally are transmitted at a 96 Hz rate during search and a 25 Hz rate during tracking. Some pseudo-random variation in the time of occurrence of the interrogations is necessary to produce a user unique pattern and reduce potential cross interference between users. Other minor adjustments in the time of occurrence are necessary such that Tacan transmit events can be scheduled around IFF and JTIDS events.

The execution of a TACAN transmit event is controlled by the time comparator circuits. The time comparator accepts inputs from the system clock, and time data from the computer. When the time data matches the system clock time a transmit trigger is generated and sent to the transmitter interface.

The TACAN processor provides continuous self test capability by scheduling test pulses which are fed forward to the antenna coupling system, and test the functioning of all circuitry in the Tacan signal processing flow path.

#### 3.5.5.5 IFF Processor

The IFF processor contains all the dedicated circuitry required to perform the IFF interrogator and IFF transponder functions.

Figure 61 shows a simplified interrogator block diagram. The IFF interrogator operates in conjunction with an APG-63 radar or similar system. The IFF mode (1,2,3 or 4) is determined by mission area operational protocol and is entered through cockpit IFF control selections. When an unknown "target" is detected by the radar, the interrogation cycle is initiated by commands from the operator and the radar control system. As shown in Figure 61, the radar trigger is applied to pulse delay circuits, and a delayed radar trigger is returned to the radar after generation of the interrogation trigger. The coder prepares the IFF interrogation in accordance with the selected mode and provides this data to the transmit event controller (in the JTIDS processor) to allow IFF interrogations to override other L-band transmissions (with the exception of IFF transponder reply transmissions which take precedence).

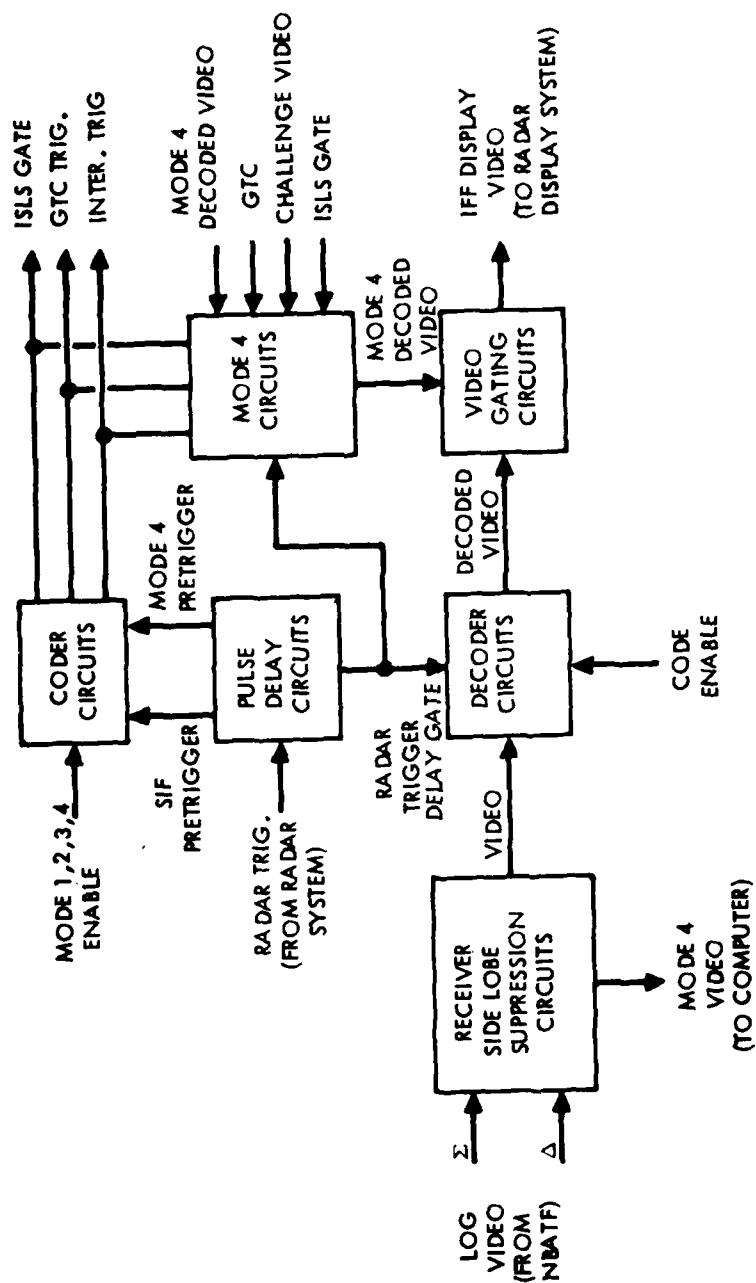


Figure 61. IFF interrogator block diagram

Since aircraft other than the interrogator's "target" may also receive an IFF interrogation message, some method of discrimination is required to reduce reply ambiguities. The interrogator utilizes sum ( $\Sigma$ ) and difference ( $\Delta$ ) pattern directional antenna elements to transmit certain pulses in a narrow beamwidth pattern and others in a wide beamwidth pattern. This technique is termed transmit sidelobe suppression. An aircraft receiving any given interrogation message compares signal strength of successive pulses to determine if the receiving aircraft is in or out of the interrogator's narrow beamwidth pattern. If in the narrow beamwidth, the aircraft replies; if out of the pattern it does not.

Since the interrogator may receive replies from aircraft being interrogated by other interrogators, as well as replies to its own interrogations, directional antenna sum and difference pattern comparisons are utilized in processing replies received by the interrogator. This technique effectively narrows the beamwidth of the directional receiving antenna, and is termed receive sidelobe suppression. In addition, range windows (controlled by the radar system) may be used to further reduce reply ambiguities. Replies received from aircraft within the narrow beamwidth pattern and within the proper range window are labeled "friend" and sent to the radar system for IFF/radar display. Lack of response from a target (after a predetermined number of successive interrogation attempts) causes the radar system to indicate "foe" on the IFF/radar display.

Figure 62 is a simplified block diagram of the IFF transponder. Log-video signals are provided to threshold detectors which determine the pulse width of incoming signals. A pulse width screen is provided to eliminate any erroneous pulse detections which are not consistent with the (approximately) 0.8  $\mu$ sec IFF pulse width. The pulse interval decoder measures the time spacing between pulses to determine the mode of interrogation. In addition, the relative amplitudes of the pulses are compared to determine whether or not the aircraft should reply (as explained above). If the aircraft should reply, a message is prepared by the reply encoder. Depending on operating mode selected, the reply message may contain aircraft altitude, ID and/or other data. The prepared reply message is then transmitted, in the appropriate mode, via the event controller (part of JTIDS), where IFF replies are given interrupt priority over other L-band transmissions.

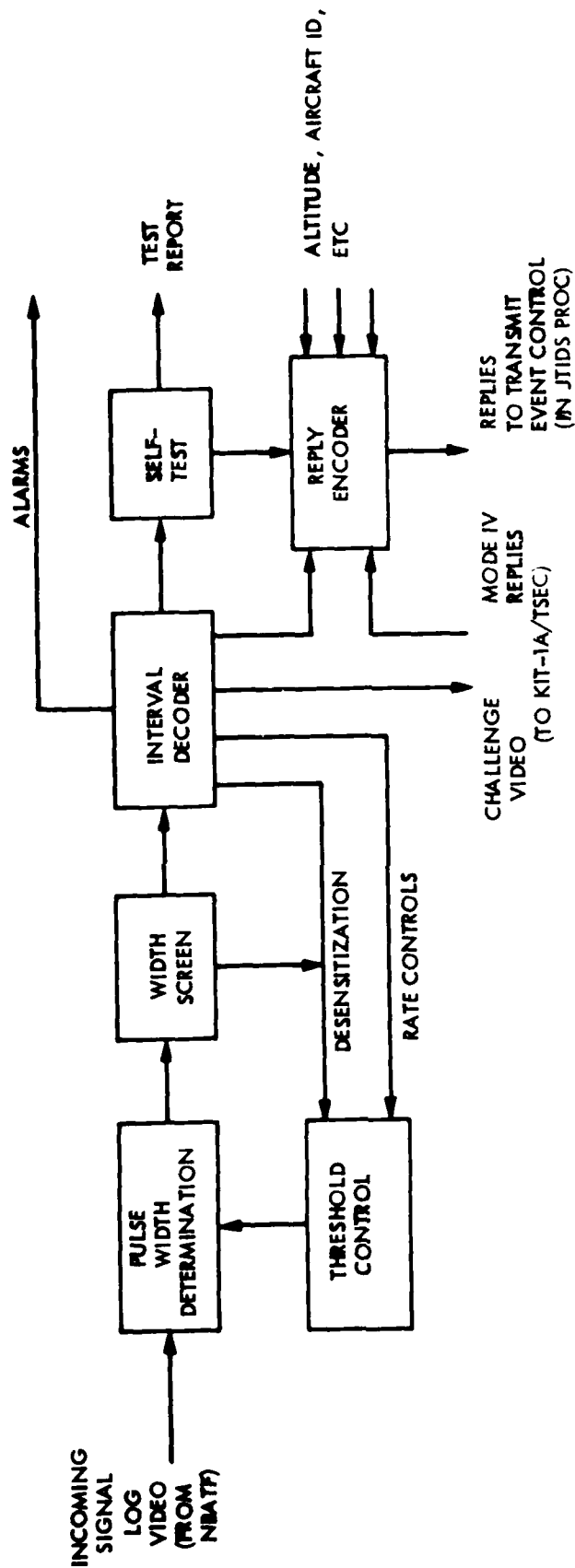


Figure 62. IFF transponder block diagram

#### 3.5.5.6 SEEK TALK Processor

Details on SEEK TALK processor design have not yet been released by the Government. Therefore, specifics must be added later. For purposes of PRICE analyses (Section 5), SEEK TALK hardware size, complexity and costs were estimated.

#### 3.5.5.7 AFSATCOM Processor

AFSATCOM processor details are to be supplied by the Government. Estimates were used for PRICE analyses. (Note that not all platforms will have AFSATCOM.)

#### 3.5.5.8 SINCGARS Processor

SINCGARS processor details are to be supplied by the Government. Estimates were used for PRICE analyses. (Note that not all platforms will have SINCGARS.)

#### 3.5.5.9 Analog Voice Processor

The function of the analog voice processor is to provide an interface with the aircraft intercom system. Figure 63 is a simplified block diagram of the analog voice processor. It is driven by outputs from the NBATF Assembly. The audio signals are, if necessary, routed to a baseband COMSEC device, such as a KY-28, for decryption. The VHF/UHF transmitter is also connected to a COMSEC interface for encryption of transmitted signals. The output I&Q squaring circuits in the NBATF Assembly provide amplitude demodulation functions. Frequency modulation/demodulation must be performed by synthesizers (previously described) and by dedicated FM detectors. The resulting detected signals are then provided to post-detection low pass audio filters and then to the aircraft intercom interface.

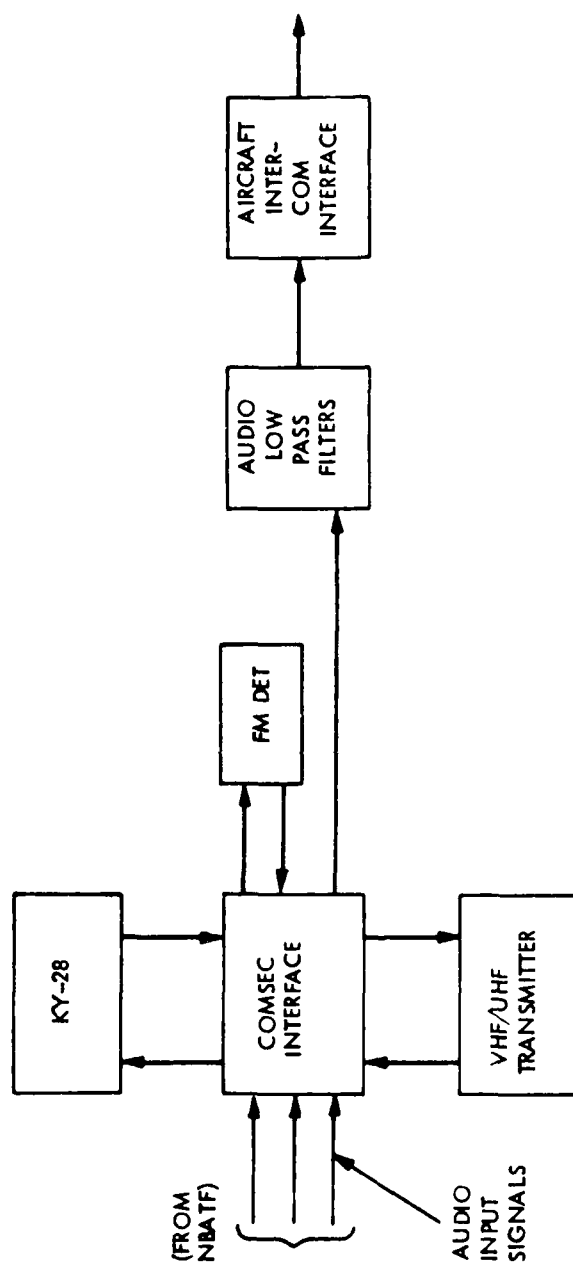


Figure 63. Analog voice processor block diagram

### 3.6 DATA AND CONTROL PROCESSOR SUBSYSTEM

The Data and Control Processor Subsystem provides six main functions for MFBARS:

- system processing
- interface (via DAIS) with externally generated control commands
- internal control of the MFBARS subsystems, in response to the externally generated control commands
- processing, formatting and routing (via DAIS, to external aircraft systems) of digital data outputs from the Signal Processor Subsystem
- formatting and routing to appropriate modulation and transmitter circuitry of messages generated on-board the aircraft for MFBARS transmission
- control of the MFBARS BITE Subsystem

The subsystem consists of a dynamically reconfigurable multiprocessor array containing:

- multiple microprocessors
- modularized main memory (in which is stored all system operating programs and the system data base)
- internal and external I/O's
- an interconnection structure

The two main reasons for selecting a multiprocessor architecture are to provide for efficient partitioning of the total MFBARS computational work load and to provide a means for fail-soft reallocation of subsystem resources in the event of failure of any element of the subsystem. Figure 64 shows the basic architecture of the Data and Control Processor Subsystem.

Specific details of the subsystem have not yet been defined. This is because there are a large number of optional multiprocessor architectures to be reviewed and many MFBARS-unique requirements to be integrated into candidate multiprocessor architectures before the best approach can be determined. Completion of these efforts is beyond the funding resources of the current contract and will be accomplished in the next phase of the program. Nevertheless, some preliminary design decisions have been made. The following paragraphs present these preliminary design decisions.

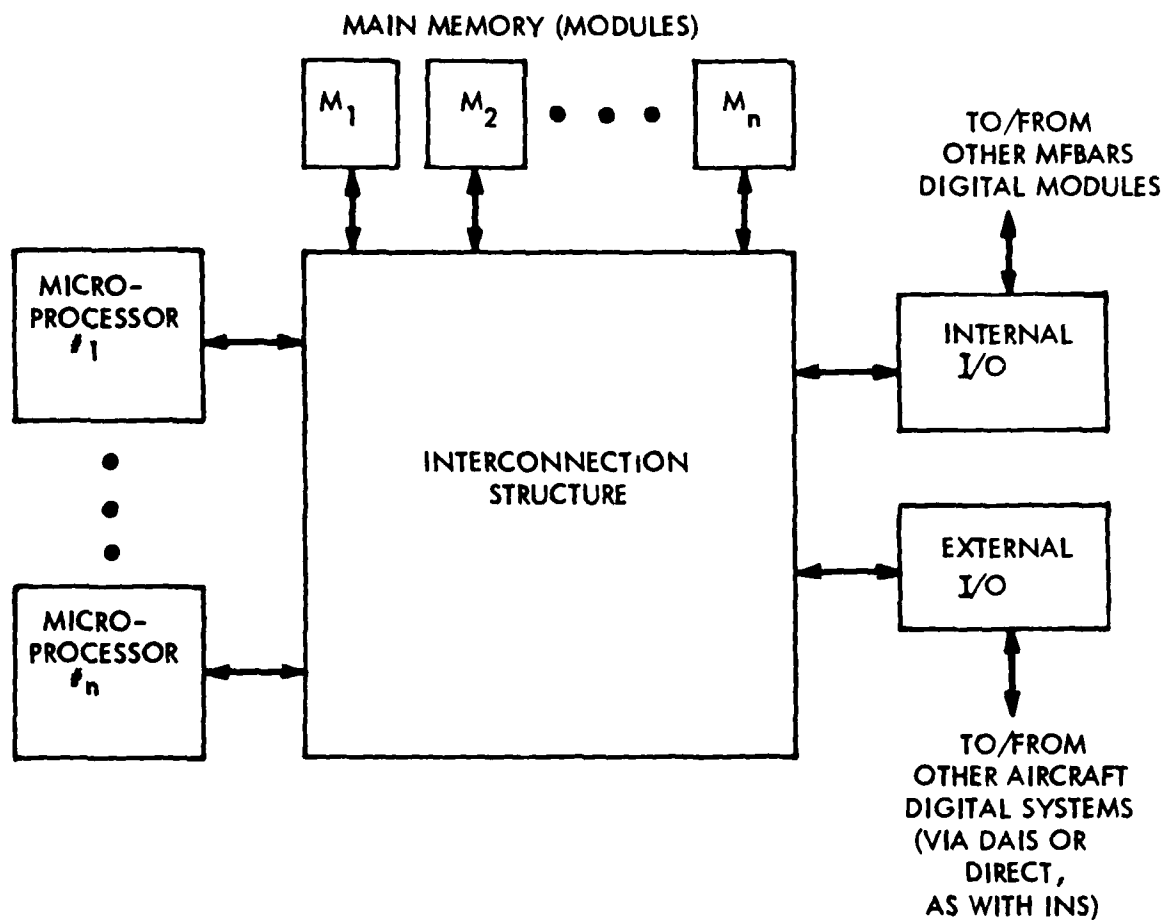


Figure 64. Data and control processor subsystem



### 3.6.1 Architecture

The basic multiprocessor architecture will be an adaptation of a tested, proven military or commercial computer multiprocessor architecture (rather than a totally new architecture), to take advantage of existing designs to reduce risk and minimize development costs. There are a number of tested, proven candidates to choose from. Although the hardware aspects of the MFBARS implementation will be quite different, the proven machines contain applicable functional designs in the areas of:

- operating system software
- memory partitioning and access techniques
- workload allocation
- failure sensing techniques
- reconfiguration techniques

Working from a proven functional design base will provide a low risk approach to this aspect of the MFBARS design.

### 3.6.2 Microprocessors

The subsystem will contain an estimated 3 or 4 advanced (1985-era) microprocessors. This projection is based on the following considerations:

- (1) Today's typical militarized microprocessor has an effective throughput rate of up to about 1 MOPS.
- (2) Processor technology has been widely projected to continue to grow at about 30 percent per year, in terms of effective throughput rate; thus, by around 1985, a conservative extrapolation of typical processor throughput capability would be almost 4 MOPS per microprocessor. VHSIC technology is expected to apply to this projected growth.
- (3) From section 3.6.6, it is seen that MFBARS processing requirements are estimated to be about 8 MOPS (including a 30 percent margin for growth).
- (4) Thus, about two 1985-era processors would be required to handle the basic projected MFBARS processing workload.
- (5) An additional one or two processors may be added for redundancy for system reliability and for further functional growth margin.

- (6) Thus, either 3 or 4 1985-era microprocessors are projected for MFBARS.

### 3.6.3 Main Memory

The subsystem will contain a modularized main memory, in which all system operating programs and the system data will be stored. The main memory will be partitioned into several memory modules. This will permit minimization of contention problems and will facilitate load leveling. There will be redundant memory for critical system functions and elements of the data base.

### 3.6.4 I/O's (Input/Output Devices)

There will be at least two I/O's in the subsystem, one for internal MFBARS digital interfaces and the other for all external interfaces between MFBARS and other aircraft digital systems (either via DAIS or directly, as in the case of INS). The I/O's may or may not be subdivided. Further study and tradeoff analysis is required before this decision can be made.

### 3.6.5 Interconnection Structure

Selection of the interconnection structure, which ties together the processors, the memory modules, and the I/O's, is the most complex design issue of the subsystem. There are three basic generic architectural approaches:

- common bus
- crossbar switch
- multi-port memory

The common bus has the advantage of simplicity of design and ease of expansion (up to some limit) for adding additional processors, memory or I/O devices. It is a relatively inexpensive and highly reliable approach. All processors would have access, through the common bus, to all main memory modules, which would facilitate load sharing and reconfiguration in the event of processor failure. The main disadvantage of the common bus approach is throughput limitations, due to contention. Also, even though highly reliable, bus failure of a common bus would cause total system failure.

The second generic approach (typified by C.mmp) is crossbar switching, in which every processor has access, via crossbar connections, to every global memory module. In this configuration, each processor can have its own local memory and dedicated I/O. The main advantage is more rapid access to the data base and the system operating programs.

Also, contention is minimized, due to local memory and I/O. The main disadvantages are system availability limitations, and difficulty in load sharing and reconfigurability because of the use of dedicated I/O's and dedicated local memories. Also, the crossbar connection hardware is expensive (currently), although 1985-era technological advances should lessen this disadvantage.

Multi-port memory solutions include a number of optional system approaches which increase the interconnection paths beyond the single path of a common bus structure without going to the extreme of complete crossbar interconnection between all processors and all memory modules. (This is the most frequent implementation used by main frame manufacturers.) Advantages of all of these approaches include: increased overall subsystem reliability and reduction of contention problems due to the multiple bus paths; and ease of expandability.

The design complexity of the interconnection structure requires considerable further study and tradeoff analysis, to be accomplished in the next phase of the program.

#### 3.6.6 Software\*

All system operating software for MFBARS is stored in main memory of the Data and Control Processor Subsystem. A preliminary estimate of MFBARS software is given in Table 8. Detailed software definitions will be part of the next phase of the program.

\*Since software will be stored in (depot level replaceable) ROM's, it could more precisely be referred to as "firmware", but the more generic term "software" is used in this report, for convenience.

TABLE 8. SOFTWARE REQUIREMENTS (PRELIMINARY ESTIMATE)

	<u>KOPS</u>	<u>Memory (Bytes)</u>	<u>Comments</u>
1. Multiprocessor Operating System	850	40K	
2. Application Programs			
JTIDS	1400	256K	DTDMA/TDMA (worst case)
GPS	870	46K	Draper Labs projection
SEEK TALK	480	30K	Estimate
AFSATCOM	460	50K	Estimate
Nav	470	60K	
Comm	400	20K	
Data Base	-	256K	
3. Support Programs	1100	60K	AGC, math routines, etc.
Subtotal	<u>6030</u>	<u>818K</u>	
4. Growth Margin	1810	245K	30% (typical design margin)
Total	<u>7840</u>	<u>1063K</u>	
<p>Estimated* Instructions = <math>\frac{\text{Total Bytes} - \text{Data Base}}{2.4}</math></p> <p style="text-align: center;">= <math>\frac{1063 - 256}{2.4}</math> K = 336.25K</p> <p>*Based on JTIDS experience of average instruction length of 2.4 bytes/instruction</p>			

### 3.7 BITE SUBSYSTEM

The BITE Subsystem is a major subsystem of the selected MFBARS system architecture. It contains both analog and digital test signal generators and analog and digital monitoring and evaluation circuitry to maintain a constant check on system health. It is under control of the Data and Control Processor Subsystem for normal automatic, periodic system checkout. Also, operator initiated action can activate BITE checkout routines for fault isolation of known or suspected out-of-limit performance. Working in conjunction with the Data and Control Processor Subsystem, detected failures can be bypassed or minimized by reconfiguration of the system. Memory elements within the BITE subsystem will provide a record of detected failures to aid post-flight system maintenance.

Analog and RF circuitry will be checked by means of test tone generators, receive and transmit signal strength measurements, and VSWR measurements. Digital circuitry will be checked by means of digital test words, as well as monitoring of parity bits and other digital checks built into message structures.

The special purpose processors in the Signal Processing Subsystem each have built-in digital test words and logic checks which enable self-test during normal operation and automatic fault indication reporting when a fault is detected.

The Data and Control Processor Subsystem has built-in test sequences for self monitoring and checkout of digital command and data flow between itself and other MFBARS subsystems and external aircraft digital systems (e.g. DAIS bus interface).

Details of the BITE Subsystem have not been completed. Table 9 summarizes the BITE function for one subsystem, the RF Subsystem. An example of one of the monitoring circuits follows. Other details and other subsystem BITE functions will be defined in a future phase of the program.

Figure 65 illustrates a typical circuit for one of the RF BITE monitors, the bottom L-band antenna for JTIDS. Monitor coupler No. 1 includes three directional couplers, one for sampling the forward signal (in transmission), one for the reflected signal, and one for coupling a low level signal into the line back to the receiver.

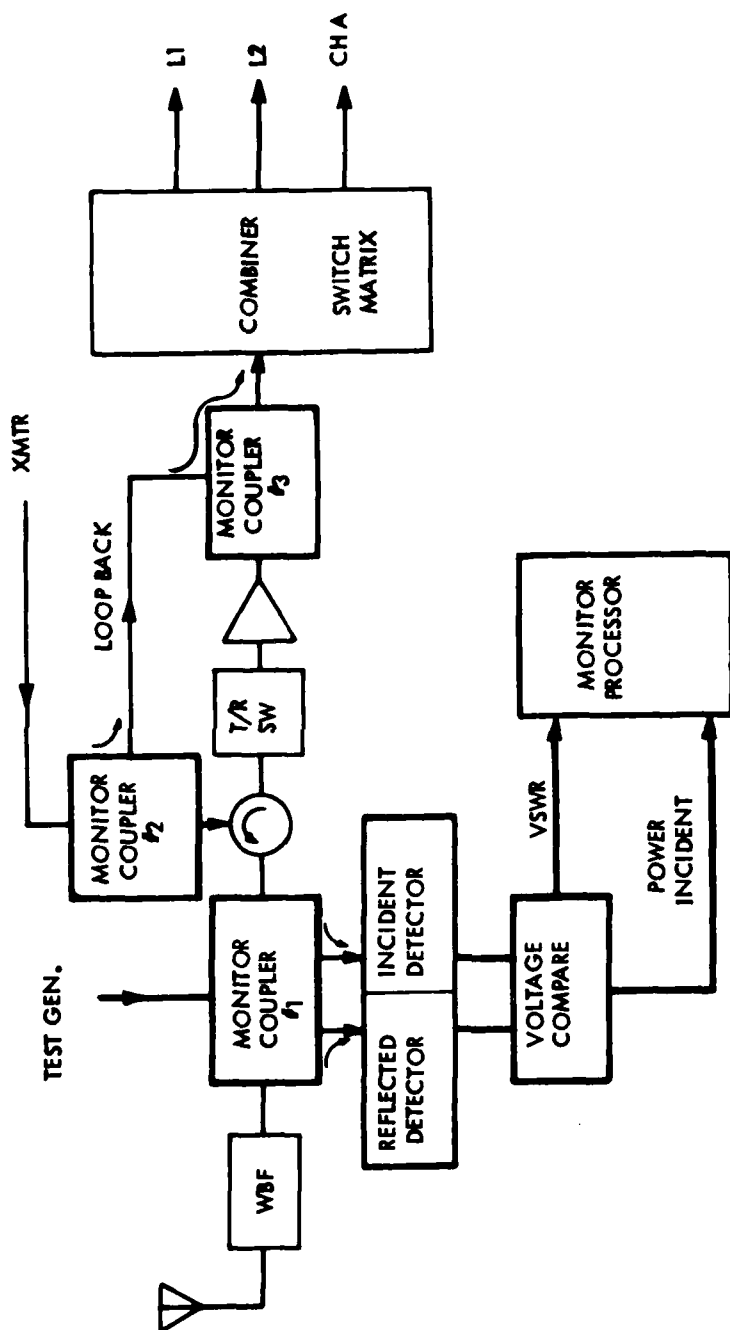
The incident and reflected signals are compared to measure antenna VSWR, and the incident signal is used directly for

TABLE 9. RF SUBSYSTEM BITE FUNCTIONS

Test or monitor	Function	Monitor location(s)	Action in case of default	Comment
VSWR	Monitor Antenna VSWR	Top L-Band Ant., Bottom L-Band Ant., IFF Interr. Ant.	Turn Off X-Mitter Power Amplifier IF VSWR >3:1	
Power Monitors	Monitors Transmitted Power	Top L-Band Ant., Bottom L-Band Ant., IFF Interr. Ant.	Alarm IF Transmitted Power Outside of Allowed Limits	
Overheating	Monitors Transmitter Power Amplifier Temperature	X-Mitter Power Amplifier	Switch to Lower Power Mode if preferred otherwise Alarm	
Pulse Width	Monitors Width of Transmitted Pulse	At Logic Lines which Drive the X-Mitter On-Off Circuits	Limit Pulse Width to Safe Values, Alarm	
Pulse Duty Cycle	Monitors Duty Cycle of Transmitted Pulse Train	At Logic Lines which Drive the X-mitter On-Off Circuits	Limit Transmissions to Safe Limits and Alarm	
Loop-Back	Sample all Transmissions and Process the Signals in Receiver and then Compare with Original Data	At Input (from Transmitter) of the Antenna Coupling Network	Computer Decision	

TABLE 9. RF SUBSYSTEM BITE FUNCTIONS (Continued)

Test or monitor	Function	Monitor location(s)	Action in case of default	Comment
Sensitivity Self Test (SST)	Periodically to Test JTIDS, TACAN, IFF X-ponder, IFF Interr., and GPS Reception Sensitivity	Signals taken from X-Mitter Low Level Stages (X-Mitter Power Amp'l OFF) are fed into the B.P. Filters at the Ant. Ports	Alarm IF Receiver Sensitivity Poor	GPS Test Signals are from the GPS Test Generator
Freq Hopping Monitor	Ascertains that Freq Hopping is occurring in a Pseudo-Random Fashion at the proper Frequencies	Transversal Filter (TF) tracks the Transmitted Signal via Loop-Back. Logic Signals at TF and at X-Mitter Freq Synth-monitored	Shutdown Transmitter if improper Freq Hopping	If Reception via Loop Back is obtained Transmitter is then assumed ok. Psudom-random hopping is then ascertained by weighting the average dwell at each freq word
IFF Guard Bands	Detects Excessive JTIDS and Tacan X-Mitted Spectrum Spill-over into 1030 or 1090 MHz IFF Bands	Monitored in the IFF Receiver during JTIDS or Tacan Transmissions via Loop Back	Shutdown Transmitter if excessive Spectrum Spill-over detected	



NOTE: MONITOR PORTIONS  
OF CIRCUIT HAVE HEAVY  
LINES

Figure 65. Block diagram of monitor circuit for typical antenna channel



monitoring transmitter power. The low level signal is derived from the transmitter, (or from a test generator in the case of receive only systems such as GPS and AFSATCOM) and coupled into the receive path for receiver sensitivity self-test. The transmitter tests are performed during normal transmission; the receiver sensitivity self-test is performed during an off-time.

An additional loop back test is performed during normal transmissions, whereby a small portion of the transmit signal is coupled (monitor coupler No. 2) back into the receiver path beyond the T/R switch and preamplifier (monitor coupler No. 3). This signal is processed in the receiver and then compared with the original data that was to be transmitted.

### 3.8 PHYSICAL DESCRIPTION

The packaging concept used for MFBARS is essentially the same as that used in the Draper Integrated GPS/JTIDS/INS Report<sup>(1)</sup>. This packaging approach was chosen because it simplifies the task of comparison between the Draper results and the selected MFBARS architecture.

All LRU's are approximately 3/4 ATR (long) packages. The digital boards are dual multilayer printed circuit boards with a corrugated aluminum core for forced convective cooling. Integrated circuits are packaged in flatpacks, and it was assumed that up to 160 flatpacks could be accommodated per digital module. The RF and analog circuitry was, for the most part, either discretes or thick film hybrids (TFH's) packaged on drilled-through printed circuit boards mounted in thick wall modules.

Each functional module of the selected architecture was estimated in size and weight consistent with the above assumptions. The result was a MFBARS packaged in three LRU's. Figures 66, 67 and 68 are isometrics of the three LRU's, also showing the size and location of the various functional modules.

Table 10 is a summary of the most important physical characteristics of the selected architecture.

TABLE 10. SUMMARY OF PHYSICAL CHARACTERISTICS

	<u>LRU no. 1</u>	<u>LRU no. 2</u>	<u>LRU no. 3</u>	<u>Totals</u>
Width (in)	7.6	7.6	7.6	-
Height (in)	7.62	7.62	7.62	-
Length (in)	19.4	21.4	21.4	-
Volume (ft <sup>3</sup> )	0.595	0.65	0.65	1.895
Weight (lbs)	50	57	54	161
Power Requirements (watts)	1404	441	488	2333

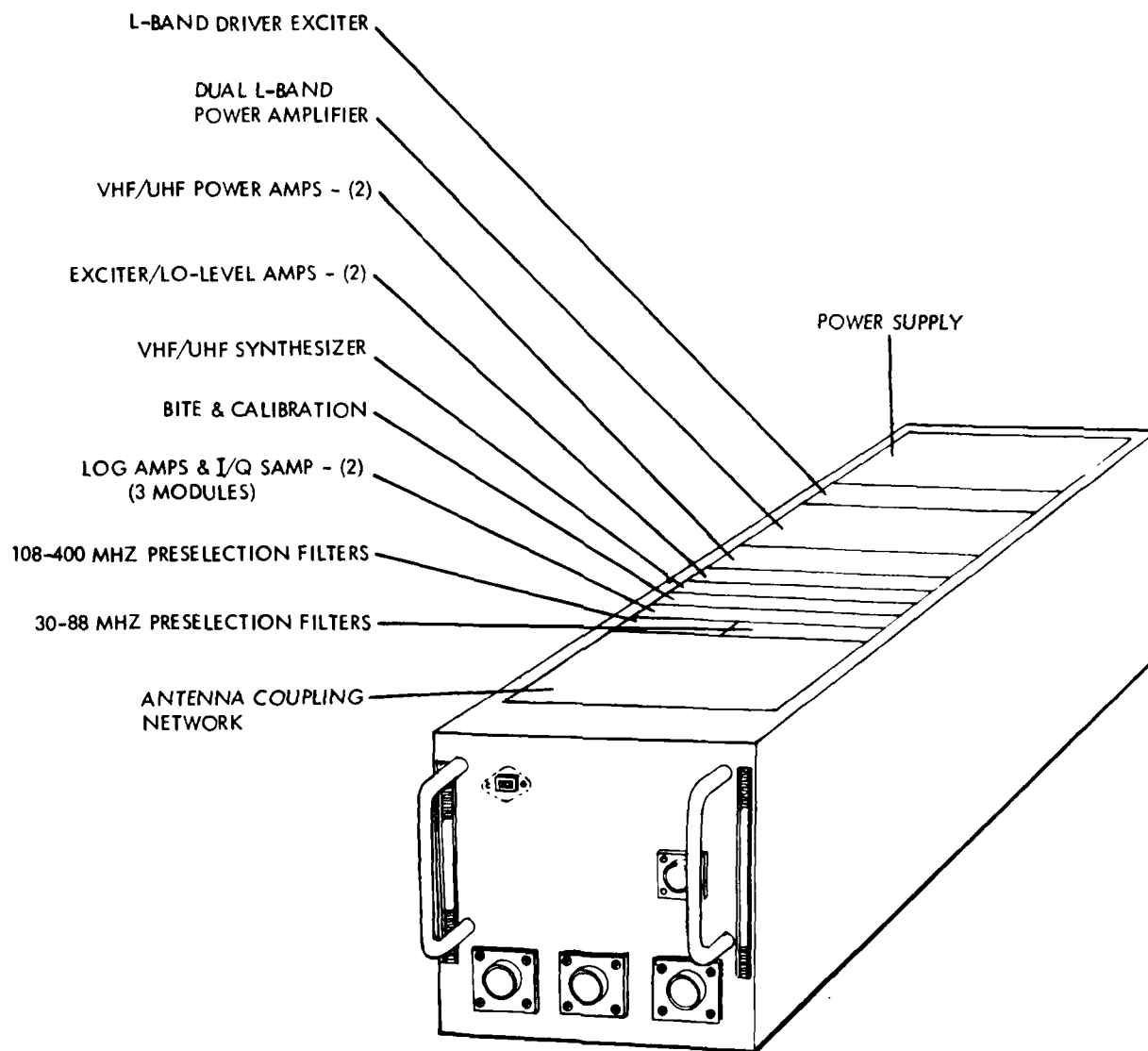


Figure 66. MFBARS Phase II, LRU no. 1

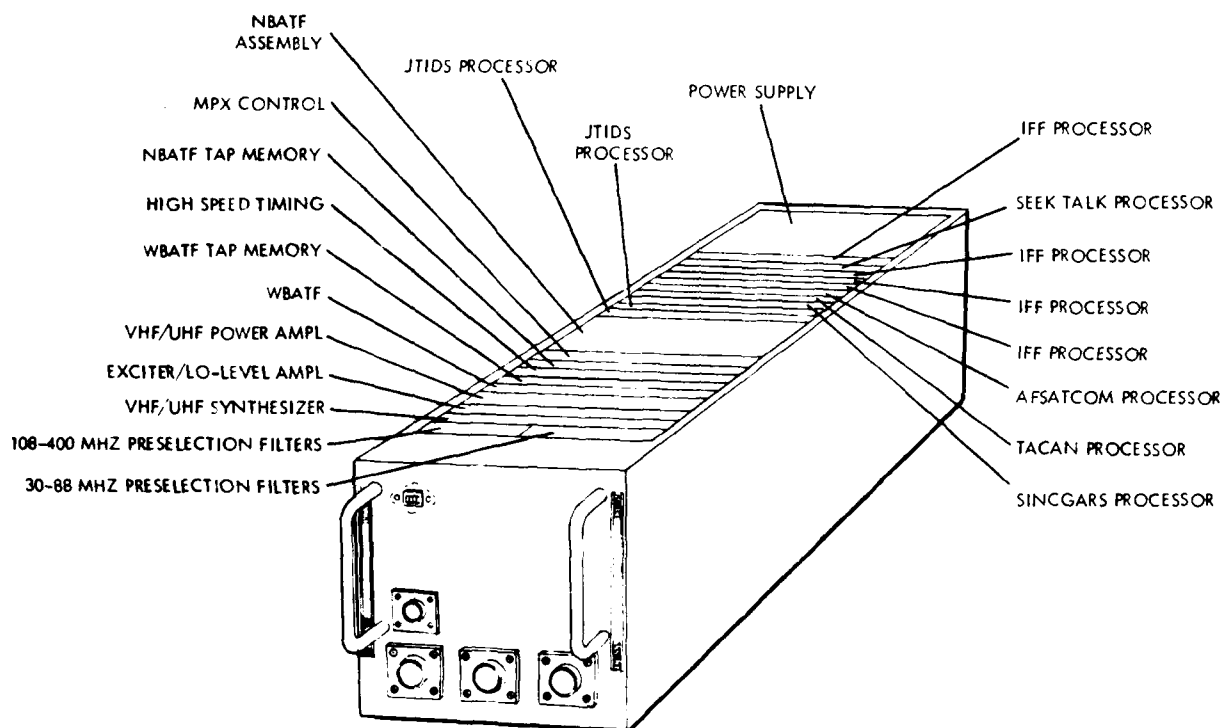


Figure 67. MFBARS Phase II, LRU no. 2

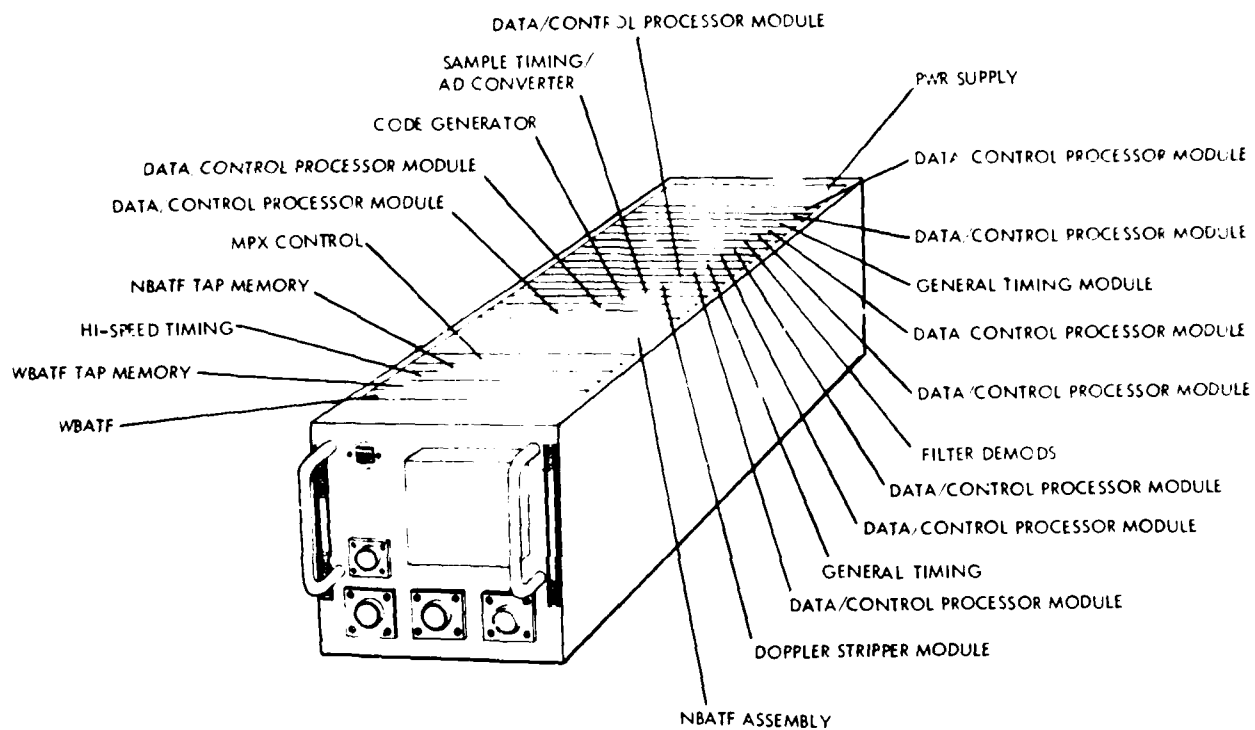


Figure 68. MFBARS Phase II, LRU no. 3

#### 4. TECHNOLOGY PROJECTIONS

As part of the study objectives, the Government directed that candidate system designs were to be based on technology projected to be available in 1985, the planned start of hardware development, rather than technology in-hand at the start of the studies (1978). This was done to avoid constraining the designs by technology which would be seven years old before system hardware development started.

ITTAV approached 1985 technology projection in two ways:

- assessment of how far MFBARS-related technology would progress, independent of MFBARS requirements
- assessment of how far MFBARS-related technology could progress if technological developments were driven by MFBARS requirements

An example of the first type might be forecasts of digital memory densities and speed, for which some history exists and for which trends can be predicted. This type of technology growth has a wide base of application and would proceed with or without MFBARS. An example of the second type would be the development of advanced, special purpose, programmable agile transversal filters for MFBARS applications. These devices are very specific in application and would require influence from the MFBARS program for initiation of the necessary development efforts.

Three areas of projected technology emerged as having the greatest impact on ITTAV's candidate system architectures. The most advanced projected technology for all three areas was utilized in architecture No. 3, the system design with the highest projected performance, and the greatest cost and size savings. This was the architecture selected by the Government for more detailed design effort during Phase II of the study. The three technology areas were:

- wideband agile transversal filters (WBATF's)
- digital circuits
- SAW preselection filters

#### 4.1 WBATF TECHNOLOGY

There are several possible device technologies which could theoretically provide the means to implement WBATF's. They are:

- Digital (Hardware) Filters
- Fiber Optics
- Surface Acoustic Wave (SAW) Devices
- Magneto-Static Wave (MSW) Devices
- Charge Coupled Devices (CCD)

A fully digital hardware filter using digital memories and/or shift registers for delay would require A/D converters with very wide dynamic range ( $>16$  bits) and high conversion rates (870 MHz). Development of such A/D converters does not seem likely in the MFBARS time frame. Another even more severe limitation involves the number of computations that would have to be performed on each digitized sample. Assuming sampling each of 14 output signals at a 15 MHz rate, there must be a calculated output value from the filter every  $1/(15 \times 10^6) \times (14) = 4.8$  nanoseconds. If it is further assumed that the filter will have 500 taps, then 500, 16 bit multiplies and additions must be performed every 4.8 nanoseconds. This is equivalent to over 100,000 million multiply and accumulate operations per second. As a point of reference, the state-of-the-art for a single LSI device today is ten million multiply and accumulate operations per second. This device dissipates about one watt of power. For these reasons, a digital (hardware) filter approach was not considered a realistic approach.

Optical fibers are mentioned because of their wide bandwidth capabilities. Although fairly long fibers might be required (approximately 0.2 kilometers due to speed of light propagation velocities) to achieve the necessary delay time, the fibers are small in diameter and could be contained in a reasonably small volume. The most significant problem with this approach was the transducers (lasers, light emitting diodes and photo-diodes) because internal noise limits useful dynamic range. Also significant is mechanical complexity due to alignment problems of the individual fibers. Therefore, this technology was not considered a realistic approach.

The technology areas that offered the greatest promise for economical implementation were SAW's, MSW's, and CCD's. Each of these types of devices has attributes which make

it attractive. Figure 69 shows current relative operating regions for each. As technology advances, so will the performance of these devices. MFBARS requirements could be met with realistically achievable advances in any one of these technologies.

MSW and SAW devices are similar in their nature, differing primarily in the mode of signal coupling to an acoustic substrate. MSW devices have demonstrated their ability to operate at L-band frequencies, and the acoustic propagation velocity is about 100 times faster than SAW's, which tends to ease photolithography problems associated with short interval tap spacing. On the other hand, MSW device technology is several years behind SAW technology. Continued development would be required before either SAW or MSW devices could be available for MFBARS. However, there is a high probability that MFBARS requirements could be met by 1985.

CCD's offered the greatest promise for ultimate cost effective WBATF implementation. Although at present, silicon CCD's are nominally limited to operating frequencies around 50 MHz, new developments in both silicon and gallium arsenide (GaAs) semiconductor technology are expected to open the way to new frontiers of performance. Some developers feel that gigahertz CCD's are only a few years away. Indeed, at this time a fixed, 64 tap, CCD with in excess of 70 dB of dynamic range has been built and operated at clock speeds greater than 500 MHz. Another very important aspect of CCD's is that they can be produced monolithically, including support circuitry (such as clock drivers, summing busses, etc. all on one chip).

Table 11 summarizes current and projected CCD capabilities, compared to MFBARS requirements.

TABLE 11. CCD WBATF PERFORMANCE PROJECTIONS

<u>Parameter</u>	<u>MFBARS requirements</u>	<u>Projected capability</u>	<u>Present capability</u>
Clocking Rate	870 MHz	1 GHz in next two years	50 MHz (Silicon) 500 MHz (GaAs)
Dynamic Range	95 dB	100 dB	70-75 dB
Number of Taps	500-650	1000	500



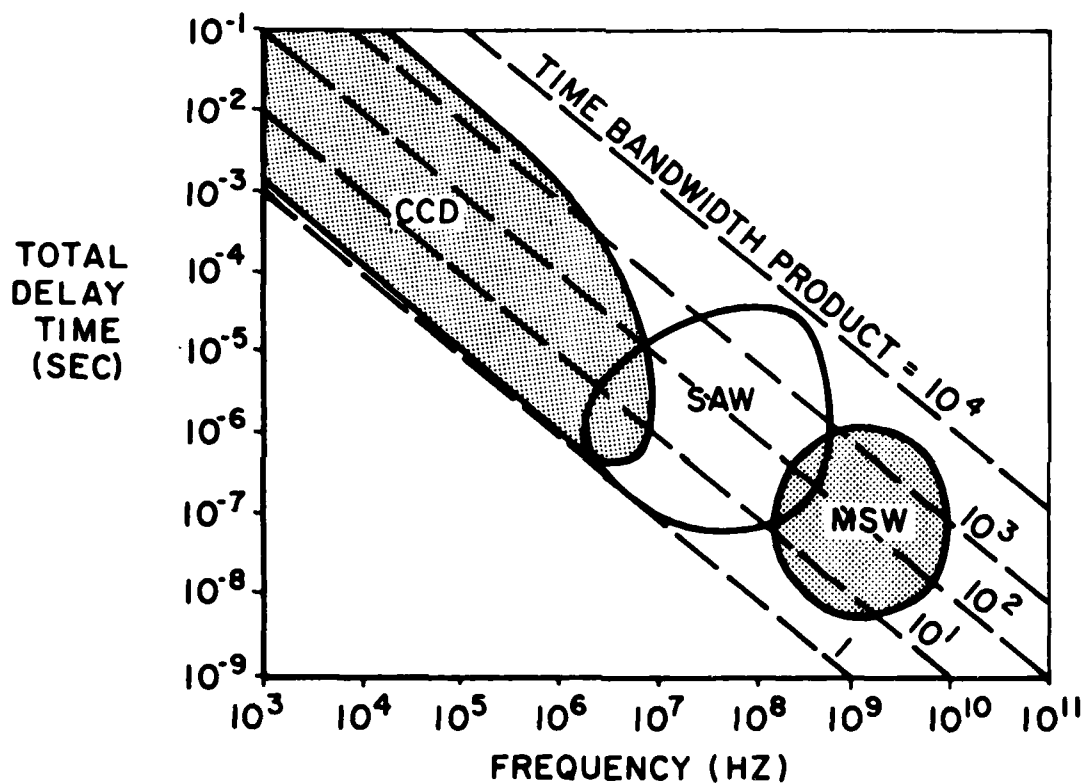


Figure 69. Domain of operation for various transversal filter technologies

It is believed that either silicon (in concert with the DoD VHSIC program) or GaAs CCD technology could be ready for WBATF implementation for MFBARS. In order for this to happen, however, a considerable development effort would have to be undertaken immediately.

(NBATF's, also required for the system, are considerably simpler than WBATF's. In fact, the NBATF is considered within today's state-of-the-art.)

#### 4.2 DIGITAL CIRCUITS

The selected MFBARS design employs a considerable amount of digital hardware, including federated microcomputers, digital control of subsystems, digital signal processing modules, and digitally-controlled BITE. Status of integrated digital circuits at the time of hardware development start has a great deal of influence on ultimate system cost and size.

The steady increase in speed and density of digital circuits is expected to continue at essentially the same rate it has historically, with a potential for additional emphasis generated by the VHSIC program. Technological thresholds are centered about X-ray lithograph techniques which will permit penetration into the sub-micron domain. By 1982, the reduced feature size will lower stray capacitance making a higher speed-power product cell available. With the reduction in the power per cell, permissible circuitry per chip will increase. This increased density will alleviate the I/O problem; that is, pin limitations and partitioning of functions, and permit entire functions on a chip, thereby increasing modularity. What also seems to be increasing is a much greater mix of digital and analog circuitry on the same chip, which further improves functional modularity.

Estimates of size for MFBARS digital functions were arrived at by first estimating the number of integrated circuits required to perform comparable functions using today's technology. Then the various functions were analyzed to see what impact improvements in speed would have on fundamental designs. This included consideration of transferring entire sub-functions to a general purpose digital microprocessor where as previously they may have been implemented in discrete logic. Speed improvements also allowed some functions to be implemented by time-sharing rather than using dedicated, multiple sets of identical hardware. The overall reduction of integrated circuits based on speed and density considerations amounted to approximately a factor of four for the mid-1980's time frame. Once the number of integrated circuits was estimated, a reduction factor was applied to reflect expected

continuation of historic trends. The final estimates provided considerable savings in system size and cost.

In addition to these savings, VHSIC technology will be maturing in the mid-80's. It is expected that further savings will be possible from the use of standardized VHSIC modules.

#### 4.3 SAW PRESELECTION FILTERS

The use of a WBATF for an RF preselection device introduces insertion losses which must be overcome. At L-band, this problem is avoided by use of a wide-band preselector and amplifier with sufficient gain to establish the required system noise figure. This technique runs into difficulties in the VHF/UHF band, however, because many octaves of frequency (30-400 MHz) must be handled simultaneously, and non-linearities in the wideband preselection amplifier result in signal interaction distortions which desensitize the receiving system.

A possible design solution (at VHF/UHF) is to sub-divide the 30-400 MHz band into smaller sections, each of which is no larger than a semi-octave, and employing separate, parallel filtering and amplification in each path. The outputs are then summed together and sent to the WBATF for further filtering. The sub-division of the VHF/UHF band may be performed by contiguous fixed center frequency filter banks implemented in SAW technology.

In this manner, SAW filters with the required insertion loss can be fabricated in the MFBARS time frame. The realizability of such filters is at the edge of the state-of-the-art today. Table 12 shows current and projected capabilities. The most significant element of risk involves the ultimate production cost of these devices, which is considered a low to medium risk.

TABLE 12. SAW FILTER PERFORMANCE COMPARISON

<u>Parameter</u>	<u>MFBARS requirement</u>	<u>Present capability</u>	<u>Projected</u>
Insertion Loss	3 dB	4-5 dB	3 dB
Out-of-Band Rejection	40 dB	30 dB	40 dB
Ripple, Pass Band	.2 dB	.2 dB	.2 dB
Cost per Filter Bank	\$30.00	\$150.00	\$30.00
Internal Matching	Yes	Yes	Yes

## 5. COST ANALYSES

Evaluations and comparisons of MFBARS architectures with respect to government supplied baselines were performed using the RCA "PRICE" cost modeling programs. Three cost categories were evaluated: Hardware, Software and Life Cycle Cost, using the appropriate PRICE model. PRICE-H was used to project hardware costs for both Phase I and Phase II MFBARS architectures. PRICE-S and PRICE-L were used only for Phase II.

### 5.1 BASELINE DATA AND ESTIMATING GROUND RULES

Government-supplied baseline data is summarized in Table 13. These numbers already incorporate applicable product improvements for baseline equipments, so that comparison with MFBARS is fair.

Schedule information supplied by the Government (for comparative cost analyses purposes only, not necessarily the actual planned program schedule) included:

- 1/78 - start of development (ADM)
- 1/85 - start of EDM phase
- 11/85 - first EDM prototype
- 8/86 - last EDM prototype (10 prototypes)
- 1/88 - start production
- 1/90 - complete production (1050 systems)

LCC Parameters supplied by the Government included:

- 1050 MFBARS Systems
- 20 organization levels
- 20 intermediate levels
- 2 depots
- 30 hours/month aircraft operating time
- 10 year support period

TABLE 13. CNI BASELINES

Radio	Band/Type	(a)			(a)		
		Phase I Baseline		Weight (lb)	Phase II Baseline		Cost (b)
		Volume (cu. ft.)	Cost (b)		Volume (cu. ft.)	Cost (b)	
ARC-112	HF Comm	69.8	1.93	69.8	1.93	\$14.93K	-
ARC-131	Low VHF Comm (30-88 MHz)	27.2	.50	27.2	.50	19.06	\$19.06K
ARC-115	High VHF Comm (108-156 MHz)	8.5	.16	8.5	.16	3.31	3.31
ARC-164	UHF Comm	10.2	.16	10.2	.16	6.03	6.03
ARN-108	VHF ILS/VOR	9.0	.17	9.0	.17	9.91	9.91
ARN-118	L-band TACAN	33.5	.58	33.5	.58	8.44	8.44
APX-76	L-band IFF Interrogator	14.3	.22	14.3	.22	24.06	24.06
APX-101	L-band IFF Transponder	51.8	.98	51.8	.98	13.77	13.77
JTIDS	L-band Spread Spectrum Comm/NAV	196.0 (c)	2.27 (c)	196.0 (c)	2.27 (c)	100.33 (c)	100.33 (c)
GPS	L-band Spread Spectrum Nav						
SEEK TALK	UHF Spread Spectrum Comm	-	-	-	30.0 (d)	.50 (d)	20.00
SINGGARS	VHF Freq Hop Comm	-	-	-	4.0 (d)	.07 (d)	2.50
AFSATCOM	UHF Satellite Comm	-	-	-	71.0 (d)	1.18 (d)	120.00
		420.3	6.97	\$199.84K	6.79	\$327.41K	

(a) Baseline product improvements already incorporated

(b) 1978 \$

(c) For combined GPS/JTIDS set, per Draper Labs GPS/JTIDS/INS study

(d) Based on EDM design goals

Advanced Development Phase (ADP) costs (computed for Phase II only) were based on the following:

- Two parallel system definitions studies (two contractors)
- Hardware and software design development and assembly of two complete flyable brassboards (one contractor)
- Factory test and integration (one contractor)
- Laboratory testing with simulated signals (one contractor)
- Flight test and evaluation (contractor assistance to Government)

ADP costs were computed for MFBARS only, not the baseline. To allow fair LCC comparisons, it was assumed there would be an approximately equivalent ADP cost for applicable product improvements to baseline equipments. (Inasmuch as ADP costs are only about 10 percent of total LCC costs, errors introduced by this assumption would not appreciably change results.)

Software development costs (computed for Phase II only) were based on the software functions shown in Table 14. The RCA PRICE-S model was used to assist in estimating the total cost of software programming. The ground rules for software cost estimating were:

- 1978 constant dollars
- All new software, all new coding
- PRICE complexity (CPLX) = 1.3 (except for integration and test (I & T) where 1.0 was used)
- Draper labs integrated GPS/JTIDS/INS study was used to estimate special purpose coding (the bulk of the estimated special purpose processing)
- ITTAV estimates were used for other system software requirements

TABLE 14. SOFTWARE REQUIREMENTS (PRELIMINARY ESTIMATE)

	<u>KOPS</u>	<u>Memory (Bytes)</u>	<u>Comments</u>
1. Multiprocessor Operating System	850	40K	
2. Application Programs			
JTIDS	1400	256K	DTDMA/TDMA (worst case)
GPS	870	46K	Draper Labs projection
SEEK TALK	480	30K	Estimate
AFSATCOM	460	50K	Estimate
Nav	470	60K	
Comm	400	20K	
Data Base	-	256K	
3. Support Programs	1100	60K	AGC, math routines, etc.
Subtotal	<u>6030</u>	<u>818K</u>	
4. Growth Margin	1810	245K	30% (typical design margin)
Total	<u>7840</u>	<u>1063K</u>	
Estimated* Instructions = $\frac{\text{Total Bytes} - \text{Data Base}}{2.4}$			
= $\frac{1063 - 256}{2.4}$ K = 336.25K			
*Based on JTIDS experience of average instruction length of 2.4 bytes/instruction			

## 5.2 RESULTS

Table 15 summarizes results of Phase I and Phase II cost analyses. As shown, at the end of Phase I there were significant cost differences between all MFBARS architectures and the Phase I baseline. The relative advantages of architecture No. 3 were especially large, and were major factors in the Government's selection of architecture No. 3 for Phase II. The final results of Phase II cost analyses show even greater relative savings for the MFBARS architecture, compared to the Phase II baseline.



TABLE 15. COST COMPARISONS (1978 \$)

	Phase I Baseline	MFBARS No. 1	MFBARS No. 2	MFBARS No. 3	Phase II Baseline	Phase II (Improved No. 3)
Weight	420#	290#	253#	215#	455#	161#
MFBARS Savings	-	31%	40%	49%	-	65%
Volume	7.0 cu.ft.	3.9 cu.ft.	3.3 cu.ft.	2.6 cu.ft.	6.8 cu.ft.	2.0 cu.ft.
MFBARS Savings	-	44%	53%	63%	-	71%
Unit Prod Cost*	\$200K	\$176K	\$168K	\$152K	\$327K	\$121K
MFBARS Savings	-	12%	16%	24%	-	63%
ADP Costs	(Not computed)			(Not computed)	(Not computed)	\$ 2M
System Definition						15
Hardware						7
Software						
Subtotal					\$24M(est)****	\$ 24M
EDP Costs	\$ 6M	\$ 7M	\$ 7M	\$ 8M	\$ 10M	\$ 6M
Design	296	224	214	195	484	155
Production**	\$302M	\$231M	\$221M	\$203M	\$494M	\$161M
Subtotal						
MFBARS Savings	-	24%	27%	33%	-	67%
Support Costs***	\$ 35M	\$ 21M	\$19M	\$17M	\$57M	\$14M
MFBARS Savings	-	40%	46%	51%	-	75%
Total Life Cycle Costs	n/a			n/a	\$575M	\$199M
MFBARS Savings	n/a			n/a	-	65%

\*1050 units

\*\*1050 units, includes non-recurring production as well as recurring

\*\*\*10 years

\*\*\*\*Not computed, estimated equivalent to MFBARS ADM costs to allow LCC comparison

## 6. INTEGRATED NAVIGATION CONCEPTS

During the basic MFBARS study, the Government asked ITTAV to conduct a preliminary investigation of the feasibility of an optional higher level of system integration; namely, integration of MFBARS navigation signals with each other and with the on-board inertial navigation system (INS). Two concepts were explored:

- integration of GPS and JTIDS signal processing
- integration of GPS/JTIDS/INS signal processing

### 6.1 SUMMARY OF RESULTS OF INTEGRATED NAVIGATION FUNCTION STUDY TASK

Preliminary results of the integrated navigation function study task were promising. Both hardware integration opportunities and operational benefits were identified. However, more detailed analysis is required to determine cost-performance effectiveness across the entire user community. If cost effective, an integrated navigation function could either be merged into the basic MFBARS program at this time or could follow as a subsequent program task.

#### 6.1.1 Opportunities for Hardware Integration

GPS, JTIDS, and the INS all make use of similar navigation computations, all using Kalman filtering techniques. An integrated set of navigation algorithms, with common Kalman filtering, could lead to savings in navigation processor hardware and inertial system and aircraft interfaces. Section 6.2.1 provides details.

#### 6.1.2 Operational Benefits to JTIDS Users

The greatest potential operational benefit to JTIDS (of an integrated navigation function) would be the ability to utilize GPS inherent higher accuracy timing and geodetic position location capability. GPS provides high accuracy, receive-only, position location and timing information, in one common world-wide geodetic coordinate reference grid, for all GPS users. In contrast, JTIDS provides relative navigation (relnav) capability by means of two-way position location message interchanges between participants in any given JTIDS network. Each JTIDS network establishes its own independent navigation reference grid and time reference.

Geodetic benchmarks are required (for each JTIDS network) to permit position location repeatability and exchange of target data and other ground-related data between cooperating aircraft and between aircraft and air tactical control centers. Use of GPS common worldwide geodetic coordinates would simplify establishing common geodetic benchmarks for JTIDS networks.

Furthermore, the total mix of navigation data available to the Kalman filter from an integrated GPS/JTIDS would permit rapid navigation signal reacquisition not possible with independent systems.

#### 6.1.3 Operational Benefits to GPS Users

The primary operational benefit to GPS users (of an integrated navigation function) would come about when a GPS user could not directly receive a sufficient number of GPS satellite signals for accurate GPS position location computations. At least four GPS satellite signals must be received to complete each computation. Furthermore, the four satellites must have adequate angular separation, for geometric reasons. Under many foreseeable circumstances (including deliberate enemy jamming, atmospheric attenuation anomalies, nonoptimum or incomplete GPS constellation configurations, and other factors), a GPS-user may receive some, but not all, of the necessary GPS signals required for accurate position location computations. In those cases, if the missing signal(s) could be obtained by other GPS-equipped platforms at locations sufficiently different to receive the missing signals, and if the missing information could be fulfilled using the JTIDS relative grid and/or could be transferred via JTIDS messages, then each GPS user could complete its own GPS computations, even though some of the inputs would be received indirectly. Importantly, during periods of GPS signal loss, the JTIDS timing data, properly filtered by the Kalman algorithms, could maintain close synchronism with the virtual GPS signal code. Thus, when the GPS signal returned to a detectable level, almost immediate reacquisition would be possible. Section 6.2.5 discusses this concept in more detail.

## 6.2 DETAILS OF INTEGRATED GPS/JTIDS/INS NAVIGATION FUNCTION

Figure 70 shows a block diagram of a fully integrated GPS/JTIDS/INS navigation function. There are three sets of navigation data available. One is derived from the inertial navigation system (INS). The second is derived from JTIDS messages, and the third is derived from GPS pseudo-range measurements. The right hand side of the block diagram is essentially the GDM GPS receiver.

Inertial system outputs, (at a rate of approximately once every 250 milliseconds) are inertially estimated navigation states of the system, resulting from a baro-damped inertial navigator. These outputs are "pseudo" differentiated so that Kalman filter estimated velocity and tilt error resets can be directly applied (avoiding nonlinearity problems). Then these corrected functions are integrated again in order to obtain an optimal estimate of the full state of the system with respect to the geodetic grid and relative grid. Outputs also include associated rotation states of the vehicle.

The geodetic information resulting from this state computation, along with the vehicle attitude information and certain accelerometer outputs from the IMU (inertial measurement unit), are fed into the high data rate satellite range rate computer algorithm which provides rate aiding to the GPS tracking loops.

An important distinction between previous GPS implementations, such as the General Development Model (GDM), and the fully integrated GPS/JTIDS/INS navigation function involves the navigation state being used to drive the rate aiding computations. In the GDM it may not be important whether pure inertial information or Kalman filter corrected state information is fed into the range rate computations. In the fully integrated model the Kalman filter estimated navigation state data is critical for enhanced operation. This is because the filter function, combined with the source selection function, can operate so as to provide precise geodetic position and rate data regardless of the state of jamming on the GPS receiver internal to the platform of interest. Precise GPS time may also be available (through other functions). Thus the potential exists for slewing the code and phase tracking loops consistent with GPS range even during times when GPS signals cannot be tracked. This information can be critical when relocking GPS tracking loops after the jammer to signal ratio has been reduced.

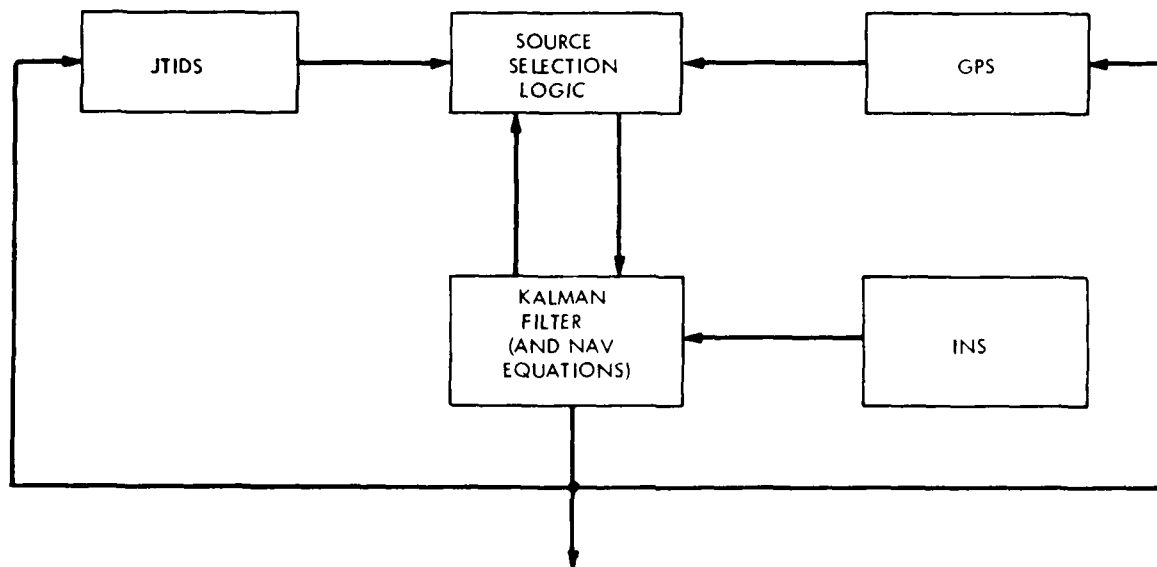


Figure 70. Fully integrated system structure  
GPS/JTIDS/INS

The inputs to the GPS tracking loops are the rate aiding data, the GPS RF, clock information, and various inputs from the tracking loop control function (which controls the time constants and the satellites to be tracked). The loops output pseudo-ranges, pseudo-delta ranges, and any loop lock loss alarms. (If a particular tracking loop is not locked to the required signal, an alarm is generated.) A possible additional input to the tracking loops is the binary data code for the 50 Hz satellite message. If this is available, either from previous receptions or from a JTIDS link, it is possible to eliminate some of the nonlinear operations in the costas phase tracking loop and thus obtain a 5 or 6 dB advantage in S/N performance. The tracking loop outputs feed the source selection and Kalman filter functions. Lock indicators identify the validity of the observed pseudo-ranges.

Now consider the JTIDS transceiver function. When a "P message" is sent, JTIDS can detect time of arrival, position and time quality from the message, and geodetic and relative position states of the transmitted message. If an RTT reply is received, JTIDS can also detect synchronization error between a donor (remote) clock and own (local) clock. Input to the JTIDS receiver function is JTIDS corrected time, which results from correction of the master oscillator.

Next, consider the navigation filter and source selection functions. When GPS and JTIDS are both operational, the measurement source selection process operates on an alternating time sequence basis. First, it selects GPS derived data, then JTIDS derived data, alternately, for inclusion in the navigation filter. If all satellite pseudo-range measurements are available, as indicated by the lock alarm indicators, the source selection routine samples the pseudo-ranges, which are used to calculate geodetic positions during the next filter cycle, while the source selection routine operates on JTIDS information. For JTIDS, a conventional source selection algorithm consistent with relative navigation-only measurement is implemented. If GPS data were collected during the previous source selection interval, the filter function generates pseudo-range divergences, the measurement matrix and noise matrix, and performs a Kalman update on the geodetic information. If JTIDS information were collected during the previous cycle, relative data is then fed to the navigation filter function which then sets up the proper TOA divergences and measurement matrices for a Kalman filter relative grid update.

In the completely integrated JTIDS/GPS/INS navigation function, when one or more of the GPS tracking loops has lost lock, and the source selection routine is screening for geodetic data, it also scans the JTIDS received data for the potential of deriving highly precise geodetic data from other members of the navigation community. This source selection can take the relative geometry of the pseudo-ranges still being tracked and the location of the donor JTIDS terminal into account in order to round out the set of geodetic measurements needed in the navigation filter function.

The net result is that the source selection algorithm, in combination with the filter function, will provide its own platform with very precise geodetic data in a smooth and continuous fashion regardless of whether or not all or any of the GPS receiver tracking loops are fully operational. So long as there is at least one other GPS/JTIDS receiver (in the same relative navigation community and within line-of-sight), operating with both capabilities should always enable maintaining lock on highly precise geodetic information. The highly precise geodetic information\* can then be used to rate aid the GPS tracking loops until jamming has diminished, and/or can be used to slew the tracking loop code generators to the point where lock-on is possible without performing a complete initialization or search procedure. Reinitializing tracking or tolerating reduced geodetic quality may only be necessary during those rare periods of time when all GPS receivers within JTIDS line of sight are fully jammed.

Now consider other factors in source selection. In a situation where GPS signals are not available, the source selection routine will revert to that consistent with the current JTIDS concepts, mixing both relative and geodetic information provided in the "P" message.

When GPS signals are available or partially available (and during that portion of time when the source selection routines are not scanning for geodetic data), the source selection routine scans strictly for relative data and performs relative position updates. In this way no interoperability problems should arise among those members of the JTIDS community without GPS.

---

\*Accurate enough to estimate range to satellite within 100 feet.

Regarding synchronization, with the separate GPS and JTIDS functions, the source selection routine would be consistent with the current concepts now being implemented. When required, a JTIDS RTT request would be transmitted. In the integrated GPS/JTIDS/INS, the source selection routine has a potential of being modified so that GPS time can be used to stabilize relative time so that JTIDS RTT requests are not required as often, being used primarily for consistency checks.

#### 6.2.1 GPS Tracking Loops

This section discusses the concept of a time locked loop (a generalization of a code tracking loop) for GPS. The discussion includes the types of rate aiding and slewing which can characterize the tracking loops. Then the modes of rate aiding and slewing which can be implemented are identified, along with problems and solutions involved with mode switching. Finally, a candidate tracking loop control algorithm for mode switching is presented.

The time of arrival observed at the GPS receiver is delayed proportional to the range from the receiver to the satellite. See Figure 71. The receiver clock, which can be considered a servo-controlled clock, consists of a local reference oscillator which is slewed with a signal proportional to the range rate difference between the receiver and the satellite. That is, it is rate-aided. If there were no error on the clock, the output of the onboard clock time at "A" would be  $t-R/C$ , exactly that observed from the satellite clock.

In practice, however, there would be a synchronization error. The code comparison circuits of the GPS tracking loops take the difference between the estimated time at point A and the observed time from the satellite. The error is then fed back through the tracking loop filter (in the case of a noncoherent tracking loop, a second order filter) so as to drive the clock output to the observed GPS time. The time difference between the oscillator time output and the servo-control output is a measure of the "pseudo-range" to the satellite. It is the true range to the satellite, plus the time error in the local clock, with a noise term added. Note that the steady state output of the tracking loop filter is an estimate of the oscillator clock error.



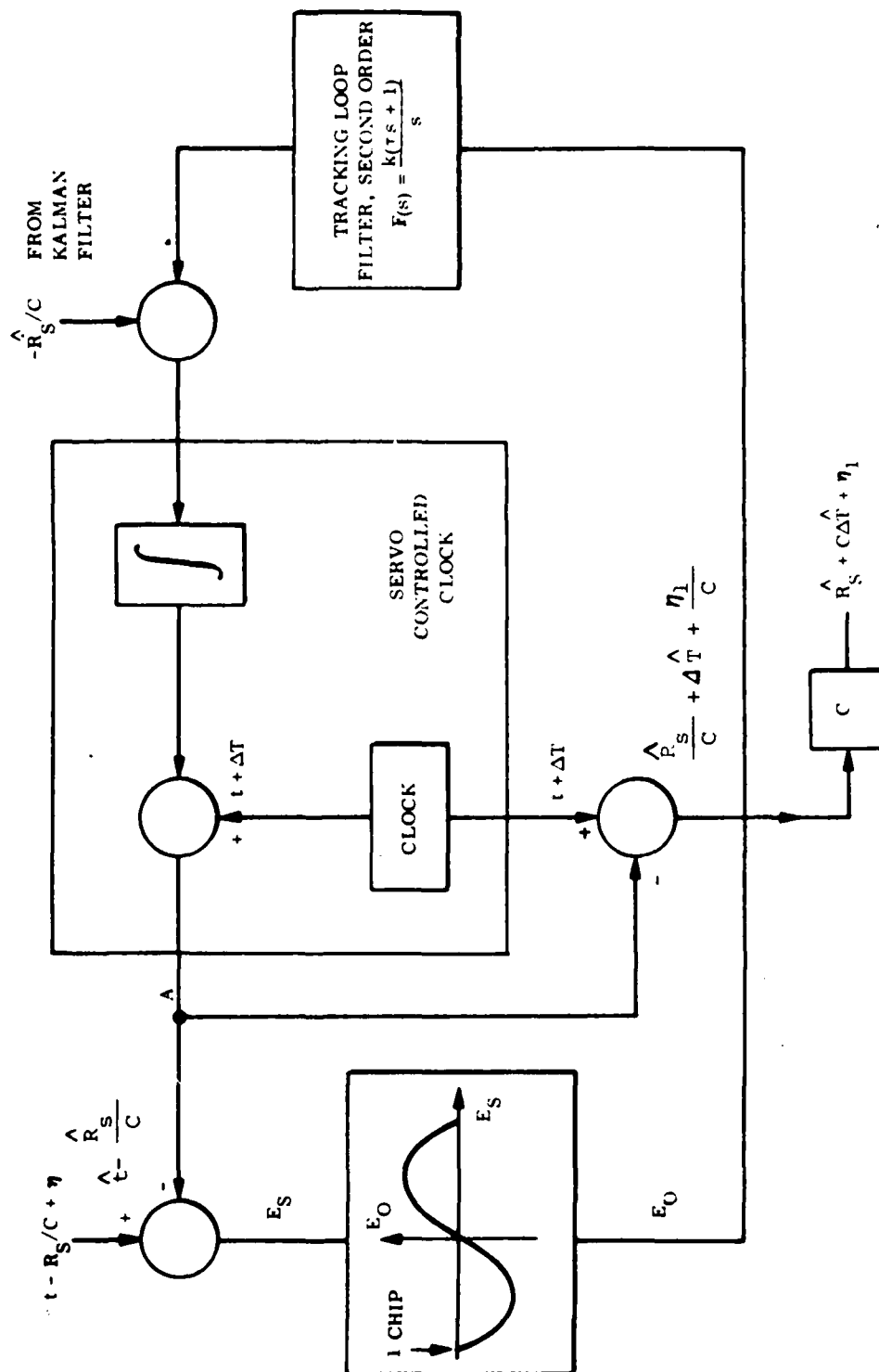


Figure 71. Time-locked loop, normal operation

When jamming becomes too great, there will be no observed correlation between input signal and the internally generated signal used for time or code comparison. The result is that a noisy zero average signal enters the delay lock loop filter and a "Lost Signal" detection circuit located in the AGC module. The loop will continue to be slewed via the rate aiding signal. If rate aiding were nearly perfect, the loop would continue to be slewed correctly; however, noise from the error detector would tend to cause the code to walk off the ideal "zero error" position. Ideally, when the noise is diminished and a valid phase comparison made ( $E_s < 1$  chip), the loop would be in a position to lock back on.

However, rate aiding is not perfect, even when controlled by the Kalman filter. Thus, there is an additional tendency for the tracking loop code to walk off from the true code. Cumulatively, the resulting drift could cause a zero output in  $E_0$  even though an error greater than one chip in  $E_s$  is experienced. In a "conventional" receiver, search procedures would eventually have to be instituted when S/N was large enough to allow this.

In the fully integrated GPS/JTIDS/INS navigation function, however, an accurate estimate of pseudo-range,  $R_s$ , is usually available -- if not from internally measured information then from JTIDS net derived information.  $R_s$  can then be used to slew the tracking loops in the range slewing mode as is shown in Figure 72 (with the switches in the position as shown).

Estimated range rate and clock frequency error (which together make up pseudo-range rate) are input to the integrator in the servo-controlled clock. The output is an estimate of  $t - R_s/C$ . The time difference generated between the servo-control clock and the local oscillator represents an estimate of the pseudo-range. The pseudo-range estimate from the Kalman filter can then be differenced with this estimate, resulting in an error signal used to slew the loop. This will maintain the loop essentially synchronized with the incoming signal, even though it is not observable.

The logic blocks on this diagram represent high duty cycle logic for determining whether the loop is locked, and for mode switching. The lock indicators, which should be a direct result of the circuitry involved in the time comparison of the code loops, can be used to indicate when lock is again achieved (the satellite is observable).

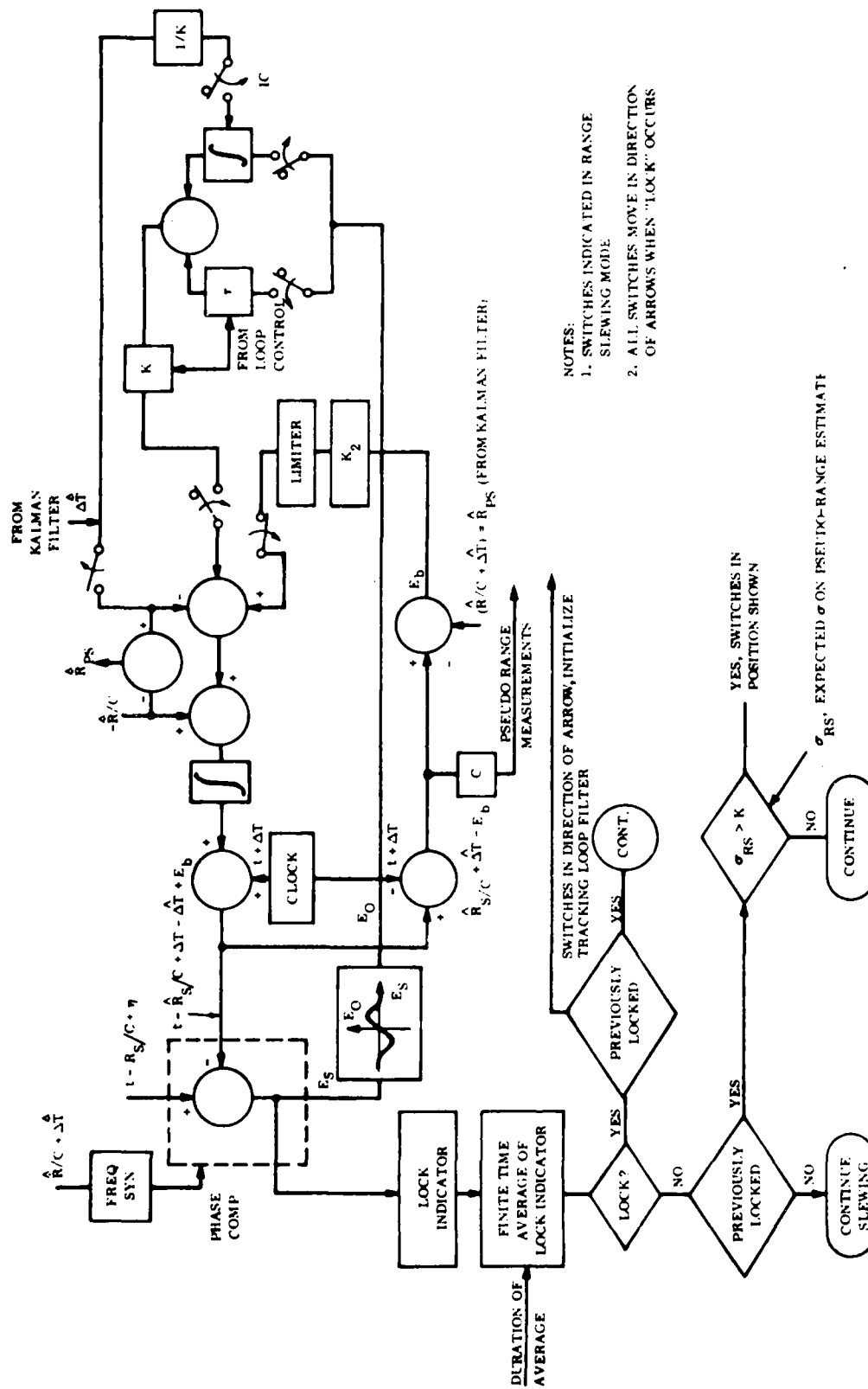


Figure 72. Combined conventional tracking and loop slewing

When lock has been reestablished, the mode can immediately be switched to the long time constant tracking loop shown in Figure 71. This mode switching can be accomplished without significant transients as the switches are moved from the position shown to the position indicated by the arrows. The estimate of clock frequency would be cut off from the loop in one location and would be used to initialize the integrator in the tracking loop filter as indicated on the right hand side of the diagram. This is done because a steady state output of the tracking loop filter should equal the clock error rate. The loop would only have to cope with any small accumulated time and frequency drift errors developed during the signal "down time". Conventional tracking with the long tracking loop time constants is immediately implemented.

Now assume that the lock has been lost again. The expected standard deviation of the pseudo-range estimate from the Kalman filter is then computed and tested against some small value. If the estimated standard deviation is low enough, indicating the potential for good range slewing, the modes are switched back to the "shown position". This type of processing can continue back and forth between one mode and the other, for individual tracking loops, in any combination or sequence.

Note that this type of operation in the tracking loops would be impossible without a fully integrated system since the precise pseudo-range information and the quality of the pseudo-range information would not be developed unless integration was designed into the depths of the GPS tracking loops.

With these two mode capabilities in addition to the conventional coherent mode, and with a properly functioning fully integrated system, it is then possible to have lock and unlock in the tracking loops as a matter of course, without instituting any particular search procedures and their resulting transients. Also note that violent maneuvers which cause temporary loss of lock should require no specialized initialization. The performance appears limited only by the amount of "noise drift" experienced before the "lost signal" detector switches modes.

### 6.2.2 Kalman Filter

This section is organized in the following way. First, the basic functions of the Kalman filter and its inputs and outputs, are described. The filter follows the model of the filter derived for the Hughes improved terminal, augmented with states suggested by Draper. It is suggested that either the basic Kalman filtering algorithm used by Hughes\* or by Singer\*\* be a model for the completely integrated receiver Kalman filter. Alternate approaches towards the Kalman filter algorithm and its implementation are well documented. Modifications required for the fully integrated filter are not serious.

Concentration will be on the fundamental functions of the filter and those particular inputs and outputs which enhance the system. In addition, some general commentary will be given on the relative merits of the Singer approach versus the Hughes approach. The exact form of the filter should have little impact on accuracy in a fully integrated GPS/JTIDS/INS navigation function, so long as the minimal number of states is included in the filter.

The navigation data set selection algorithm, that is the algorithm which makes the decisions as to which measurements should be utilized by the Kalman filter, is critical to proper performance of the integrated JTIDS/GPS/INS navigation function. This is detailed after the general Kalman filter description. A candidate mechanization for source selection is then presented.

#### 6.2.2.1 Filter State Structure

The outputs of the navigation equations are listed in Table 16. The navigation equation effectively integrates derived corrected velocity information transformed to the appropriate coordinate systems in order to output these variables. All the states outlined have error components.

- 
- \* Reference: Hughes JTIDS Rel Nav for Hughes Aircraft Company, Intermetrics Corporation Report, 25 August 1978.  
\*\* Reference: Navigation Program Specification for JTIDS, Kearfott Division of Singer Corporation.

TABLE 16. OUTPUTS OF NAVIGATION EQUATIONS

$P_u, P_v$	Grid Position (usually North and East)
$P_w$	Altitude above u, v plane
$L, \lambda, Z$	Geodetic latitude, longitude and altitude
$V_u, V_v, V_w$	Grid Velocities
$V_e, V_n, V_z$	Geodetic Velocities

In terms of vectors, the relative and geodetic states can be written as follows:

$$\underline{R} = \underline{G} - \underline{0} \quad (8)$$

where  $\underline{R}$  is the relative position vector;  $\underline{G}$  is the geodetic position vector; and  $\underline{0}$  equals the grid origin position vector. This is the origin of the relative grid. Equation 9 shows

$$\delta \underline{R} = \delta \underline{G} - \delta \underline{0} \quad (9)$$

that errors on the relative grid, geodetic grid and errors in positioning the grid origin are related. In the Hughes JTIDS relnav implementation it is assumed that relative errors are a linear combination of independent geodetic and origin error as defined in equation 9. This approach makes generation of coordinates algorithmically simpler.

In the Singer JTIDS relnav approach, equation 9 is re-written as follows:

$$\delta \underline{0} = \delta \underline{R} - \delta \underline{G} \quad (10)$$

where here, origin error is dependent upon the independent grid errors and geodetic errors. The advantage of the Singer approach is that, in the absence of any geodetic fixes, one need only model relative errors even if fixes were normally considered geodetic. (With an inertial system that means that tilts, heading, etc. are all "relative".) With all vehicles having the same type of dead reckoning system, it is possible to implement highly precise relative navigation.

It appears that the Singer approach, in the absence of highly accurate geodetic information, will yield improved grid accuracy and reliability and has a potential for greater stability. However, with the presence of both highly accurate geodetic information and relative grid information it is doubtful whether one mechanization will have any clear cut advantage over the other. Neither one really models the mixing of relative and geodetic data correctly or optimally. However, both should work quite well when the plethora of highly precise geodetic and relative information is available.

The error states which should be modeled in the system are listed in Table 17.

TABLE 17. ERROR STATES USED IN THE KALMAN FILTER

$\delta L, \delta \lambda, \delta Z$	Geodetic errors
$\delta V_n, \delta V_e$	Geodetic velocity errors
$\delta \theta_e, \delta \theta_n, \delta H$	Inertial platform tilt errors
$\delta B$	Baro-altitude error
$\delta V_z$	Vertical velocity error
$\delta X_o, \delta Y_o$	Grid origin errors
$\delta V_{x_o}, \delta V_{y_o}$	Grid origin velocity errors
$\delta \beta$	Grid origin rotation rate error
$\delta T_j, \delta T_f$	JTIDS time and frequency errors
$\delta T_g, \delta \dot{T}_g$	GPS clock and drift errors

This is consistent with the Hughes implementation, with the addition of GPS clock and drift errors and vertical velocity and baro-altimeter error, to account for the vertical positioning capabilities of GPS. These additions are consistent with the approach taken by Draper in its filter mechanization.\*

\*The Draper mechanization effectively used the Singer definition of states with the addition of the four states mentioned above.

Relative errors would then be:

$$X_R = X_G - X_0$$

or

$$\begin{bmatrix} \delta P_u \\ \delta P_v \\ \delta P_w \end{bmatrix} = G \begin{bmatrix} \delta X_r \\ \delta Y_r \\ \delta Z_r \end{bmatrix} \quad \text{Where } G \text{ is a transformation matrix to account for relative grid location}$$

Two types of fixes are possible for this system. One is relative, and the other is geodetic. A separate loop which may be implemented is a direct synchronization of the JTIDS time or GPS time.

The filter actually processes measurement divergences.

That is:

$$\text{Divergence} = \left[ \hat{z}_{t_i/t_{i-1}} - z_{(t_i)} \right] = H \delta X_{t_i/t_{i-1}} + n \quad (11)$$

where  $\hat{z}_{t_i/t_{i-1}}$  represents the estimate of the measurement, given data up to the previous time, and  $z_{(t_i)}$  represents the measurement at that particular instant of time. This can be represented by the linear combination of errors,  $\delta X_{t_i/t_{i-1}}$ , in the system.  $H$  is the measurement matrix.

Added to this is additional noise,  $n$ .  $H$  will be a row vector identifying the various weights associated with the system errors.

When a geodetic fix is taken,  $H$  has one of the three forms shown in equation 12.

$$\begin{array}{l} \text{GEOID} \quad \text{ORIGIN} \quad T_j \quad T_g \\ H = [XX \dots X \mid 0000 \mid 00 \mid XX] \\ \text{or} \qquad \qquad \qquad \mid XX \mid 00] \\ \\ \text{or} \qquad \qquad \qquad 00 \mid 00] \end{array} \quad (12)$$



Note that the elements of the H matrix pertinent to geodetic states may have non-zero values. Elements pertaining to origin errors will all have zero values. If a GPS fix is involved in the measurement then the elements associated with JTIDS time state will be zero and the elements associated with GPS time may be non-zero. If the geodetic fix uses time of arrival from the JTIDS terminal along with geodetic information from the donor platform, then the JTIDS time element may be filled, and GPS time elements are zero.

The H matrix may take many forms dependent upon the measurements made available, such as offset geodetic fix, relative fix and round-trip timing.

There are other measurements which potentially can be taken which are unique to the fully integrated GPS/JTIDS/INS navigation function, and depend upon P message transmission of GPS/JTIDS clock offset, and reported pseudo-ranges. One is the offset clock synchronization measurement and the other is the offset GPS fix. Offset clock measurements may replace some or all JTIDS RTT messages. The offset GPS fix involves using reported pseudo-ranges between donor platform and GPS satellites, along with computation of the JTIDS relative positions of the two vehicles, to formulate a fix. This type of measurement will be useful for geodetic positioning in a community when only two or three satellites are available in the community.

#### 6.2.2.2 Filter Timing

The filter processes each of the measurements in the source selection buffer in time sequence until the point in time when the reset was applied to the navigation equations. At this time, the effect of the reset is subtracted from the filter error estimate and the filtering continues. At the end of the second filtering interval the optimal estimate of the error state is predicted ahead and another reset is applied to the navigation equations. This process continues.

An important point which should be remembered is that measurements obtained at one particular time may not be applied to the system, through the filter, until 16 to 40 seconds after the measurement is actually taken. The filter lags behind real time by about 20 seconds, but it properly predicts error projections to the precise time.

The above description is generic in nature. It is not necessarily precisely the same as the timing for either a Hughes or a Singer terminal. However, it represents the essence of the timing requirements.

### 6.2.2.3 Filter Operation

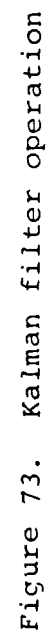
Figure 73 shows the operation of the Kalman filter. The information in the source selection buffers is the input. First, the filter propagates the Kalman covariance,  $P$ , and the estimate of the state error to the time of the first measurement, as indicated by the source selection buffers. Then, the measurement residual is formed and the associated measurement matrix,  $H$ , and noise value,  $R$ , are generated. The values of the  $H$  elements will depend upon whether the fix is geodetic or relative. The value for  $R$  will depend upon geometry, some fixed value, and quality numbers transmitted by the donor source (if applicable).

Next, the measurement residual is checked for consistency. The combination of the quality numbers transmitted and the user's own covariance matrix can be used to determine the value associated with the measurement divergence. If the magnitude of the measurement divergence is too large (4 to 5 sigma) then the measurement is rejected and suitable indicators are sent to the error control function along with the bad data. If the data passes a consistency check, the Kalman measurement update is performed, updating the Kalman covariance and updating the estimate of the error states.

At this point, the covariance matrix is checked to assure that all diagonal values are large enough (and none of them are negative). If there is a problem, appropriate changes are made to the covariance matrix to assure numerical stability. Also at this point, if the error control function has determined that there is a problem with the Kalman filter (divergence or the like), it may also signal that certain elements of the covariance matrix should change to eliminate the problem.

The Kalman covariance information is sent to the source selection routines so that it can be used in selecting the next measurement which should be used in the filter.

Next, the algorithm tests to see if this is the last fix in the source selection interval. If it is not, the program loops back and propagates to the next measurement event. If necessary, the estimated error vector is reset.



If the last fix has occurred, the filter then extrapolates the error states in the system to current time and resets the navigation and (potentially) the time errors with this information. The reset information is also stored for later use in compensating for the resets in the filter.

If the JTIDS receiver is in the RTT mode, a special filter for estimating JTIDS time (involving two states) is implemented on a four-second cycle (Singer's approach). These corrections, rather than the corrections from the navigation filter, are used to correct clock time. If the receiver is in this mode, the measurement matrix associated with the navigation measurements is, of course, modified to assume that JTIDS time is perfect.

The key features which distinguish the fully integrated JTIDS/GPS/INS filter from the JTIDS-only filter are:

- Pseudo-range divergences from GPS are used directly in the fully integrated filter.
- The fully integrated filter models GPS clock error states.
- A wider variety of consistency checks is available in the fully integrated filter.
- The error control function of the fully integrated filter may be more complex and may actually be used to control the RF tracking loops.
- Additional measurements (offset time, offset GPS) are possible in the fully integrated filter.

#### 6.2.3 Navigation Data Set Source Selection

The key to maximizing the synergistic benefits of having a fully integrated navigation function lies in the source selection routines used to choose the measurements operated upon by the Kalman filter. Below is a description of a candidate mechanization for this source selection algorithm.

Inputs to the source selection algorithm are:

- JTIDS P messages received from donor members.
- Satellite ID's used for navigation.

- Own navigator's quality, as determined from the Kalman covariance.
- Tracking loop parameters: loop lock indicators and tracking loop time constant.

The source selection routine has been set up so that alternate screening takes place for geodetic information and for relative information on alternate source selection intervals. Note that alternating geodetic and relative source selection is reasonable because:

- The time constant associated with the GPS tracking loops is so long.
- The geodetic grid is established through GPS and is initialized through the C/A mode if possible.
- Both time references are set independently.

Figure 74 shows a functional flow diagram of the source selection algorithm. First, assume that both JTIDS and GPS are operational, that it is time for geodetic fix, and that the program is at the beginning of the source selection interval labeled START. The pseudo-ranges from the GPS receiver are sampled for at least four pseudo-ranges. If the lock indicators indicate that the tracking loops are locked, these pseudo-ranges are stored. If the costas loop is operable, as indicated by the phase tracking loop indicator, and if the time constant in the tracking loop is small, then the  $\Delta R$ 's from the frequency tracking loop are also stored. Note that if the time constants of the phase locked loops are large, the  $\Delta R$ 's are really more dependent upon the rate-aiding errors than they are to true velocity errors. Thus, they really contain no additional information of use to the filter.

If there are no missed measurements, the source selection routine simply waits until the end of the source selection interval. It then checks the lock indicators again. If all loops are in lock, the original pseudo-ranges are replaced with the pseudo-ranges sampled at the end of the source selection interval. In this way, satellite data is made as current as possible. If only some of the loops indicate lock, then only these pseudo-ranges are used to replace the original set of the pseudo-ranges.

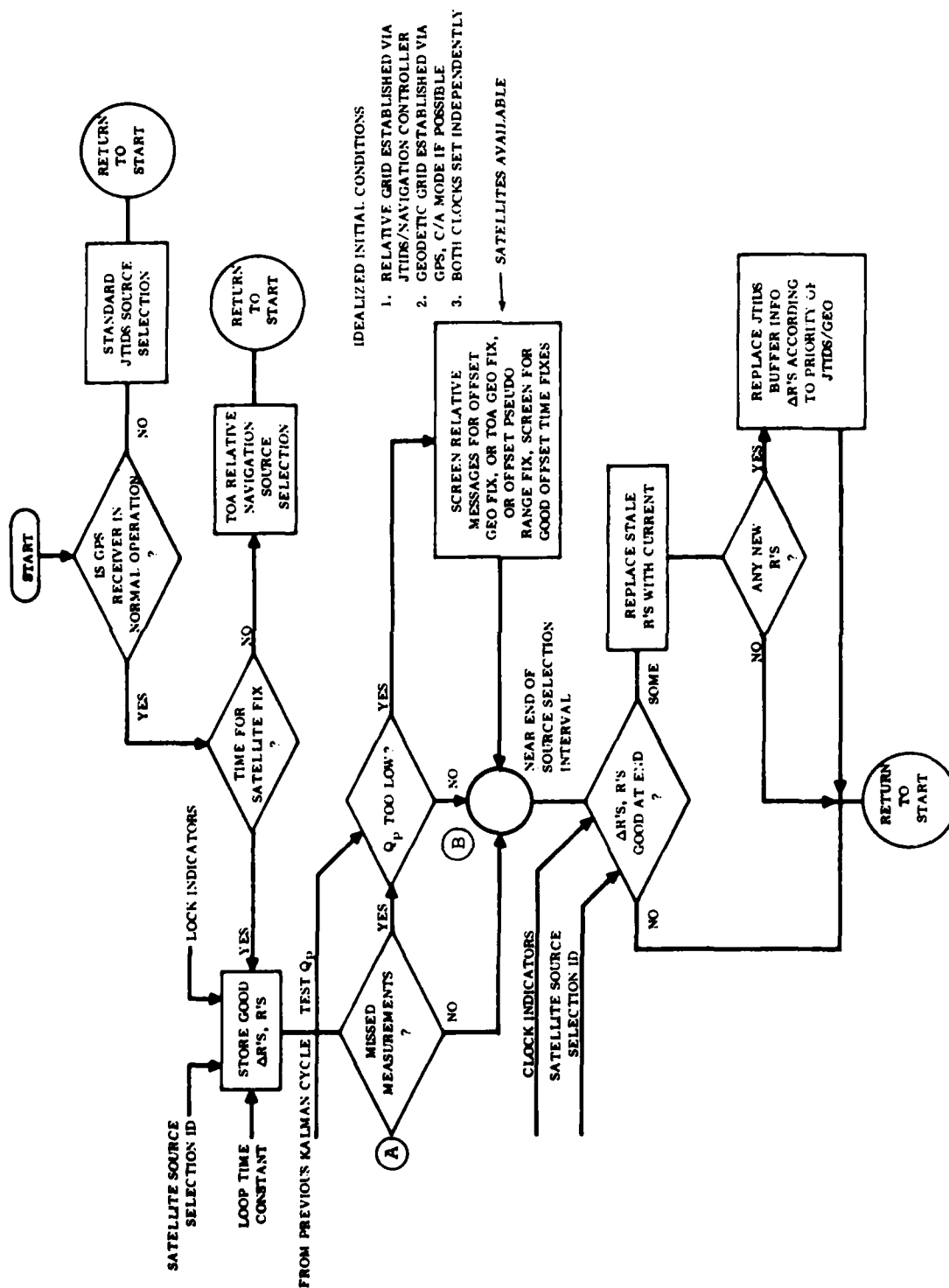


Figure 74. Source selection algorithm functional flow chart

Returning to point A on Figure 74, if some of the measurements are missed, the algorithm then tests the quality of navigation. If position quality,  $Q_p$ , is high enough, the algorithm simply proceeds as before (going down to point B). If there is degraded geodetic position quality, however, the source selection routine scans the P messages derived from JTIDS. These P messages and measured TOA may be used to arrive at a JTIDS related geodetic measurement. The source screening algorithm here may be quite complex. If only some of the pseudo-ranges are observed, the screening algorithm may choose to use a TOA measurement from a high quality source member which has the proper geometry in order to round out knowledge of geodetic fix. If availability of satellites is low and/or if  $Q_p$  from available sources is low, and if geometry is correct, P-message-reported pseudo-ranges may also be used as a source of an offset pseudo-range fix.

Near the end of the source selection interval the lock indicators are again sampled. More current pseudo-ranges are entered into the source selection buffers, if indicated, and, if there are any new pseudo-ranges, an appropriate algorithm is implemented to eliminate some of the JTIDS derived information in favor of the new pseudo-ranges.

If it is time for relative navigation fixes, a source selection routine consistent with that for screening only relative data is performed as implemented by current JTIDS designs.

If GPS is not operating, then the standard JTIDS source selection routines which potentially mix geodetic and relative information are implemented during every source selection cycle.

#### 6.2.3.1 Dynamic Behavior of Navigation Data Set Source Selection

A discussion of the dynamic behavior of the source selection routine in the presence of jamming and/or high dynamic vehicle maneuvers is noteworthy. When all tracking loops in the GPS are operational, precise geodetic navigation will result. When, because of jamming or high dynamic maneuvers, some or all of the tracking loops lose lock, the source selection routine will operate in such a way that, so long as the remaining GPS information is good enough to maintain a high quality of geodetic information, there is no mixing of JTIDS information to derive geodetic information. However, when the Kalman filter indicates that geodetic quality is degrading, the source selection automatically reverts to using JTIDS information for

updating. It will use the highest quality geodetic information available in the community, which characteristically will be derived from another platform which is receiving GPS. Thus GPS quality navigation can be maintained so long as one or more members in the community is still locked on to GPS. Also, if there are only two satellites in sight of the community and community geometry is suitable, accurate geodetic fixing is possible by sharing of GPS pseudo-range information.

When the GPS receiver is jammed or loses lock because of maneuvers, high quality position and velocity information pertaining to the grid can be maintained by the program. Precise time can also be maintained. Thus the rate-aiding of the tracking loops may maintain high enough quality so that the tracking loops can be slewed through the period of jamming and naturally relock on to the GPS signal when jamming is diminished.

#### 6.2.4 Acquisition and Maintenance of Timebase

For JTIDS relative navigation, there are two distinct timebase possibilities: 1) the timebase controller has GPS available to it, and resets its local oscillator with GPS time, so that JTIDS time will effectively be the same as GPS time; or 2) the timebase controller is independent of GPS time.

If JTIDS time is locked to GPS time, and if some of the GPS loops lose lock, causing the Kalman filter to indicate that GPS time is being degraded, the frequency correction made to the GPS time reference should be the correction made for the JTIDS time reference. The GPS covariance value should be allowed to grow (no change is made to the Kalman algorithm). This procedure should be continued until such time as there are sufficient satellite measurements that control of GPS time can be allowed to revert back to the GPS navigation filter. If this, along with the positioning source selection is properly implemented, it may be possible to allow the GPS tracking loops to run open loop for minutes on end and still have them ready to lock on to the GPS signals when they again become available.

If JTIDS time is not locked to GPS time, then JTIDS clock precision generally will be no better than the precision of the JTIDS oscillator. The best one can do in this situation is to simply use the last best estimate of GPS time and frequency, and extrapolate time forward. Obviously clock errors will grow, soon making it impossible to automatically relock on to the GPS signal without special initialization procedures.



There is a third possibility, however. This involves having other community members with an integrated JTIDS/GPS receiver transmit two quantities on the variable message field of the JTIDS P message:

- Estimated quality of GPS clock.
- Time offset between JTIDS and GPS.

Source screening can then be carried out to find the highest quality geodetic time during the source selection cycle. Then an offset time fix could be accomplished relating JTIDS time to GPS time. The result would be highly accurate GPS time, which could be applied to the Kalman filter.

#### 6.2.5 Geodetic Navigation With Less Than Four GPS Satellites in View

At times, there will be less than four GPS satellites in view of a user (or less than four with adequate angular separation), as required for accurate GPS computations. If, however, there are several JTIDS/GPS receivers displaced over a relatively broad area, and if the relative locations of these receivers are known via JTIDS, and if they are within line-of-sight of one another, then it can be shown by geometric analysis that as few as two satellites within view of each user can provide relatively high accuracy geodetic positioning for all users in the area.

For example, see Figure 75. The positions of three platforms are indicated by the ends of the triangle. The hyperbolic lines on the figure represent LOPs from two navigation satellites (altitude assumed known). If the relative ranges between the platforms is known via JTIDS, there is only one position and orientation for this triangle if each of the vehicles is to lie on the LOPs indicated. Note that GDOP may be relatively severe if the curvature of the LOPs is small. However, the Kalman filter operating on the information will have information to this affect. The source selection routines will use this information to minimize GDOP impact.

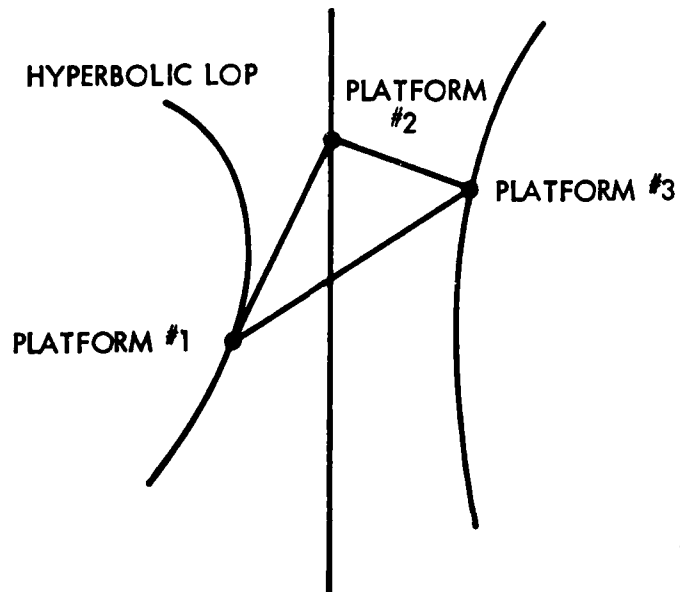


Figure 75. Geometry of three platforms in a field of hyperbolic LOP's

What follows is a preliminary design of how this synergistic benefit between JTIDS and GPS can be implemented

Assume that the variable data field of the JTIDS P message contains the following information:

$P_u, P_v, P_w, L, \lambda, Z, \dots Q_T, Q_P, Q_{AR}, Q_{PR},$

to which is added:

-  
New Data

$\overbrace{R_1, R_2, R_3, R_4, \dots T, Q_{GPS}}$

Note that the additional information on the P message contains the pseudo-ranges to the various satellites tracked by the donor platforms (the R's), the estimated time difference between GPS clock and JTIDS clock, T, and the quality number,  $Q_{GPS}$ , indicating the anticipated quality of GPS time.

Note that several methods of data compression are possible for the pseudo-range reports. One alternative is to send pseudo-range divergences like those used as inputs, to the donor platform's Kalman filter. The second alternative is to simply transmit the "least significant bits" of the pseudo-range measurement where own receiver can utilize reported latitude-longitude in order to reconstruct the entire pseudo-range measurement. Also required is a report of "staleness" of each pseudo-range measurement.

Own receiver would then have the capability of taking an offset satellite geodetic fix. The source selection algorithm would first screen the augmented P messages for the best source of offset satellite fix. The first key parameter of the screening would be the quality of the relative position and the second, the time error of the donor platform. The third key parameter would be the availability of offset measurement. The fourth key parameter would be the relative geometry errors pertinent to the potential offset measurements. The quality of this offset method of fix will not be as high as the quality of a direct geodetic fix. However, in the absence of enough satellites to take a self-contained fix, this procedure offers an acceptable alternative to not using GPS at all.

## 7. CONCLUSIONS AND RECOMMENDATIONS

### 7.1 REVIEW OF THE STUDY FINDINGS

All the findings to date lead to the conclusion that a flexible, software controlled, advanced technology MFBARS offers substantial size, weight and cost advantages over upgraded but non-integrated discrete CNI radios. These savings can be attributed, in large part, to a new concept in radio signal processing employing programmable agile transversal filters as flexible, general purpose signal processing elements, both in the radio frequency domain (WBATF's) and at baseband (NBATF's). Conventional radio systems are usually limited by fixed designs rigidly optimized for each particular application. The flexible aspects of the WBATF and NBATF allow MFBARS to be dynamically reconfigured under software control to any signal structure consistent with filter input bandwidths.

The further ability of the WBATF's and NBATF's to be time-shared in a high speed fashion without signal to noise ratio degradation, results in further savings. And by using sampled data techniques and implicit frequency conversion, there can be simplification in the area of frequency synthesizer complexity.

The efficiency of these advanced techniques, coupled with projected advances in integrated digital circuit designs, produces overall projected size and weight savings illustrated very dramatically in Figure 76. This very significant reduction in size and weight would ease severe hardware space limitation problems in tactical aircraft. Another, less obvious, advantage of the selected MFBARS architecture is its growth flexibility. Software, rather than hardware, changes can reconfigure the system for additional radio service and/or a change in mix of radio service.

In any integrated design where many functions depend upon the health of one set of equipment, reliability can be a problem if it is not carefully factored into the design. Redundant paths must be provided such that no single failure can cause a catastrophic mission failure. Again, flexibility in design provides some help in this area. The proposed MFBARS design provides redundant processing paths which are each flexible enough to perform a critical subset of processing functions at full performance levels, or all functions at reduced levels of performance. The system design allows the available system resources to be applied as required by a particular mission requirement.

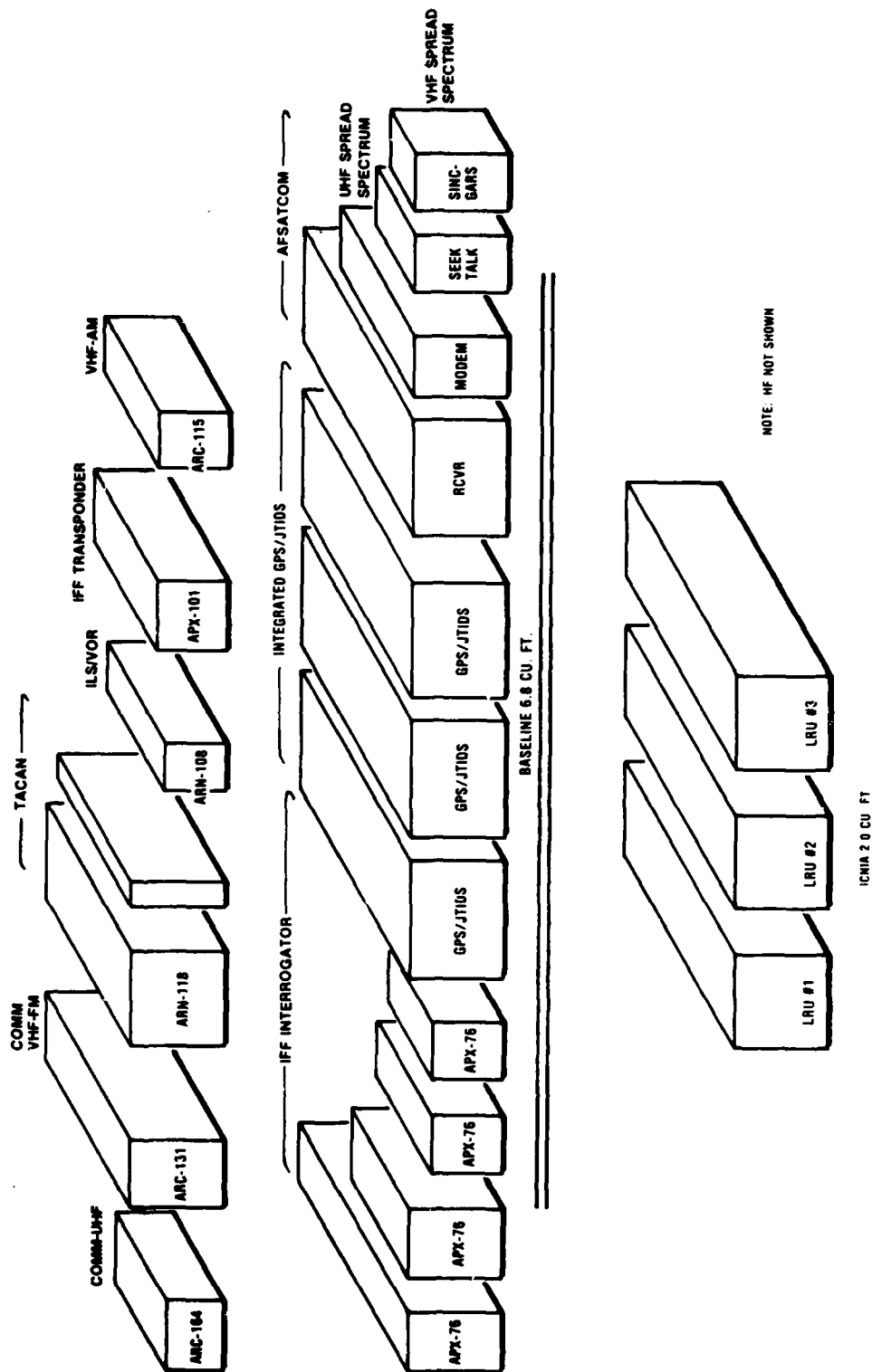


Figure 76. Comparison, MFBARS versus baseline

Finally, the fully integrated CNI/Nav concepts merit further work to evaluate whether a higher level of integration would be cost-effective and feasible at this time.

## 7.2 RECOMMENDATIONS FOR FUTURE DEVELOPMENT

With the completion of Concept Definition, (essentially MFBARS Phases I and II), the program is ready to enter two parallel follow-on phases, Concept Validation Tasks and Support (or Operational Impact) Tasks. Concept Validation Tasks are those which will reduce program risk by demonstrating feasibility of critical system concepts before proceeding to ADM. Support (or Operational Impact) Tasks are those tasks which involve interactions between MFBARS and other systems, deployment and support interactions, life cycle cost, etc. Upon completion of both of these groups of tasks, the program can proceed to Concept Refinement and then to ADM with minimum risk. Figure 77 shows the general interrelationship of these groups of follow-on program tasks.

## 7.3 SUGGESTED PROGRAM PLAN

Figure 78 shows a more detailed program plan, with major tasks identified. (The tasks are numbered to tie in with the top level grouping of Figure 77).

Tasks 2.1 through 2.14 represent a logical and progressive demonstration of validity of the most innovative aspects of the system concept, starting with development and demonstration of an innovative new technology device, the wideband agile transversal filter (WBATF) (tasks 2.1 through 2.5). As shown, there is a high degree of interaction between tasks 2.3 and 2.4, the device development and the parallel development of demonstration hardware and software. Upon completion of development of both the device and the demonstration hardware/software, task 2.5 demonstrates and evaluates WBATF signal processing and integrated adaptive antenna processing.

A similar grouping of tasks (2.6 through 2.10) provides for device development and concept demonstration of narrowband agile transversal filter (NBATF) signal processing, another critical system function. There are similar interactive relationships between some of the tasks, as in the case for the WBATF.

Upon completion of WBATF and NBATF demonstration and evaluation, results can be used for refinement of device parameters (task 2.11) to allow progression from prototype device status to more refined devices (task 2.12) for the ADM phase of the program.

AD-A106 052

ITT AVIONICS DIV NUTLEY N J

F/G 17/2.1

MODULAR MULTI-FUNCTION MULTI-BAND AIRBORNE RADIO SYSTEM (MFARS--ETC(U)

JUN 81 R A REILLY; C W WARD; A LEE

F33615-78-C-1518

UNCLASSIFIED

AFWAL-TR-81-1077-VOL-2

NL

3 of 3

40 4  
11-8052

													END DATE FILMED 11-81 DTIC

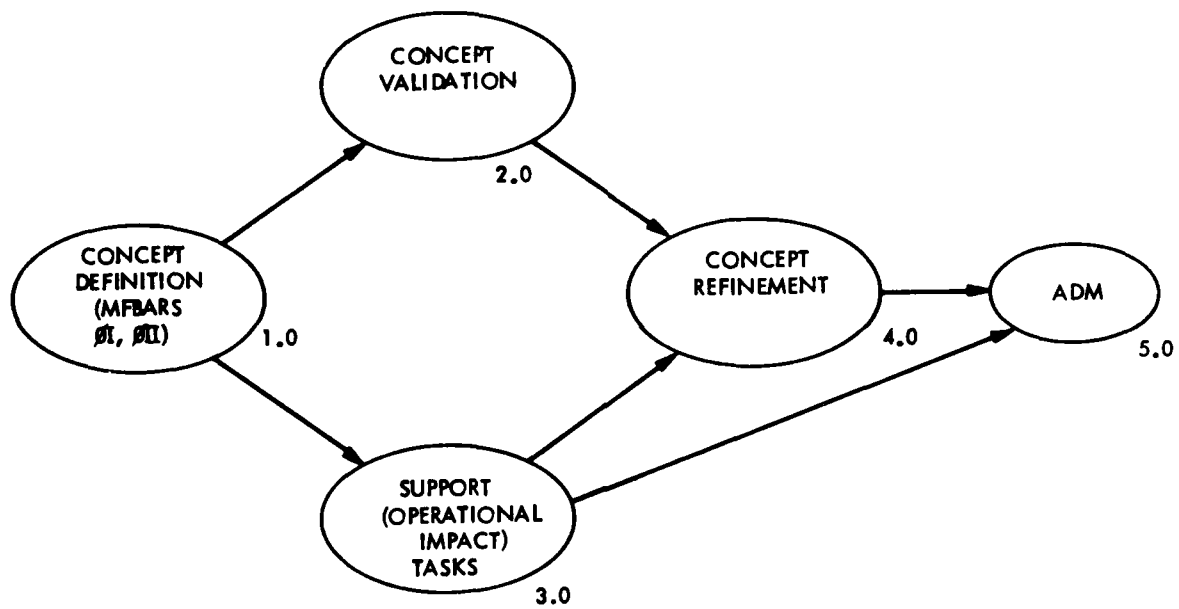
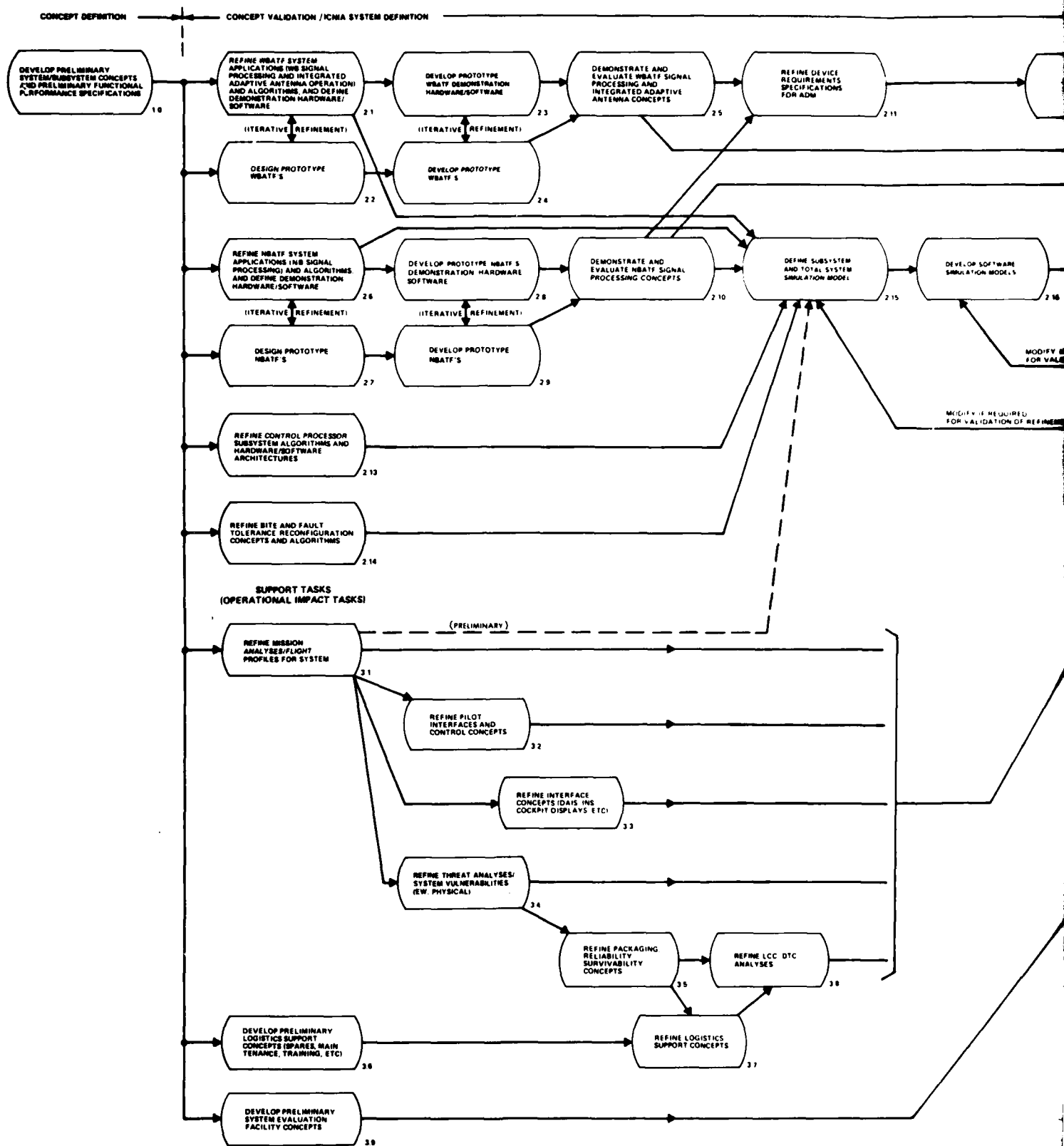


Figure 77. Program flow chart







Tasks 2.13 and 2.14 provide refinement of other design areas not completed in depth in MFBARS Phase II.

Upon completion of these four areas of group 2.0 tasks (WBATF, NBATF, control processor, and BITE/fail-soft reconfiguration capability), the major innovative aspects of the system will have been individually demonstrated and evaluated. The next step will be to validate their interactions with each other and with other less innovative aspects of the system design concept. At this point in system validation, a simulation model is the most practical means of demonstrating overall integrated system performance concepts. Tasks 2.15 through 2.17 involve development and operation of a system simulation model and evaluation of the integrated results. Note, that the model also utilizes inputs from the group 3.0 tasks, the support or operational impact tasks. The group 3.0 tasks provide inputs needed by the model in terms of realistic timelines, system signal loads, control and display time-sharing, pilot interactions, impact of external threats (EW and physical) which might interfere with system operation, etc. Without these group 3.0 inputs, system load could not be realistically simulated.

Group 3.0 tasks serve other purposes as well as providing inputs to the system simulation model. Tasks 3.1 through 3.3 represent refinements of other earlier data which provided rough mission constraints and requirements information for initial development of MFBARS system concepts. Now that a system concept has been developed, it is necessary to review the constraints and requirements information to make sure that the missions would still be performed the same way as originally defined or whether refinements may be appropriate. This could be considered a type of "sensitivity analysis" to validate that the resultant overall system capabilities are still well matched and balanced to the overall mission requirements. In addition, some inputs, such as pilot interfaces, need refinement which could not be done prior to availability of a specific system concept.

Task 3.4, in addition to providing an input to the system simulation model, also provides critical inputs to refinements of packaging, survivability, and reliability concepts for the system (task 3.5). These, in turn, provide needed inputs to tasks 3.7 and 3.8, which are refinements of logistics support concepts and life cycle cost and design to cost (LCC/DTC) analyses. Preliminary logistics concepts can be started (task 3.6) using basic system concept information, but refinement (task 3.7) requires packaging inputs from task 3.5.

Finally, among the support tasks is a very important task (3.9) which initiates definition of a System Evaluation Facility required to support ADM development and ADM test and evaluation. The multiple signals and complex interactions the system must handle requires a System Evaluation Facility beyond any now available. Initial concepts must be started early to assure availability of the necessary facility at the proper time.

Completion of all group 2.0 and 3.0 tasks enables initiation of task 4.0, refinement of system/subsystem concepts and functional performance specifications, as appropriate. Although shown as only a single task in the program plan (plus feedback to earlier tasks), it could be a very significant task and may be broken into smaller subtasks later, depending upon the outcome of system simulations and task group 3.0 inputs. Also, although not shown on the diagram for reasons of clarity, many of the other task outputs may also influence task 4.0. As shown, significant changes are fed back to tasks 2.15 through 2.17, as required, to make sure refinements are validated before proceeding to ADM. Also, group 3.0 tasks will be refined as appropriate, although refinement details are not shown, for clarity.

When the system concepts have been refined and validated to the satisfaction of the Government, then the program can proceed to ADM with minimal risk. Only six ADM (group 5.0) tasks are shown on the program plan at this time. Each represents a significant program effort and could be subdivided into more detail later. The major relationships are evident, however, including input of task 2.12 refined ADM devices, which have been developed in parallel with other tasks. Upon completion of ADM (task 5.6), the program can proceed to EDM and subsequently to production.

## APPENDIX A. DETAILED DESCRIPTION OF WIDEBAND AGILE TRANSVERSAL FILTER (WBATF) DESIGN

A WBATF is a special form of a generic device called a transversal filter, which utilizes a tapped delay line and summing bus to detect matches between input signals and a stored reference signal. The major differences between the generic transversal filter and the specific WBATF are: an extraordinarily wide input bandwidth (400 MHz); extraordinarily high speed sampling of the input signal (900 MHz), and the special ability to change the tap weights rapidly (6 ns), under software control, as the sampled input signal propagates through the device.

The function of the WBATF is to perform RF frequency selective filtering (preselection) of incoming radio signals in the range of 30-400 MHz, or 960-1215 MHz. The filter can be rapidly timeshared among several input signals without the usual timesharing losses with respect to signal to noise ratio. Further, the filter is fully programmable in terms of center frequency and bandshape, making it useful for processing various signal formats in a multi-function environment.

Figure A-1 is a simplified functional block diagram of the WBATF. The wideband antenna inputs are bandpass filtered by conventional filters and provided to the switch preceding the WBATF. Therefore, each WBATF (of two in the system) will be receiving either VHF/UHF signals or L-Band signals, but not both simultaneously. This limits the bandwidth of the incoming signals to less than 400 MHz, which the delay medium of the WBATF is designed to accommodate.

The maximum time delay between taps is determined by the bandwidth and center frequency of the signals which are input. At any given instant of time the information which can be extracted from the tapped delay line is limited to discrete values of the input signals at times corresponding to the tap delays. For equal delay ( $T$ ) between successive taps, we can consider this to be a regular sampling process on the input signals at a rate equal to  $1/T$ . We know from sampling theory that the choice of sampling frequency is important in avoiding aliasing errors due to spectrum overlapping. That is to say, when we sample an input signal characterized by a given frequency spectrum, the resulting sampled signal spectrum is periodic and consists of the original input spectrum replicated at all integer

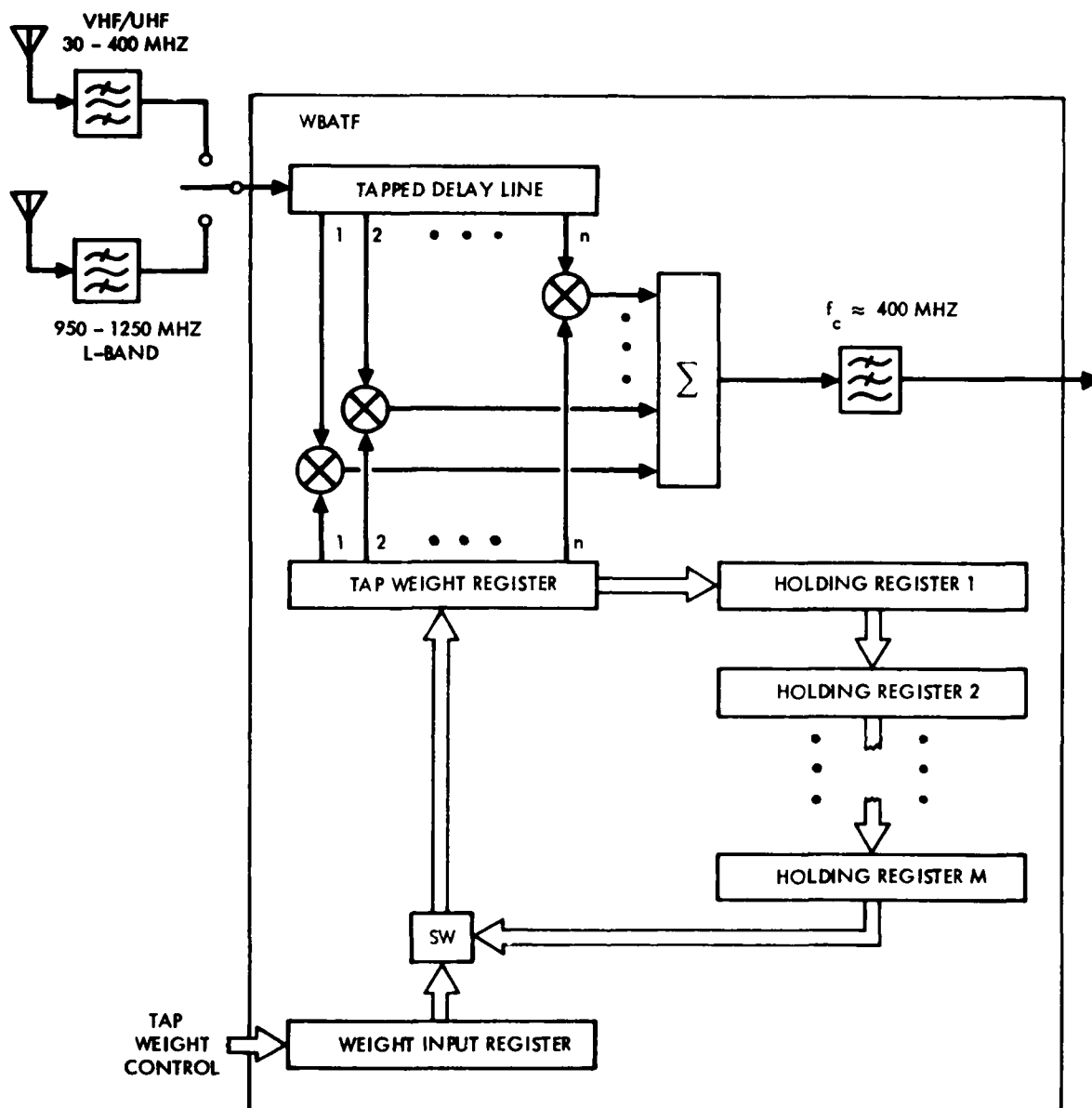


Figure A-1. WBATF block diagram

multiples of the sampling frequency. Therefore, if the sampling frequency is improperly chosen, the multiple images of the spectrum may overlap, causing a distortion of the input signal's original spectrum. This situation is depicted in Figure A-2 for the case where the input signal is characterized by both a low pass spectrum and a bandpass spectrum.

For the case of a low pass spectrum, the minimum sampling rate ( $f_s$ ) to avoid aliasing is twice the highest frequency ( $f_h$ ) present in the spectrum, which is the well known Nyquist rate. The case for a bandpass spectrum is similar except that, in general, sampling at a rate equal to twice the highest frequency in the spectrum is not necessary. By the very nature of a bandpass signal spectrum there are gaps between zero frequency and the inner edges of the spectrum. This gap may accommodate several replications of the original spectrum, and for this reason a sampling rate on the order of twice the bandwidth of the input signal may be sufficient. Actually, the relationship between the center frequency and bandwidth enter into the problem and sampling at twice the bandwidth is the minimum rate which will avoid aliasing but only for particular center frequencies. This situation is described by the following relationships.

If a given input signal has a spectrum which is band-limited such that the highest frequency present is  $f_2$  and the lowest frequency present is  $f_1$ , then the range of permissible sampling frequencies which guarantee no aliasing are given by:

$$\frac{2f_2}{m+1} < f_s \leq \frac{2f_1}{m} \quad (A-1)$$

where  $m=0, 1, 2, \dots$

While the above equation gives a listing of all possible sampling rates it is often of particular interest to know the minimum sampling rate, which is given by:

$$f_{s_{\min}} = 2B \left( 1 + \frac{k}{M+1} \right) \quad (A-2)$$

where

$$B = f_2 - f_1 = \text{input signal bandwidth}$$

$$M = \text{int}(f_1/B) = \text{integer part of } (f_1/B)$$

$$K = (f_1/B) - M = \text{fractional part of } (f_1/B)$$

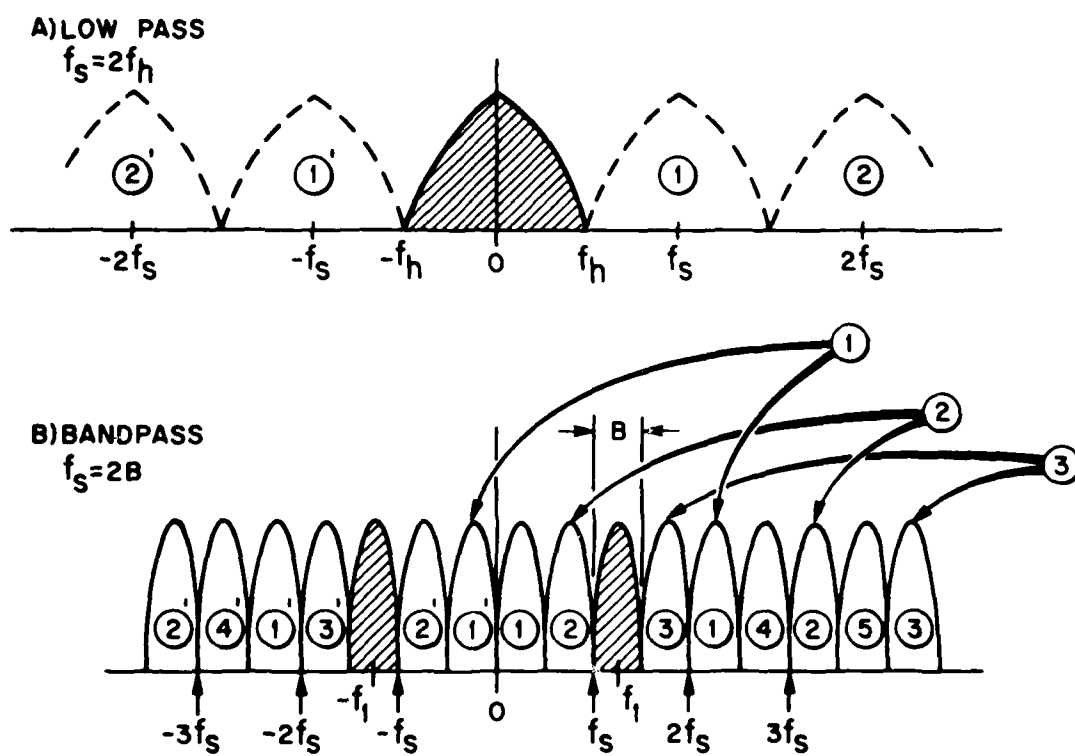


Figure A-2. Low pass and band pass sampling theory



This equation demonstrates the point made earlier, that the minimum sampling rate for bandpass signals is  $2B$ , providing that  $f_1$  is an integer multiple of  $B$  (i.e.,  $k=0$ ).

If we wish to use one common WBATF to process either VHF/UHF or L-Band signals it would be of interest to find a tap spacing (sampling rate) which would be satisfactory for both frequency bands. Table A-1 is a tabulation of permissible sampling rates computed from equation (A-1) for these frequency bands. The equation is evaluated for higher values of  $m$  until the inequality is no longer satisfied. For the VHF/UHF band we see that any frequency exceeding 800 MHz is acceptable. For L-Band there are several ranges of frequency acceptable, and the minimum frequency range which also satisfies the VHF/UHF requirements is 810 MHz to 960 MHz.

Any sampling rate in this range would be acceptable providing the input signal's spectrum is perfectly bandlimited to the assumed frequencies ( $f_1$  and  $f_2$ ). In practice, the wideband input filters will have attenuation skirts which must be considered. Figure A-3 shows as shaded areas the L-Band frequency range of interest. An ideal input filter would have a perfectly rectangular passband matched to this frequency range. The equivalent sampling process performed by the tapped delay line produces replications of the spectrum spaced at  $f_s$ , the sampling frequency, as shown in the figure.

TABLE A-1. ACCEPTABLE VALUES OF SAMPLING RATES  
FROM EQUATION (1)

<u>VHF/UHF band</u>	<u>L-band</u>
$f_1 = 30 \text{ MHz}$	$f_1 = 960 \text{ MHz}$
$f_2 = 400 \text{ MHz}$	$f_2 = 1215 \text{ MHz}$
$800 \text{ MHz} \leq f_s \leq \infty$	$2430 \text{ MHz} \leq f_s \leq \infty$
$m = 0$	
$m = 1$	$1215 \text{ MHz} \leq f_s \leq 1920 \text{ MHz}$
<del><math>400 \text{ MHz} \leq f_s \leq 60 \text{ MHz}</math></del>	$810 \text{ MHz} \leq f_s \leq 960 \text{ MHz}$
$m = 2$	
$m = 3$	$607.5 \text{ MHz} \leq f_s \leq 640 \text{ MHz}$
$m = 4$	<del><math>486 \text{ MHz} \leq f_2 \leq 480 \text{ MHz}</math></del>

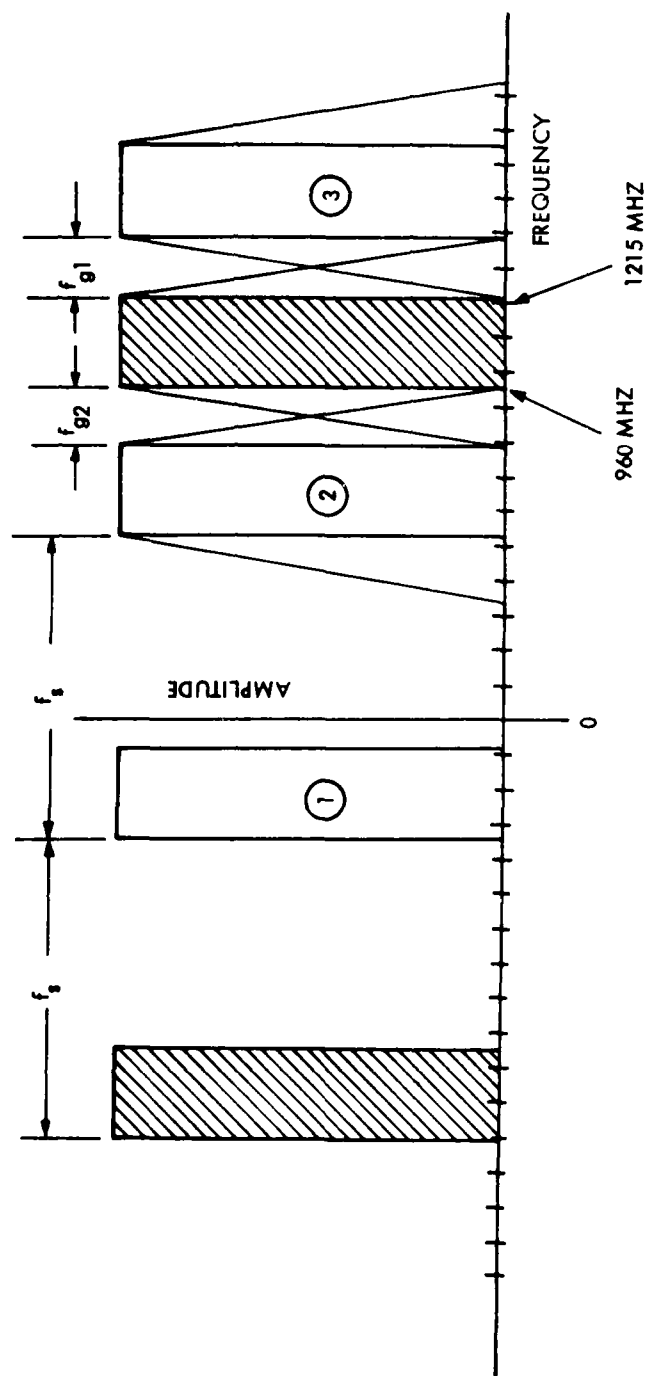


Figure A-3. Input filter selectivity requirements (L-band)

Notice that the original spectrum on the positive frequency axis is bordered by the second and third harmonic image of the negative frequency portion of the original spectrum. The gaps on either side of the original spectrum,  $f_{g1}$  and  $f_{g2}$ , are a function of the sampling rate. The gaps must be wide enough to accommodate the skirts of the real input filter. As shown in the figure, if the skirts are symmetrical, the gaps  $f_{g1}$  and  $f_{g2}$  should be equal. This also uniquely defines the sampling frequency or tap spacing. The gap space is then the allowable frequency range over which the skirt attenuation must reach some desired value. Note that the skirts overlap each other, but not any portion of the original spectrum which is the region of interest. For the MFBARS application the ultimate attenuation required over the gap width is on the order of 100 dB. This level is determined by the maximum level of an interfering signal at the gap width or greater from the desired signal's spectrum band edge. Simple algebra will yield the specific sampling frequency which will produce the symmetrical gaps, and for the example shown this becomes  $f_s = 870$  MHz.

A similar analysis could be conducted for the application of the WBATF to the lower frequency VHF/UHF frequency band. The results of this analysis indicate that even a better input filter in terms of its rate of cutoff is required. This is due to the wider bandwidth (30-400 MHz) of the input spectrum. If these filters are realized using conventional, recursive, lumped constant designs, many poles may be required, and this would result in large time delay variations in the region near the skirts. This differential time delay over the passband is an error source for precise ranging systems such as JTIDS, and therefore, must be compensated for by equalization networks, or use of transversal filters which are inherently more flexible.

Each of the tap outputs from the delay line (see Figure A-1) is connected to one input of a four quadrant multiplier. The other input of the four quadrant multiplier is connected to the corresponding output of a tap weight register. The tap weight register is a memory device which holds  $n$  signed numbers, where  $n$  corresponds to the number of taps in the delay line. All of the outputs from the four quadrant multipliers are summed, and the output can be described mathematically by:

$$y(k) = \sum_{v=0}^n w(v) X(k-v) \quad (A-3)$$

where  $k$  = integer denoting a time index so that one unit of time corresponds to the tap spacing

$$T = 1/f_s.$$

$X(k)$  = the input signal to the delay line at the  $k$ th instant of time.

$w(v)$  = the  $v$ th value of the tap weight.

$y(k)$  = the filter output at the  $k$ th instant of time.

A linear discrete time filter can be completely specified by its impulse response. Substituting the delta-dirac ( $\delta$ ) function for  $X(k)$  in equation (A-3):

$$y(k) = \sum_{v=0}^n w(v) \delta(k-v) = w(k) \triangleq h(k) \quad (A-4)$$

We arrive at the obvious conclusion that the impulse response of the filter,  $h(k)$ , is simply equal to the tap weights. In the frequency domain the filter transfer function,  $H(z)$ , can be obtained by taking the z-transform of the impulse response:

$$H(z) = \sum_{v=0}^n h(v) z^{-v} \quad (A-5)$$

By setting  $z = \exp(j2\pi fT)$  we can examine the frequency response:

$$G(f) = H(\exp(j2\pi fT)) = \sum_{v=0}^n h(v) \exp(-j2\pi fTv) \quad (A-6)$$

which gives the magnitude and phase response of the filter. In filter design the magnitude and phase response is usually the starting point, and consequently the problem is worked backwards to determine the impulse response which defines the tap weights. A similar relationship exists for continuous time filters except it is the Fourier Transform which relates the impulse response to the transfer function. Figure A-4 illustrates several Fourier Transform pairs which provide some insight into the interdependence between the time domain and the frequency domain. It can be seen that for a rectangular impulse response (A), (approximated in the discrete time case when all tap weights are equal) the corresponding frequency response has a  $\sin x/x$  form. Notice that the width of the main lobe of

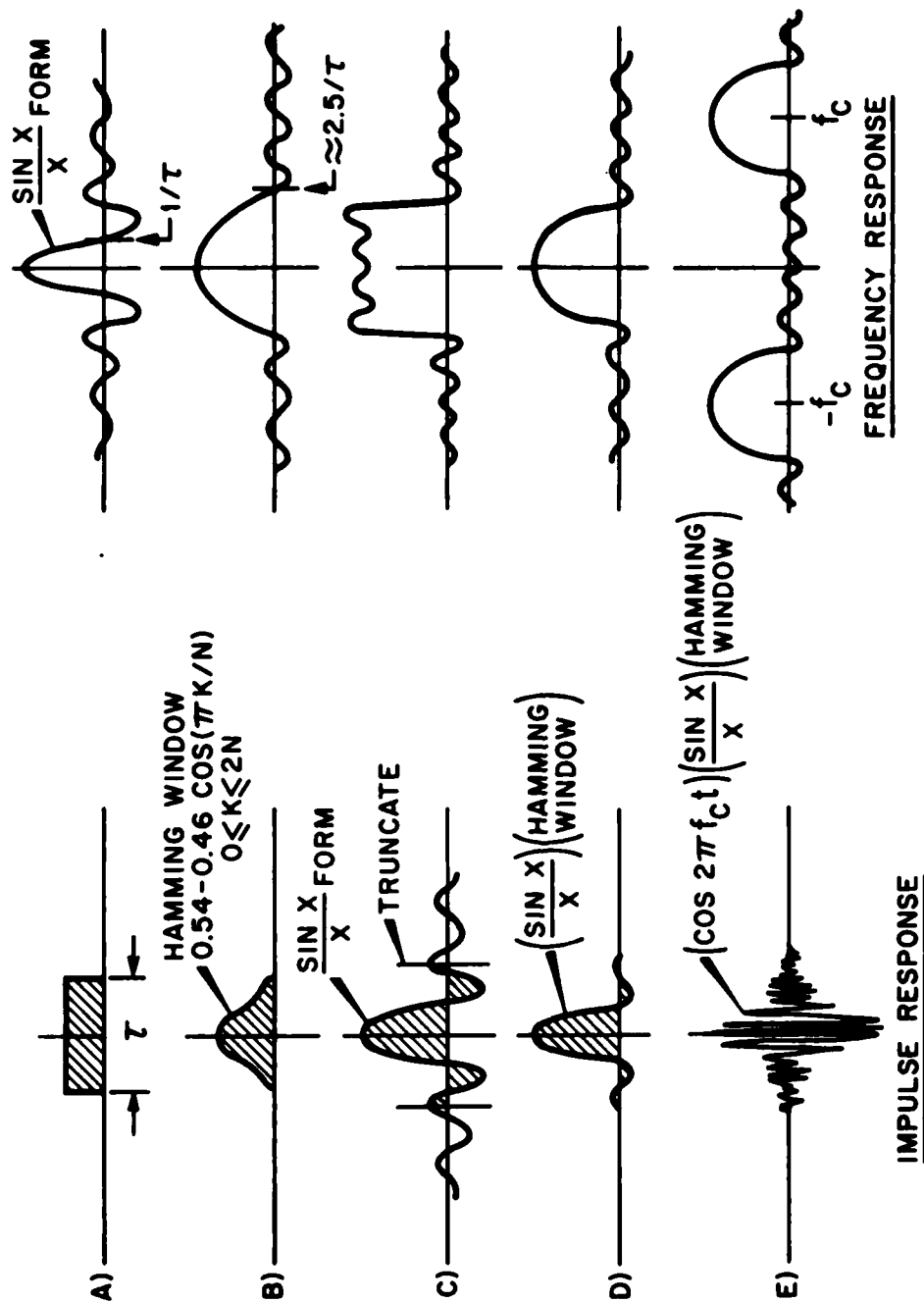


Figure A-4. Fourier transform pairs

the  $\sin x/x$  form is the reciprocal of the impulse response duration. This illustrates the important fact that the narrower the desired filter bandwidth is the longer the impulse response duration must be. Therefore, once a tap spacing has been selected based on input bandwidth considerations, output bandshape considerations determine how many taps are required. The term "bandshape" was used here to denote that other factors in addition to bandwidth, such as passband ripple, stopband ripple, and ultimate attenuation enter into the problem.

Figure A-4(B) shows the effect of one commonly used weighting function known as a Hamming Window. Window functions of this type are usually employed to improve the rate of cutoff and suppress sidelobe responses with respect to the  $\sin x/x$  form. The price paid for this is a wider passband.

Figure A-4(C) illustrates the reciprocal nature of Fourier Transform pairs by attempting to achieve ideal (rectangular) passband by using a  $\sin x/x$  impulse response. The theoretical  $\sin x/x$  function extends to infinity in both directions along the time axis, and in a practical implementation requires truncation at some point. The resultant frequency response does exhibit very sharp cutoff characteristics but also produces large ripples\* at the cutoff frequencies due to the truncation.

Figure A-4(D) is a combination of a truncated  $\sin x/x$  function and a Hamming Window. This is a form which is useful in many practical applications since it retains some of the sharp cutoff characteristics while suppressing the ripple in the passband.

Figure A-4(E) demonstrates how a low pass filter transfer function can be transformed into a bandpass transfer function centered at carrier frequency  $f_c$ , simply by multiplying the low pass impulse response by  $\cos 2\pi f_c t$ . This is a direct consequence of the frequency shifting theorem.

The above descriptions were presented to provide an understanding of the interrelationships between the time and frequency domain, rather than to suggest a design approach. For practical designs, particularly where very high performance is required, computer programs have been written which produce optimal designs efficiently (2).

\*This is due to Gibbs Phenomenon; see Papoulis, The Fourier Integral and its Applications, page 30.

By returning to equation (A-6) and noting that the filter transfer function consists of a sum of complex exponentials, we can see that the transfer function is periodic over the interval  $T$  which is equivalent to the tap spacing interval. Therefore, as an unavoidable consequence of the discrete time nature of the filter, the filter will have multiple harmonic responses every  $1/T$  Hz. Figure A-5 illustrates this situation where the WBATF has been programmed to perform a bandpass filtering function at a center frequency of 300 MHz. The drawing is approximately to scale where each tic mark on the horizontal axis represents 100 MHz. Note that the fundamental response (consisting of both the positive and negative frequency images) is replicated about multiples of  $f_s = 1/T = 870$  MHz. Some of the responses are indicated by dotted lines because they fall outside the input filter responses. That is, the WBATF does indeed have natural responses at those frequencies but the VHF/UHF and L-Band input filters prevent any signals at these frequencies to ever enter the WBATF. Also note that although both the VHF/UHF and L-band input filter responses are shown in the figure, as was mentioned earlier, only one at a time is used. See Figure A-1 for switching at the WBATF input. Therefore, by a simple switching operation at the input, the filter will respond to the selected band. This is an important simplification because it eliminates the need for generating additional tap weight programming information for each frequency band. The small horizontal arrows above each of the output responses indicate the direction that the response will move with an increase in programmed center frequency. This indicates that both the VHF/UHF and L-band responses track in magnitude and direction. For the particular example shown in Figure A-5 the tap weight programming of the WBATF to produce a narrow bandpass response at 300 MHz also produces a response at  $f_s + 300$  MHz, or 1170 MHz.

The exact nature of the narrowbanded output signal from the WBATF is, to some extent, dependent upon the tapped delay line structure. If the delay line medium is time continuous such as a transmission line would be, then the output signal will also be time continuous. If the delay medium is a discrete time device such as a Charge Coupled Device (CCD), then the output will be discrete time in nature. The various possibilities are shown in Figure A-6. An example of a continuous delay medium which might be used in a practical implementation of a WBATF is a Surface Acoustic Wave (SAW) device. A CCD, on the other hand, stores values of the input signal at discrete instants of time as charge packets. The output in this case must also be discrete time in nature, although a continuous signal could be recovered by appropriate filtering, providing the Nyquist sampling criterion was satisfied. As is also shown in the figure, if for some reason

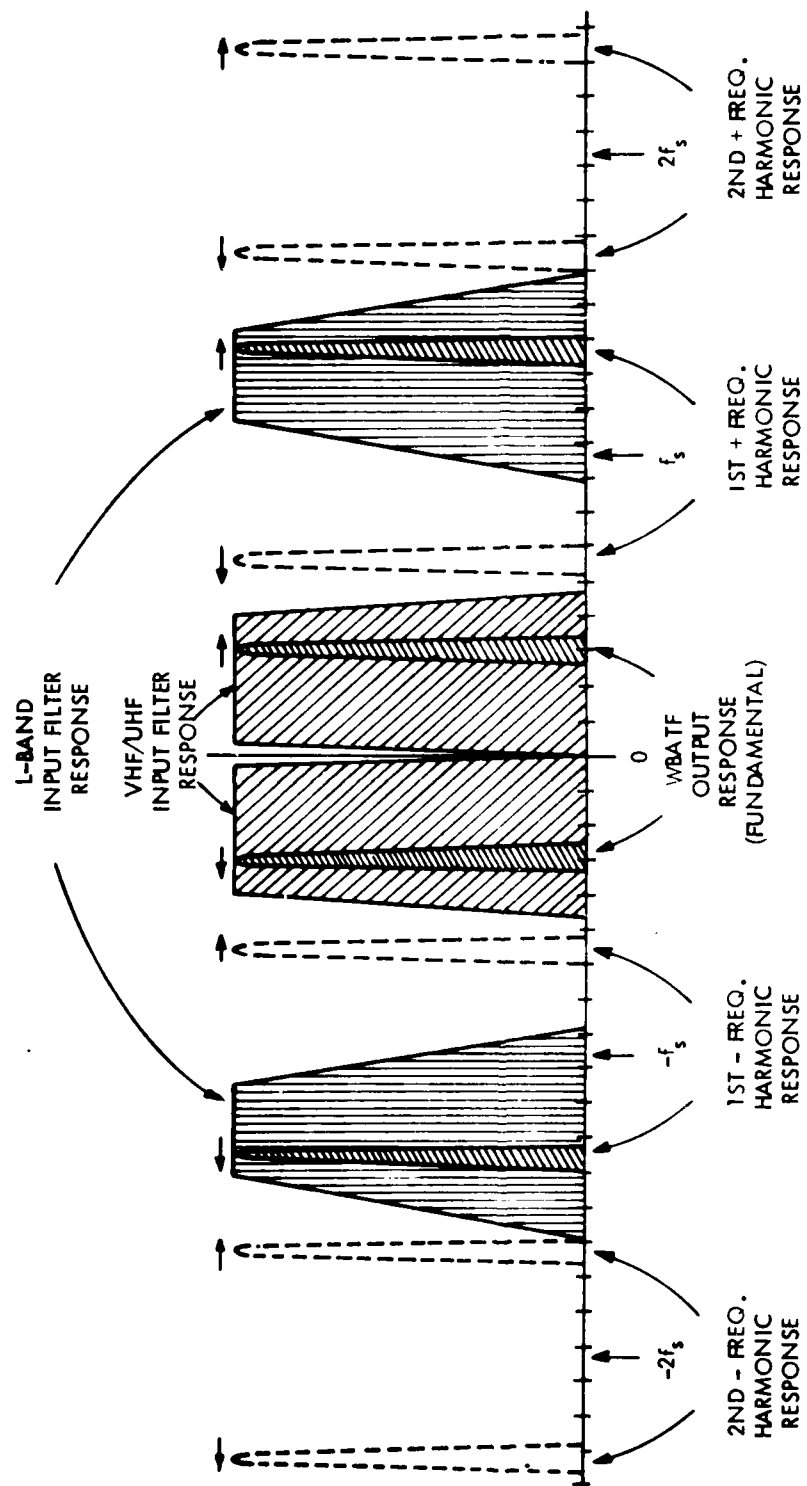


Figure A-5. WBATF input/output frequency responses



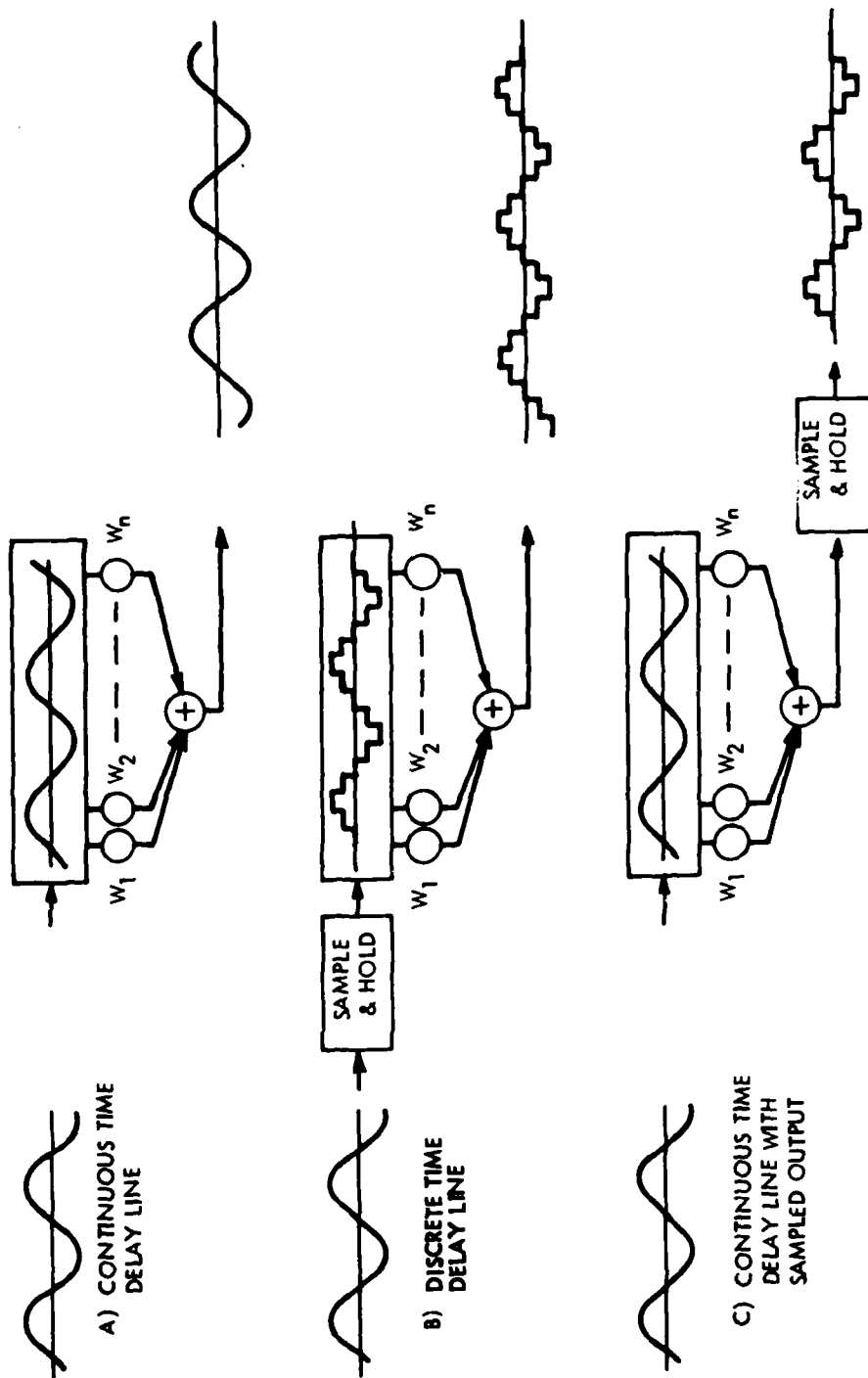


Figure A-6. Continuous versus discrete time filters

a discrete time output is desired, a sample and hold circuit at the output of a continuous time filter produces an equivalent result.

There are some very distinct advantages to sample data filters for a MFBARS type system. Some of these are device oriented and will be discussed later. A particular advantage results from the implicit frequency downconversion resulting from bandpass sampling. It was just demonstrated that the WBATF produces complementary frequency responses at multiples of  $f_s = 1/T$  where  $T$  is the tap spacing delay. This is true whether the delay line is time continuous or not. For a time continuous delay line these responses are at the same frequency as the input. But a sample-data delay line produces a sampled data output which has natural ambiguities with respect to frequency. This situation is depicted by Figure A-7. Suppose that we sample two different input signals, one at 300 MHz and the other at 1170 MHz, at the assumed tap rate of 870 MHz. If a previous sample is held at its last value until a new sample is taken, we call this function a zero-order sample and hold.

This is exactly the function performed by a CCD delay line. The two different frequency inputs are shown in the figure, approximately to scale, and their values at the sampling times (multiples of  $1/T$ ) are found to be identical. This means that once the sampling process has been performed on the input signal, it is impossible to determine from the samples themselves what the actual input frequency was. This is not very surprising, however, since the sampling rate was chosen on the basis of bandpass sampling theory which presumes knowledge of the frequency limits (bandwidth) of the input signal. Due to the presence of the zero order hold (capacitor) circuit which functions as a low pass filter, the sampled output most closely resembles the lower frequency (300 MHz) signal. An appropriately designed low pass filter following the sample and hold would result in a more precise reproduction of the lower frequency signal. In many applications it may be simpler to operate on the lower frequency signal.

One of the primary system benefits of using the WBATF is their signal processing capability in a multi-function radio environment. They can be time-shared among several continuous simultaneous signals in a high speed fashion such that there is negligible loss of available signal power for each of the processed signals. To fully appreciate this point it is necessary to understand the intimate relationship between integration and filters.

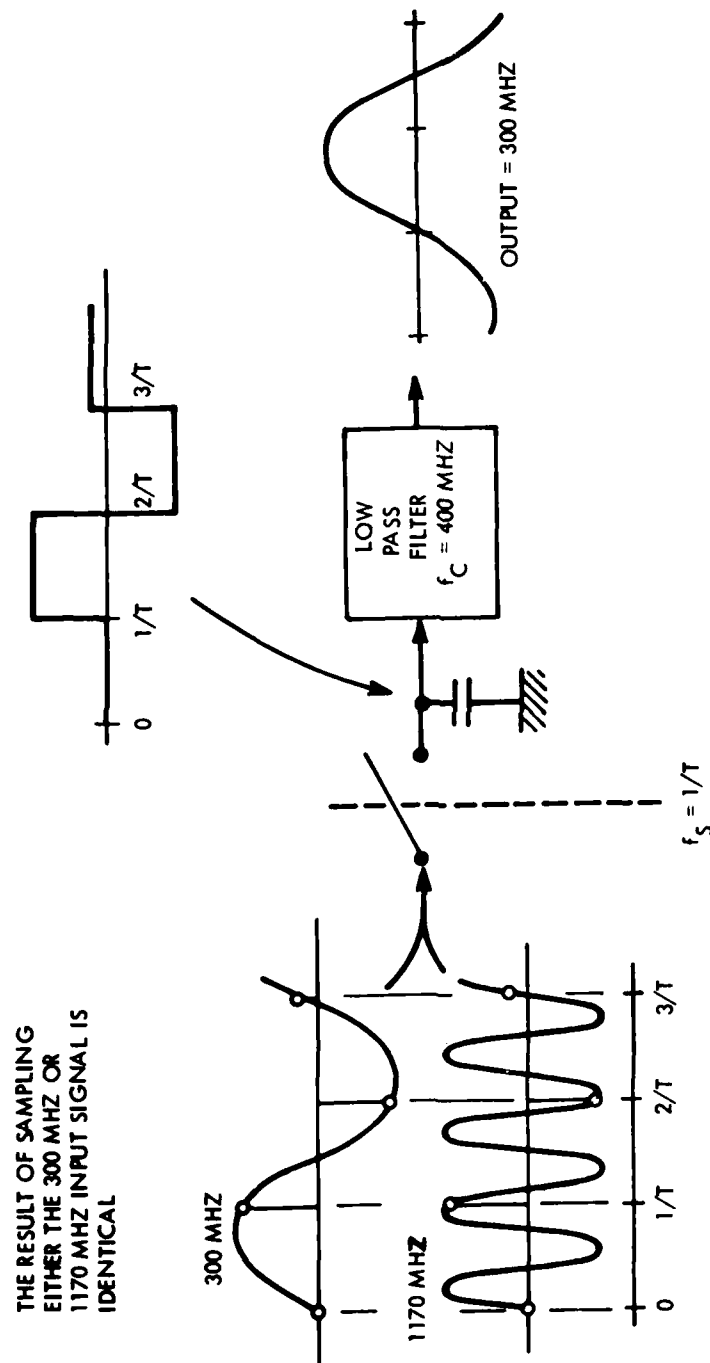


Figure A-7. Bandpass sampling and implicit down-conversion

All filters implicitly contain integrating elements such as capacitors or digital accumulators. In fact, the matched filter<sup>(3)</sup> for a rectangular input pulse of duration  $t$  seconds is an integrator circuit which is allowed to operate over the  $t$  seconds corresponding to the duration of the pulse. The matched filter (by definition) maximizes the output signal-to-noise ratio of the input signal. The improvement in signal-to-noise power ratio is proportional to the integration time. This is clear if we consider the input signal to consist of a constant voltage  $v_k$  representing a signal of interest, and a noise voltage which is a zero mean random variable.

$$s(t) = v_k + n_v(\tau) \quad (A-7)$$

Providing these signals to a linear integrator over an interval  $t$  seconds yields:

$$\int_0^t (v_k + n_v(\tau)) d\tau = v_k t + \int_0^t n_v(\tau) d\tau \quad (A-8)$$

The voltage at the output of the integrator due to the signal of interest increases in proportion to the integrating time. The contribution due to the noise may not be directly evaluated in the time domain since  $n_v(\tau)$  is a non-deterministic function. Instead we can use a frequency domain approach if we assume that  $n_v(\tau)$  represents noise of flat single-sided spectral density  $N_0$ . Any filter has a single-sided noise bandwidth defined by:

$$B_n = \int_0^\infty |H(j\omega)|^2 df \quad (A-9)$$

where  $H(j\omega)$  = the Fourier transform of the filter impulse response  $h(t)$

$$f = \text{frequency} = \omega/2\pi$$

A perfect integrator operating for  $t$  seconds has an impulse response which is a rectangular pulse of unity amplitude and  $t$  seconds duration. It is well known that the Fourier transform of a unity amplitude pulse is:

$$F[h(t)] = t \frac{\sin(\pi t f)}{(\pi t f)} = |H(j2\pi f)| \quad (A-10)$$

substituting this result into equation (A-9) yeilds:

$$B_n = \int_0^{\infty} t^2 \frac{\sin^2(\pi t f)}{(\pi t f)^2} df \quad (A-11)$$

Using the fact that:

$$\int_0^{\infty} \frac{\sin^2 x}{x} dx = \pi/2 \quad (A-12)$$

Results in:

$$B_n = \frac{t^2}{\pi} \cdot \frac{\pi}{2} = \frac{t}{2} \quad (A-13)$$

The noise bandwidth of an integrator is therefore proportional to its integrating time, and the total noise power at integrator output is  $N_0 B_n = N_0 t/2$ . Since the total noise power increases in proportion to the integrating time, and the signal of interest voltage increases in proportion to integrating time we can write the output signal to noise ratio as a power ratio proportional to the integrating time  $t$ .

$$\frac{S}{N}_{OUT} = \frac{(\frac{v_k t}{N_0 t})^2}{\frac{N_0 t}{2}} \quad \frac{S}{N}_{IN} t \quad (A-14)$$

In conventional timeshared systems it is desired that a single piece of hardware be used to process a number of similar signals, rather than using additional sets of identical hardware. These systems usually contain filters, and if the signals to be processed are simultaneous, then some degradation in signal to noise ratio must result. For example, if four simultaneous, equal duration signals are to be processed with one filter (integrator), we could divide their common interval into four equal parts and allow the filter to operate on each signal in succession but for only one-fourth the time. The output signal to noise from the filter for each signal is then one-fourth, or 6 dB less than if no timesharing had been attempted.

The simple signal integrator matched filter described above requires knowledge of the Time of Arrival of the incoming signals in order to properly time the integration intervals. This information is not always known and, therefore,

a more general form of filter consists of a system of integrators operating continuously. Figure A-8 is a block diagram of a generalized  $n$ th order filter which has a voltage transfer function:

$$H(s) = \frac{a_0 + a_1 s + \dots + a_{n-1} s^{n-1} + a_n s^n}{b_0 + b_1 s + \dots + b_{n-1} s^{n-1} + b_n s^n} \quad (A-15)$$

Note that for the filter to be stable, the feedback gain  $b_0$ , at least, must be non-zero. If this were not so,  $H(s)$  would have at least one pole at the origin, implying that any zero frequency input would cause the filter output to increase without bound. It is the existence of this feedback which restricts the use of conventional filters in time sharing systems. If a particular filter characteristic is chosen by assigning values to the gain elements in Figure A-8, then the integrators will accumulate voltages which are specific to that assumed characteristic. To change the filter characteristic we can change the gain elements, but the output cannot respond instantly because of the stored signals in the integrators. We must wait for the old signals to decay as well as the new signal to reach steady state.

The transversal filter is a special case of what is often called a digital filter, and is shown in Figure A-9. The term "digital" is generally used only because digital hardware was most often used to implement these filters, although in principle, there is no reason why analog hardware could not be used. A more correct term, particularly when describing discrete time devices such as CCD's, is "sample-data filter". The transfer function is most conveniently described using  $z$ -transforms and is given by:

$$H(z) = \frac{\sum_{k=0}^m a_k z^{-k}}{1 + \sum_{k=1}^r b_k z^{-k}} \quad (A-16)$$

Note that there is a great deal of similarity between the conventional filter and the sample-data filter. The most obvious difference is the substitution of  $T$  second delay elements for the integrators. For this situation all the feedback gains,  $b_1$ - $b_r$ , can be made zero and the filter becomes a Finite Impulse Response (FIR), or transversal, filter. Providing the number of stages ( $m$ ) and the tap weights,  $a_0$ - $a_m$ , are finite, the output will be unconditionally stable.

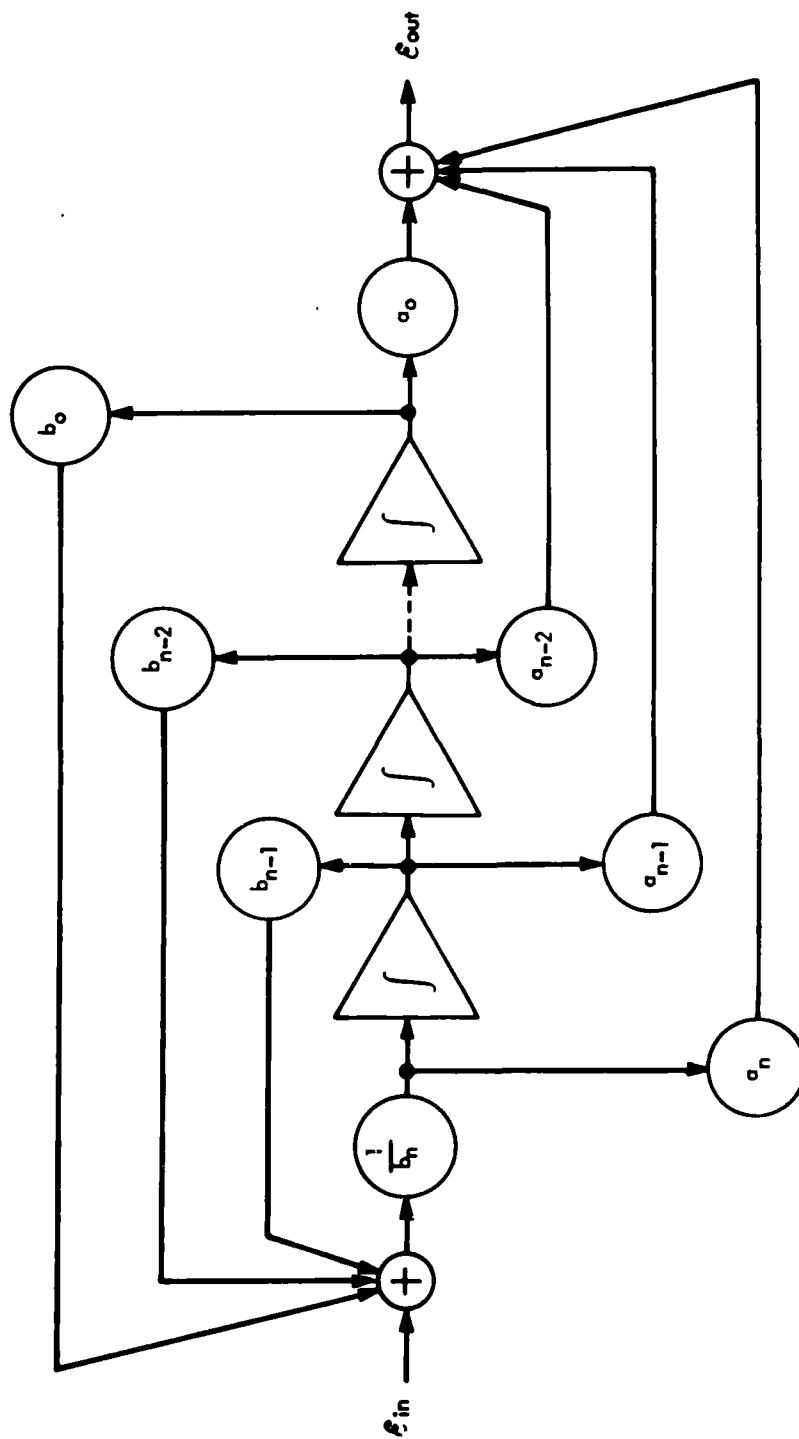


Figure A-8. State variable infinite gain form of a general filter

Also note that the transversal filter performs integration by virtue of the output summation, but that this integration does not corrupt a history of the input signal stored in the delay medium over a period of  $mT$  seconds. Therefore, this time segment of input signal could be processed several different ways if desired. Furthermore, if we are observing the output of the filter we need not observe it continuously. That is, if all the tap weights were equal, for example, then we could sample the output every  $mT$  seconds without losing any available signal energy. This is true because we have replaced the continuous serial processing of a signal by an equivalent parallel processing in batches of  $mT$  seconds. In a practical situation, the tap weights will not be all equal (in order to achieve a desired frequency selective function) and sampling at a somewhat higher rate will be required. The output sampling rate can be computed using the considerations described earlier for avoiding aliasing resulting from the sampling process. There is a natural tradeoff between the total time delay length of the filter (related inversely to the output bandwidth), and the output sampling rate. The filter is therefore designed for the minimum required bandwidth which is approximately 3 MHz<sub>3dB</sub> for a JTIDS PN chip matched filter. Simplifications in subsequent processing hardware can be realized if the output sampling rate is an integer multiple of both the center frequency spacing (3 MHz) and the code chipping rate (5 MHz) of JTIDS. This subject is discussed in more detail in Section 3.5 where the theory of operation of follow-on processing circuits is described. It will suffice at this point to state that a sampling rate of 15 MHz, both I&Q (in-phase and quadrature phase) has been selected.

Once it is recognized that the output of the WBATF can be sampled periodically with no loss of signal to noise ratio, it is asked what can be done during the time interval between these samples? The answer is, reprogram the tap weight gains to correspond to other tuning characteristics and sample the other filtered signals resulting at the output.

It must be remembered that the tapped delay line contains the sum of all signals within its input bandwidth. Which of these signals is passed to the output with minimal attenuation is determined by the tap weight gains, which in principle can be modified instantly. This modification does not change the contents of the tapped delay line, so we may change the weights in any conceivable way as long as we restore them to their original state corresponding to the original signal for which the next adjacent time segment sample is due.



Figure A-10 illustrates this concept of high speed, lossless timesharing of one set of hardware. Note that each of the three input signals is being sampled at a rate equivalent to the Nyquist rate at the output of the transversal filter. The sample times are staggered, however, such that there is never a conflict. In practice, as many simultaneous signals can be processed in the interval  $1/B$  as there is time for the weights to be changed and the output of the filter to respond. This limit will be determined by the physics of the material used to implement the WBATF.

For a MFBARS type system the most stressing requirement for parallel channel processing occurs at L-Band. This is primarily due to JTIDS which requires the equivalent of up to eight parallel receivers to process (without A/J loss) the synchronization preamble. A worst case estimate for the total number of parallel channels is:

<u>Function</u>	<u>Channels</u>
JTIDS (for synchronization)	8
Tacan	1
IFF Transponder	1
IFF Interrogator (sum and difference antenna)	2
GPS (double freq. sampling due to 10 MHz BW)	<u>2</u>
TOTAL	14

By dividing this number into the reciprocal of 15 MHz we can determine the maximum permissible response time of the WBATF output to a change of tap weights, which is approximately five nanoseconds. This estimate is termed worst case because some of the listed functions (GPS and IFF) are fixed frequency systems, and if achievable performance became critical these functions could be implemented fairly economically with dedicated hardware. This is particularly true of the IFF Interrogator function which would require some signal manipulation prior to insertion to the WBATF. This is so because the sum (  $\Sigma$  ) and difference (  $\Delta$  ) antenna outputs carry identical signals differing only in amplitude. Once these signals are combined at the WBATF input it becomes difficult to separate their respective amplitudes.

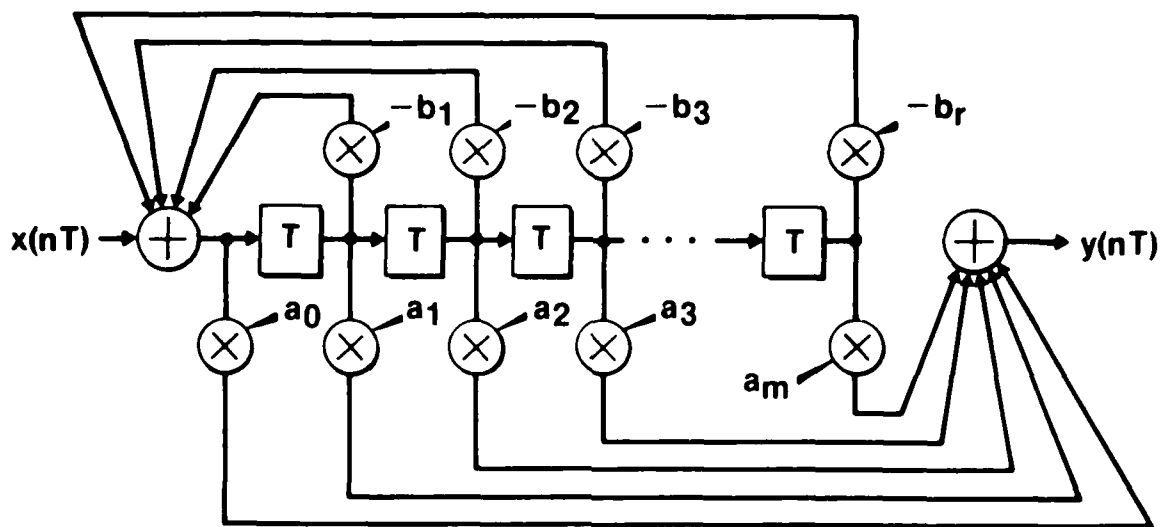


Figure A-9. The general form of a digital filter

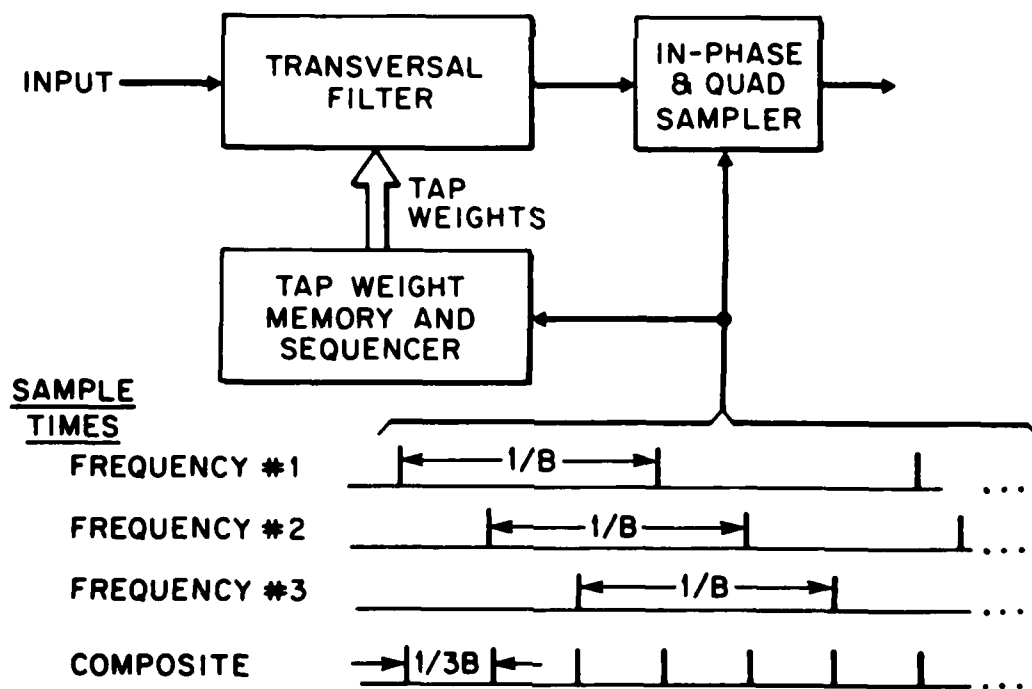


Figure A-10. High speed lossless transversal filter timesharing

To achieve the rapid rotation of tap weights in the WBATF, a system of local memory consisting of registers to hold the desired tap weights is required. This situation is depicted in Figure A-1. The registers hold M sets of tap weights which are parallel transferred from one register to the next. Each set of tap weights is cyclicly introduced to the tapped delay line producing the required transfer function. In this way the WBATF "scans" a set of M frequencies and produces a natural time division multiplexed output signal sequence. At some point in the cyclic path of the tap weight registers a switch is placed such that new values of tap weights can be introduced where required.

The maximum rate at which new tap weight sets must be introduced may be calculated as follows. The radio function that requires the maximum agility from a tunability standpoint is JTIDS. During the message portion of a JTIDS transmission, approximately each 12 microseconds, a new pulse arrives at a pseudo-randomly selected frequency. The duration of the pulse is approximately 6 microseconds, leaving an equal gap between successive pulses. During this gap, a completely new set of tap weights must be introduced to the WBATF. As an example, if the WBATF employed 500 taps, then the tap loading rate is  $(500/6 \times 10^{-6} \text{ seconds}) = 83 \text{ MHz}$ .

The required accuracy for the tap weights was studied by computer analysis. A 500 tap filter was designed by the computer program referred to earlier. Several different center frequencies were considered. These designs were optimum in the sense that the tap weights were assumed to have infinite resolution, and this resulted in a uniform attenuation ripple over the reject band of the filter. The ideal values of the tap weights were then quantized by rounding the tap weight value to the nearest multiple of  $1/(2^n - 1)$ . This binary quantization allows one bit for sign. The frequency response of the quantized filter was then computed and the peak and average values of the reject band attenuation were recorded for various values of n. The result of this analysis is shown in Figure A-11. It can be seen that in the region where attenuation is being determined by the quantization effects (rather than the ultimate attenuation characteristics of the filter), the attenuation is directly proportional to the quantization level. That is, for a one bit change in quantization (factor of 2) there is a 6 dB (factor of 2) change in attenuation. The effect of tap weight quantization on the passband response is negligible and need not be considered. For the 500 tap filter shown, 12 bit quantization provides performance only 5 dB from the optimum theoretical peak rejection. The desirable ultimate peak rejection would be approximately 100 dB. This level of rejection would

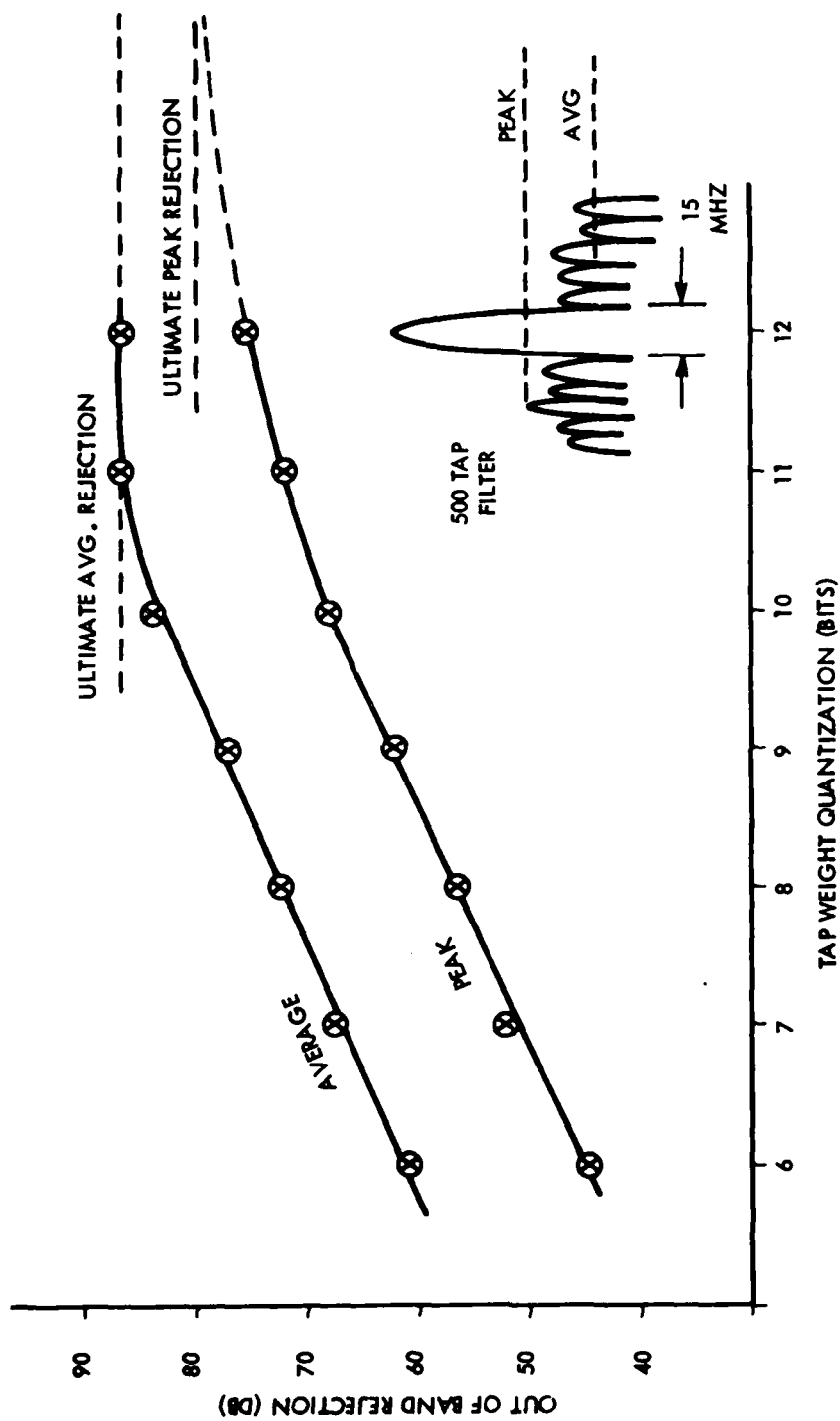


Figure A-11. Effects of tap weight quantization errors

guarantee excellent performance in all respects. To achieve this, however, might require as much as 650 taps with 16 bits of quantization. This specific problem has not been run on the computer due to core memory limits which preclude filter designs in excess of 500 taps without extensive program modification. Departures from the ideal rejection levels will produce some small measure of performance degradation from the ideal under some circumstances, and further work in this area is needed to further refine estimates of the total number of taps and weight quantization.

The dynamic range of the WBATF is defined as the ratio of the maximum input signal for linear operation to the internal RMS noise referred to the input. If we assume that the maximum input signal that we must handle is 0 dBm, and that the effective input noise due to the WBATF is to be at least 10 dB less than thermal noise we may compute the required dynamic range. The thermal noise power in a 400 MHz bandwidth and assuming a 5 dB noise figure pre-amplifier prior to the WBATF is:

$$10 \log_{10}(kT/1 \times 10^{-3}) = -174 \text{ dBm/Hz}$$

$$\text{for a 400 MHz BW} = + 86 \text{ dB}$$

$$\text{for a 5 dB Noise Figure} = \underline{+ 5 \text{ dB}}$$

$$\text{Total Thermal Noise Power} = - 83 \text{ dBm}$$

If the WBATF effective input noise is to be 10 dB below this, then the dynamic range required is from 0 dBm to -93 dBm or simply 93 dB.

A convenient way of describing the interrelationship between dynamic range, WBATF power gain (or insertion loss), and the overall system specifications for noise figure and maximum input signal level, is shown in Figure A-12. Here the assumptions are that the maximum input signal level will be 0 dBm, and that the overall system noise figure must be less than or equal to 7 dB. These numbers were chosen because they are consistent with JTIDS and Tacan specifications. These specifications may be somewhat overstated from a practical standpoint, however, they serve as a reference point. The curves in the figure are developed by using the well known formula for overall noise figure of cascaded amplifier stages:

$$F_0 = F_1 + \frac{F_2 - 1}{G_1} + \frac{F_3 - 1}{G_1 G_2} \dots \quad (\text{A-17})$$

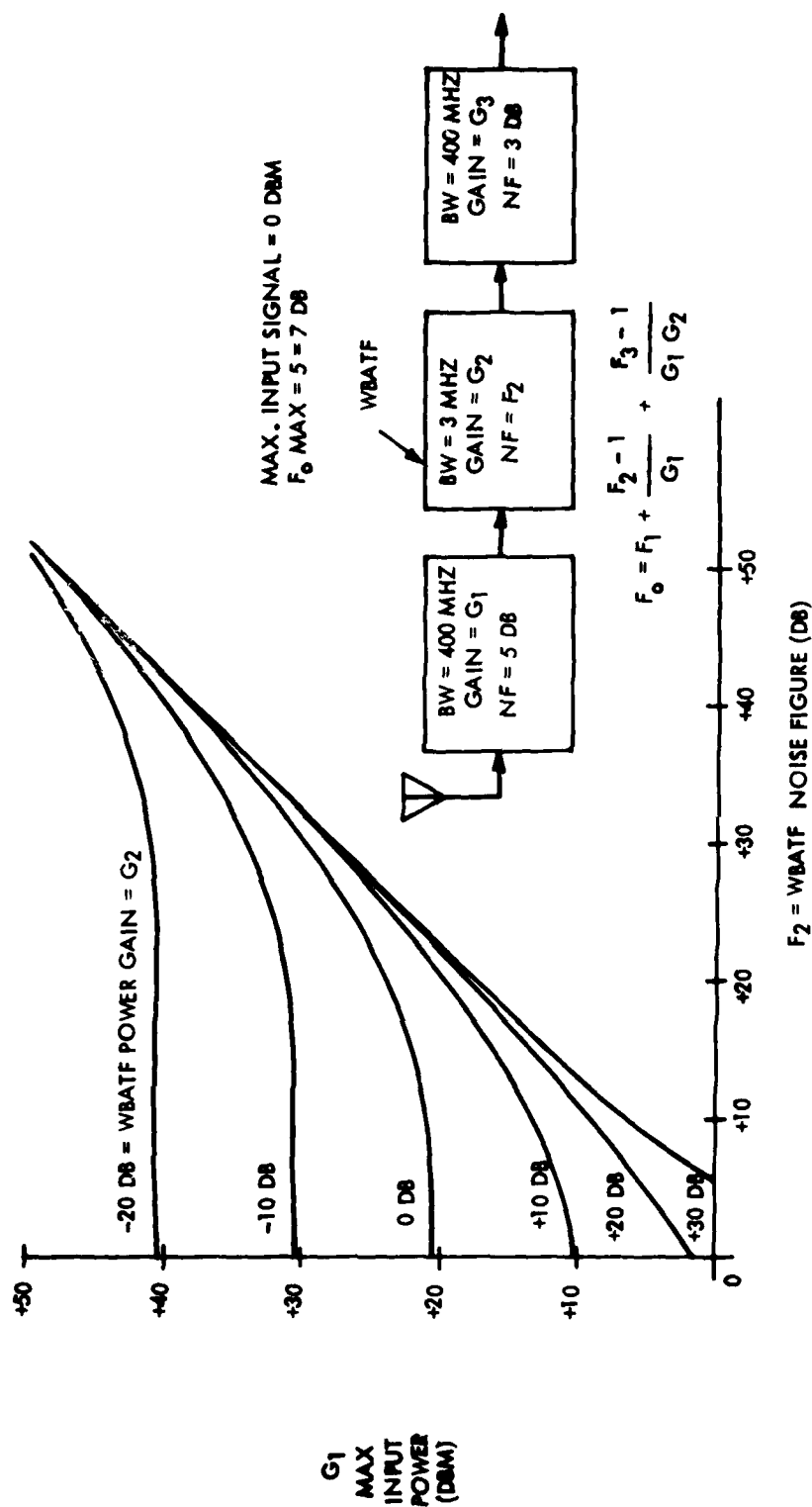


Figure A-12. WBATF noise performance

where:

$F_0 = 5.01$  (7 dB) Overall system noise factor.

$F_1 = 3.16$  (5 dB) Input Amplifier noise factor.

$G_1$  = Input Amplifier power gain, and also the max.  
input level to the WBATF (if system input level  
is 0 dBm).

$G_2$  = Power Gain (or Insertion Loss) of WBATF.

$F_2$  = Noise Factor of WBATF.

$F_3$  = Noise Figure of Amplifier following WBATF, assumed  
to be 3 dB, but due to the larger BW (400 MHz)  
with respect to WBATF the effective noise figure  
is:

$$3 \text{ dB} + 10 \log_{10} \frac{400 \text{ MHz}}{3 \text{ MHz}} = 24.2 \text{ dB}$$

Solving equation (A-17) for  $G_1$  in terms of  $G_2$  and  $F_2$   
yields the curves shown in Figure A-12.

Note that if the noise figure of the WBATF is increased,  
then the maximum input power that the filter must handle  
is also generally larger. This figure also demonstrates  
the importance of keeping the insertion loss as low as  
possible, since it directly reduces dynamic range.

We have not, to this point, discussed how the values of  
the tap weights which will be provided to the WBATF are to  
be generated. There are several possibilities which we  
will consider, and they are:

1. Calculation from a given frequency response.
2. Table look up in digital memories.
3. A combination of table look up of key parameters  
and calculation.

The first approach is the most general and flexible. It  
involves calculation of the required tap weights using a  
computer algorithm similar to that which was mentioned  
earlier, and used for filter design. Any bandshape and  
center frequency could be obtained in this manner. The  
bandshape could even be adaptively controlled to be respon-  
sive to a changing threat environment. The only disadvan-  
tage of this approach is the very large number of computa-  
tions required to generate the tap weights to the required

accuracy. As an example, it takes 15 minutes on an SEL-32/55 computer to calculate one 500 point impulse response.

An alternative approach would store all necessary sets of tap weights corresponding to various bandshapes and center frequencies in digital memories. This approach is much less flexible, but can produce the tap weights very quickly and with a simple memory addressing scheme. The size of the memory required to store all the tap weights can be estimated. Since there is still some uncertainty regarding the exact number of taps and their quantization in bits, a range of possibilities will be calculated. Another variable which enters into this calculation is the frequency resolution of the output. Since the WBATF will have an output bandwidth on the order of several megahertz, a frequency resolution of one megahertz should be more than adequate. On the outside, by making minor compromises in the bandshape, it might be possible to use three megahertz resolution. These results may be summarized as follows.

	<u>Minimum</u>	<u>Maximum</u>
BITS/TAP	12	16
TAPS/WBATF	500	650
FREQUENCY RESOLUTION	3 MHz	1 MHz
TOTAL BITS	738,000	4,848,000

Although these memory requirements are quite large, using reasonable predictions for memory densities in the MFBARS production timeframe, it can be shown that it would be possible to implement on a single digital card.

The third alternative is a hybrid approach combining digital memories and computation. It is based on the fact (see Figure A-4) that the bandshape of a bandpass filter is determined by the envelope of the impulse response, and the center frequency by the cosine function modulated by that envelope. This implies that we could store an envelope function one time, and a quarter cycle of the cosine function, and obtain the desired tap weights by multiplying the sampled values of these components. This technique is illustrated in Figure A-13. The advantage of this approach is that less memory is required than the previous approach. In addition, a very fine center frequency resolution can be obtained with only a modest increase in memory size. The size of this tap weight generator varies with the details of particular implementations; however, preliminary analysis has indicated that there is at least a 60 percent saving in hardware over the previously discussed approach.



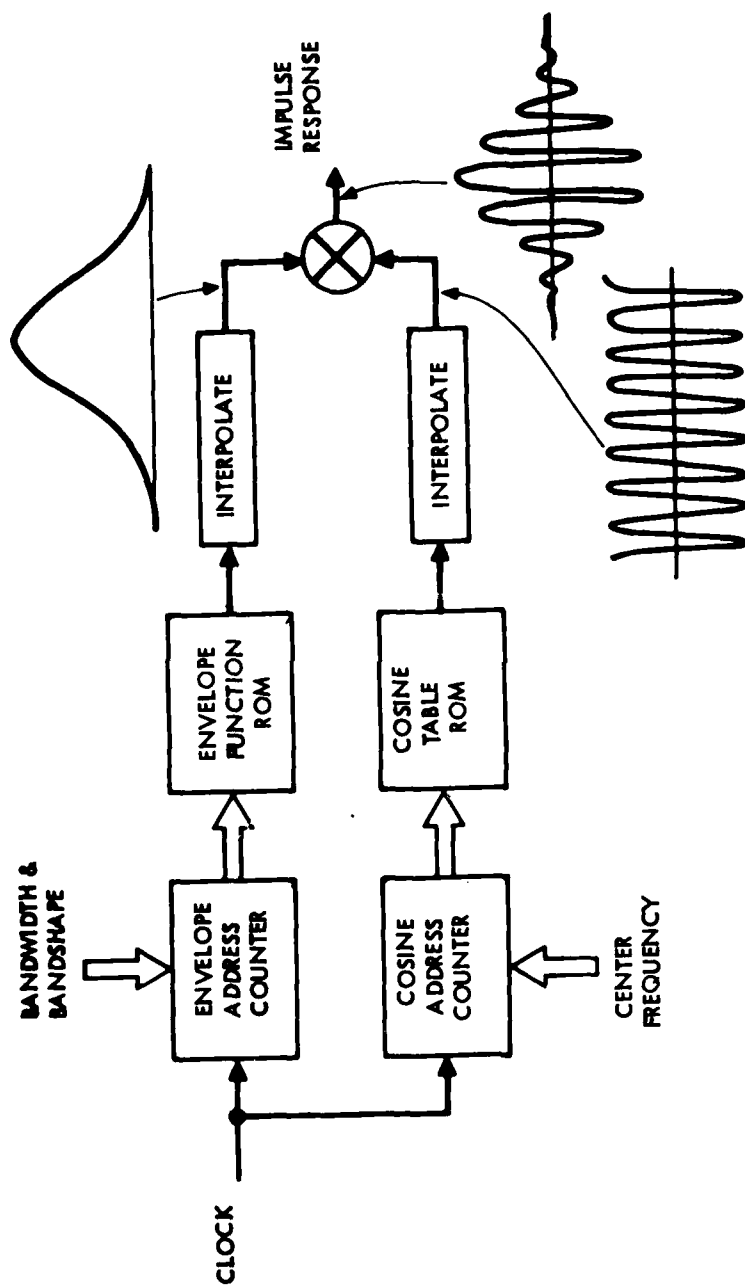


Figure A-13. A tap weight generation technique

#### REFERENCES

- (1) GPS/JTIDS/INS Integration Study Final Report, prepared by Charles Stark Draper Laboratories, Inc., April 1978.
- (2) J.H. McClellan, T. W. Parks, and L. R. Rabiner, A Computer Program for Designing Optimum FIR Linear Phase Digital Filters, IEEE Trans. Audio Electroacoust. Vol. AU-21, Dec. 1973, pages 506-525.
- (3) M. Schwartz, Information Transmission, Modulation, and Noise, pages 282-291, McGraw-Hill Book Co., Inc. 1959.
- (4) Richard J. Swan, The Switching Structure and Addressing Architecture of N Extensible Multiprocessors: CM\*, August 1978 PhD Dissertation, Carnegie-Mellon University, Dept. of Computer Science.
- (5) Final Technical Report for JTIDS Class 3 Terminal Conceptual Study, prepared for JTIDS Joint Program Office, Deputy for Control and Comm. Systems (AFSC) on Contract No. F19628-77-C-0192-0002, June 1978.

## BIBLIOGRAPHY

1. B. Widrow, et al, "Adaptive Antenna Systems," Proc. of the IEEE, Vol. 55, No. 12, Dec. 1967, pp. 2143-2159.
2. B. S. Abrams, et al, "Interference Cancellation," General Atronics Corp. Final Report RADC-TR-74-225, Sept., 1974.
3. W. D. White, "Artificial Noise in Adaptive Arrays," IEEE Trans. on AES, Vol. AES-14, No. 2, March 1978, pp. 380-384.
4. R. T. Compton, Jr., "An Adaptive Array in a Spread Spectrum Communication System," Proc. of the IEEE, Vol. 66, No. 3, March 1978, pp 289-298.
5. M. J. DiToro, "Communication in Time-Frequency Spread Media Using Adaptive Equalization," Proc. of the IEEE, Vol. 56, Oct. 1968, pp. 1653-1679.
6. L. E. Brennan, E. L. Pugh, I. S. Reed, "Control Loop Noise in Adaptive Array Antennas," IEEE Trans on AES, Vol. AES-7, No. 2, March 1971, pp. 254-262.
7. B. Widrow and J. M. McCool, "A Comparison of Adaptive Algorithms Based on the Methods of Steepest Descent and Random Search," IEEE Trans. on Ant. and Prop., Vol. AP-24, No. 5, Sept. 1976, pp. 615-637.
8. A. J. Berni, "Weight Jitter Phenomena in Adaptive Array Control Loops," IEEE Trans. on AES, Vol. AES - 13, No. 4, July 1977, pp. 355-361.
9. Papoulis, "The Fourier Integral and Its Applications" page 30.

## ABBREVIATIONS AND ACRONYMS

AAS	Adaptive Antenna System
ADM	Advanced Development Model
ADP	Advanced Development Program
AFSATCOM	Air Force Satellite Communications
AGC	Automatic Gain Control
A/J	Anti-Jam
ASL	Average Signal Loss
ATC	Air Traffic Control
ATDMA	Advanced Time Division Multiple Access (Proposed JTIDS signal format)
ATF	Agile Transversal Filter
BIT	Built-In-Test
BITE	Built-In-Test Equipment
BPSK	Bi-Phase Shift Keying
CAS	Collision Avoidance System
CAS	Close Air Support
CCD	Charge Coupled Device
CCSK	Cyclic-Code-Shift-Keying
COMSEC	Communication Security
CNI	Communication Navigation Identification
CP	Circular Polarized
CPSM	Continuous Phase Shift Modulation
CPLX	Complexity
CTD	Charge Transfer Device
DABS	Discrete Address Beacon System
DAIS	Digital Avionics Information System

DTC	Design-to-Cost
DTDMA	Distributed Time Division Multiple Access (Proposed JTIDS signal format)
ECCM	Electronic Counter-Countermeasures
EDM	Engineering Development Model
FIR	Finite Impulse Response
FS	Frequency Synthesizer
FSK	Frequency Shift Keying
GPS	Global Positioning System
HOL	Higher Order Languages
ICNIA	Integrated CNI Avionics
IMU	Inertial Measurement Unit
INS	Inertial Navigation System
JTIDS	Joint Tactical Information Distribution System
LCC	Life Cycle Cost
LOP	Line of Position
LRU	Line Replaceable Unit
MIC	Microwave Integrated Circuit
MLS	Microwave Landing System
MPX	Multiplexer
MSW	Magneto-Static Wave
NBATF	Narrow Band Agile Transversal Filter
NIS	NATO Identification System
P-MESSAGE	JTIDS Message Type (Position Information)
PRICE	Programmed Review of Information for Costing and Evaluation
PMS	Processor-Memory-Switch
PSK	Phase Shift Keying

PN	Pseudo-Noise
ROM	Read Only Memory
RTT	Round-Trip-Timing
SAW	Surface Acoustic Wave
SEEK TALK	A Secure Voice UHF system
SINGARS	A Secure Voice VHF system
SDU	Service Data Unit
TBD	To Be Determined
TDMA	Time Division Multiple Access (Proposed JTIDS signal format)
TOA	Time of Arrival
TFH	Thick Film Hybrid
TFHM	Thick Film Hybrid Module
TRANSEC	Transmission Security
WBATF	Wide Band Agile Transversal Filter

**MED**  
**-8**